An exploration of the interplay between HSV-1 and the non-homologous end joining proteins PAXX and DNA-PKcs

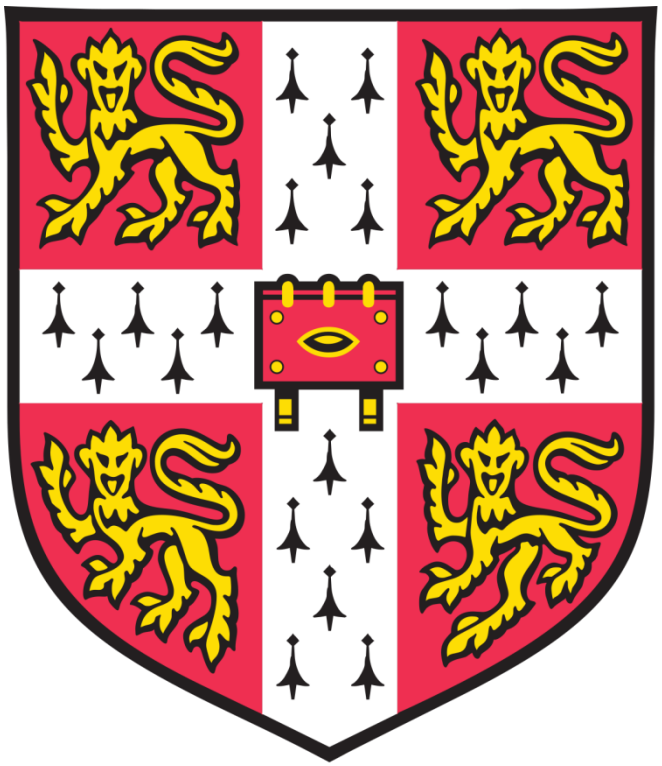

Benjamin James Trigg

Gonville and Caius College

This dissertation is submitted for the degree of

Doctor of Philosophy

September 2017

An exploration of the interplay between HSV-1 and the non-homologous end joining proteins PAXX and DNA-PKcs

Benjamin James Trigg

Abstract

DNA damage response (DDR) pathways are essential in maintaining genomic integrity in cells, but many DDR proteins have other important functions such as in the innate immune sensing of cytoplasmic DNA. Some DDR proteins are known to be beneficial or restrictive to viral infection, but most remain uncharacterised in this respect. Non-homologous end joining (NHEJ) is a mechanism of double stranded DNA (dsDNA) repair that functions to rapidly mend broken DNA ends. The NHEJ machinery is well characterised in the context of DDR but recent studies have linked the same proteins to innate immune DNA sensing and, hence, anti-viral responses. The aim of this thesis is to further investigate the interplay between herpes simplex virus 1 (HSV-1), a dsDNA virus, and two NHEJ proteins, DNA protein kinase catalytic subunit (DNA-PKcs) and paralogue of XRCC4 and XLF (PAXX).

PAXX was first described in the literature as a NHEJ protein in 2015, but whether it has any role in the regulation of virus infection has not been established. Here we show that PAXX acts as a restriction factor for HSV-1 because *PAXX*$^{-/-}$ (KO) cells produce a consistently higher titre of HSV-1 than the respective wild type (WT) cells. We hypothesised that this could be due to a role of PAXX binding viral DNA and directly inhibiting HSV-1 replication or activating an anti-viral innate immune response. We have been able to, at least partially, rule out both of these initial hypotheses by showing that there was a reduced number of viral genomes present in KO cells during active lytic infection, and that an identical level of type I interferons are produced from WT and KO cells during HSV-1 infection. Although further characterisation of HSV-1 infection in WT

and KO cells has not defined the molecular mechanism of restriction of HSV-1 by PAXX, we have uncovered a potential role for PAXX in mitogen-activated protein kinase (MAPK) signalling. In addition, and consistent with its function in restriction of HSV-1 infection, we show that infection with this virus in WT cells induces a loss of nuclear PAXX protein. Preliminary data suggest that these changes in localisation may occur as a result of stimulation of the cells with DNA, but not the RNA analogue poly(I:C).

The role of PAXX in the regulation of HSV-1 infection *in vivo* was investigated by studying KO mice. Despite previous observations that mice lacking NHEJ proteins have brain defects related to autoinflammatory pathology, there were no obvious defects in the development of *Paxx*$^{-/-}$ mice, and they had brains of normal weight. No significant difference in viral spread or viral protein expression was observed between WT and KO HSV-1 infected mice, and KO mice did not exhibit abnormal pathology. There were, however, small but significant differences in the cellular immune response to infection which might be explained by reduced MAPK signalling in KO cells.

DNA-PKcs is another component of the NHEJ machinery that acts to assist in dsDNA break repair in the nucleus and as an innate sensor of cytoplasmic viral DNA, but the effect of DNA-PKcs on HSV-1 infection has not been fully explored. Murine skin fibroblasts (MSFs) derived from wild type and *PRKDC*$^{-/-}$ (DNA-PKcs deficient) mice were cultured *ex vivo* and used for innate immune studies. Although HSV-1 was able to infect and stimulate these cells, no differences in the stimulation of innate immune gene expression between the two genotypes was observed, suggesting that DNA-PKcs does not contribute to HSV-1 sensing in MSFs. It has previously been reported that the HSV-1 protein ICP0 targets DNA-PKcs for degradation, although the reason for this is unknown. We confirmed these data, although found it to be cell-type specific and explored this interaction further using *PRKDC*$^{-/-}$ RPE-1 cells created using CRISPR/Cas9. HSV-1 infection in these cells followed unusual dynamics, and the development of cytopathic effect was accelerated as compared to WT cells. Together these observations confirm that DNA-PKcs regulates HSV-1 infection, but more work is required to fully understand the mechanisms involved.

Preface

This dissertation is the result of my own work and includes nothing which is the outcome of work done in collaboration except as declared in the Preface and specified in the text.

This dissertation is not substantially the same as any that I have submitted, or, is being concurrently submitted for a degree or diploma or other qualification at the University of Cambridge or any other University or similar institution except as declared in the Preface and specified in the text. I further state that no substantial part of my dissertation has already been submitted, or, is being concurrently submitted for any such degree, diploma or other qualification at the University of Cambridge or any other University or similar institution except as declared in the Preface and specified in the text.

This dissertation does not exceed the prescribed word limit for the Biology Degree Committee.

Acknowledgements

First and foremost, I would like to thank Dr Ferguson for his advice and guidance over the past four years. Brian's support has been unwavering, despite the many times that I have been an excellent test of his patience, and for this I shall always be grateful.

As is often the case, aspects of this project have been a team-effort. Especial thanks go to Kathi and Paula for their help with the PAXX project, and to Zhenya for helping me to navigate the strange worlds of cellular immunity and *in vivo* work. Over twenty people have passed through the lab in the time that I have been doing my PhD, and each has helped make my time in the lab considerably more enjoyable. Unfortunately it is impractical to list how each has helped me, but Christian, the master of distraction, deserves a special mention for guiding me through my first, hard year.

The number of people I would like to acknowledge outside of 'The Lab of Brian' is testament to the extent to which I have benefitted from the kindness and generosity of others. Prof. Geoffrey Smith and his lab have supported me throughout with both advice and reagents. The number of times that I bothered David Carpentier is surpassed only by his wealth of knowledge and enthusiasm to help. I have also benefitted greatly from the wisdom and charity of Helen Ewles and Yongxu Lu. The help of Heather Coleman was instrumental in facilitating many aspects of the PAXX project, and there was never a dull moment while working with her. Dan Wise provided invaluable advice on CRISPR, but was otherwise just an annoyance. Mike Hollinshead and Nigel Miller set aside a great deal of time to impart the wonders of microscopy and flow cytometry, respectively. Des Jones provided help and worldly advice in my first few years.

I would also like to thank Adrian Smith and Letitia Jean for inspiring me to embark on a PhD. Without their advice and encouragement, I probably would not be writing this today.

Thanks also to my long-suffering friends who have helped to preserve what is left of my sanity, be that through rowing, the pub quiz, or Mario Kart. To my even-longer-suffering family, a special mention goes to mum and Sam for their surprising eagerness

to help with proof-reading, but thanks also to dad and Jess for all of your support and understanding over the last four years.

Finally, thank you to Jo. After putting up with my unsocial hours and perpetual grumbling over the last four years she probably deserves a page to herself, but at this point in composing my thesis I'm not sure I can manage that much more writing. Suffice to say, she has provided essential moral, emotional, and nutritional support, without which I would probably not have had the stamina to see the PhD to the end. I could not have asked for a more patient and generous partner. Thank you.

Table of Contents

List of figures

List of tables

Abbreviations

2-ME	2 mercaptoethanol
AIM2	Absent in melanoma 2
AMPK	AMP-activated protein kinase
A-NHEJ	Alternative non-homologous end joining
APLF	Aprataxin-and-PNK-like factor
ASC	Apoptosis-associated speck-like protein containing a caspase activation and recruitment domain
ATM	Ataxia-telangiectasia mutated
ATR	ATM and Rad3-related
ATRIP	ATR interacting protein
BER	Base excision repair
BRCA1	Breast cancer 1
CARD	Caspase recruitment domain
Cas9	CRISPR-associated 9
CCL	Chemokine (C-C motif) ligand 3
CD	Cluster of differentiation
cDNA	Complimentary DNA
cGAMP	Cyclic-GMP-AMP
cGAS	Cyclic-GMP-AMP synthase
CHK-1	Checkpoint kinase 1
CMC	Carboxymethyl cellulose
CMV	Cytomegalovirus
C-NHEJ	Classical non-homologous end joining
CNS	Central nervous system
CPE	Cytopathic effect
CRISPR	Clustered Regularly Interspaced Short Palindromic Repeats
CSR	Class switching recombination
DAMPs	Damage-associated molecular patterns
DAPI	4',6-diamidino-2-phenylindole
DC	Dendritic cell
DDR	DNA damage response
DMEM	Dulbecco's Modified Eagle Medium
DNA	Deoxyribonucleic acid
DNAM-1	DNAX accessory molecule-1
DNA-PK	DNA-dependent protein kinase
DNA-PKcs	DNA-dependent protein kinase catalytic subunit
DSB	Double-strand break
dsDNA	Double-stranded DNA
ELISA	Enzyme-linked immunosorbent assay
FA	Fanconi anaemia
FAT	Focal adhesion targeting
FATC	FRAP, ATM, TRRAP C-terminal

FBS	Foetal bovine serum
G2	Growth 2 phase of the cell cycle
G2/M	Growth 2/mitosis checkpoint
GAPDH`	Glyceraldehyde 3-phosphate dehydrogenase
gB	Glycoprotein B
gC	Glycoprotein C
gD	Glycoprotein D
gE	Glycoprotein E
GFP	Green fluorescent protein
γH2AX	Phosphorylated H2AX
gI	Glycoprotein I
H2AX	Variant of histone 2A
HBV	Hepatitis B virus
HDP-RNP	HEXIM1-DNA-PK-paraspeckle components ribonucleoprotein complex
HEAT	Huntington-elongation-A-subunit-TOR
HEXIM1	Hexamethylene bis-acetamide-inducible protein 1
HFFF	Human foetal foreskin fibroblasts
HIF-1α	Hypoxia-inducible factor-1 alpha
HIN	Hematopoietic, interferon-inducible, nuclear
HIV	Human immunodeficiency virus
HPV	Human papillomavirus
HR	Homologous recombination
HSV-1	Herpes simplex virus 1
IAPs	Inhibitor of apoptosis proteins
ICP0	Infected cell protein 0
IE	Immediate early
IFI16	Interferon gamma inducible protein
IFN	Interferon
IFN-I	Type-1 interferon
Ig	Immunoglobulin
IKK	IκB kinase
IL	Interleukin
InDel	Insertion/deletion mutation
IR	Ionizing radiation
IRF	Interferon regulatory factor
IVIS	*In vivo* imaging system
JCV	JC virus
JNK	c-Jun N-terminal kinase
Kbp	Kilobase pair
KO	Knock out
LIG4	DNA ligase IV
LPS	Lipopolysaccharide
LRR	Leucine rich region
LT	Large T
MAPK	Mitogen-activated protein kinase

MAPKKK	MAPK kinase kinase
MEFs	Murine embryonic fibroblasts
MHC-1	Major histocompatibility complex 1
MEM	Minimum essential medium
MLH1	MutL homologue 1
MMEJ	Microhomology-mediated end joining
MMR	Mismatch repair
MOI	Multiplicity of infection
MRE11	Meiotic recombination 11 homolog
MRN	MRE11, RAD50, NBS1
mRNA	Messenger RNA
MSFs	Murine skin fibroblasts
MVA	Modified Vaccinia Ankara
NBS1	Nijmegen Breakage Syndrome 1
ND10	Nuclear domain 10
NEAT1	Nuclear Enriched Abundant Transcript 1
NEMO	NF-kappa-B essential modulator
NER	Nucleotide excision repair
NF-κB	Nuclear factor kappa-light-chain-enhancer of activated B cells
NHEJ	Non-homologous end joining
NK	Natural killer
NKG2D	NK group 2, member D
P/S	Penicillin/streptomycin
PAMPs	Pathogen-associated molecular patterns
PARP	Poly ADP ribose polymerase,
PAXX	Paralogue of XRCC4 and XLF
PBS	Phosphate-buffered saline
PBST	PBS with 0.025 % v/v tween 20
PCR	Polymerase chain reaction
PFA	Paraformaldehyde
PFU	Plaque forming units
PIKK	Phosphatidyl inositol 3' kinase-related kinase
PMA	Phorbol 12-myristate 13-acetate
PML	Promyelocytic leukaemia
PNKP	Polynucleotide kinase-phosphatase
PP2A	Protein phosphatase 2A
PRKDC	'Protein kinase, DNA-activated, catalytic polypeptide' (the gene encoding DNA-PKcs)
PRRs	Pattern recognition receptors
PYHIN	Pyrin and HIN
qPCR	Quantitative PCR
RAD	Ras associated with diabetes
RAG	Recombination-activating gene
RIP1	Receptor-interacting protein
RNA	Ribonucleic acid

ROS	Reactive oxygen species
RPA1	Replication protein A 1
RPA32	Replication protein A 32
RPE-1	Retinal pigment epithelia 1
S17	Strain 17
SCID	Severe combined immunodeficiency
SDS	Sodium dodecyl sulphate
SEM	Standard error of the mean
sgRNA	Single-guide RNA
SHM	Somatic hypermutation
SLE	Systemic lupus erythematosus
S-phase	Synthesis phase of the cell cycle
SSA	Single-strand annealing
ssDNA	Single-stranded DNA
STING	Stimulator of interferon genes
SV40	Simian vacuolating virus 40
TANK	TRAF family member associated NF-κB activator
TBK1	TANK-binding kinase 1
TCR	T-cell receptor
TLR	Toll-like receptor
TNFα	Tumour necrosis factor α
TOPBP1	Topoisomerase-IIβ–binding protein 1
TREX1	3′ repair exonuclease 1
UL	Unique long
US	Unique short
UV	Ultraviolet
V(D)J	Variable, diversity, joining
VACV	Vaccinia virus
Vpr	Viral protein R
WR	Western reserve
WRN	Werner Syndrome
WT	Wildtype
XLF	XRCC4-like factor
XLS	XRCC4-like-small protein (alternative name for PAXX)
XRCC4	X-ray cross-complementing protein 4

1 Introduction

1.1 The DNA Damage Response

1.1.1 Introduction to the DNA Damage Response

The genome of an organism is frequently damaged by a wide range of exogenous and endogenous processes. Exogenous factors include ionizing radiation, infection (Chumduri *et al*., 2016), and mutagenic chemicals, while endogenous factors include reactive oxygen species (ROS), errors in genome replication, and dysregulation of gene expression (Tubbs and Nussenzweig, 2017). It is estimated that on average each cell incurs over 100 genomic lesions daily (Lindahl, 1993), and each of these can interfere with genome replication and gene transcription. If the cell fails to repair lesions correctly mutations can arise, genome stability can be compromised, and cell and/or organism viability can be put at risk. Cancer, for example, arises following the accumulation of mutations in a cell genome which deregulate important homeostatic processes and result in further genomic instability.

To address the threat posed by DNA damage, mammalian cells have evolved complex and interlinked pathways collectively termed the DNA damage response (DDR). In addition to attempting to repair damaged DNA, the DDR controls activation of cell-cycle checkpoints (Iliakis *et al*., 2003), modifies chromatin (Price and D'Andrea, 2013), and controls transcription (Khanna and Jackson, 2001). If the damage of the DNA is too great, the DDR can induce various forms of cell death including apoptosis and necrosis (Surova and Zhivotovsky, 2013). DNA lesions can take a variety of forms, and the DDR responds to and repairs damaged DNA using complexes and pathways specific to the lesion type and extent of damage. These range from the replacement of damaged or mismatched nucleotides using base excision repair (BER), nucleotide excision repair (NER), or mismatch repair (MMR), to the religation of double-strand breaks (DSBs) using homologous recombination (HR) pathways or non-homologous end joining (NHEJ).

DSBs are the most toxic form of lesion, of which there are an estimated ten per day per cell (Davis and Chen, 2013; Martin *et al*., 1985). The requirements for the repair of

DSBs are different for HR and NHEJ, and the fidelity of these two pathway types also varies greatly. HR uses the sister chromatid as a template for repair which allows for faithful repair of DSBs. In contrast NHEJ does not use a template and religates free ends regardless of sequence, and so is error-prone and is more likely to introduce mutations. In human cells, most DSBs are repaired by NHEJ, and, although there are times where NHEJ is necessary because the sister chromatid is not nearby or because the DSB occurred outside of the synthesis phase (S-phase) or second growth phase (G2) of the cell cycle, it is not known why mammalian cells have evolved to preferentially use NHEJ over HR in situations where both pathways are possible (Lieber, 2010; Liu *et al*., 2014). We shall now review the mechanisms of both NHEJ and HR before considering their roles during viral infection.

1.1.2 Classical NHEJ

1.1.2.1 Overview

There are two different NHEJ pathways in mammals: the classical NHEJ (C-NHEJ) pathway and the alternative NHEJ (A-NHEJ) pathway (Davis and Chen, 2013; Lieber, 2010). A-NHEJ is an MRN (comprising MRE11 (Meiotic recombination 11 homolog), RAD50, and NBS1 (Nijmegen Breakage Syndrome 1))-dependent, Ku-independent pathway that is more error-prone than C-NHEJ, resulting in chromosome translocations and large deletions (Della-Maria et al., 2011). A-NHEJ is not used as often as C-NHEJ, which is the pathway of primary interest for this thesis. C-NHEJ is initiated when the Ku70/Ku80 heterodimer recognises and binds to the free ends of DNA at a DSB in a sequence-independent manner, an event which occurs within seconds of laser-generated DSB formation (Mari *et al*., 2006). The Ku heterodimer then acts as a scaffold to recruit other C-NHEJ factors (Davis and Chen, 2013). One such factor, the DNA-dependent protein kinase (DNA-PK) catalytic subunit (DNA-PKcs), binds the Ku heterodimer in a DNA-dependent manner to form the DNA-PK complex (Gottlieb and Jackson, 1993). Subsequent autophosphorylation of DNA-PKcs regulates the early stages of C-NHEJ, depicted in **Figure 1** (Uematsu *et al*., 2007). Independently of DNA-PKcs recruitment, Ku also recruits X-ray cross-complementing protein 4 (XRCC4) and XRCC4-like factor (XLF) (Costantini *et al*., 2007; Mari *et al*., 2006; Nick McElhinny *et al*., 2000; Yano and Chen,

2008; Yano *et al*., 2008). XRCC4 does not have any known enzymatic activity in NHEJ, but may act as a scaffold for other factors such as DNA ligase IV (LIG4). Indeed, XRCC4 and XLF can form a filament which has been proposed to act as a bridge between DSB

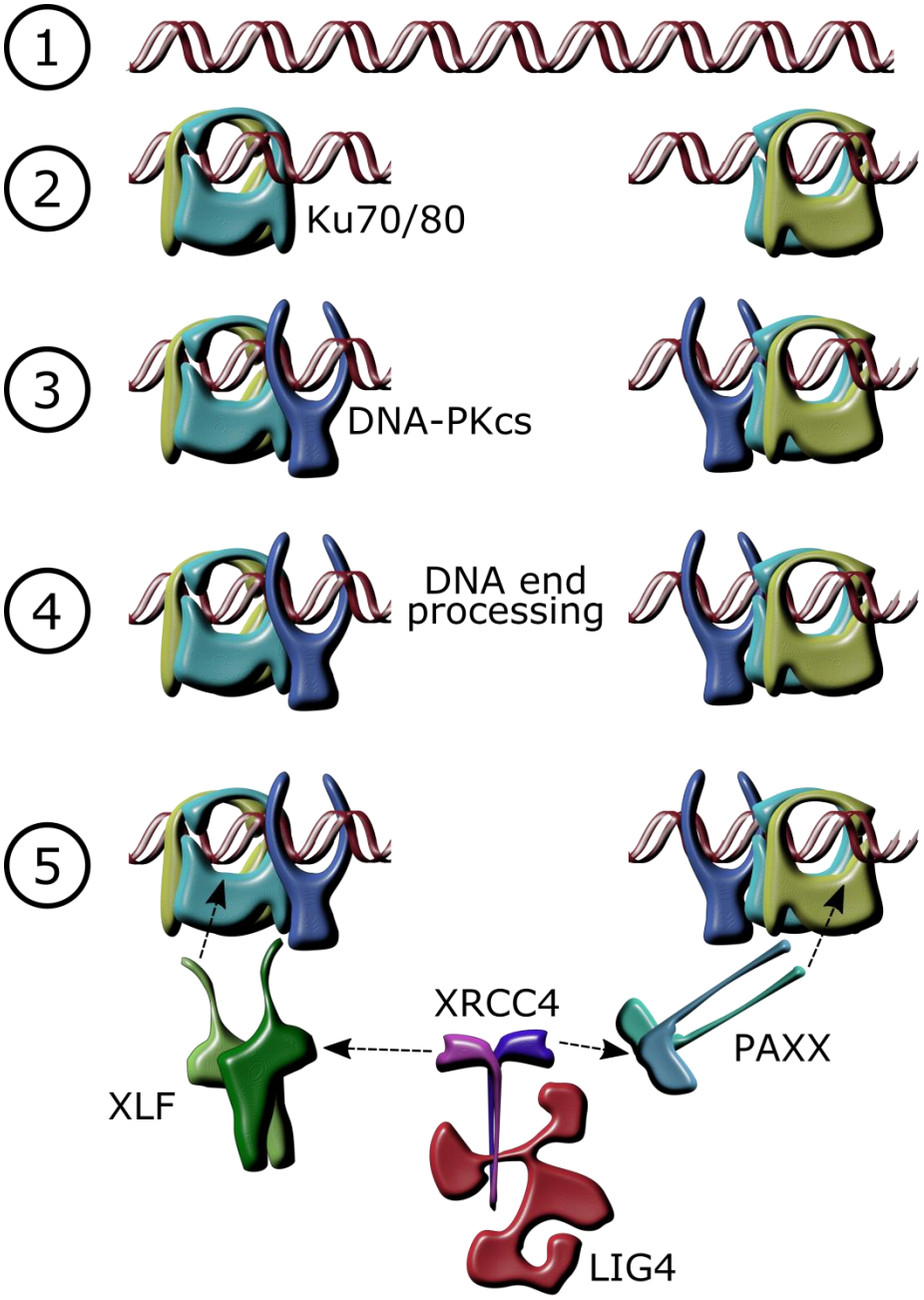

Figure 1: Schematic overview of C-NHEJ.

1) Linear DNA. **2)** A DSB caused by genotoxic damage is bound by the Ku70/80 heterodimer, which slides along the DNA to make room for subsequent complex formation. **3)** DNA-PKcs binds to the Ku70/80 heterodimer. **4)** Factors, including aprataxin, APLF, PNKP, Artemis, WRN, Polλ, and Polμ modify the ends of the DNA if necessary. **5)** PAXX and/or XLF bind Ku70/80 and recruit the XRCC4/LIG4 complex, which in turn ligates the DNA ends together.

ends. Ligation of the blunt ends of the DSB is then achieved by an XRCC4-LIG4-XLF complex. Paralogue of XRCC4 and XLF (PAXX) also binds to Ku and acts to stabilise the NHEJ complex (Ochi *et al*., 2015).

Although the above pathway can be sufficient for DSB ligation, in many cases the structure of the free ends must first be modified (Davis and Chen, 2013). 5′ or 3′ overhangs must either be cleaved off by the factors Ku (Choi *et al*., 2014; Roberts *et al*., 2010), polynucleotide kinase-phosphatase (PNKP) (Bernstein *et al*., 2005), and aprataxin (Ahel *et al*., 2006), or the complementary strand filled in to recreate the duplex structure by the DNA polymerases μ and λ. 5′ hydroxyl groups and 3′ phosphate groups must be removed by the aprataxin-and-PNK-like factor (APLF) (Li *et al*., 2011), Artemis (Ma *et al*., 2002; Povirk *et al*., 2007), and WRN (Werner Syndrome) (Perry *et al*., 2006). After these modifications, LIG4-dependent ligation can proceed as described.

Having provided the context of C-NHEJ, we shall now discuss in more detail the roles of PAXX and DNA-PKcs, the two proteins of primary interest to this thesis. Henceforth C-NHEJ shall simply be termed NHEJ.

1.1.2.2 PAXX

PAXX, also known as XRCC4-like-small protein (XLS), is the most recently-discovered NHEJ factor (Craxton *et al*., 2015; Ochi *et al*., 2015; Xing *et al*., 2015). Despite its name, it has not been determined that PAXX is a paralogue of XRCC4 and XLF in the strictest sense, but the potential misnomer arises due to its structural similarity to these proteins (**Figure 2A**). It is also true that the N-terminal sequences of these proteins have high sequence similarity, and the general domain structures are similar to that of PAXX (**Figure 2B**). PAXX also forms a homodimer in a similar manner to XLF and XRCC4 (Ochi *et al*., 2015). In contrast the C-termini of these proteins are more variable, and may help define their different functions. The long C-terminal tail of PAXX is required for binding to Ku, whilst XRCC4 binds to the N-terminal head domain (Costantini et al., 2007) and **Figure** 2**C**).

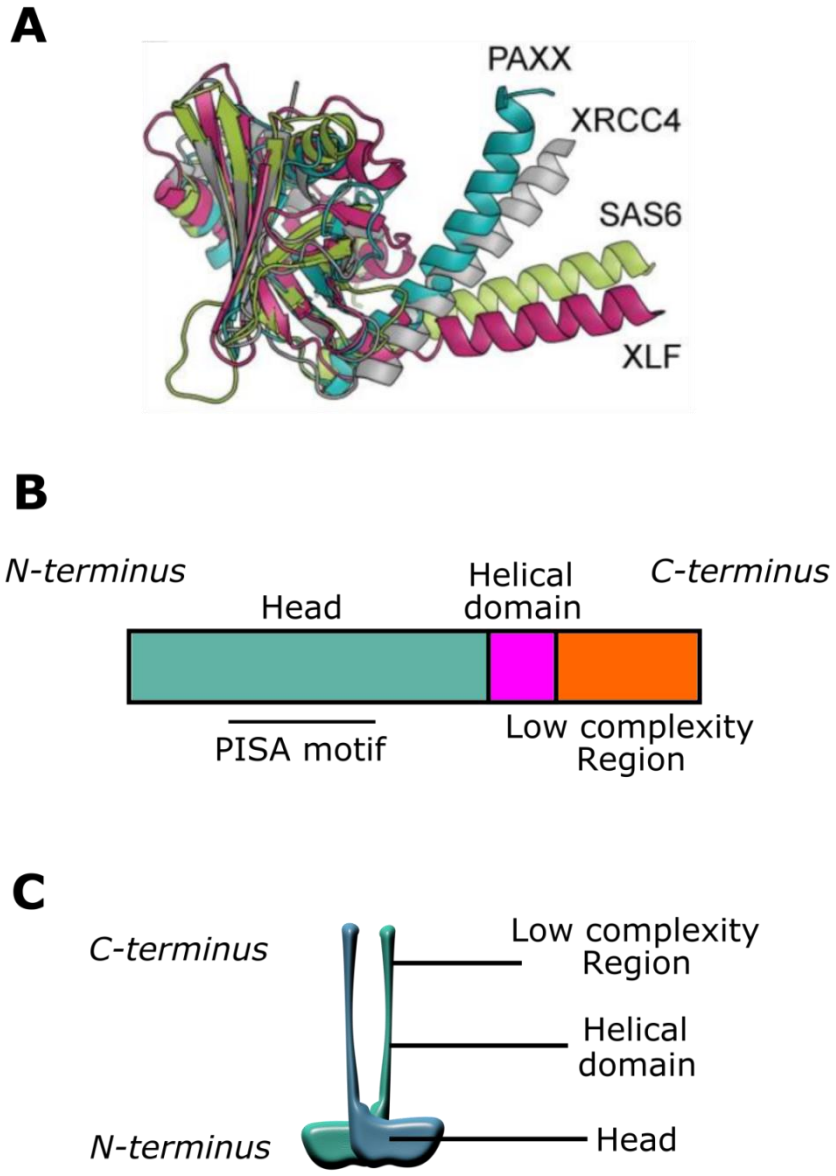

Figure 2: Schematic overview of PAXX structure.

A) Models of the structures of PAXX, XRCC4, and the other members of the XRCC4-superfamily, XLF and SAS6, are overlaid to show structural similarity. Figure from Ochi *et al*. 2015. **B)** Structure of the *PAXX* gene, including the PISA motif which is common amongst the XRCC4-superfamily. **C)** Simplified structure of PAXX showing the location of the key domains.

Following DSB formation PAXX is rapidly recruited through a direct interaction between the C-terminus of PAXX and a DNA-bound Ku heterodimer , but not with DNA itself (Ochi *et al*., 2015). PAXX stabilises the NHEJ complex, and cells without PAXX are more sensitive to induction of DSBs, although the requirement of PAXX is

dependent on the structure of the break; PAXX is redundant with XLF in the repair of 'simple' DSBs which require little processing prior to ligation, but acts in concert with XLF for 'complex' DSBs where more processing of the DNA ends is required (Chang *et al*., 2016; Kumar *et al*., 2016; Liu *et al*., 2017; Xing *et al*., 2015).

In contrast to the phylogenetically-conserved XRCC4 and XLF, PAXX is not present in most invertebrates or yeast (Xing *et al*., 2015), leading to the hypothesis that PAXX evolution has been shaped by V(D)J recombination (Mistrik and Bartek, 2015), a process required for the creation of T cell receptor diversity (described in more detail in Section 1.3.3.1). However, PAXX and XLF show functional redundancy in V(D)J recombination (Lescale *et al*., 2016; Tadi *et al*., 2016), and PAXX is not required for the production of lymphocytes (Balmus *et al*., 2016). *Paxx*$^{-/-}$ mice are viable, fertile, and grow normally despite radiosensitivity (Balmus *et al*., 2016). In contrast *Paxx*$^{-/-}$*Xlf*$^{-/-}$ mice exhibit synthetic lethality, and most embryos die before birth (Balmus *et al*., 2016; Liu *et al*., 2017).

1.1.2.3 DNA-PKcs

DNA-PKcs is a 469 kDa protein encoded by the *PRKDC* (protein kinase, DNA-activated, catalytic polypeptide) gene in humans. It was originally discovered as a regulator of SP1 (specificity protein 1) transcription complexes (Jackson *et al*., 1990), but has since been shown to have a key role in NHEJ and the DDR (Blunt et al., 1995). Although at high concentrations DNA-PKcs is able to bind to DNA in the absence of Ku (Yaneva *et al*., 1997), DNA-dependent binding to Ku is required for its serine/threonine kinase activity (Gottlieb and Jackson, 1993; Yoo and Dynan, 1999).

DNA-PKcs is a member of the phosphatidylinositol-3 (PI-3) kinase-like kinase (PIKK) family (Abraham, 2004; Hartley *et al*., 1995). This family includes two other proteins with important roles in the DDR, namely ataxia-telangiectasia mutated (ATM) and ATM and RAD3-related (ATR). ATM is responsible for orchestrating HR (Section 1.1.3), while ATR mediates ATR-CHK1 (checkpoint kinase 1) pathways in response to regions of single-stranded DNA (ssDNA) next to double-stranded DNA (dsDNA) (Maréchal and Zou, 2013). The N-terminus of the PIKK family proteins contains Huntington-elongation-A-subunit-TOR (HEAT) repeats which are thought to act as

protein-protein interaction interfaces and allow flexibility in the arms of the N-terminal pincer shape (**Figure 3A**) (Perry and Kleckner, 2003; Sibanda *et al.*, 2010). The largely α-helical N-terminus of DNA-PKcs also contains a leucine rich region (LRR) between amino acid residues 1,503 and 1,602 which has been attributed to giving DNA-PKcs its affinity for DNA (Gupta and Meek, 2005). This region is situated within the centre of the pincer shape formed by the N-terminus and is thought to reside in the channel through which the DNA passes (**Figure 3B**) (Sibanda *et al.*, 2010; Williams *et al.*, 2008). The C-terminal region is positioned on top of the N-terminal pincer. *In vitro* experiments determined that the Ku heterodimer binds to the DNA-PKcs amino acid residues 3,002-

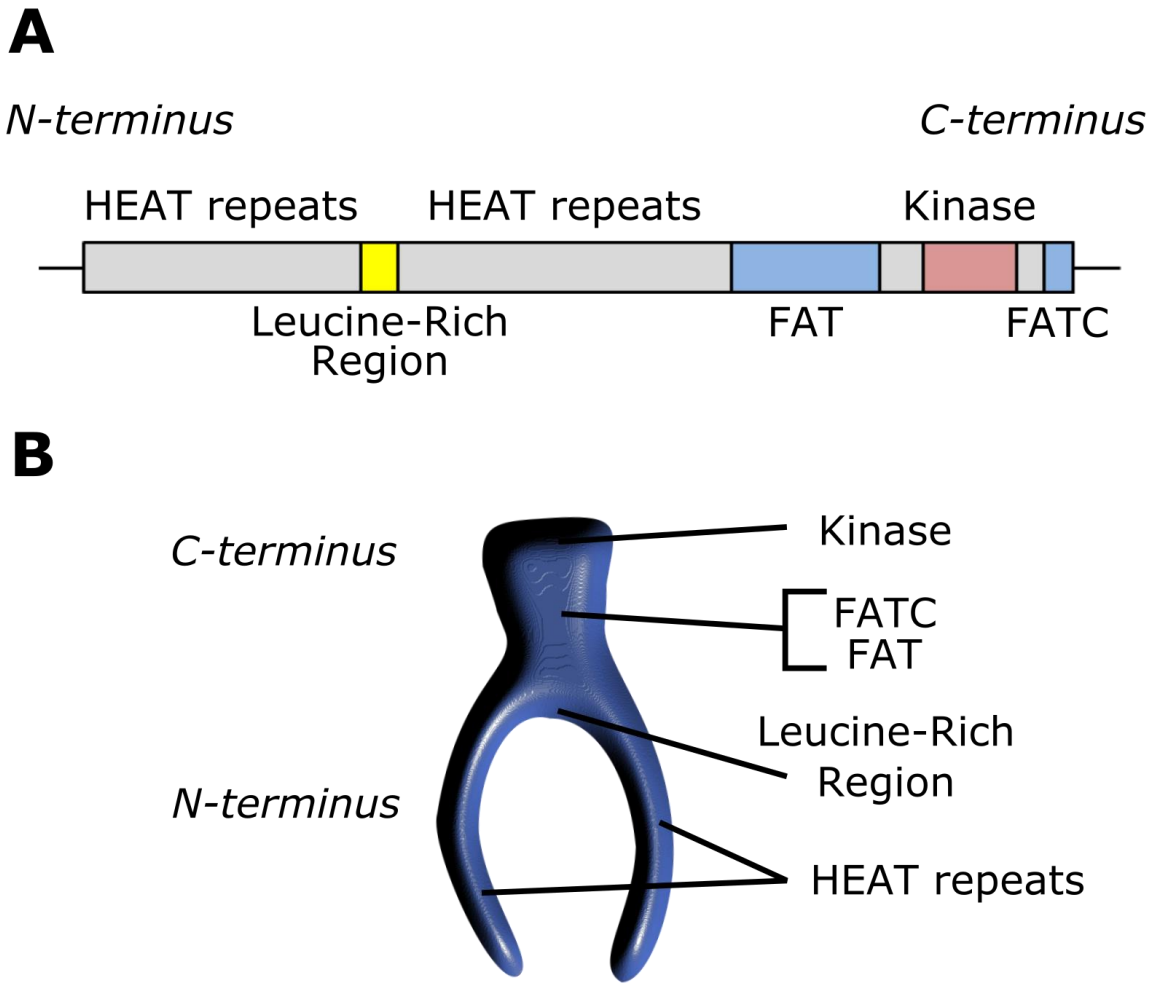

Figure 3: Domains of the *PRKDC* gene and DNA-PKcs protein

A) A map of *PRKDC* showing some of the key domains is shown. **B)** Some of the key domains of DNA-PKcs are mapped to a simplified cartoon of the structure of DNA-PKcs.

3,850 within the C-terminus (Jin *et al*., 1997), but the N-terminus is also required for the interaction with Ku (Davis *et al*., 2013). Structurally, the FAT (focal adhesion targeting) and FATC (FRAP, ATM, TRRAP C-terminal) domains are adjacent to the kinase domain and probably regulate the kinase activity of DNA-PKcs following DNA binding and mediate binding to other proteins (Lempiäinen and Halazonetis, 2009; Rivera-Calzada *et al*., 2005).

Although DNA-PKcs is not required for the recruitment of XRCC4 and XLF during NHEJ, it is critical for the NHEJ process (Dobbs *et al*., 2010; Kurimasa *et al*., 1999a). In the DDR, DNA-PKcs phosphorylates a large number of proteins including p53 (Lees-Miller *et al*., 1992), the Ku heterodimer (Chan *et al*., 1999; Douglas *et al*., 2005), H2AX (histone 2A variant) (Mukherjee *et al*., 2006; Stiff *et al*., 2004), XLF (Yu *et al*., 2008), XRCC4 (Lee *et al*., 2004; Yu *et al*., 2003), Artemis (Ma *et al*., 2005), LIG4 (Wang *et al*., 2004), and WRN (Perry *et al*., 2010; Yannone *et al*., 2001). There are also over 40 autophosphorylation sites identified within DNA-PKcs (Dobbs *et al*., 2010), and it has been proposed that the autophosphorylation of different sites has different outcomes, not only in DNA-PK-mediated DNA repair, but also in determining DNA repair pathway choice (Cui *et al*., 2005).

For the purpose of this thesis we are primarily interested in the ability of DNA-PKcs to restrict herpes simplex virus 1 (HSV-1) infection. DNA-PKcs is known to sense cytoplasmic DNA species and induce an innate immune response (Section 1.3.1.2, Ferguson *et al*., 2012), but the importance of this during HSV-1 infection has not been fully characterised and there may be mechanisms outside of innate sensing which contribute to this restriction, such as interfering with replication of the viral genome (Section 1.2.6).

DNA-PKcs also has functions in cell death, most notably apoptosis. DNA-PKcs and Ku contribute to the induction of apoptosis following shortening of the telomeres (Espejel *et al*., 2002a, 2002b), and inhibition of DNA-PK results in a diversion from apoptosis to necrosis following cisplatin treatment (Sand-Dejmek *et al*., 2011). DNA-PKcs and ATM differentially phosphorylate p53; whereas DNA-PK promotes apoptosis, ATM induces cell-cycle arrest (Wang *et al*., 2000). However, DNA-PK can also inhibit

apoptosis by activating Akt (Stronach *et al*., 2011) or stabilising apoptotic regulators such as receptor-interacting protein 1 (RIP1) and inhibitor of apoptosis proteins (IAPs) (Wang *et al*., 2017). DNA-PKcs is degraded during apoptosis (McConnell *et al*., 1997; Song *et al*., 1996), and it has been hypothesised that this is to suppress pro-survival signals from DNA-PK (Bernstein *et al*., 2002). DNA-PKcs has also been implicated in necroptosis (Baritaud *et al*., 2012).

DNA-PKcs has multiple other functions outside of NHEJ and viral restriction, and although coverage of the full extent of its roles is beyond the scope of this thesis, we will briefly address some of the salient points. DNA-PKcs activity has repeatedly been linked to various cancers, and for that reason there has been a lot of research into the inhibitors of DNA-PKcs for their potential uses as cancer therapeutics (Curtin, 2012; Goodwin and Knudsen, 2014). For instance, upregulation of DNA-PKcs is linked to resistance to radiotherapy and DNA damaging agents used in cancer treatment (Beskow *et al*., 2009; Shintani *et al*., 2003). Interestingly, even in the absence of DNA-damaging agents, DNA-PKcs expression correlates with poor prognosis for a number of cancer types (Goodwin and Knudsen, 2014; Hosoi *et al*., 2004; Tonotsuka *et al*., 2006; Xing *et al*., 2008). DNA-PK is also activated by hypoxia in the absence of DSBs, and does not result in subsequent recruitment of XRCC4, XLF, and LIG4 (Bouquet *et al*., 2011). In this context DNA-PK promotes cellular survival during hypoxia by positively regulating hypoxia-inducible factor-1 alpha (HIF-1α), a transcription factor which regulates genes required for adaptation to hypoxic conditions (Kang et al., 2008). DNA-PK also has roles in cellular metabolism, for example in the regulation of lipogenesis in response to insulin (Wong *et al*., 2009), and by phosphorylating AMP-activated protein kinase (AMPK), a master switch controlling the cellular response to changing energy levels (Amatya *et al*., 2012). In addition the DNA-PK components localise to telomeres and are essential for telomere capping (Bailey *et al*., 1999; d'Adda di Fagagna *et al*., 2001; Gilley *et al*., 2001; Goytisolo *et al*., 2001).

1.1.3 Homology-mediated repair

Homology-mediated repair is the umbrella term for DNA repair pathways which repair lesions using a homologous sequence. These pathways include homologous

recombination (HR), single-strand annealing (SSA), and microhomology-mediated end joining (MMEJ). HR is the main pathway used, and is generally the main homology-mediated pathway of interest during viral infection (Section 1.2).

HR (reviewed by Heyer *et al*. 2010; Maréchal & Zou 2013) is initiated when the MRN complex senses a DSB. MRN then activates ATM, the PIKK responsible for mediating HR, which has a large number of phosphorylation targets including H2AX, a histone variant found in 2 - 25 % of nucleosomes which helps mediate DSB DNA repair (Rogakou et al., 1998) Phosphorylated H2AX (γH2AX) recruits downstream effectors to the lesion site. Replication protein A 1 (RPA1) binds to single-stranded DNA (ssDNA) to remove secondary structures and allow for RAD51 (Ras associated with diabetes 51) filament assembly which is responsible for performing a search for homology and DNA strand invasion (Heyer *et al*., 2010). At this point, the repair machinery has the choice of three sub-pathways to complete the repair, coverage of which is beyond the scope of this thesis (reviewed Heyer *et al*. 2010).

HR generally results in the activation of the ataxia telangiectasia and RAD3 related (ATR) pathway because ATR, another PIKK, is activated by ssDNA and some of the phosphorylated substrates of ATM. ATR acts in conjunction with ATM to regulate DNA repair, recruits ATRIP (ATR interacting protein) to ssDNA-bound RPA1, and activates cell checkpoint kinases to halt the cell cycle (Maréchal and Zou, 2013). ATR also activates the Fanconi anaemia (FA) pathway which repairs DNA interstrand crosslinks, coordinates HR and SSA, and suppresses NHEJ (Adamo *et al*., 2010; Ceccaldi *et al*., 2016).

The SSA pathway is more error-prone than HR because it promotes recombination between tandemly-repeated DNA sequences when a DSB forms between two repeated sequences, and therefore introduces a deletion of the region between the repeats (Bhargava *et al*., 2016). SSA shares some components with other pathways, such as RAD52 (also used in A-NHEJ and HR), and ERCC1/XPF (also involved in MMEJ) (Bhargava *et al*., 2016).

The final pathway, MMEJ, is perhaps the most poorly understood of the three. MMEJ is very error-prone because in mammalian cells it only requires one nucleotide of

homology (Sfeir and Symington, 2015). For this reason MMEJ might only be a back-up pathway used when HR is not present (Sfeir and Symington, 2015; Wang and Xu, 2017). Perhaps of greatest consequence to our work is the involvement of MRN, a complex also involved in HR and which is often targeted during viral infection (Section 1.2). Ligation is achieved by Ligases I and III.

We have briefly reviewed how NHEJ and HR is coordinated following DSB formation, providing the background required to understand how DNA repair factors function in other contexts. This thesis is primarily concerned with the role of DNA repair proteins during viral infection, and the next section will discuss key examples of interactions between DNA repair proteins and DNA viruses during infection.

1.2 DNA repair proteins and virus infection

1.2.1 Introduction

Viruses cannot survive independently of a host and require host machinery during their infection cycle, creating philosophical debate over whether viruses should be considered as alive (Koonin and Starokadomskyy, 2016). Viruses rely upon some aspects of the DDR during replication of the viral genome and activate them accordingly (Shah and O'Shea, 2015; Sinclair *et al*., 2006; Turnell and Grand, 2012). However, given the necessity to expose the viral genome during replication, it is perhaps unsurprising that the nucleic acids can activate the DDR and, in addition to DNA repair proteins which can benefit viral infection, other DNA repair factors can be activated which act to restrict viral infection (Shah and O'Shea, 2015; Sinclair *et al*., 2006; Turnell and Grand, 2012). The term 'restriction' is used in this context to describe a factor which reduces the efficiency of viral infection.

This section will provide an insight of our current understanding of the interactions between DNA repair proteins and viral infection. Viruses requiring the DDR for replication tend to be those which undergo integration into the host genome or genome modifications. Furthermore, although RNA viruses are also affected by DDR proteins, most is known in the context of DNA viruses and retroviruses. As this context is also of greater relevance to this research, we shall focus primarily on DNA viruses. It is not

intended to be an exhaustive review, but will give important examples. It also stops short of describing the role of DNA repair proteins in the immune system, which is instead covered in Section 1.3.

1.2.2 Adenoviruses and DNA repair

Adenoviruses are non-enveloped viruses and which replicate their linear, ~36 kb dsDNA genomes within the host nucleus (Hoeben and Uil, 2013). These DNA genomes activate the DDR, and so they must inactivate DNA repair proteins to inhibit the ligation of viral genomes into concatemers that are too large to be packaged (Forrester *et al*., 2011; Stracker *et al*., 2002). During adenovirus infection, MRE11 and RAD50 are degraded by the E4 34k/E1b 55k complex, and MRN recruitment to replication centres is inhibited by E4orf3 expression, together preventing signalling of ATM and ATR pathways (Carson *et al*., 2003, 2009; Stracker *et al*., 2002). Interestingly, etoposide-induced DSBs in the cellular genome sequester MRN and allow for infection with adenovirus unable to degrade MRN (Shah and O'Shea, 2015). In addition adenoviruses degrade topoisomerase-IIβ–binding protein 1 (TOPBP1) to prevent ATM/ATR signalling (Blackford *et al*., 2010). Strangely, despite the numerous mechanisms exploited by adenoviruses to inhibit DNA repair proteins, they also recruit a number of DNA repair proteins to viral replication centres, including ATR, ATRIP, RAD9, and RAD17, and replication protein A 32 (RPA32) (Stracker *et al*., 2005; Turnell and Grand, 2012). The reason for recruitment and inhibition of the same proteins has not been confirmed, but it is possibly because they have both beneficial and restrictive roles (Turnell and Grand, 2012). However, it is important to note that the exact substrates targeted during adenovirus infection vary between serotypes (Forrester *et al*., 2011).

Adenoviruses also target NHEJ proteins. E1B55K/E4orf6 prevents dephosphorylation of threonine 2609 of DNA-PKcs, reducing DSB repair probably by preventing DNA-PK disassociation from the DSB and preventing LIG4 from accessing the break (Hart *et al*., 2004). Although E1B55K/E4orf6 do not affect the kinase activity of DNA-PK (Hart *et al*., 2004), they may also target DNA-PK due to its ability to restrict viral alternative RNA splicing (Törmänen Persson *et al*., 2012). In addition, E4 34k and E1b 55k target another NHEJ protein, DNA LIG4, for degradation (Baker *et al*., 2007).

Finally, Protein phosphatase 2A (PP2A) is inhibited by adenovirus E4orf6 to maintain γH2AX phosphorylation and induce caspase-dependent and –independent cell death (Hart *et al*., 2007).

1.2.3 Human papillomavirus and DNA repair

Human papillomaviruses (HPVs) are non-enveloped and have relatively short, circular dsDNA genomes. As with all viruses, the infection cycle of HPVs is closely linked to DNA repair proteins, but there has been a lot of research on this topic and a full review is beyond the scope of this thesis. Instead we shall focus on key points and direct readers to previous reviews (McKinney *et al*., 2015; Pancholi *et al*., 2017; Turnell and Grand, 2012).

The HPV proteins E6 and E7 induce DNA damage and enable integration of foreign DNA into the host genome, activities which may contribute to HPV-induced genomic instability, DDR activation, and cancer progression (Moody and Laimins, 2009). Viral genome replication in the suprabasal layers of the skin is dependent on the E7-induced activation of ATM, which may function to promote replication by inducing G2/M cell-cycle arrest (Moody and Laimins, 2009, 2010). Interestingly the dependency on ATM is cell-type specific; although ATM is constitutively activated in undifferentiated keratinocytes, its inhibition does not affect HPV infection (Moody and Laimins, 2009).

HPV-induced activation of DNA repair proteins extends beyond the requirement for G2/M arrest. The MRN component NBS1 is required for productive replication of HPV31 for an unidentified reason that is independent of cell cycle control, and HPV induces an increase in the levels of the MRN complex *via* E7 (Anacker *et al*., 2014). E7 also activates the FA pathway, and FA deficiency increases the risk of genome instability and HPV-induced carcinogenesis (zur Hausen, 2002; Kutler *et al*., 2003; Moody and Laimins, 2010).

In contrast to HR factors, the role of NHEJ in HPV infection has not been extensively studied. However, DNA-PK is likely to be detrimental to HPVs because HPV^+ cells from head and neck carcinomas are deficient in DNA-PK expression (Weaver *et al*., 2015). Interestingly, head and neck cancer cell lines not only have decreased NHEJ-directed

repair, but also have reduced repair by HR (Bol, 2015). This suggests that HPV exploits the beneficial HR factors, and restricts other components which may be detrimental.

It is interesting to consider that the HPV genome is circularised, and as such will not have exposed DNA ends most of the time. We have previously hypothesised that this is to avoid being detected by innate immune DNA sensors (Trigg and Ferguson, 2015), but this may also be to avoid triggering detrimental DDRs.

1.2.4 Polyomaviruses and DNA repair

The human polyomaviruses are generally benign, but some can cause complications in immunocompromised individuals (DeCaprio and Garcea, 2013). Although highly divergent, polyomaviruses have a similar genome structure comprising a single circular dsDNA genome of ~5.2 kb in length (DeCaprio and Garcea, 2013).

The canonical polyomavirus, Simian virus (SV)40, expresses large T (LT) antigen which activates ATM for efficient genome replication and infectious virus production (Dahl *et al*., 2005; Dey *et al*., 2002). ATM activity inhibits NHEJ by inhibiting recruitment of DNA-PK, and thereby prevents polyomavirus genome concatemerisation (Sowd *et al*., 2014).

JC virus (JCV) is another member of the polyomavirus family, and it expresses agnoprotein, a factor which reduces expression of the Ku heterodimer and induces Ku70 relocalisation away from the viral genome (Darbinyan *et al*., 2004). SV40, another polyomavirus, induces the degradation of MRN components *via* LT antigen (Zhao *et al*., 2008) and uses ATM to prevent NHEJ (Sowd *et al*., 2014).

1.2.5 Retroviruses and DNA repair

Retroviruses are enveloped RNA viruses which are of great medical importance. Retroviruses must integrate their genome into the host genome as a DNA provirus to replicate (Hayward, 2017), and almost half of human chromosomal DNA either originated from viral integration or have virus-like sequences (Blinov *et al*., 2017). Unsurprisingly these DNA species and the integration event stimulate the DDR. DNA-PK is required for retroviral integration and prevention of apoptosis (Cooper *et al*., 2013;

Daniel *et al*., 1999; Li *et al*., 2001), and replication is delayed in cells depleted of Ku (Jeanson *et al*., 2002). ATM is activated during human immunodeficiency virus (HIV) integration into the human genome, and small molecule-mediated inhibition of ATM suppresses replication of HIV and increases cell death in infected cells (Lau *et al*., 2005). HIV activates the ATR pathway using Vpr (Viral protein R), possibly to induce G2/M cell-cycle arrest (Lai *et al*., 2005; Roshal *et al*., 2003; Zimmerman *et al*., 2004).

1.2.6 HSV-1 and DNA repair

Herpes simplex virus 1 (HSV-1) has a 152 kbp dsDNA genome which replicates in the nucleus. HSV-1 is the viral model used in this thesis, and so an in-depth introduction to its infection cycle and structure can be found in Section 1.4. One of the reasons that HSV-1 was selected for use in our experiments is that it is already well characterised, and a great deal is already known about HSV-1 and DNA repair proteins. This has been comprehensively reviewed in the literature (Lilley *et al*., 2005; Smith and Weller, 2015; Turnell and Grand, 2012), and this section will more briefly address some of the most pertinent points.

HSV-1 genome replication occurs in the nucleus where it can access beneficial DNA repair factors, although this also exposes the genome to factors which may be deleterious. HSV-1 overcomes this by activating and inhibiting factors, as required (**Figure 4**). The HSV-1 genome is unusual in that it contains gaps and nicks (Section 1.4.3), and these contribute to DDR stimulation along with the free ends of the HSV-1 genome (Smith *et al*., 2014). These gaps and nicks trigger DNA-PK activity, and the HSV-1 infected cell protein 0 (ICP0)-induced degradation of DNA-PKcs is required to relieve the DNA-PK-dependent restriction of viral infection caused by these gaps (Lees-Miller *et al*., 1996; Parkinson *et al*., 1999; Smith *et al*., 2014). Indeed, *PRKDC*$^{-/-}$ human malignant glioma cells produce a higher titre of infectious HSV-1 after two days of infection than their wildtype (WT) counterparts (Parkinson *et al*., 1999). In addition, Ku-deficient murine embryonic fibroblasts (MEFs) yield almost 50-times more infectious HSV-1 (Taylor and Knipe, 2004). The HSV-1 genome also has a single-nucleotide 3' overhang (Mocarski and Roizman, 1982) which may need to be processed by APLF (Section 1.1.2) before the recruitment of other NHEJ factors can occur (Davis and Chen, 2013). To our

knowledge the role of APLF in the context of HSV-1 infection has not been studied. Interestingly, although the NHEJ components Ku and DNA-PKcs restrict HSV-1 infection, other NHEJ factors promote HSV-1 genome replication. Knockdown of LIG4 or XRCC4 delays and reduces the production of infectious HSV-1, probably because these proteins are required for the formation of endless replication intermediates (Muylaert and Elias, 2007). This is despite the fact that LIG4 inhibits HR (Kurosawa *et al.*, 2013).

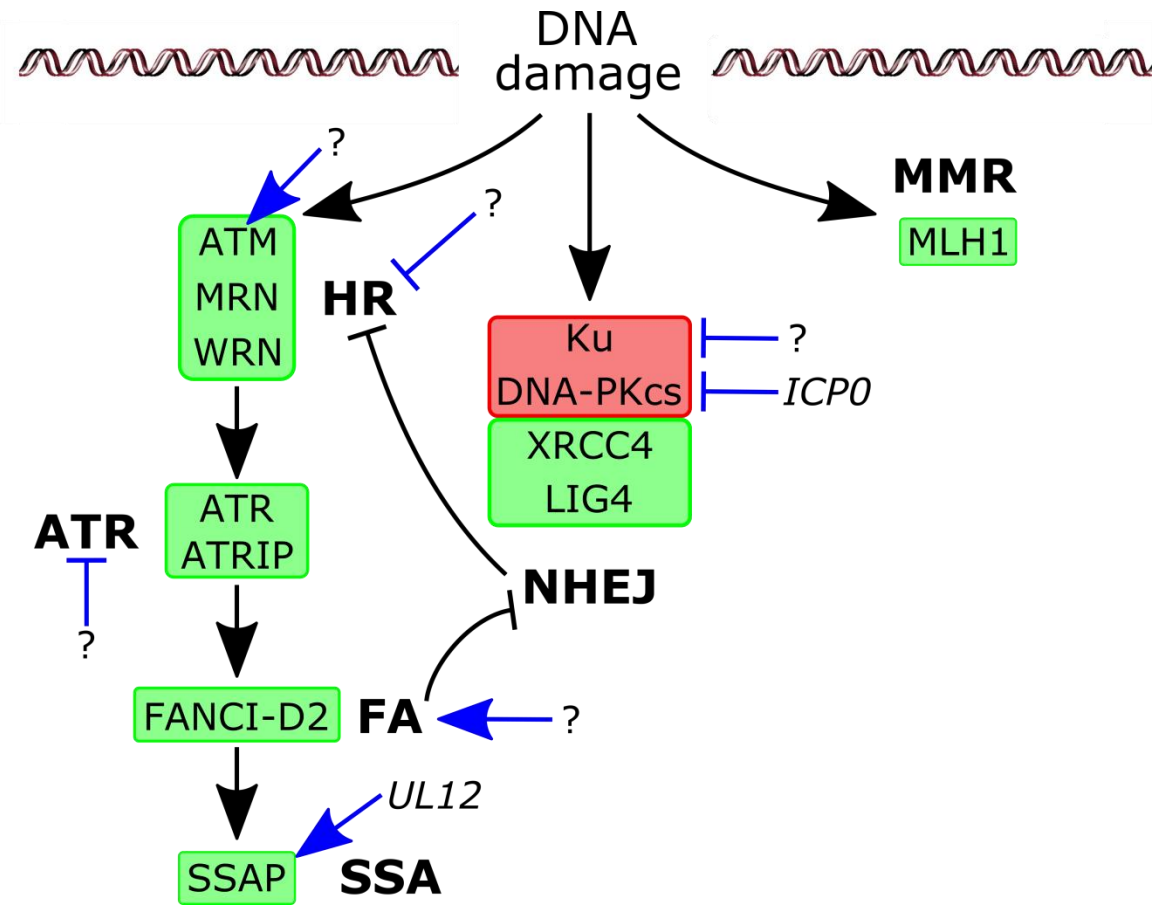

Figure 4: Interactions between HSV-1 and the DDR.

Following DNA damage multiple DDR pathways (black arrows) are activated, including HR, NHEJ, and MMR, and these can subsequently activate (black arrows) or inhibit (black blunt-ended line) other DDR pathways. Many proteins in these pathways are beneficial to HSV-1 infection (green boxes), but some are detrimental (red box). HSV-1 expresses proteins (italics) which activate (blue arrow) or inhibit (blue blunt-ended line) these proteins *via* different mechanisms (not shown). Question marks indicate undefined HSV-1 interactions.

In addition to the activation of DNA repair proteins by the HSV-1 genome, HSV-1 proteins activate beneficial factors. The FA pathway is activated by HSV-1 during infection, and defects in FA result in impaired HSV-1 genome replication and gene transcription (Karttunen *et al*., 2014). Interestingly, inhibition of DNA-PKcs partially alleviates restriction caused by FA defects, leading to the proposal that FA-mediated inhibition of DNA-PKcs may be important (Karttunen *et al*., 2014). The FA pathway is also able to stimulate SSA, and SSA is activated by the HSV-1 recombinase complex component, alkaline nuclease (UL12), leading to suggestions that SSA is the homology-mediated repair pathway used by HSV-1 (Schumacher *et al*., 2012). This was established using chromosomally-integrated GFP correction assays which also showed that HR, NHEJ, and MMEJ were inhibited (Schumacher *et al*., 2012).

DNA mismatch repair (MMR) pathway factors localise to the HSV-1 replication compartments, and are required for efficient replication, probably due to defects in immediate early gene expression in the absence of the MMR factor MutL homologue 1 (MLH1) (Mohni *et al*., 2011). Infected cell protein 0 (ICP0) induces the degradation of many components of nuclear bodies, but MLH1 protein levels are unaffected by ICP0.

The role of DNA repair proteins in HSV-1 infection is not always straightforward. ATR signalling is inhibited despite the fact that ATR and ATRIP are both recruited to the HSV-1 replication centre and are beneficial for HSV-1 infection (Mohni *et al*., 2010; Wilkinson and Weller, 2006). Similarly, although chromosomally-integrated GFP correction assays suggest that HR is repressed (Schumacher *et al*., 2012), HSV-1 production is deficient in cells lacking MRN and WRN (Balasubramanian *et al*., 2010; Smith and Weller, 2015). Investigations into the importance of ATM are inconclusive; some studies report that HSV-1 infection activates ATM, but ATM inhibition does not have a large effect on HSV-1 genome replication (Gregory and Bachenheimer, 2008; Shirata *et al*., 2005), while others conclude that ATM defects reduce production of HSV-1 (Alekseev *et al*., 2014; Smith and Weller, 2015).

The role of exogenous DNA damage on herpesvirus infection is also uncertain. Although exogenous DNA damage induction reduces the infectivity of murine gammaherpesvirus 68 by inducing an antiviral state (Mboko *et al*., 2012), there is

evidence that DNA damage induced by topoisomerase inhibitors can promote HSV-1 immediate early gene expression (Volcy and Fraser, 2013).

Finally, it is interesting to consider that the accumulation of DNA lesions reported in neurodegenerative diseases may explain the correlation observed between HSV-1 infection and conditions such as Alzheimer's Disease (De Chiara *et al*., 2012; Itzhaki, 2014). Indeed, HSV-1 infection restricts DNA repair in rat cortical neurones (De Chiara *et al*., 2016). Furthermore, HSV-1 infection induces ROS (reactive oxygen species) which could also contribute to the lesion formation and inflammation observed in neurodegenerative disease (Gonzalez-Dosal *et al*., 2011).

1.3 DNA repair proteins and the immune system

1.3.1 DDR factors and the sensing of foreign DNA

1.3.1.1 Overview of DNA sensing

The innate immune system has evolved pattern recognition receptors (PRRs) to recognise pathogen-associated molecular patterns (PAMPs) and damage-associated molecular patterns (DAMPs) that initiate appropriate transcriptional responses. In the context of virus infection, recognition of viral nucleic acids is essential for initiating a type-1 interferon (IFN-I) response and inflammatory processes, responses which create an anti-viral environment and recruit leukocytes (Mansur *et al*., 2014). The innate sensing of DNA by these PRRs also has consequences for parasite and bacterial infection, carcinogenesis, and vaccine development (Kobiyama *et al*., 2013; Mansur *et al*., 2014; Woo *et al*., 2015).

The first PRR shown to recognise DNA was Toll-like receptor (TLR) 9, which recognises CpG DNA in endosomal compartments (Hemmi et al., 2000). It was thought that TLR9 might be the only DNA sensor, but further experiments showed this not to be the case. Cytoplasmic DNA is usually kept at low levels in the cell by nucleases such as the lysosomal endonuclease DNase II (Evans and Aguilera, 2003). In macrophages, DNaseII is responsible for digesting the DNA from phagocytosed apoptotic cells and in DNase knock-out mice DNA accumulates in macrophages and induces interferon-β (IFNβ)-driven immunopathology causing the mice to die *in feto* (Krieser et al., 2002). Unexpectedly, crossing *DNaseII*$^{-/-}$ mice with *TLR3*$^{-/-}$ or *TLR9*$^{-/-}$ mice did not prevent CXCL10 and IFNβ expression in fetal liver macrophages and failed to rescue the embryonic-lethal DNaseII knock-out phenotype (Okabe et al., 2005). MyD88 and TRIF are adaptor proteins which interact with activated TLRs and initiate down-stream signalling, and every TLR able to respond to nucleic acids requires one of them (McGettrick and O'Neill, 2004), but *MyD88*$^{-/-}$/*TRIF*$^{-/-}$ mice also continued to express CXCL10 and IFNβ, which suggested that there is a TLR-independent DNA sensing pathway (Okabe et al., 2005).

A large number of cytoplasmic DNA sensors have since been proposed (Unterholzner, 2013). Most recent research has focused on cyclic GMP-AMP (guanosine monophosphate–adenosine monophosphate) synthase (cGAS) which activates STING via the secondary signalling molecule circular guanidine-adenosine monophosphate (cGAMP) (Ablasser *et al*., 2013; Sun *et al.*, 2013; Wu *et al.*, 2013).

Cytosolic DNA sensing pathways converge at an adaptor protein known as the stimulator of interferon genes (STING) (Surpris and Poltorak, 2016). Once activated, STING translocates to punctate perinuclear structures and recruits tank binding kinase 1 (TBK1), which in turn phosphorylates and activates an IFN regulatory factor (IRF)3-dependent response (Ishikawa *et al.*, 2009; Saitoh *et al.*, 2010; Stetson and Medzhitov, 2006; Tanaka and Chen, 2012). STING has also been shown to activate the transcription factor NF-κB, although by a mechanism that is less clear (Abe and Barber, 2014).

The activation of IRF3 and NF-κB results in the expression of IFNI and cytokines which mediate antiviral responses in bystander cells (Schoggins and Rice, 2011). The antiviral state is achieved through the expression of interferon-stimulated genes (ISGs), of which there are a vast number of varying potency. These restrict viral infection by targeting different stages of the viral infection cycle or by enhancing the propagation of the antiviral response (Schoggins and Rice, 2011). Tetherin, for example, is an ISG which inhibits viral release from the cell surface (Perez-Caballero *et al*., 2009), while protein kinase R is an example of an ISG which promotes the antiviral state by stabilising IFN mRNA (Schulz *et al.*, 2010). IFNs and chemokines also influence the adaptive immune response. Chemokines attract leukocytes and drive their maturation (Jin et al., 2008), while IFNs and cytokines increase expression of factors such as MHC (major histocompatibility complex) which are important in the activation of lymphocytes (Grabowska et al., 1990; Panek and Benveniste, 1995).

Interestingly, many of the PRRs important in the recognition of foreign cyt DNA are also DDR factors (Trigg and Ferguson, 2015). As might be expected, the recognition of mislocalised self DNA or damaged self DNA is also able to induce an antiviral response, although it is not yet clear whether the same pathways are stimulated (reviewed Section 1.3.2). Therefore, it stands that the DNA damage response has considerable implications

in the DNA-induced stimulation of the immune system, and here we review the functions of DDR factors in the innate sensing of exogenous DNA.

1.3.1.2 DNA-PK

It has long been established that DNA-PK detects damaged DNA in the nucleus, but it also functions to sense cytoplasmic DNA and induce an innate immune response. Karpova *et al.* reported that Sendai virus infection activates DNA-PK via an unknown mechanism, and that this subsequently interacts with and activates the innate immune transcription factor, interferon regulatory factor 3 (IRF3) (Karpova *et al*., 2002). In 2012 Ferguson *et al.* showed that DNA-PK detects cytoplasmic DNA and activates the stimulator of interferon genes (STING), TANK-binding kinase 1 (TBK1), and IRF3 (Ferguson *et al*., 2012). They showed that DNA-PK immunoprecipitates with exogenous cytoplasmic DNA, and that DNA-PK localises to vaccinia virus (VACV) replication factories. Depletion of DNA-PK diminishes the IRF3-dependent and p65-independent induction of interferon (IFN) transcription in response to DNA, but not to RNA, and this is independent of the kinase activity of DNA-PK.

More recently it has been demonstrated that DNA-PK is a component of a ribonuclear complex termed the HEXIM1-DNA-PK-paraspeckle components ribonucleoprotein complex (HDP-RNP) (Morchikh *et al*., 2017). The core components of the complex are hexamethylene bis-acetamide-inducible protein 1 (HEXIM1), and the long non-coding RNA, NEAT1 (nuclear enriched abundant transcript 1). The HDP-RNP also contains the paraspeckle proteins SFPQ (splicing factor proline- and glutamine-rich), NonO (non-POU domain-containing octamer-binding protein), PSPC1 (paraspeckle component 1), RBM14 (RNA binding motif protein 14), and Matrin3. Morchikh *et al*. showed that the HDP-RNP interacts with a previously-identified DNA sensor, cyclic-GMP-AMP synthase (cGAS), and that HDP-RNP is required for the activation of the cGAS-STING-IRF3 pathway. DNA-PK has further links to immunity due to its role in V(D)J recombination during lymphocyte production (discussed in more detail in Section 1.3.3.1) (Blunt *et al*., 1995; Kirchgessner *et al*., 1995; Kurimasa *et al*., 1999b).

DNA-PK has also been shown to sense hepatitis B virus (HBV) infection (Li *et al*., 2016). However, unlike the mechanisms already described, STING and IRF3 are not reported to be involved in the signalling pathways activated, and instead DNA-PK assembles PARP (Poly ADP ribose polymerase) at the site of recognition and signals *via* IRF1 to induce expression of CCL3 (chemokine (C-C motif) ligand 3) and CCL5, two ligands important in hepatitis (Li *et al*., 2016).

1.3.1.3 IFI16

Interferon gamma inducible protein (IFI16) is a human DDR factor and, as a member of the PYHIN protein family, contains a pyrin domain and two DMA-binding HIN (hematopoietic, interferon-inducible, nuclear) domains (Cridland *et al*., 2012). AIM2 (absent in melanoma 2) is also a PYHIN protein, and upon binding dsDNA it recruits ASC (apoptosis-associated speck-like protein containing a caspase activation and recruitment domain) and activates caspase-1 (Hornung *et al*., 2009). During HSV-1 infection, IFI16 is stimulated and relocalises from the nucleus to the cytoplasm, and cooperates with cGAS to induce IFNβ in an ASC-independent, STING-dependent manner (Almine *et al*., 2017; Orzalli *et al*., 2012; Unterholzner *et al*., 2010). There is evidence that IFI16 can also associate with ASC to form an inflammasome and induce IL-1β maturation (Johnson *et al*., 2013). Indeed, IFI16 and AIM2 upregulation and inflammasome formation have been linked to inflammatory bowel disease (Vanhove *et al*., 2015). Interestingly, another DDR factor, BRCA1 (breast cancer 1), may be required for IF16-dependent responses to DNA sensing (Dutta *et al*., 2015).

1.3.1.4 MRE11 and RAD50

MRE11 and RAD50 are members of the MRN complex of HR (Section 1.1.3). They were amongst the first cytoplasmic dsDNA receptors proposed, and act upstream of the STING, TBK1, and IRF3 pathway (Kondo *et al*., 2013). RAD50 can induce IL-1β *via* CARD9 (caspase recruitment domain-containing protein 9) and NF-κB (nuclear factor kappa-light-chain-enhancer of activated B cells) in dendritic cells (Roth *et al*., 2014), and there is evidence that MRN may be involved in NF-κB signalling following Kaposi sarcoma-associated herpesvirus infection (Sun *et al*., 2014).

1.3.2 Immune response to DNA damage

Following DNA damage the DDR machinery regulates many downstream signalling responses, including those regulating the cell cycle and programmed cell death. Given the role of DDR proteins as sensors of exogenous DNA, it is perhaps unsurprising that genotoxic damage and DSB formation are also able to induce an innate immune response (Jackson and Bartek, 2009). One of the first studies linking DNA damage with the immune response showed that ultraviolet B (UV-B) was able to induce interleukin (IL) 8 expression (Kondo *et al*., 1993), and shortly after UV-C and γ-radiation were found to activate NF-κB *via* different mechanisms (Li and Karin, 1998). Since then a variety of genotoxic agents have been identified as stimulators of multiple innate immune pathways. Topoisomerase inhibitors and ionizing radiation (IR) induce ATM to relocalise to the cytoplasm, associate with IKK, and NF-κB signalling in a NEMO-dependent manner (Wu *et al*., 2006). ATM-dependent NF-κB activation is required for the activation of IRF1 and IRF7, important transcription factors for *IFNα* and *IFNλ* expression following etoposide treatment (Brzostek-Racine *et al*., 2011; Honda *et al*., 2005). Interestingly, ATM may have a role in negatively regulating IL-1β secretion, and activation of ATM by topoisomerase inhibitors can protect mice from sepsis during bacterial infection or LPS (lipopolysaccharide) treatment (Figueiredo *et al*., 2013).

Genotoxic stress also activates the JNK (c-Jun N-terminal kinase) MAPK (mitogen-activated protein kinase) pathway, which then activates IRF7 (Kim *et al*., 2000). Additionally, IRF3 is phosphorylated and activated by a MAPKKK (MAPK kinase kinase)-related pathway following DNA damage (Kim *et al*., 1999; Servant *et al*., 2001). DNA-PK has been linked to IRF3 phosphorylation during virus infection, but this has not been shown in the context of DNA damage (Karpova *et al*., 2002).

DNA damage can also induce innate immune responses indirectly. In healthy cells, small amounts of damaged self-DNA can escape from the nucleus and mitochondria, although these fragments are normally broken down by DNases such as DNaseII in endosomes, and 3′ repair exonuclease 1 (TREX1) in the cytoplasm. Mutation of these nucleases in mice and humans leads to the build-up of mislocalised DNA, causing the systemic autoinflammation and interferonopathy observed in diseases such as

Aicardi-Goutières syndrome (Ablasser *et al*., 2014; Crow *et al*., 2006; Stetson *et al*., 2008; Yoshida *et al*., 2005). Even in the absence of these mutations, extensive DNA damage can result in leakage of genomic fragments into the cytoplasm where they can stimulate cytosolic DNA sensors such as cGAS (Glück et al., 2017a). Furthermore, UV-B radiation can induce DDR-driven apoptosis, resulting in genome fragmentation and the release of nuclear autoantigens responsible in systemic lupus erythematosus (SLE) (Caricchio *et al*., 2003).

The immune response to DNA damage has implications in disease outcomes. IR induces cytokine and IFN expression which are useful in cancer immunotherapy (Friedman, 2002; Hong *et al*., 1999). Induction of the DNA damage-driven immune response can also protect against infection, as has been demonstrated with mouse gammaherpesvirus type 68 (Mboko *et al*., 2012). However, the importance of DNA repair proteins in immunity is not limited to the innate immune system, and we shall now consider their role in the creation of the adaptive immune response.

1.3.3 DNA repair and lymphocytes

1.3.3.1 V(D)J recombination and SCID

In jawed vertebrates, lymphocytes are arguably the primary cell type in the adaptive immune response. B lymphocytes express immunoglobulins (Ig; also called antibodies) which contribute to the humoral response, and T lymphocytes have a T-cell receptor (TCR) which enables them to recognise unhealthy or infected cells. Variation in the Ig and TCR repertoire is an essential feature of the adaptive immune response created during lymphocyte development by a process called V(D)J recombination which rearranges the variable (V), diversity (D), and joining (J) gene segments that encode the Ig and TCR (Schatz and Ji, 2011). V(D)J recombination is essential for B and T lymphocyte production, and jawed vertebrates unable to carry it out have severe combined immunodeficiency (SCID; also called alymphocytosis).

V(D)J recombination requires a number of DNA repair factors from both HR and NHEJ (Xu, 2006). DSBs are introduced at recombination signal sequences by the recombination-activating gene (RAG) 1 and RAG2. This allows for the somatic recombination of the V, D, and J gene segments of the lymphocyte antigen receptors (Arya and Bassing, 2017; Xu, 2006). These DSBs activate ATM, which then coordinates the recruitment of DSB repair factors, phosphorylates proteins involved in cell cycle checkpoints, and activates NF-κB which induces transcription of important genes in lymphocyte development and antiapoptotic proteins (Arya and Bassing, 2017).

The DNA repair factors required for V(D)J recombination are Artemis, DNA-PKcs, LIG4, XRCC4, Ku70 and Ku80 (Moshous *et al*., 2000, 2001; Xu, 2006). As such, *Prkdc*$^{-/-}$ mice (Blunt *et al*., 1995; Kirchgessner *et al*., 1995; Kurimasa *et al*., 1999b) and humans with mutations in *PRKDC* cannot make B and T lymphocytes and exhibit a SCID phenotype (Woodbine *et al*., 2013). Mice lacking Ku70 and Ku80 are also SCID, but *Xrcc6*$^{-/-}$ (Ku70$^{-/-}$) mice can achieve reduced levels of V(D)J sufficient to produce a few abnormal T lymphocytes (Gu *et al*., 1997; Taccioli *et al*., 1994). XLF and PAXX are involved in V(D)J recombination, but display redundancy (Ijspeert *et al*., 2016; Lescale *et al*., 2016).

1.3.3.2 Class switching recombination and somatic hypermutation

Class switching recombination (CSR) and somatic hypermutation (SHM) are required for effective Ig responses (Xu, 2006). CSR allows for the creation of different Ig subtypes (e.g. IgG, IgA) by switching the constant region. SHM introduces mutations which are important in affinity maturation of the antibody (Xu, 2006). Ku70 and Ku80 are the only DNA repair factors currently known to be required for CSR or SHM, although many others are involved, including LIG4, DNA-PKcs, NBS1, and ATM (Xu, 2006).

1.3.3.3 DNA repair and cytotoxic lymphocyte activation

DNA repair proteins have another important role in regulating the innate and adaptive immune responses. NKG2D (NK group 2, member D) and DNAM-1 (DNAX accessory molecule-1) are receptors expressed on the surface of natural killer (NK) cells, activated cluster of differentiation 8-positive ($CD8^+$) T lymphocytes, and some other immune cells (Cerboni *et al*., 2014; Raulet, 2003). The ligands for NKG2D and DNAM-1 are not normally expressed on healthy cells, but genomic instability caused by genomic lesions or viral infection induces their expression, inducing the cytotoxic killing of the affected cells by both NK and $CD8^+$ T lymphocytes (Cerboni *et al*., 2014; Xu, 2006). The expression of these ligands is dependent upon ATM or ATR activity, and the inhibition of ATM can prevent their expression (Cerboni *et al*., 2014; Gasser *et al*., 2005). Furthermore, in response to DNA damage, fibroblasts upregulate MHC-1 , an important complex in antigen presentation to cytotoxic lymphocytes, further suggesting that the DDR is used to alert the immune system to stressed and unhealthy cells (Tang *et al*., 2014).

Rag2$^{-/-}$ and *Prkdc*$^{-/-}$ mice are SCID and lack B and T lymphocytes, but do still produce NK cells (Karo *et al*., 2014). DNA repair is important in all cells, but the rapid proliferation of lymphocytes makes them more susceptible to DNA damage than most, and this may explain why *Prkdc*$^{-/-}$ NK cells die considerably faster than WT NK cells *in vivo* (Karo *et al*., 2014). Interestingly, NK cells from *Prkdc*$^{-/-}$ mice were activated more than those from WT mice – whether this is due to increased DNA damage in somatic cells

and the associated increase in expression of activating NK cell ligands has not been explored.

1.4 HSV-1

1.4.1 Background

Herpes simplex virus (HSV-1) is a member of the *Herpesviridae* family, a family of enveloped, dsDNA viruses. Herpesviruses get their name from the Greek word "*herpein*" ("to creep") because typical infections are characterised by recurring cycles of latent and lytic infection (Novak and Peng, 2005). It is estimated that 3.4 billion people worldwide are infected with HSV-1, but most maintain the virus in the latent stage and remain symptomless (Gilden and Nagel, 2016; Looker *et al*., 2015). However, HSV-1 infection can cause skin sores and, rarely, encephalitis (Gilden and Nagel, 2016) or blindness (Royer *et al*., 2015). There is also increasing interest in the link between HSV-1 and neurological disorders such as Alzheimer's disease (Itzhaki, 2014, 2017) and cognitive decline in patients with schizophrenia (Bhatia *et al*., 2017; Prasad *et al*., 2012). HSV-1 has also been linked to Bell's palsy, a form of facial paralysis (Schirm and Mulkens, 1997). The virus is treated with antiviral drugs which interfere with HSV-1 enzymes, including Acyclovir, Famciclovir, and Cidofovir, but these have clinical side-effects (Baram-Pinto *et al*., 2010). No vaccine is currently available, although ongoing research appears to be promising (Royer *et al*., 2016).

1.4.2 HSV-1 Infection cycle

HSV-1 initially infects epithelial cells and keratinocytes in the oral mucosa and ocular areas of the human host (Kollias *et al*., 2015). Lytic infection of these cells produces infectious virions which can then infect neighbouring cells, eventually infecting sensory nerve endings and travelling by retrograde transport to local ganglia (Kollias *et al*., 2015; Smith, 2012). Here the virus may continue productive infection and induce encephalitis, or, more commonly, enter latency where it will remain dormant until it reactivates (Smith, 2012). Mechanisms controlling HSV-1 latency and reactivation remain unclear.

At the molecular level, HSV-1 virions express glycoprotein C (gC) on their envelope which binds to heparan sulphate or chondroitin on host cells and mediates viral attachment (Baram-Pinto *et al*., 2010; Campadelli-Fiume and Menotti, 2007; Svennerholm *et al*., 1991). Subsequently other glycoproteins on the viral envelope, for example gB and gD, induce fusion with the cell membrane and release of the viral capsid and tegument into the host cytoplasm (Cai *et al*., 1988; Campadelli-Fiume and Menotti, 2007; Turner *et al*., 1998). The HSV-1 tegument contains viral transcripts, 23 viral proteins important in initiating infection, for example ICP0 (Section 1.4.4), and host factors which can help induce an antiviral state, for example cyclic GMP-AMP (cGAMP) (Gentili *et al*., 2015; Huffman *et al*., 2017; Smith *et al*., 2011).

The HSV-1 capsid then travels *via* microtubule transport to the nucleus, and docks to nuclear pores (Sodeik, 1997). The pressure of the packaged HSV-1 genome is thought to drive initial translocation of viral DNA across the nuclear pore, although the mechanism by which this is initiated is not known (Huffman *et al*., 2017). Once inside the nucleus, transcription of HSV-1 genes begins. Over 80 viral genes are expressed in different phases, termed immediate early (IE; expressed immediately after entry of the viral genome into the nucleus. Exact timing is dependent on the cell type, but is usually between one and four hours after infection), early (expression is regulated by IE proteins and so usually detectable after about four hours), late (delayed expression, but detectable in the absence of viral genome replication by about 6 hours), and true late (γ; only after viral genome replication, roughly eight hours after infection) (Huffman *et al*., 2017; Roizman, 1985; Weir, 2001). HSV-1 genome replication (Section 1.4.3) produces concatemers of the viral genome which are cleaved into monomers and packaged into viral capsids (Tong and Stow, 2010; Vlazny *et al*., 1982). The nuclear pores are too small for capsids to exit the nucleus, and so mature capsids wrap themselves in the inner nuclear membrane, which subsequently fuses with the outer nuclear membrane and releases the capsid into the cytoplasm (Hellberg *et al*., 2016). The virion tegument is sequentially packed around the capsid, and the capsid and tegument are wrapped in intracytoplasmic membranes, the outer of which fuses with the cell membrane to release the virion (Mettenleiter, 2002). Capsids are not required for tegumentation and

wrapping, leading to the production of non-infectious light (L) particles which are also released, and may contribute to the infectivity of infectious particles (Mettenleiter, 2002).

After HSV-1 virions exit the cell, most remain associated with the cellular membrane, and cell-to-cell spread occurs across tight junctions or neural synapses (Sattentau, 2008). A small proportion of virions is released into the tissue fluid where they travel by diffusion. Some strains of HSV-1 form cellular syncytia because the glycoproteins left on the cell membrane induce neighbouring cells to fuse (Sattentau, 2008).

1.4.3 HSV-1 genome structure, replication, and packaging

HSV-1 has a linear 152 kbp (kilobase pair) dsDNA genome which has short 3′ overhangs at each end which may promote genome circularisation during replication (Mocarski and Roizman, 1982). The genome comprises of nicks and gaps approximately 30 bases in length, although the purpose of these is unknown and virus genomes that have been modified so that the gaps are filled do not lose infectivity (Smith *et al*., 2014). The genome consists of two unique regions (unique long, UL; unique short, US) adjacent to inverted repeats, and has three origins of replication (Ward and Weller, 2011). HSV-1 infection induces nuclear reorganisation to create replication compartments within which factors beneficial for replication are recruited, and detrimental factors are excluded (Weller and Coen, 2012). Replication of the genome requires seven viral proteins: UL9 (also called the origin-binding protein, OBP), UL30 (the catalytic subunit of DNA polymerase), UL42, UL5, UL8, UL52, and UL29 (also called infected cell protein 8, ICP8) (Weller and Coen, 2012). ICP8 and UL9 distort the duplex genome at an origin of replication and allow the subunits of the helicase/primase (UL5, UL8, and UL52) to unwind the DNA and synthesise primers for UL30 to elongate, achieving synthesis of leading and lagging strands of the replication fork (Weller and Coen, 2012).

Inside the virion the genome is linear, but endless forms of the genome form during replication (Weller and Coen, 2012). It remains controversial whether concatemeric, endless genomes are formed by HR, or created by rolling circle replication following circularisation of the genome (Weller and Coen, 2012). There is evidence for both hypotheses: HR is thought to be important due to the upregulation of SSA during HSV-1

infection (Weller and Coen, 2012), but knockdown of XRCC4 and LIG4 abrogate the formation of endless genomes, suggesting that NHEJ may play an important role in their formation (Muylaert and Elias, 2007). The HSV-1 genome is also branched, although little is known about why this occurs or whether it is advantageous to the HSV-1 infection cycle (Severini *et al*., 1996). It is possible that the branches are caused by replication forks and that the branched structures are simply replication intermediates (Severini *et al*., 1996).

These branched HSV-1 concatemers are cleaved into monomers and packaged into the icosahedral viral capsids (Homa and Brown, 1997). Cleavage of the genome is achieved by the HSV-1 terminase, a heterotrimeric complex of UL15, UL28, and UL33 (Heming *et al*., 2014). The dogma in the field is that packaging is required for simultaneous genome cleavage (Heming *et al*., 2014; Muylaert and Elias, 2007). There is evidence that packaging can be aborted after genome cleavage, however this has only been observed using a virus with a mutation in the terminase component, UL15 (Yang *et al*., 2011).

1.4.4 ICP0

Infected cell protein 0 (ICP0) is a 775-amino acid protein with IE expression. It has multiple functions which make it important during HSV-1 infection, and viruses lacking ICP0 expression are attenuated in most cell types, especially at low multiplicities of infection (MOIs) (Smith *et al*., 2011). As is the case with many IE proteins, ICP0 is a HSV-1 transactivator (Cai and Schaffer, 1992; Everett, 1984), meaning that it activates the transcription of other HSV-1 genes. However, it also has extensive roles in overcoming intrinsic cellular resistance to infection. ICP0 has E3 ligase activity which allows it to ubiquitinate and induce the proteasomal degradation of target proteins (Lilley *et al*., 2010; Smith *et al*., 2011). PML (promyelocytic leukaemia) and other components of nuclear domain 10s (ND10s) are able to repress HSV-1 infection by localising to the viral genome and repressing gene expression, but ICP0 induces degradation of PML and thereby prevents the accumulation of the other factors (Chelbi-Alix *et al*., 2007; Cliffe and Knipe, 2008; Gu *et al*., 2013; Smith *et al*., 2011; Wang *et al*., 2012). ICP0 also induces the degradation of IFI16 and DNA-PKcs to prevent their restrictive effects on viral infection

(Section 1.2.6) (Lees-Miller *et al*., 1996; Orzalli *et al*., 2016; Parkinson *et al*., 1999; Smith *et al*., 2011). Indeed, the ability of ICP0 to tip the balance against HSV-1 latency has been attributed to its ability to degrade DNA-PKcs (Smith *et al*., 2014).

ICP0 also directly inhibits the immune response. IRF3 and IRF7 signalling are inhibited by ICP0, and as a result ICP0 mutants are hypersensitive to IFN-I (Eidson *et al*., 2002a; Lin *et al*., 2004a; Mossman *et al*., 2000, 2001). ICP0 also inhibits toll-like receptor 2 (TLR2) and NF-κB signalling (van Lint *et al*., 2010). Finally, ICP0 degrades CD83 on mature dendritic cells, which may help diminish T lymphocyte responses (Heilingloh *et al*., 2014; Kummer *et al*., 2007).

1.4.5 HSV-1 Restriction factors

Restriction factors are cellular proteins which reduce the efficiency of viral infection, and cells express such factors against most, if not all, viruses. The first reported example was the murine protein, Friend-virus-susceptibility-1 (Fv1), which protects mice from murine leukama (Lilly, 1970) by blocking a step between reverse transcription and integration of the viral genome (Jolicoeur and Baltimore, 1976; Sveda and Soeiro, 1976). Another famous example is APOBEC (apolipoprotein B mRNA editing enzyme, catalytic polypeptide-like) 3G which inhibits HIV-1 infection through the hyper-editing of the viral genome (Sheehy et al., 2002).

We have already explored how some DNA repair proteins restrict HSV-1 infection (Section 1.2.6), but most HSV-1 restriction factors are not found in this pathway. These restriction factors are diverse and act *via* a multitude of mechanisms, meaning that a full review is beyond the scope of this thesis. However, it is worthwhile considering some key examples to help provide further context to the role that restriction factors have during HSV-1 infection.

Autophagy is a process by which excess or disfunctional proteins or organelles can be broken down and recycled, but it is also an important anti-viral defence. Tripartite motif 23 (TRIM23) drives the autophagy of HSV-1 and other viruses (Sparrer et al., 2017).

MxB inhibits uncoating of viral DNA in a GTPase-dependent manner, preventing the viral genome from entering the nucleus for replication (Crameri et al., 2018). Genome expression is required for subsequent replication of genomes that successfully enter the nucleus, and there are factors such as IFI16 (Section 1.2.6) and the upstream binding factor (UBF) (Ouellet Lavallée and Pearson, 2015), which are able to reduce viral gene expression. The sirtuin family of proteins also restricts HSV-1 gene expression (Koyuncu et al., 2014).

SAMHD1 is a restriction factor better known for inhibiting retroviral reverse transcription, but also inhibits HSV-1 replication, possibly by reducing the availability of deoxynucleotide triphosphates (dNTPs) (Kim et al., 2013). Restriction factors often target viral genome replication, with other examples including PML and other components of the ND10s (Section 1.4.4), or the genome itself. APOBEC3C hyper-edits the HSV-1 genome through cytidine deamination, introducing mutations and reducing viral viability (Suspène et al., 2011).

Restriction factors can also act to inhibit viral egress and spread. Tetherin is a restriction factor that is very effective at targeting a wide range of viruses, including HSV-1, and does so by preventing new virions from dissociating from the surface of the host cell, thereby preventing spread to neighbouring cells (Blondeau et al., 2013).

1.5 HSV-1 infection in mice

1.5.1 Overview

HSV-1 has human tropism, and mice are not a natural host for the virus. However, studying the virus in humans is difficult because infection is generally asymptomatic. Furthermore, the neurotropic nature of HSV-1 mean that human samples are often limited to *post-mortem* studies. It is therefore necessary to study many aspects of infection in an alternative host, and mice are often used because their genetic, immunological, and neurological biology is already well-characterised (Kollias *et al*., 2015). Here we describe the use of mice as a model for studying HSV-1 infection, with a particular focus on aspects of consequence for our study.

1.5.2 Pathology

There are numerous infection routes commonly used for studying HSV-1 in mice, and the location of inoculation and the amount of virus inoculated will determine the pathology observed (Kollias *et al*., 2015). In most cases infection is asymptomatic, but mice with a reduced propensity to control HSV-1 infection or mice inoculated with a high dose of HSV-1 may experience pathology and, in extreme cases, mortality (Kollias *et al*., 2015). There is also variation based upon age and strain of mice (Ben-Hur *et al*., 1983; Kastrukoff *et al*., 2012; Kollias *et al*., 2015).

The most common signs of pathology observed are ruffled coats (a generic symptom of mouse distress), weight loss, and loss of mobility due to neurological damage (Kollias *et al*., 2015). In the case of inoculation of HSV-1 in the lip, spread of HSV-1 infection to the brain is often observed in mice unable to effectively control HSV-1 infection (Kastrukoff *et al*., 1982). This makes this inoculation route useful in the study of potential HSV-1 restriction factors, because mice which are deficient in the factor of interest can be tested for their ability to control HSV-1 infection. It is, however, important to remember that mouse pathology differs from that of humans; for instance, HSV-1 infection of the mouse brain spreads diffusely, as compared to the focal lesions observed in human brains (Kollias *et al*., 2015).

1.5.3 The immune response to HSV-1 infection

The innate immune response to HSV-1 infection is primarily driven by nucleic acid sensors. TLR9 recognises the HSV-1 genome and induces IFNα production (Hochrein *et al*., 2004). A number of the proposed intracellular DNA sensors have either not been verified *in vivo*, or have been found to be redundant during HSV-1 infection of mice (Ishii et al., 2008; Unterholzner, 2013). Those that have been shown to contribute to the innate immune response to HSV-1 *in vivo* are cGAS (Li *et al*., 2013) and DNA-PK (Ferguson *et al*., 2012), both of which signal *via* the STING-TBK1-IRF3 pathway to induce IFN-I (Unterholzner, 2013).

The cellular immune response to HSV-1 is primarily driven by $CD8^+$ T lymphocytes which secrete IFNγ (Cantin *et al*., 1995). IFNγ receptor-null mice are more susceptible to

HSV-1 infection and reactivation (Cantin *et al*., 1999, 1995; Knickelbein *et al*., 2008; Liu *et al*., 2000), possibly because IFNγ amplifies the antiviral effects of IFNβ (Halford *et al*., 2005a, 2005b; Pierce *et al*., 2005). HSV-1-specific $CD8^+$ cells are retained at sites of latency (Khanna *et al*., 2003). CD4 T lymphocytes also produce IFNγ in response to HSV-1 infection, along with tumour necrosis factor α (TNFα), interleukin-2 (IL-2), and IL-4 (Johnson *et al*., 2008). $CD8^+$ and $CD4^+$ T lymphocytes can respond directly to HSV-1 antigens, of which gB is thought to be the immunodominant antigen (Johnson *et al*., 2008; Khanna *et al*., 2003; Wallace *et al*., 1999).

There is evidence that $CD8\alpha^+$ dendritic cells (DCs) are the key DC subset for priming $CD8^+$ T lymphocytes (Smith *et al*., 2003), but the priming of $CD8^+$ and $CD4^+$ T cells is performed by both migrant and resident DCs, and the infection route determines their relative importance (Lee *et al*., 2009).

Other cell types are less important in the cellular and adaptive immune responses. *Rag2*$^{-/-}$ mice unable to produce T and B lymphocytes retain some resistance to HSV-1 which is not dependent on NK cells (Halford *et al*. 2005). Neutrophils are also nonessential in the response to HSV-1 infection (Hor *et al*., 2017). B lymphocytes are not essential for clearance of lytic HSV-1 infection, but they may contribute to preventing the spread of HSV-1 through the nervous system in mice (Simmons and Nash, 1987). B lymphocytes are also not required for resistance to secondary infection of HSV-1 (Simmons and Nash, 1987). This is interesting because the HSV-1 IgG Fc receptor, a complex comprised of gE and gI (Johnson *et al*., 1988), is important to protect HSV-1 against human IgG, but does not bind murine IgG and so would not provide protection against IgG during infection of mice (Nagashunmugam *et al*., 1998).

1.6 Aims of the project

The primary aims of this project are to consider the roles of two NHEJ factors, PAXX and DNA-PKcs, during viral infection. To achieve this HSV-1 will be used as a model virus. More specifically, we have the following aims:

- To determine whether PAXX influences HSV-1 infection.
- To determine whether PAXX has a function in innate immune sensing during HSV-1 infection.
- To determine whether *Paxx*$^{-/-}$ mice can restrict HSV-1 infection.
- To further investigate the role of DNA-PKcs in HSV-1 infection.

We hope that addressing these points will help contribute to the understanding of the interactions between NHEJ factors and HSV-1.

2 Materials and Methods

2.1 Cell culture

Cells were incubated at 37 °C, 5 % CO_2, and 3 % O_2. Human foetal foreskin fibroblasts (HFFFs) and U2OS (human osteosarcoma) cells were grown in Dulbecco's Modified Eagle Medium (DMEM; Gibco) with 10 % volume per volume (v/v) heat-inactivated foetal bovine serum (FBS; Seralab), and 50 μg/mL of penicillin/streptomycin (P/S; Gibco). Retinal pigment epithelia (RPE-1) cells were cultured in DMEM-F12 with Glutamax, 10 % v/v FBS, 0.2 % weight/volume (w/v) sodium bicarbonate, and 50 μg/mL P/S. Murine embryonic fibroblasts (MEFs) were maintained in DMEM-F12 with Glutamax (Gibco), 15 % v/v FBS, 0.001 % v/v 2-mercaptoethanol (2-ME), non-essential amino acids (glycine, L-alanine, L-asparagine, L-aspartic acid, L-glutamic acid, L-proline, L-serine; all 100 nM), 1 mM sodium pyruvate, and 50 μg/mL P/S. Primary cells grown *ex vivo* were maintained in DMEM-F12 + Glutamax-I with 15 % FBS. All cells were routinely tested for contamination with mycoplasma using the MycoAlert detection kit (Lonza).

2.2 Transfection

2.2.1 TransIT-LT1 transfection

TransIT-LT1 (Mirus) is a cationic, lipid-mediated transfection reagent. For optimum transfection efficiency cells were seeded to be 70-80 % confluent at the point of transfection. TransIT-LT1 was mixed with OptiMEM (Gibco) at a ratio of 1:33 and incubated at room temperature for 5 minutes. DNA was then added at a ratio of 1 μg DNA:3 μl TransIT-LT1, and incubated for a minimum of 15 minutes. The transfection mix was then added to the cells directly into the culture medium.

2.2.2 Nucleofection

Cells were seeded to be 80 % confluent on the day of nucleofection. The cells were washed in phosphate-buffered saline (PBS), and disassociated from the tissue culture plate using trypsin (Gibco). The cells were washed in an excess of medium containing FBS to inactivate the trypsin, and then washed in PBS to remove the medium, and

resuspended in PBS. Cells were counted, and 1.2 x 10^6 were centrifuged, resuspended in 120 μl of resuspension buffer (Neon Transfection System, ThermoFisher), and added to 8 μg of DNA. The cell-DNA mixture was taken up in a gold-coated tip and nucleofected at 1400 V for a single pulse of 30 milliseconds using the Neon Transfection System (ThermoFisher).

2.3 PMA stimulation

Cells were counted and seeded so as to be 70-80 % confluent at the time of stimulation. The next day they were starved of serum for three hours prior to stimulation with 10 ng/mL of phorbol 12-myristate 13-acetate (PMA) in serum-free media. At appropriate time points the RPE-1 cells were harvested and the RNA isolated for use in qPCR (Section 2.6.3).

2.4 Viruses

2.4.1 HSV-1 viruses

For consistency, all HSV-1 viruses were grown on U2OS cells because they are permissive for viruses lacking ICP0. Strain 17+ (S17) HSV-1 virus was used as the wild-type strain and was a kind gift from Professor Stacey Efstathiou. An S17 virus lacking ICP0 (referred to in the literature as dl1403) was a kind gift from Professor Gill Elliot (Stow and Stow, 1986). dl1403 contains a 2 kb deletion within both the TR_L and IR_L copies of *Vmw110* (ICP0) which instead encode 105 amino acids from the original N-terminus followed by 56 amino acids altered by a frame shift. It should be noted that it has recently been published that, in addition to the loss of ICP0, dl1403 also lacks functional gC expression (Cunha *et al*., 2015). For the purpose of simplicity, dl1403 will henceforth be termed ΔICP0 HSV-1. S17 VP26-GFP was a gift from Professor Geoffrey Smith (Hollinshead *et al*., 2012). The ΔgE/VP26-YFP virus derived from a strain-16 (S16) parent and was a gift from Dr Colin Crump. *In vivo* studies used S16 HSV-1 virus expressing firefly luciferase under a cytomegalovirus (CMV) promoter, a gift from Professor Stacey Efstathiou.

2.4.2 Preparation of HSV-1 stocks

U2OS cells were infected at an MOI of 0.01. Once cytopathic effect was observed in all cells (approximately 3 days *post* infection), cells were scraped into the media and centrifuged at 1900 g for 30 minutes. The pellet was resuspended in PBS and freeze-thawed three times before being centrifuged again. The resulting supernatant was aliquoted and frozen. Aliquoted stocks were thawed no more than twice to prevent deterioration of the stock.

2.4.3 Plaque assay titration of HSV-1

U2OS or Vero cells were seeded into 6-well plates to be confluent at the time of titration. The virus stock was serially diluted ten-fold in DMEM plus 2.5 % v/v FBS, and applied to the cells. The plates were rocked every 15 minutes for 1 hour, and then the medium was replaced with 1.5 % carboxymethyl cellulose (CMC) complemented with a final concentration of 1x minimum essential medium (MEM). The plates were incubated at 37 °C, 5 % CO_2 and 3 % O_2 until plaques were observed. The semi-solid overlay was then removed and cells were fixed and stained with 5 % v/v crystal violet (Sigma) and 25 % v/v ethanol for 1 hr, washed with water, and the plaques were counted.

2.4.4 Plaque assay titration of VACV

The Western Reserve (WR, hereafter referred to as wildtype, WT) and modified vaccinia Ankara (MVA) strains of vaccinia virus (VACV) were kindly provided by Professor Geoffrey Smith. The stocks were serially diluted in duplicate, and titrated onto monolayers of BSC-1 cells in 6-well plates cultured in DMEM with 2.5 % v/v FBS and 50 μg/ml of P/S. The plates were incubated at 37 °C for one hour and rocked every 15 minutes. The medium was then replaced with 1.5 % carboxymethyl cellulose (CMC) complemented with a final concentration of 1x minimum essential medium (MEM) and the plates were incubated until large plaques were observed. The cells were stained and counted as described for HSV-1 titration.

2.4.5 Virus growth curves

Cells of interest were counted using a Countess (Invitrogen) automated cell counter and seeded so that the cell numbers of different genotypes would be within 5 % of each other at the time of infection. MEFs were seeded into 6-well plates, and RPE-1 cells were seeded into T25 flasks. Prior to infection cells were counted to ensure that different genotypes had total numbers within 5 % of each other, and this count was also used to calculate the volumes required for specific multiplicities of infection (MOI) between cell types. At the desired time *post* infection, cells were scraped into the growth medium. The cell suspensions of all samples were freeze-thawed three times in parallel, and stored at -80 °C. Infectious virion numbers were determined by titration of each sample in duplicate (Section 2.4.3).

2.4.6 MOI calculations

Viral stocks of known titre were used to infect cells at specific MOIs. MOI is calculated by dividing the total number of infectious virions by the number of cells. The MOI used gives an indication of the proportion of cells which we expect to be infected when applied to the Poisson distribution (Fields et al., 2007). A simplification of the Poisson distribution can be used to calculate the number of cells infected with one or more virions.

$$P(k) = e^{-m}m^k/k!$$

The Poisson distribution: The proportion of cells infected with k virions, $P(k)$, can be determined using the MOI, m.

$$P(>0) = 1 - e^{-m}$$

The Poisson distribution can be simplified to show the number of cells infected with at least one virion.

The above formulae can be used to show that we expect infecting cells with an MOI of 0.01 should result in <1 % of cells infected, whilst MOI 4 should infect over 98 % of cells.

2.5 DNA manipulation

2.5.1 Polymerase chain reaction

The polymerase chain reaction (PCR) was used to amplify DNA sequences of interest for the purposes of cloning and genotyping. Primers were specifically designed for this purpose (Table 1). PCR was carried out using a Veriti thermocycler (Applied Biosystems). When high-fidelity replication was required, Platinum Pfx DNA polymerase (ThermoFisher) and its reaction buffer were used. For analyses which did not require the maintenance of sequence integrity, for example mouse genotyping by PCR, HotStarTaq polymerase (Qiagen) was used.

Name	Sequence (5′-3′)
Paxx WT (genotyping - F)	TCAACCTTGAGTACCGCC
Paxx WT (genotyping - R)	GCTGCCTGCCTTAAGACCTA
Paxx KO (genotyping - F)	GTTCCAGTTAGGGAGGCCAT
Paxx KO (genotyping - R)	CATACAGTACCTGCCAGCCG

Table 1: Primer sequences used in PCR reactions.

F = forward primer, R = reverse primer

2.5.2 Agarose gel electrophoresis

Agarose gel electrophoresis was used to analyse DNA samples, including PCR products. Agarose powder was dissolved in Tris, acetic acid, EDTA (TAE) buffer to a concentration of 1 or 2 % w/v, and SYBR Safe DNA gel stain (ThermoFisher) was mixed in at 1x concentration prior to the gel setting. Gels were run at 100 V until the dye in the molecular weight marker (HyperLadder 1kb; Bioline) reached the end of the gel. The gel was visualised using an ultraviolet (UV) lamp.

2.5.3 Purification of DNA from an agarose gel

DNA bands were excised from agarose gels using a clean scalpel under blue light. The QIAquick gel extraction kit (Qiagen) was then used to dissolve the gel and purify

the DNA. The concentration and purity of the DNA product was then analysed using a NanoDrop 2000 Spectrophotometer.

2.5.4 Restriction enzyme digestion

Restriction enzymes (New England Biosciences (NEB)) were used with their recommended buffers as supplied by the manufacturer. DNA was digested for 5 hours at 37 °C followed by an overnight incubation at 22 °C.

2.5.5 DNA ligation

50 ng of vector DNA and insert DNA were incubated in the presence of one unit of T4 DNA ligase (Promega) in the buffer provided by the manufacturer at 16 °C overnight. The amount of insert was initially adjusted to a molar ratio of 1:3 between the vector and the insert, but this ratio was optimised for each ligation reaction. If ligation was intended at two sites where the complementary ends are of the same sequence (e.g. insertion of a sequence at a single restriction site), prior to ligation 1.7 μg of the vector was incubated in a total volume of 20 μL containing one unit of shrimp alkaline phosphatase (SAP) and 1x buffer supplied by the manufacturer for one hour at 37 °C, followed by heat inactivation of the SAP at 65 °C for 15 minutes. SAP treatment increases the specificity of the ligation by removing the 5′ phosphate from the ends from the vector, preventing religation to recreate the original, undigested vector.

2.5.6 Creation of chemically competent E. coli

Competent DH5α *Escherichia coli* (*E. coli*) were generated using the following protocol: 5 μL of DH5α *E. coli* were added to 3 mL of super-optimal broth (SOB) and incubated at 37 °C in a shaking incubator overnight. The broth was added to a further 200 mL of SOB, and incubated at 37 °C until the optical density at 595 nm (OD595) reached 0.3 - 0.4 relative to a non-inoculated control. The broth was then centrifuged at 1200 g for 20 minutes at 4 °C. The pellet was resupsended in RF1 buffer (100 mM KCl, 50 mM $MnCl_2$-$4H_2O$, 30 mM Potassium acetate, 10 mM $CaCl_2$-$2H_2O$, and 15 % v/v glycerol, adjusted to pH 5.8 with 10 % v/v glacial acetic acid, and filter-sterilised through a pre-rinsed 0.22 μm membrane), and centrifuged at 1200 g for 20 minutes at 4 °C. The pellet was resuspended in filter sterilised RF2 buffer (10 mM MOPS pH6.8, 10 mM KCl,

75mM $CaCl_2$-$2H_2O$, and 15 % v/v glycerol), incubated on ice for 15 minutes, and then aliquoted, flash-frozen and stored at -80 °C.

2.5.7 Transformation of E. coli, and purification of plasmid DNA

To propagate DNA plasmids, chemically competent *E. coli* were mixed with 50 ng of the plasmid DNA, and the mixture was incubated on ice for 30 minutes. The *E. coli* were then heat-shocked at 42 °C for 30 seconds, and then placed back on ice for a further two minutes. The *E. coli* were allowed to recover in SOB at 37 °C for 1 hour before plating onto an agar plate containing 50 μg/mL kanamycin or 100 μg/mL carbenicillin. Plates were then incubated for 16 hours at 37 °C. Bacterial colonies were then picked, and allowed to grow in 5 mL or 50 mL of LB broth containing 50 μg/mL of kanamycin or 100 μg/mL of carbenicillin at 37 °C for 16 hours. From this culture DNA plasmids were isolated using QIAprep miniprep and maxiprep kits (Qiagen).

2.5.8 DNA sequencing

Sanger DNA sequencing was performed by the Department of Biochemistry, University of Cambridge. The non-standard primer used to sequence the PX458 plasmid at the BbsI site was GGCTGTTAGAGAGATAATTGG. Sequencing results were analysed using MEGA or SnapGene.

2.5.9 Creation of concatemerised immunostimulatory DNA

Immunostimulatory DNA was produced as previously described (Ku and Ferguson, 2014). Oligomeric ssDNA constructs with complementary sequences (Table 2) were ordered from Integrated DNA Technologies (IDT) and resuspended in water to a concentration of 10 μg/μl, mixed in equal concentration, and heated to 75 °C for 15 minutes to remove secondary structures. Subsequent cooling to RT allowed for the annealing of the oligomers to create dsDNA oligomers. 50 μL of 60 % w/v PEG8000 (Sigma) was added to increase the effective concentration of solution, and polynucleotide kinase (PNK; Promega) was added in the presence of PNK buffer and incubated at 37 °C for 2 hours to phosphorylate the DNA ends in order to increase ligation efficiency. 3 units (U) of T4 DNA ligase (Promega) were then incubated with the products at 37 °C for 16 hours to ligate the oligomers together and create DNA concatemers.

Forward ssDNA	TACAGATCTACTAGTGATCTATGACTGATCTGTACATGATCTACA
Reverse ssDNA	TGTAGATCATGTACAGATCAGTCATAGATCACTAGTAGATCTGTA

Table 2: ssDNA constructs used in the creation of immunostimulatory DNA

2.5.10 Phenol/chloroform DNA extraction

Prior to purification, the total volume of the solution was increased by adding 300 μL of water. DNA was then purified by mixing with 400 μL of phenol (Fisher Chemical), centrifuging at 15,000 g for 1 minute, and isolating the aqueous layer. Phenol was added to this again, and the process was repeated three times or until evidence of proteinaceous contaminants was no longer visible. 400 μL of chloroform (Fisher Chemical) was added to the aqueous layer, and the solution centrifuged at 15,000 g for 1 minute to remove any phenol contamination. DNA was precipitated by adding 800 μL of 100 % ethanol that had been pre-chilled to -20 °C, incubating at -20 °C for 16 hours, centrifuging at 15,000 g for 10 minutes, and aspirating the supernatant. The pellet was resuspended in 1 mL of 70 % v/v ethanol, and the solution was centrifuged again at 15,000 g for 10 minutes. The supernatant was removed, and the pellet was allowed to

air-dry in the fume hood. Once dry, the pellet was resuspended in 50 μL of endotoxin-free water. The length distribution of the constructs was analysed using gel electrophoresis (Section 2.5.2), and the concentration ascertained using a NanoDrop 2000 Spectrophotometer.

2.5.11 Alternative immunostimulatory DNA creation

As an alternative to the concatemerised immunostimulatory DNA described in Section 2.5.9, complementary ssDNA sequences of 90 bp in length comprised of the same sequence used in the concatemerised DNA, but repeated twice (Table 1), were resuspended in endotoxin-free water and mixed at a concentration of 500 ng/μL. The mixture was heated to 75 °C and cooled to room temperature to allow the DNA strands to anneal.

Forward ssDNA	TACAGATCTACTAGTGATCTATGACTGATCTGTACATGATCTACATACA GATCTACTAGTGATCTATGACTGATCTGTACATGATCTACA
Reverse ssDNA	TGTAGATCATGTACAGATCAGTCATAGATCACTAGTAGATCTGTATGTA GATCATGTACAGATCAGTCATAGATCACTAGTAGATCTGTA

Table 3: ssDNA used to make alternative immunostimulatory DNA

2.6 Nucleic acid detection assays

2.6.1 Cellular RNA extraction

Cells were lysed *in situ* using 250 μL of lysis buffer containing 4 M guanidine thiocyanate, 25 mM Tris pH 7, and 143 mM 2-ME. 250 μL of ethanol was added, and the solution was applied to a silica column (Epoch) and centrifuged; all centrifugation steps were for 30 seconds at 16,000 g unless stated otherwise. 500 μL of buffer containing 1 M guanidine thiocyanate, 25 mM Tris pH7, and 10 % ethanol was applied to the column which was then centrifuged. The column was centrifuged with 500 μL of a second wash buffer containing 25 mM Tris pH 7 and 70 % v/v ethanol, before a further 500 μL was added and centrifuged for 2 minutes at 16,000 g. The RNA was then eluted by adding 30 μL of nuclease-free water and centrifuging at 16,000 g for 1 minute. The resulting

eluent was then passed back through the same column. RNA concentration was determined using a NanoDrop 2000 Spectrophotometer.

2.6.2 cDNA synthesis

Complementary DNA (cDNA) was generated from 500 ng of RNA. 1 μL of a 10 mM deoxynucleotide (dNTP) mixture and 500 ng of oligo(dT) (both Thermo Scientific) were incubated with the RNA at 65 °C for 5 minutes in a total volume of 13 uL. 40 U of RNaseOUT recombinant RNase inhibitor (Invitrogen), 50 U of Superscript III Reverse Transcriptase (Invitrogen), 2 μL of 10x first strand buffer, and 1 μL of 0.1 M dithiothreitol (DTT) were then added and the volume made up to 20 μL. This solution was incubated for 1 hour at 50 °C, and then at 72 °C for 15 minutes.

2.6.3 Quantitative real time-polymerase chain reaction (qPCR)

cDNA was diluted 1:3 in nuclease-free water prior to analysis. Each sample was analysed in duplicate, as a minimum. 2 μL of cDNA was added to the wells of a MicroAmp Fast Optical 96-well or 384-well reaction plate (Applied Biosystems). A mastermix was made containing 5 μL Fast SYBR Green Master Mix (Life Technologies) and 1 μL of 10 mM stocks of each of a forward and reverse primer per well, and 7 μL was added per well. The primers used for SYBR Green qPCR listed by species in

Table 4. The plate was centrifuged for 1 minute at 180 g before being analysed on a 7500 Fast Real-Time PCR System (Applied Biosystems). Following an initial 30 second melting step, 40 cycles of 3 seconds at 95 °C, and 30 seconds at 60 °C were used. The Ct value was exported and analysed relative to a housekeeping gene and control sample, where applicable.

Gene	Forward Primer	Reverse Primer
Human		
PPIA	TCCTGGCATCTTGTCCATG	CCATCCAACCACTCAGTCTTG
GAPDH	ACCCAGAAGACTGTGGATGG	TTCTAGACGGCAGGTCAGGT
PRKDC	CTGTGCAACTTCACTAAGTCCA	CAATCTGAGGACGAATTGCCT
PAXX	TTCGTGTGCTACTGCGAAGG	GTGAAGCAGGTGCTCCAAAG
XRCC5	AGAAGAAGGCCAGCTTTGAG	AGCTGTGACAGAACTTCCAG
EGR1	AGCACCTGACCGCAGAGTCT	AGATGGTGCTGAGGACGAGG
CFOS	CTGGCGTTGTGAAGACCAT	TCCCTTCGGATTCTCCTTTT
Murine		
Hprt	GTTGGATACAGGCCAGACTTTGTTG	GATTCAACTTGCGCTCATCTTAGGC
Cxcl10	ACTGCATCCATATCGATGAC	TTCATCGTGGCAATGATCTC
Egr1	TCCTCTCCATCACATGCCTG	CACTCTGACACATGCTCCAG
*Ifna**	ARSYTGTSTGATGCARCAGGT	GGWACACAGTGATCCTGTGG
Ifnb	CATCAACTATAAGCAGCTCCA	TTCAAGTGGAGAGCAGTTGAG
Isg15	GCAAGCAGCCAGAAGCAGACTCC	CGGACACCAGGAAATCGTTACCCC
Isg54	ATGAAGACGGTGCTGAATACTAGTGA	TGGTGAGGGCTTTCTTTTTCC
Cjun	CCAGAAGATGGTGTGGTGTTT	CTGACCCTCTCCCCTTGC
Cfos	CCTTCGGATTCTCCGTTTCTCT	TGGTGAAGACCGTGTCAGGA
Nfkbia	CTGCAGGCCACCAACTACAA	CAGCACCCAAAGTCACCAAGT
HSV-1		
ICP27	GTGCAAGATGTGCATCCACCACAACCTGCC	GCCAGAATGACAAACACGAAGGATGCAATG
gB	TGTGTACATGTCCCCGTTTTACG	GCGTAGAAGCCGTCAACCT
US11	CTTCAGATGGCTTCGAGATCGTAG	TGTTTACTTAAAAGGCGTGCCGT
ICP4	GACGTGCGCGTGGTGGTGCTGTACTCG	GCGCACGGTGTTGACCACGATGAGCC
US1	ATGCAATGCTACGGCGCTCGGT	ACAGCTGATTGATACACTGGCGC

Table 4: Primer pairs used in qPCR

*Murine *Ifna* primers detect all *Ifna* subsets except *Ifna4*

2.6.4 Isolation of cellular and viral DNA for quantification by qPCR

qPCR was used to quantify the relative numbers of viral genomes in HSV-1 infected cells. Infected cells were scraped into growth medium, centrifuged for 5 minutes at 400 g, and the resulting pellet was resuspended in lysis buffer consisting of 5 μM sodium dodecyl sulphate (SDS), 10 mM Tris-HCl pH 8.3, and 100 μg/mL proteinase K. The amount of lysis buffer added was approximately 10x the volume of the cell pellet. The cells and buffer were then incubated at 50 °C for 90 minutes, before the proteinase K was deactivated by heating to 95 °C for 10 minutes.

2.6.5 Quantification of viral DNA by qPCR

For qPCR of cellular and viral genomes, primers and probes against the promoter regions of human *GAPDH (*glyceraldehyde 3-phosphate dehydrogenase) and HSV-1 *ICP0* were used (Table 5), and these were tagged with the fluorophores Cy5 (cyanine5) and FAM (6-carboxyfluorescein), respectively, coupled with the BlackBerry quencher (BBQ). A mastermix was created with final concentrations of 8 mM MgCl2 (Qiagen), 0.8 mM dNTPs (Thermo Scientific), 5 % v/v DMSO, 0.8 U of HotStarTaq DNA polymerase (Qiagen), and Taq polymerase buffer. Primers and probes (TIB Molbiol) were added at concentrations that were previously optimised (Table 5). 19 μL of this mastermix was added per tube. Samples were analysed in triplicate by adding 1 μL of isolated cellular viral DNA (Section 2.6.4) to the appropriate tubes. A plasmid containing the *GAPDH* promoter region and one with the *ICP0* promoter region were mixed and serially diluted at known concentrations. 1 μL of each of the dilution series were mixed with 19 μL of the mastermix and analysed to create a standard curve. qPCR of the samples and standards was carried out simultaneously on a Rotorgene 3000 (Corbett Research). The reaction was held at 95 °C for 15 minutes, before 45 cycles of 95 °C for 30 seconds, and 60 °C for 60 seconds (the latter being the acquisition stage).

Name	Sequence	Final concentration
ICP0 (forward primer)	GGAAAGGCGTGGGGTATAA	24 nM
ICP0 (reverse primer)	AACGTAGGCGGGGCTTC	72 nM
ICP0 probe	6FAM-TCGCATTTGCACCTCGGCAC-BBQ	50 nM
GAPDH (forward primer)	CGGCTACTAGCGGTTTTACG	72 nM
GAPDH (reverse primer)	AAGAAGATGCGGCTGACTGT	24 nM
GAPDH probe	Cy5-CACGTAGCTCAGGCCTCAAGACCT-BBQ	50 nM

Table 5: Primers and probes used in TaqMan qPCR of cellular and viral DNA.

2.6.6 Isolation of viral DNA for southern blotting

Infected cells were scraped into the growth medium, and centrifuged at 400 g for five minutes. The pellet was resuspended in 1.6 mL of buffer containing 10 mM Tris, 50 mM EDTA, 0.5% SDS w/v and 163 mg/ml proteinase K before incubation at 37 °C overnight. The next day an equal volume of phenol and was added and gently mixed before the solution was centrifuged for 10 minutes at 1600 g and 20 °C. The top, aqueous layer was transferred to a clean tube, and the phenol wash was repeated. An equal volume of chloroform was added to the aqueous layer, and the solution was centrifuged for 10 minutes at 1600 g and 20 °C. The aqueous layer was isolated and NaCl was added to a final concentration of 0.2 M. After mixing gently but thoroughly, absolute ethanol was added to a final concentration of 29 % v/v, and the solution mixed gently but thoroughly once more. The sample was then kept at -20 °C overnight before 15 minutes of centrifugation at 2900 g and 4 °C. The supernatant was removed and the precipitated DNA pellet was allowed to air-dry for several hours before being gently resuspended in 300 μL of 10 mM Tris and 1 mM EDTA. The samples were then heated to 65 °C to increase the accuracy of the measurement of concentration by a NanoDrop 2000 Spectrophotometer. The samples were stored at 4 °C until they were used.

2.6.7 Creation of hybridisation probe for southern blotting

The HSV-1 BamHI K fragment (nucleotides 123459 to 129403 of strain S17) (McGeoch *et al*., 1988) was excised from a donor plasmid (pAT153 containing fragment Kpn A) and gel-purified. 100 ng of the excised fragment was added to nuclease-free water to a total volume of 34 μL. After boiling for 5 minutes, the solution was placed on ice for five minutes. A dNTP mix was created with final concentrations of 0.17 mM biotin-14-dATP (Invitrogen), 0.17 mM biotin-14-dCTP (Invitrogen), and 0.98 mM of each of dATP, dTTP, dGTP, and dCTP. The BamHI K fragment was then added to 5 μL of the dNTP mix, 1 μL of Klenow enzyme (NEB), and 10 μL of 5x labelling mix (NEB) and incubated at 37 °C for 3 hours. 200 μg of salmon sperm DNA and 30 μL of water were added prior to purification using a Qiagen PCR purification kit.

2.6.8 Southern blotting

Prior to southern blotting, isolated DNA (as described in Section 2.6.6) was digested with BamHI. The samples were then analysed on a NanoDrop 2000 Spectrophotometer, and an equal mass of DNA from each sample was loaded onto a 0.8 % w/v agarose gel containing ethidium bromide. Biotinylated molecular weight markers (NEB) were also loaded. The gel was run at 16 V overnight, and once sufficient separation of the samples was observed, the gel was rocked in 0.25 M HCl for 20 minutes to inefficiently hydrolyse the DNA and thereby improve transfer efficiency. The gel was then rocked in 0.4 M NaOH for 30 minutes. The semi-dry transfer apparatus was assembled on a layer of clingfilm (**Figure 5**). Four sheets of grade 3MM blotting paper (Sartorius Stadium Biotechnology) were soaked in 0.4 M NaOH, and air bubbles were excluded by rolling the paper flat. The gel was carefully placed on top and bubbles were rolled out. Biodyne B filter paper was wetted with water, briefly soaked in 0.4 mM NaOH, and placed on top of the gel. Four pieces of dry 3MM blotting paper followed by paper towels were stacked on top, and weights were applied to maintain pressure on the gel. The transfer was left overnight.

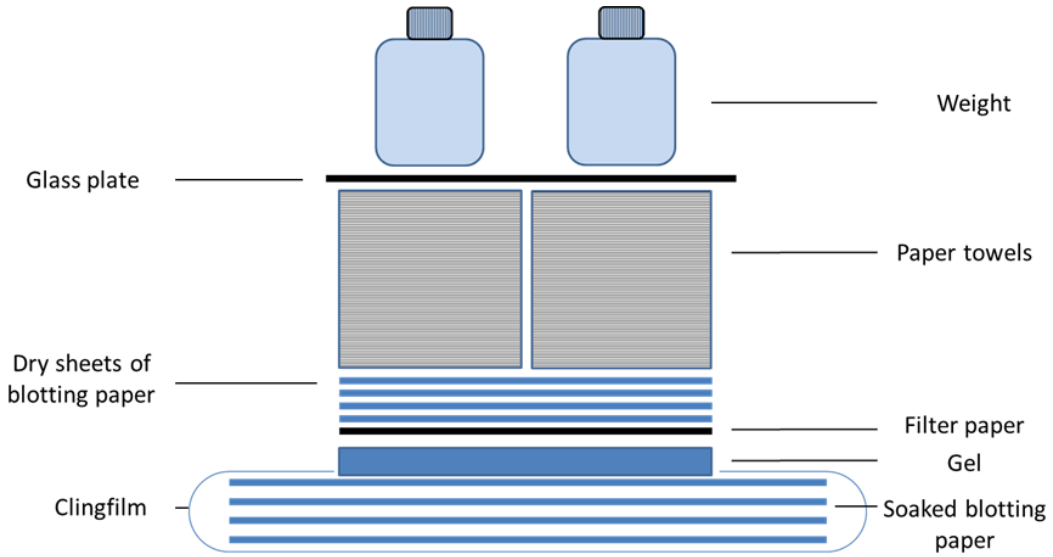

Figure 5: Schematic representation of the system used to transfer DNA from an agarose gel to filter paper.

The filter paper was washed in 4x standard saline phosphate EDTA (SSPE, pH 7.4; 750 mM NaCl, 800 mM NaH2PO4.H2O, and 20 mM Na2EDTA.2H2O) for 30 minutes. The filter paper was blocked in prehybridisation buffer (final concentrations of 1x Denhardt's solution, 200 μg/ml boiled salmon sperm DNA, 4x SSPE, 2 % w/v SDS, and 10 % w/v dextran sulphate) at 65 °C in a hybridisation oven for a two hours. The probe (Section 2.6.7) was then added to the prehybridisation buffer and allowed to hybridise at 65 °C overnight. The filter paper was washed twice in each of three wash buffers (2x SSPE; 2x SSPE, 1% w/v SDS; 0.1x SSPE) for 15 minutes at 65 °C. The filter paper was then incubated at room temperature in Odyssey block (LI-COR Biosciences) containing 1.2 % w/v SDS for 30 minutes, followed by a 30 minute incubation in Odyssey block, 1.2 % w/v SDS, and Streptavidin-IRDye 800 CW (LI-COR Biosciences). The filter paper was washed in PBST three times, and visualised using a LI-COR imaging system.

2.7 Cellular genome manipulation

2.7.1 CRISPR/Cas9 sgRNAs and plasmids

Clustered Regularly Interspaced Short Palindromic Repeats (CRISPR) and CRISPR-associated 9 (Cas9) were used to manipulate the *PRKDC* gene which encodes DNA-PKcs in RPE-1 cells. Single-guide RNAs (sgRNAs) creating a truncation within the

kinase domain (in the 83rd exon at approximately the 11782nd nucleotide of the coding sequence) of the *PRKDC* gene were designed and provided in the plasmid pD1301-AD as a kind gift by Horizon Biotechnology. pD1301-AD contains Cas9 under the CMV IE1 promoter and enhancer, and the sgRNAs were under the control of the U6 promoter. DasherGFP is also encoded as a selection marker. sgRNAs targeting the 2nd exon of PRKDC (cutting at approximately the 205th nucleotide of the coding sequence) were designed using the human genomic *PRKDC* sequence available on Ensembl (ENSG00000253729, www.ensembl.org). Exons which were potential targets for CRISPR were analysed for sgRNA binding sites using the Broad Institute sgRNA Designer (www.broadinstitute.org/rnai/public/analysis-tools/sgrna-design). This tool provides information on the predicted on-target efficiency and probability of off-target effects for each sgRNA. In addition, sgRNAs containing PAM or repetitive sequences were avoided. sgRNAs were commercially synthesised as complementary DNA oligonucleotides, which were annealed and cloned into PX458 under the control of the U6 promoter and adjoining the sgRNA scaffold using a Bbs1 restriction site. PX458 was created by the Zhang lab (Ran *et al*., 2013), and encodes Cas9 under the control of the chicken β-actin promoter and CMV enhancer. It also encodes EGFP for selection purposes. The guide RNA sequences and the plasmids that they were delivered in are shown in Table 6.

Name	Plasmid	sgRNA
PRKDC N-terminal sgRNA	PX458 (Cas9; EGFP)	TTAACTCTTTAGCAATGCCT
PRKDC Kinase sgRNA1	pD1301-AD (Cas9; GFP)	GATCACGCCGCCAGTCTCCA
PRKDC Kinase sgRNA2	pD1301-AD (Cas9; GFP)	CAGACATCTGAACAACTTTA

Table 6: The plasmids and sgRNAs used to induce mutations in *PRKDC* with CRISPR-Cas9

2.7.2 *Nucleofection, sorting, and isolation of CRISPR/Cas9 clones*

Transfection of RPE-1 cells with TransIT-LT1 is toxic, and so 8 μg of plasmids containing Cas9 and sgRNAs (Table 6) were nucleofected into RPE-1 cells (Section 2.2.2). Following nucleofection the cells were allowed to recover in a 10 cm dish in full media. After 48 hours GFP-positive cells were sorted into a well of a 6-well plate using an Astrios cell sorter. Once confluency was reached, the cells were seeded into a 6 cm dish

at a density of 500 cells per dish, and allowed to grow out into individual colonies. Once a sizeable colony was formed, trypsin was used to dissociate the cells from the dish so that a single colony could be picked and transferred to a well of a 96-well plate (this approach was taken because when cells were sorted individually into wells of a 96-well plate the RPE-1 cells did not survive). The clones were expanded, and the seeding of 500 cells per dish was repeated, and further sub-clones created. The expression of the protein of interest was analysed by immunofluorescence and immunoblotting.

2.8 Microscopy

2.8.1 Immunofluorescence

Coverslips with a diameter of 13 mm were sterilised in a 24-well plate by submerging in 70 % v/v ethanol for 10 minutes, and were subsequently washed twice in sterile PBS. Cells were seeded in standard growth medium onto sterile coverslips to be 60-70 % confluency at the time of fixation, unless 100% confluency was required for infection. Cells were fixed by aspirating the medium and then incubating in 250 mM pH 7.4 4-(2-hydroxyethyl)-1-piperazineethanesulfonic acid (HEPES) with 4 % w/v paraformaldehyde (PFA) at 4 °C, and then a further 10 minutes in 8 % PFA and 250 mM pH 7.4 HEPES. The coverslips were washed twice in PBS, permeabilised in 1 % v/v triton X-100 in PBS for 5 minutes, and washed twice more in PBS. 5 % w/v milk from powder (Premier Food Groups) in PBS was used as a blocking agent for 1 hour at room temperature on a rocking platform. Primary antibodies (Table 7) were diluted to their working concentrations in 1 % w/v milk in PBS, and 50 μL of the dilution was pipetted onto a sheet of Parafilm M (Bemis). The coverslips were placed sample-side down onto the antibodies, and incubated at room temperature in a humidified chamber in the dark for 1 hour. Following this incubation, the coverslips were washed three times in PBS, and then incubated for 30 minutes in 200 μL of fluorophore-conjugated secondary antibodies (anti-rabbit or anti-mouse conjugated to Alexa Fluor488 or Alexa Fluor546; Invitrogen) diluted 1:1000 in 1 % w/v milk. The plates were washed twice in PBS and once in water. Coverslips were mounted onto slides using 10 μL of mounting solution (25 % glycerol v/v, 0.1 M Tris pH 8.5, 10 % Mowiol 4-88 w/v containing 4',6-diamidino-2-phenylindole (DAPI)) and allowed to set in the dark overnight.

Samples were visualised and imaged using a Zeiss Pascal Confocal Microscope at 63x magnification through oil, and images were collected using Zeiss LSM Image Browser.

Antibody target	Source	Dilution
DNA-PKcs (monoclonal cocktail)	Thermo Scientific (MS423P1)	1:250
DNA-PKcs (N-terminus)	Abcam (ab1832)	1:250
PAXX	Sigma (**HPA045268)**	1:1,000

Table 7: Primary antibodies used in immunofluorescence microscopy

2.8.2 Electron microscopy

Samples were prepared as previously described (Hollinshead *et al*., 2012). 3.5 cm dishes were infected at an MOI of 4 on ice for 1 hour to synchronise the infection, before being moved to 37 °C. After 12 hours at 37 °C the cells were fixed in their dish using a fixation buffer comprising 0.5 % v/v glutaraldehyde in 200 mM sodium cacodylate buffer for 30 minutes, and washed in fresh fixation buffer. Secondary fixation was achieved in 1 % w/v osmium tetroxide and 1.5 % w/v potassium ferricyanide for 60 minutes. The samples were washed in distilled water and stained overnight in 0.5 % w/v magnesium uranyl acetate. The next day samples were washed again in distilled water, dehydrated in graded ethanol, and embedded in Epon resin in the dish. Ultrathin sections (typically 50-70 nm) were cut parallel to the dish and examined using an FEI Tecnai electron microscope with CCD camera image acquisition.

2.9 Immunoblotting

2.9.1 Preparation of whole cell lysates

Cells were scraped into the medium, and the suspension was centrifuged at 1900 g for 5 minutes. The supernatant was aspirated, and the pellet resuspended in PBS before centrifuging at 1900 g for 5 minutes. The supernatant was aspirated again, and the cells were lysed in 250-500 μL of lysis buffer (150 mM NaCl, 20 mM Tris-HCl (pH 7.4), 10 mM $CaCl_2$, 0.1% v/v triton X-100, and 10 % v/v glycerol) on ice for 30 minutes. When immunoblotting for phosphorylated proteins 10 mM sodium orthovanadate and 50 mM sodium fluoride were added to the lysis buffer to inhibit phosphatase activity, and cOmplete Mini EDTA-free protease inhibitors (Roche) were used to prevent protease

activity. After the 30 minutes the cell lysate was centrifuged at 16,000 g at 4 °C for 10 minutes to pellet genomic DNA. The supernatant was flash-frozen in liquid nitrogen and stored at -80 °C. Prior to loading onto a gel, a bicinchoninic acid (BCA) assay (Thermo Scientific) was used to determine protein concentrations, allowing for the equal loading of protein samples. 6x sample loading buffer (300 mM Tris-HCl (pH6.8), 12 % w/v SDS, 60 % v/v glycerol, 0.6 % w/v bromophenol blue, and 600 μM 2-ME) was added to the samples before they were heated to 94 °C for 5 minutes prior to electrophoresis.

2.9.2 Separating protein samples into cytoplasmic and nuclear fractions

To create separate cytoplasmic and nuclear protein samples for immunoblotting a NE-PER nuclear and cytoplasmic extraction kit (Thermo Scientific) was used. This kit allows for the lysis of the outer cell membrane and nuclear membrane independently, and therefore soluble protein from these compartments can be harvested separately.

2.9.3 Sodium dodecyl sulphate polyacrylamide gel electrophoresis (SDS-PAGE)

SDS polyacrylamide gels were created using a Bio-rad Protean III system. The running gel comprised of 12 % v/v polyacrylamide, 0.39 M Tris (pH 8.8), 0.1 % w/v SDS, 0.1 % w/v ammonium persulphate (APS), and 0.04 % w/v tetramethylethylenediamine (TEMED). The stacking gel comprised of 5 % v/v polyacrylamide, 0.13 M Tris (pH 6.8), 0.1 % w/v SDS, 0.1 % w/v APS, and 0.1 % w/v TEMED. Running buffer contained 2.5 mM Tris Base, 19.2 mM glycine, and 0.01 % w/v SDS. Samples were loaded in the wells in the stacking gel, and the system was run at 190 V for 55 minutes prior to analysis by immunoblotting.

2.9.4 Nu-PAGE

Precast 4-12 % bis-Tris gradient Nu-PAGE gels (Invitrogen) were used to blot higher molecular weight proteins. Gels were run in MES-SDS running buffer (Invitrogen) using the Novex Mini-Cell (Invitrogen) at 190 V for 50 minutes.

2.9.5 Semi-dry transfer

SDS-PAGE and Nu-PAGE gels were equilibrated in transfer buffer (20 % v/v methanol, 2.5 mM Tris Base, and 19.2 mM glycine) for 5 and 15 minutes respectively. Nitrocellulose membrane (GE Healthcare) and blot paper (BioRad) were soaked in the transfer buffer, and a stack was created comprising (from bottom to top) blotting paper, nitrocellulose membrane, the equilibrated gel, and another layer of blotting paper. Air bubbles were removed from the stack using a roller. To transfer the bottom of the stack was placed next to the positive electrode. The proteins were transferred from the SDS-PAGE gel to the nitrocellulose paper using a Trans-Blot Turbo semi-dry transfer machine (BioRad) at 25 V for 30 minutes. Protein was transferred from Nu-PAGE gels to nitrocellulose membrane using a Transblot SD semi-dry transfer cell (BioRad) for 26 minutes at 18 V.

2.9.6 Immunoblotting

Following transfer of proteins to nitrocellulose membrane, the membrane was blocked in 5 % w/v milk for 1 hour. The membrane was washed three times in PBS with 0.025 % v/v tween 20 (PBST), and incubated overnight at 4 °C in primary antibody (Table 8) diluted in PBST. After three washes in PBST the membrane was incubated for two hours in 5 % w/v milk containing horseradish peroxidase (HRP)-conjugated secondary antibodies (Table 8). The membrane was washed three times in PBST. Enhanced chemiluminescent (ECL) reagent (125 mM luminol, 0.4 mM curaric acid, 0.1 M Tris pH 8.8) was applied to the membrane, and the signal detected using developing film (Kodak or GE Healthcare) in a dark room using a film processor (SRX101A, Konica Minolta).

Target	Source	Dilution
DNA-PKcs (monoclonal cocktail)	Thermo Scientific (MS423P1)	1:3,000
DNA-PKcs (N-terminus)	Abcam (ab1832)	1:1,000
PARP-1	Abcam (ab6079)	1:1,000
ICP0	Abcam (ab6513)	1:2,000
Ku80	Santa Cruz (sc1483)	1:500
Ku70	Abcam (ab3114)	1:1,000
Tubulin	Millipore (05-829)	1:15,000
PAXX	Sigma (HPA045268)	1:1,000
HSV-1 VP22	Gift from G. Smith (AGV031)	1:20,000
Mouse antibody (HRP-conjugated)	Sigma (A4416)	1:10,000
Rabbit antibody (HRP-conjugated)	Sigma (A6154)	1:20,000
Goat antibody (HRP-conjugated)	Sigma (A5420)	1:20,000

Table 8: Antibodies and their respective dilutions used in western blotting

2.10 In vivo and ex vivo work

2.10.1 Mice

This research has been regulated under the Animals (Scientific Procedures) Act 1986 Amendment Regulations 2012 following ethical review by the University of Cambridge Animal Welfare and Ethical Review Body (AWERB). *Paxx*$^{-/-}$C57BL/6 mice and their WT counterparts were a kind gift from Professor Steve Jackson (Gurdon Institute, University of Cambridge). Mice were maintained under pathogen-free conditions. During experiments mice were weighed daily Mice set aside for breeding were not subsequently used in experiments. Mice were culled by dislocation of the cervical vertebrae.

2.10.2 Genotyping mice

Prior to experimentation the genotypes of the mice were confirmed by PCR. Genomic DNA was extracted from an ear clip by incubating it in 75 μL of alkaline lysis reagent (25 mM NaOH and 0.2 mM EDTA) at 95 °C for one hour. The sample was cooled to 4 °C, and 75 μL of neutralisation buffer (40 mM Tris HCl, pH 5) was added. 1 μL of the resultant solution was used as a template for PCR using HotStar Taq and the PAXX genotyping primers shown in Table 1 (Section 2.5.1).

2.10.3 Infection

Luciferase-expressing HSV-1 virus stocks were diluted in sterile PBS to a concentration of 2.5 x 10^7 plaque-forming units (PFU)/ml. 20 μL of the diluted stock was injected intradermally into each whisker pad of the mice to be infected, resulting in the delivery of 1 x 10^6 PFU per mouse. Mice to be left uninfected were injected with equivalent volumes of sterile PBS. Injections were carried out under isofluorane anaesthesia. All virus dilutions were back-titrated (*per* normal HSV-1 titration) to ensure that the inoculation doses were accurate.

2.10.4 Detecting luciferase activity using an in vivo imaging system (IVIS)

The mice were injected intraperitoneally with 150 μg of luciferin (Xenogen) in 10 μL of PBS per gram of bodyweight under isofluorane-induced anaesthesia. After 20 minutes an *in vitro* imaging system (IVIS) Lumina Series (Perkin Elmer) machine was used to detect the luciferase-catalysed oxidation of luciferin. Living Image software (Perkin Elmer) allowed for the quantification of light emitted in photons/second.

2.10.5 Isolation of cells from the spleen

The spleen of each mouse was harvested under sterile conditions, and they were kept separately on ice in PBS. Tissue was forced through a 70 μm cell strainer (Falcon) using a sterile microcentrifuge tube, and the filter was then washed 3 times with PBS. The resulting cell suspension was centrifuged at 400 g for 5 minutes at 4 °C. The supernatant was discarded and the pellet resuspended in BD Pharm Lyse (BD Biosciences) to lyse erythrocytes. The cells were washed twice by centrifuging at 300 g for 5 minutes at 4 °C in RPMI media containing 50 μg/mL of penicillin and streptomycin, and 10 % v/v FBS. The pellet was resupended in fresh media, and passed through a 70 μm pre-separation filter (Miltenyi). The cells were counted using trypan blue and an automated cell counter (Countess, Invitrogen) and resuspended to a concentration of one million cells per mL, and 6 mL was used per T25 flask.

2.10.6 Lymphocyte stimulation

A protein transport inhibitor cocktail (eBioscience) containing brefeldin A and monensin (used at final concentrations of 10.6 nM and 2 nM, respectively) were added directly to the media of all conditions to prevent degranulation of the lymphocytes and promote the retention of synthesised protein. Lymphocytes were stimulated by one of two methods. The primary method was the addition of a cell stimulation cocktail (eBioscience) directly to the media. This contained PMA and ionomycin (used at final concentrations of 81 nM and 1.34 μM, respectively). The second method of stimulation involved the addition of a synthesised section of the HSV-1 peptide gB2 (AnaSpec). This peptide consists of amino acids 498-505 of gB (SSIEFARL) and was certified as 97 % pure by high pressure liquid chromatography by the supplier. The gB2 peptide was used at concentrations within the range 10^{-7} to 10^{-6} M. Following the addition of the appropriate stimulant, lymphocytes were incubated at 37 °C, 5 % CO_2, and 3 % O_2 for four hours. Transport inhibitor cocktail was added simultaneously during PMA stimulation, but for gB stimulation the inhibitor was added one hour after the peptide was added. Following stimulation, cells were scraped from their flasks and washed twice in PBS and stained for flow cytometry (Section 2.10.8).

2.10.7 Isolation of cells from lymph nodes

Lymph nodes were harvested under sterile conditions, and placed on ice in PBS. Lymph nodes were forced through a 70 μm cell strainer (Falcon), which was then washed 3 times with PBS. The resulting cell suspension was centrifuged at 400 g for five minutes at 4 °C. The supernatant was discarded and the pellet resuspended in BD Pharm Lyse (BD Biosciences) to lyse erythrocytes. The cells were washed twice by centrifuging at 300 g for 5 minutes at 4 °C in PBS. The pellet was resuspended in PBS, and passed through a 70 μm pre-separation filter (Miltenyi). The cells were counted using trypan blue and an automated cell counter (Invitrogen).

2.10.8 Staining cells for flow cytometry

Cells were counted and resuspended to a concentration of 5 million cells/mL in PBS. Zombie Green dye (BioLegend) was diluted 1:400 in the cell suspension, and the

suspension was incubated at room temperature for 20 minutes in the dark. The cells were washed once in PBS at 300 g for 4 minutes, and the pellet resuspended in 100 μL of PBS. 2 μL of purified rat anti-mouse CD16/CD32 (Mouse BD Fc Block) was added to each sample at 4 °C for 5 minutes. Antibodies (Table 9) were added to perform surface staining, and incubated for 20 minutes in the dark at room temperature. The samples were then washed in 200 μL of PBS for 4 minutes at 300 g, resuspended in 4 % w/v PFA in PBS, and transferred to FACS tubes for analysis. Cells were analysed by flow cytometry using an LSR Fortessa.

Antibody	**Catalogue Numbers**	**Source**
Alexa Fluor® 647 Mouse IgG1, κ Isotype Ctrl	400155	BioLegend
CD19-BV421 (1D3)	562701	BD
CD3-APC (145-2C11)	553066	BD
CD3ε-BV605 (145-2C11)	100351	BioLegend
CD3ε-BV605 (145-2C11)	100351	BioLegend
CD4-APC-H7 (GK1.5)	560181	BD
CD44-BB515 (IM7)	564587	BD
CD45-PerCP (30-F11)	557235	BD
CD62L-APC-Cy7 (MEL-14)	104428	BioLegend
CD62L-APC-Cy7 (MEL-14)	104428	BioLegend
CD8α-APC-R700 (53-6.7)	564983	BD
CD8α-PE (53-6.7)	100708	BioLegend
CXCR5-APC-R700 (2G8)	565503	BD
GzmB-AF647 (GB11)	515406	BioLegend
IFNγ-PE (XMG1.2)	505808	BioLegend
TNFα-APC (MP6-XT22)	506308	Biolegend
NK1.1-BV421 (PK136)	562921	BD
NK1.1-BV605 (PK136)	108739	BioLegend
PD1 (CD279)-APC (J43)	562671	BD
PE Rat IgG1, κ Isotype Ctrl Antibody, κ Isotype Ctrl	400408	BD

Table 9: Antibodies used in the flow cytometry analysis of murine tissue

2.10.9 Isolation and culture of murine skin cells

WT C57BL/6, or WT or *Prkdc*$^{-/-}$ C129 mice were euthanised in a carbon dioxide chamber by increasing carbon dioxide concentration, and immediately dissected. The fur of the mouse was sterilised with 70 % v/v ethanol, and skin sections of approximately 1 cm^2 were taken from the armpit or scalp. These regions were preferential due to their relatively low levels of fat which can interfere with enzymatic digestion. Skin was stored in sterile phosphate buffer saline (PBS) on ice and then the tissue was chopped up into fine pieces using scalpels before digesting with 0.14 Wünsch U/mL of liberase (Roche) in 10 mL of DMEM/F12 media (Gibco) at 37 °C until the tissue became white and fibrous. The digested tissue was plated into 6 cm dishes and cultured in DMEM with 50 μg/mL penicillin-streptomycin and 15 % v/v FBS at 37 °C.

3 The role of PAXX in HSV-1 infection

3.1 Introduction

There are many interactions between proteins in the DDR and viruses. Our laboratory became specifically interested in the NHEJ machinery in this context following identification of the DNA-PK complex as an innate immune sensor of foreign intracellular DNA (Ferguson *et al*., 2012). These findings have since been confirmed by other labs (Li *et al*., 2016; Morchikh *et al*., 2017; Sui *et al*., 2017) and, along with the literature describing how other DDR proteins can affect innate immunity (Section 1.3.1) and contribute to DNA virus restriction (Section 1.2), led us to hypothesise that other NHEJ proteins might regulate innate immune responses to DNA viruses. Our laboratory identified PAXX as a cytoplasmic DNA-binding protein (B. Ferguson, unpublished data) and so, since any function of PAXX in infection is unknown, we aimed to establish whether PAXX regulates the host cell response to DNA virus infection.

For these experiments, HSV-1 was selected as a model virus because it is regulated by other members of the NHEJ complex, including XRCC4 and LIG4 (Muylaert and Elias, 2007) and has been established as a model system for studying innate sensors of intracellular, foreign DNA (Ferguson *et al*., 2012; Orzalli *et al*., 2015; Unterholzner *et al*., 2010). The primary aim of the experiments presented in this chapter is, therefore, to establish whether PAXX affects the HSV-1 infection cycle.

3.2 PAXX restricts production of infectious HSV-1 virions

To establish whether PAXX functions to regulate HSV-1 infection we infected RPE-1 cells in which the *PAXX* gene has been deleted by CRISPR/Cas9 (previously described, Ochi *et al*., 2015). Infectious virus was then titrated onto Vero cells to determine the production of plaque-forming units (infectious virions; PFU) by WT and *PAXX*$^{-/-}$ RPE-1 cells. RPE-1 cells were chosen because they are human epithelial cells which have retained epithelial characteristics despite immortalisation (Davis *et al*., 1995). Epithelial cells are naturally infected by HSV-1, and RPE-1 cells are also interesting in the context of HSV-1 because the ocular infection model through the cornea is frequently used in mouse models of HSV-1 infection (Kollias *et al*., 2015). Under the assumption that all

viable virions infect a cell, infection at MOI 4 should result in infection of over 98 % of cells according to the Poisson distribution (**Section 2.4.6**) (Fields *et al*., 2007). Therefore infection at MOI 4 results in single-step growth curves whereby virion production can be measured without considering confounding variables such as cell-to-cell spread. Infection at MOI 0.01 results in less than one percent of cells becoming infected (**Section 2.4.6**), and as such a multi-step growth curve is created whereby the amount of infectious virus produced is reliant upon secondary infection as well as virion production. Although I contributed towards the infections, titrations, and analysis, the growth curves shown here were primarily conducted by a colleague. WT or *PAXX*$^{-/-}$ RPE-1 cells were infected at an MOI of 0.01, 2, or 4, and the amount of infectious virus produced was quantified by titration on Vero cells (**Figure 6**). After 48 hours of infection

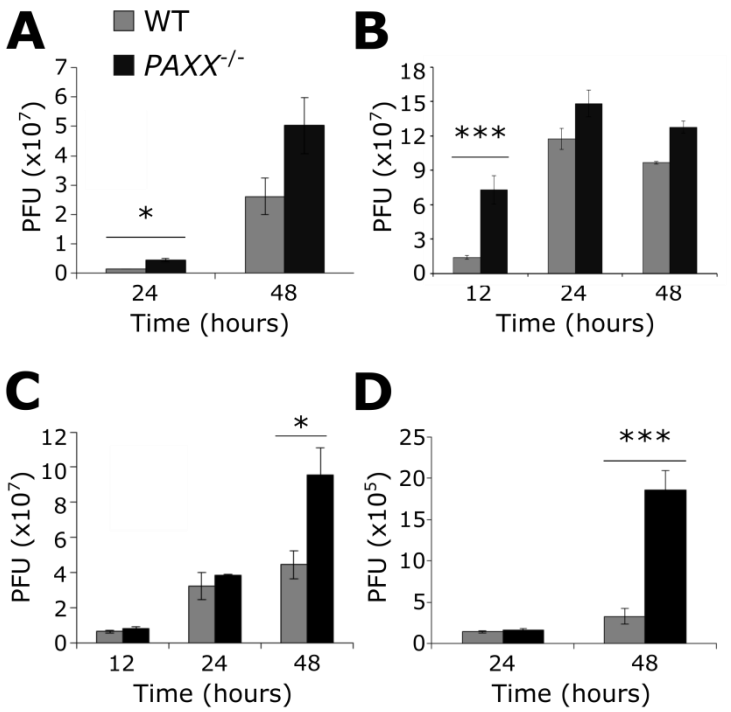

Figure 6: PAXX-deficient cells produce more infectious HSV-1 virions.

WT and *PAXX*$^{-/-}$ RPE-1 cells were infected with HSV-1 at an MOI of **A)** 0.01, **B)** 2, or **C)** 4 for the time indicated, and subsequently infectious virus was titrated onto Vero cells. **D)** WT and *Paxx*$^{-/-}$ MEFs were infected at an MOI of 0.01 for the indicated times, and infectious virus was titrated onto Vero cells. All data points are the mean of a triplicate, and the data are representative of at least three independent experiments. Error bars show intra-experimental mean +/- standard error of the mean (SEM), and statistical significance, calculated using the Student's t-test, is indicated using stars - * = $p<0.05$, *** = $p<0.01$.

at MOI 0.01, there were significantly more infectious virions in the *PAXX*$^{-/-}$ cells than in WT cells (**Figure 6A**). This phenotype was also observed after 12 hours at MOI 2 (**Figure 6B**), and 48 hours at MOI 4 (**Figure 6C**).

RPE-1 cells are derived from an immortalised cell line, and it is likely that mutations in key pathways will have arisen. This risk is amplified by the fact that *PAXX*$^{-/-}$ cells were clonally selected following the CRISPR/Cas9 protocol. As such growth curves were carried out in MEFs to complement the growth curves carried out in RPE-1 cells. Although immortalised, these MEFs have not been passaged as many times and are therefore less likely to have accrued mutations. The difference in infectious virion production in WT and *Paxx*$^{-/-}$ MEFs infected at an MOI of 0.01 was more significant than the difference observed in RPE-1 cells (**Figure 6D**), although WT cells had more advanced CPE (data not shown). Infection of MEFs with HSV-1 at MOI 4 induced early and advanced CPE, and so we decided that this experiment was not appropriate for investigating infectious virus production. These data suggest that HSV-1 infection of *PAXX*$^{-/-}$ human cells and *Paxx*$^{-/-}$ murine cells produces more infectious virions than infection of their WT counterparts.

3.3 HSV-1 genome replication is restricted in PAXX$^{-/-}$ cells

Having shown that PAXX reduces the titre of infectious HSV-1 virions following infection, we wanted to establish the mechanism responsible. PAXX is a core member of the NHEJ pathway (Section 1.1.2), components of which have already been shown to influence HSV-1 genome replication (Section 1.2.6), and so we hypothesised that PAXX may function to directly or indirectly restrict HSV-1 genome replication. To test this hypothesis, WT or *PAXX*$^{-/-}$ RPE-1 cells were infected at an MOI of 4 and total DNA (including cellular and viral DNA) was extracted at specified times *post* infection. This DNA was analysed by qPCR using TaqMan probes and primers which anneal to the promoter regions of human *GAPDH* and HSV-1 *ICP0* so that only genomic DNA, and not mRNA, would be amplified. We conducted two experiments - one with an expanded time course where each time *post* infection was only sampled once (n=1; **Figure 7A**) to get an overview of the dynamics of viral genome replication, and one at fewer times *post* infection in triplicate (n=3; **Figure 7B**) to allow for statistical analysis. HSV-1 genome

replication was not overtly different between WT and *PAXX*$^{-/-}$ cells at any time sampled during the first six hours (**Figure 7A**). However, after 8 and 12 hours of infection, WT cells reproducibly had statistically higher numbers of viral genomes per cell in than *PAXX*$^{-/-}$ cells (**Figure 7B**). 12 hours *post* infection there were approximately twice as many viral genomes in WT cells than in *PAXX*$^{-/-}$ cells. Quantification of viral genomes present in WT and *PAXX*$^{-/-}$ cells infected for 12 hours at MOI 0.01 was also attempted, but genome copy numbers were not high enough for the sensitivity of the assay. These data indicate that, in contrast to what may have been predicted from the growth curve data, PAXX does not restrict viral genome replication, and may in fact contribute to efficient replication.

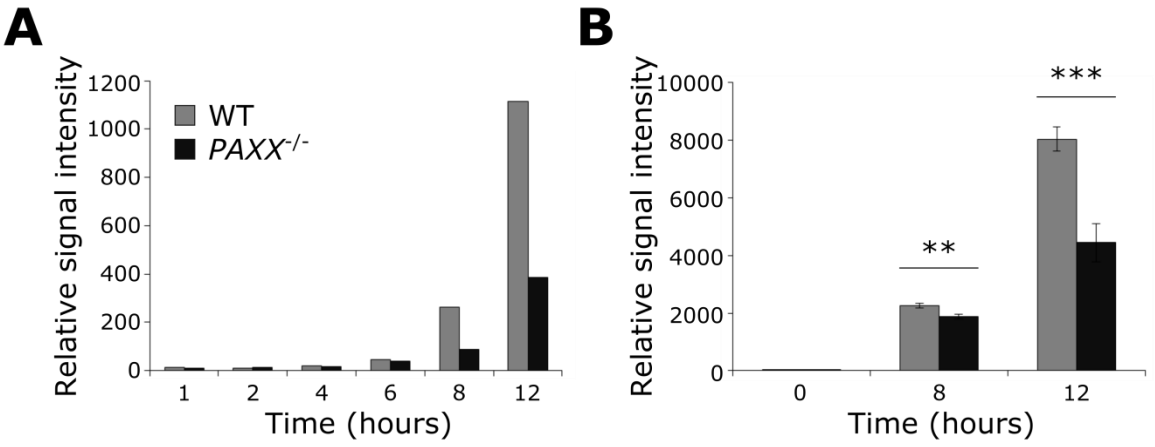

Figure 7: *PAXX*$^{-/-}$ cells support reduced HSV-1 genome replication.

WT and PAXX-/- RPE-1 cells were infected with HSV-1 at MOI 4, and the total DNA extracted at the indicated times *post* infection. qPCR was then used to determine relative levels of host and viral genome copy numbers, using *GAPDH* and *ICP0* respectively. Relative signal intensity is used because it would be incorrect to assume that this is equivalent to calculating the number of virions per cell. The experiment was either carried out where **A)** n=1 at more times *post* infection (representative of three experiments), or **B)** in triplicate at fewer times. Error bars show intra-experimental mean +/- SEM. Statistical significance, calculated using the Student's t-test, is indicated using stars - ** = $p<0.02$. Data is representative of three independent experiments.

3.4 PAXX may promote efficient endless HSV-1 genome formation during replication

Components of DNA damage repair machinery have previously been shown to influence the processing of HSV-1 genomes (Section 1.2.6), for example the formation of endless (either circular or concatemeric) genomes is enhanced by LIG4 and XRCC4 (Muylaert and Elias, 2007), and DNA-PK has also been proposed to contribute to HSV-1 genome circularisation and thereby induce latency (Smith *et al*., 2014). In an attempt to explain why *PAXX*$^{-/-}$ cells produce more infectious virions despite promoting viral genome replication, we hypothesised that PAXX contributes to processes which initially support genome replication, but which are subsequently deleterious. More specifically, PAXX may support the formation of the endless HSV-1 genomes required for replication, but PAXX binding may inhibit subsequent cleavage and packaging of the genome. Alternatively, increased circularisation could result in the induction of latency as has been proposed for DNA-PK. Another explanation is that PAXX aids early replication but also contributes towards the creation of abnormal genome structures (e.g. through ligation of viral genomes to the nicks and gaps in other copies of the genome) that may affect subsequent processes, such as the packaging of the viral genome into capsids. During HSV-1 genome replication, endless forms of the HSV-1 genome are produced in the nucleus, and cleavage of the endless forms into the mature, monomeric form occurs during packaging (Section 1.4.3). Therefore, observing the levels of the endless and monomeric forms in *PAXX*$^{-/-}$ cells would indicate whether PAXX is required for endless genome formation and whether the presence of PAXX affects genome packaging, thereby testing our hypotheses.

To experimentally investigate the formation of endless or monomeric genomes, southern blotting of the repetitive elements of restriction digested HSV-1 genomes can be used. Digesting the HSV-1 genome with BamHI creates DNA fragments named K, Q, and S (**Figure 8A**), amongst others. The Q and S fragments flank the long (U_L) and short (U_S) regions of the genome, respectively, and are formed of repetitive sequences (annotated with lower case letters in **Figure 8A**). The fact that they flank the U_L and U_S regions of the genome means that the ends of a linear genome will be either a Q or an S

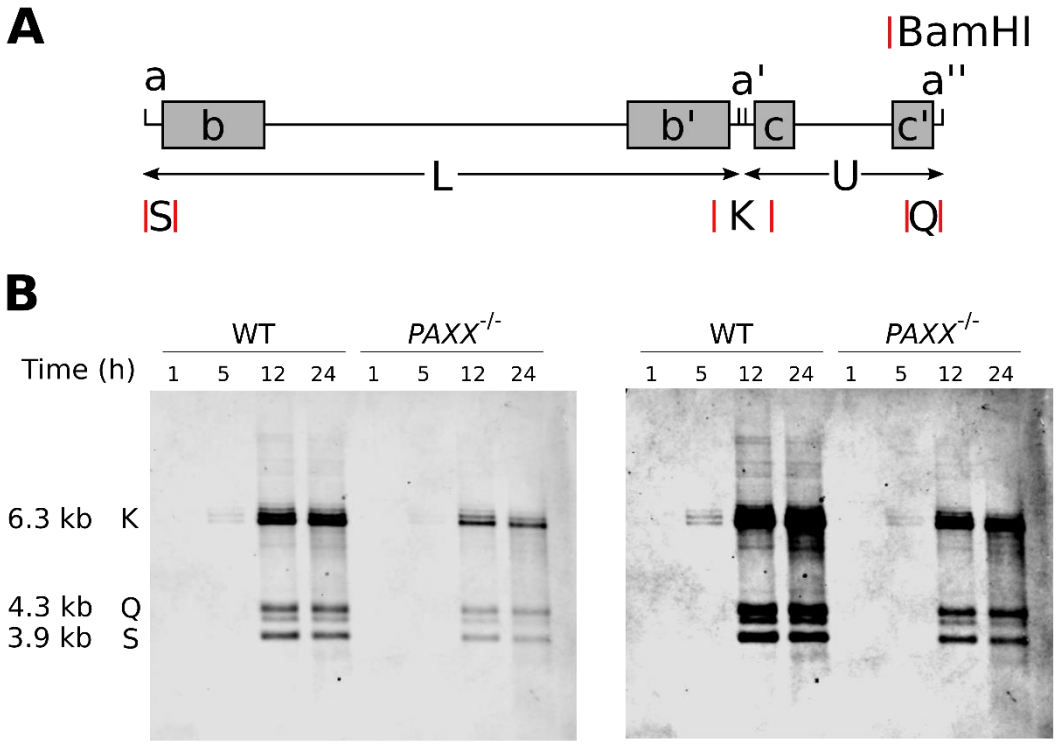

Figure 8: PAXX does not affect the proportion of endless HSV-1 genomes.

Southern blotting was used to determine the relative levels of monomeric and endless viral genomes. **A)** The linear structure of the HSV-1 genome, indicating repetitive elements a, b, and c (e.g. a, a', a'' consist of the same, repeated sequence). Relevant BamHI restriction sites are shown by a red line, and the resultant S, Q, and K fragments created following cleavage are labelled. **B)** WT and *PAXX*$^{-/-}$ RPE-1 cells were infected at MOI 4, and total cellular and viral DNA was isolated at specified times *post* infection. The DNA extracts were digested with BamHI, and analysed by Southern blotting. The same mass of DNA was added to each well, and visualisation was achieved using random primers raised against the K fragment. These random primers anneal to each of the S, Q, and K fragments of the HSV-1 genome because of the repetitive 'a' sequence. The positioning of the repetitive sequences means that in concatemeric or circular genomes the S and Q fragments combine to form additional K fragments. This means that the relative ratio of K fragments to total signal indicates the relative level of endless genome forms. Two different exposures of the same blot are shown, and the sizes of the S, Q, and K fragments are indicated. The data is representative of two independent experiments.

fragment. Within a concatemer, a circular genome, or in the middle of a monomer, the Q and S fragments combine to form the intra-genomic K fragment. The fact that the K fragment is composed of the Q and S fragments means that randomly-primed, biotinylated, ssDNA probes created against the BamHI K fragment can be used to detect

all three fragment types. Southern blotting with these primers can reveal the ratio of K fragments to Q and S fragments, which is an indicator of the proportion of endless genomes in the viral population. This method is therefore appropriate to identify potential defects in endless viral genome formation. It is important to note that the K fragment is present in both circular and concatemeric genomes, meaning that these species are not distinguishable by this assay, and they are instead considered together as endless genomes.

WT and *PAXX*$^{-/-}$ RPE-1 cells were infected with HSV-1 at MOI 4, and analysed by southern blotting using this method. No signal above background was detected in uninfected cells of either genotype (data not shown) or in cells infected for one hour (**Figure 8B**), demonstrating that the generated probe does not bind significantly to cellular genomic DNA and that the input virus DNA is below the detection limit of the assay. Only endless viral genomes could be detected five hours *post* infection, an observation previously reported early in HSV-1 infection (Muylaert and Elias, 2007), and WT cells had higher levels than *PAXX*$^{-/-}$ cells (**Figure 8B**). After 12 and 24 hours of infection both endless and monomeric forms of the viral genome could be detected, and the ratio between endless and monomeric species was similar for both genotypes. Although the total DNA loaded onto the gel prior to southern blotting was normalised, a lower signal was observed in the *PAXX*$^{-/-}$ cells, suggesting that viral DNA made up a lower proportion of total DNA, which would support the qPCR data quantifying viral genome numbers (Section 3.3). These data suggest that PAXX may be required for the efficient formation of endless genomes, and that PAXX defects may therefore result in less viral genome replication.

3.5 Virion number and structure does not appear to be affected by PAXX

Packaging is required for the cleavage of the HSV-1 genome (Heming *et al*., 2014; Muylaert and Elias, 2007), and therefore the creation of S and Q fragments observed by southern blotting suggest that efficient packaging is occurring. However, in some contexts packaging can be aborted after genome cleavage (Yang *et al*., 2011), and so we

wanted to explore the hypothesis that PAXX could affect packaging using an alternative method.

Intracellular virions can be categorised into 3 types based on their contents, as previously described (Desai *et al*., 1994). Example electron microscopy images of the three capsid types are shown in **Figure 9A**. Type B capsids are the first to be formed and are comprised of the virion capsid and of structural proteins. These structural proteins

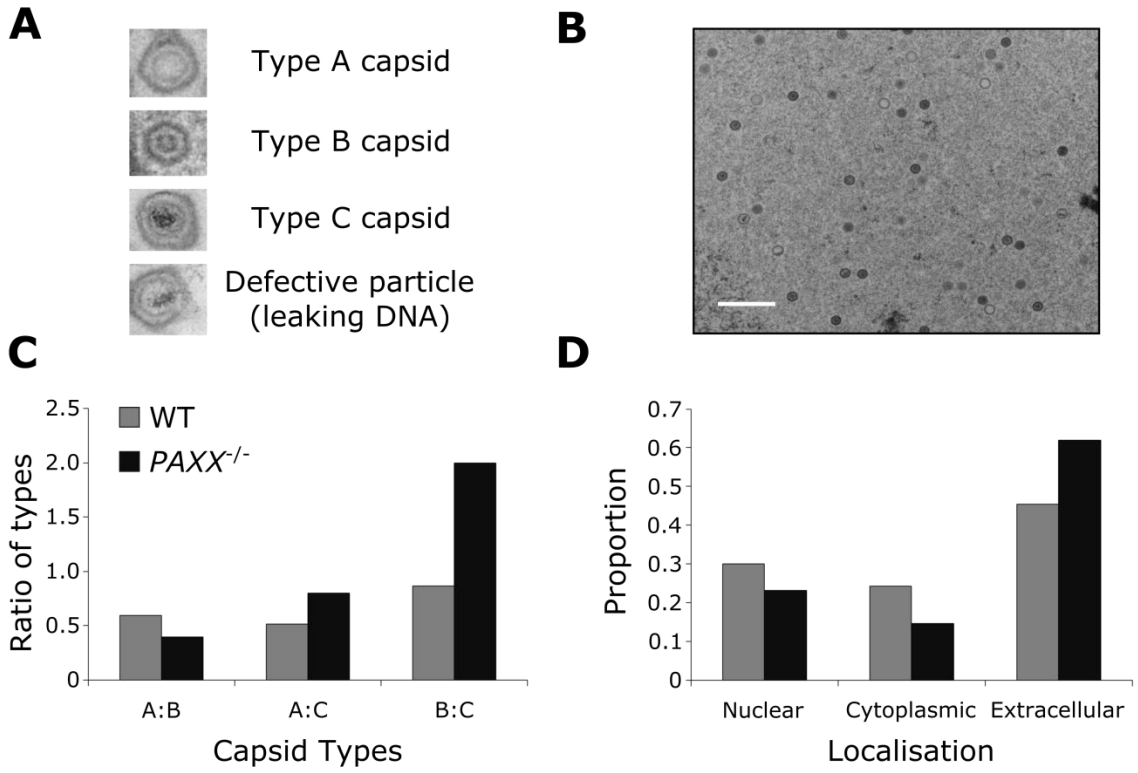

Figure 9: Electron microscopy does not reveal virion structural or localisation differences in the absence of PAXX.

WT or *PAXX*$^{-/-}$ RPE-1 cells were infected with HSV-1 at MOI 4 for 12 hours, fixed, and processed for electron microscopy imaging as described in Section 2.8.2. **A)** Example electron microscopy images of the different capsid types, as observed in RPE-1 cells. **B)** An example of a typical field of view within the nucleus of an infected RPE-1 cell following 12 hours of infection at an MOI of 4. The scale bar represents 0.5 μm. **C)** The relative ratios of the three capsid types to each other in the nucleus. **D)** The proportion of total virions found in each cellular location for each genotype. In total a minimum of 255 virions were counted per genotype. These virions were sampled from a minimum of 6 different cells per genotype. As explained in the main text, this experiment was only conducted once.

help in capsid assembly and genome packaging, and are lost as the genome is inserted into the capsid. The resultant DNA-containing capsids lacking structural proteins are termed type C capsids. Type A capsids are formed when genome packaging is aborted; the scaffold proteins are lost due to initiation of packaging, but the genome is not successfully packaged creating an empty capsid. We hypothesised that if packaging was affected by PAXX, this may be observable in changes in the ratio of these different capsid types inside cells during lytic HSV-1 infection.

To compare the number and genomic status of virions, WT and *PAXX*$^{-/-}$ RPE-1 cells were infected with HSV-1 at MOI 4 and observed using electron microscopy. Infection at MOI 4 was used to ensure that as many cells were infected as possible whilst maintaining consistency with experiments where previous phenotypes were observed. Samples were fixed after 12 hours because genome copy numbers were significantly different from eight hours onwards (**Figure 7**), and we wanted to leave sufficient time after this for packaging to occur. The fixed samples were processed and analysed in a blinded manner to avoid unconscious bias in data collection and analysis. The ratios of nuclear type A to type C, and type A to type B capsids were not strikingly different between genotypes (**Figure 9C**). However, *PAXX*$^{-/-}$ cells exhibited a small increase in the ratio of scaffold-only to DNA-containing virions (type B to type C), meaning that a smaller proportion contained DNA. The experiment was only done once and so its reproducibility is unclear, but this assay might indicate defects in the initiation of DNA packaging. This analysis is also limited by only observing a single plane through the capsid, because a capsid may be falsely determined to be type A if the plane misses DNA or structural protein. For this reason, capsids where the plane clearly does not pass through the middle were discounted. It is also true that this error should be consistent between samples, and so it is reasonable to assume that it should not affect analysis. Visibly defective particles (e.g. DNA trailing out of the capsid, as shown in **Figure 9A**) were not observed at a noteworthy frequency in either genotype.

In addition to considering the types of capsid present, we also analysed the localisation of capsids during infection of WT and *PAXX*$^{-/-}$ cells. A slightly higher proportion of virions were extracellular in *PAXX*$^{-/-}$ cells, but the difference was not

significant (**Figure 9D**). There were no notable differences in the proportion of virions in the nucleus or cytoplasm, and a comparison of total numbers of virions in each cellular location showed a similar pattern (data not shown). Together these data do not provide reason to suspect that PAXX influences the efficiency of viral genome packaging. This conclusion could be tested by extracting viral protein and viral DNA from purified virions, and comparing the protein:DNA ratio observed in WT and *PAXX*$^{-/-}$ cells. This would indicate what proportion of virions contain viral genomes.

3.6 PAXX may alter the proportion of cell-associated virions produced during infection.

We have shown that WT and *PAXX*$^{-/-}$ cells contain similar numbers of virions, and that the packaging of genomes into these virions is not defective in either genotype. It also showed that the localisation of the virions was similar between WT and *PAXX*$^{-/-}$ cells, but it does not address the fate of virions upon egress. Ku70 is important in the internalisation of the bacterium *Rickettsia conorii* (Chan *et al*., 2009; Martinez *et al*., 2005), a novel function for DNA repair proteins. We therefore decided to test whether PAXX affects the egress of HSV-1. WT and *PAXX*$^{-/-}$ cells were infected at an MOI of 0.01 or 4 for 24 hours and the cell-associated virions and virions in the growth medium were titrated separately. As is previously published (Sattentau, 2008), WT cells infected at both MOI 0.01 and MOI 4 had more infectious cell-associated virions than were present in the growth medium (**Figure 10A** and **B**). Interestingly, the ratio of cell-associated to free virus was much lower in *PAXX*$^{-/-}$ cells at MOI 0.01 (**Figure 10C**). This suggests that PAXX may function to regulate HSV-1 egress or binding of HSV-1 to the cell membrane. However, the data shown is only representative of two technical repeats of the experiment, and further repetition of the experiment is required before we base hypotheses on these conclusions. The conclusions should also be tested with other experiments such as viewing the egress of tagged virions using confocal microscopy, or measuring the rate of plaque growth when cells are infected in a semi-solid medium.

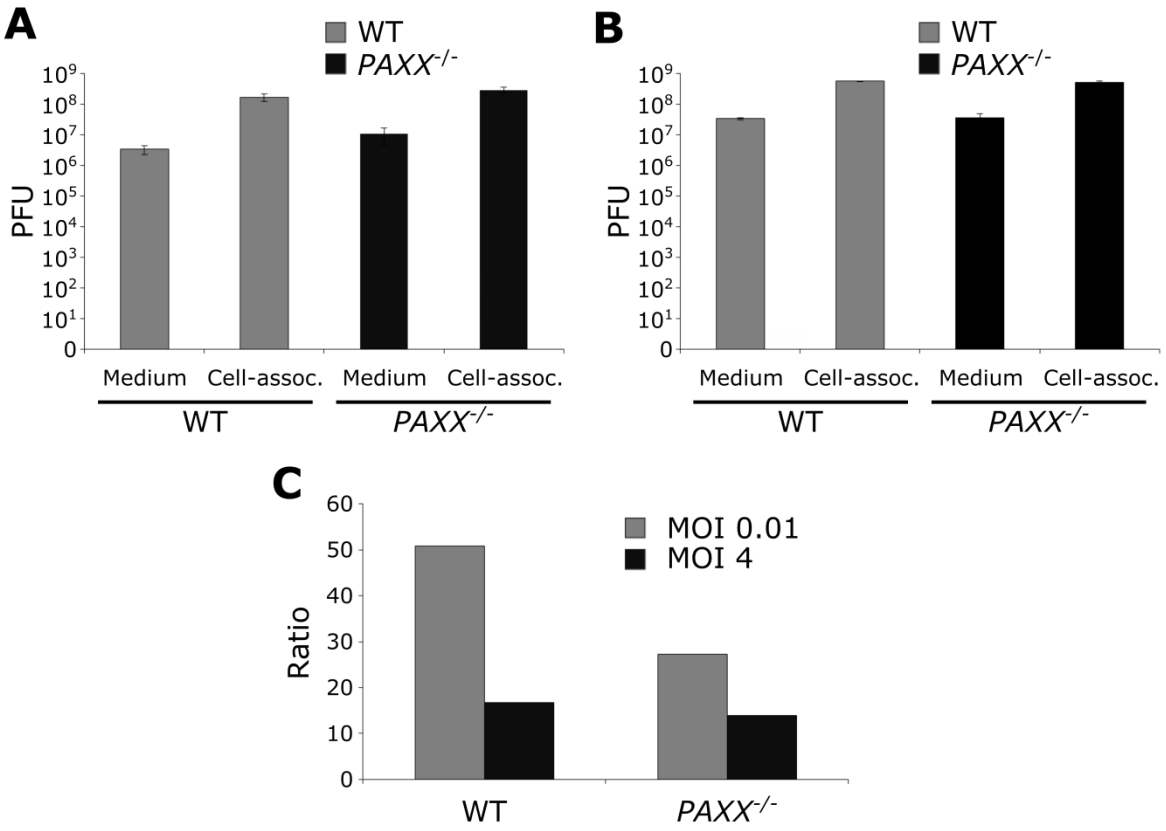

Figure 10: A lower proportion of virions from PAXX$^{-/-}$ cells remain cell-associated.

WT or *PAXX*$^{-/-}$ RPE-1 cells were infected with HSV-1 for 24 hours at an MOI of **A)** 0.01 or **B)** 4, and the growth medium and cell-associated virions were titrated separately. **C)** The ratio of cell-associated infectious virions to infectious virions in the growth medium. All data points are the mean of a biological triplicate, and error bars show intra-experimental mean +/- standard error of the mean (SEM). Statistical significance, calculated using the Student's t-test, is indicated using stars - * = $p<0.05$, *** = $p<0.01$. The data is representative of two technical repeats.

3.7 PAXX may affect innate immune signalling pathways

Some DDR proteins have already been linked to innate immune responses to exogenous DNA and viral infection (Section 1.3.1). DNA-PKcs and IFI16 have been shown to detect the HSV-1 genome and initiate transcriptional responses *via* the STING and IRF3 pathway (Ferguson *et al*., 2012; Orzalli *et al*., 2012; Unterholzner *et al*., 2010). It has been proposed that Mre11 is able to sense cytoplasmic DNA and induce IFN-I transcription, although cells lacking Mre11 did not respond differently to HSV-1 infection (Kondo *et al*., 2013). Following genotoxic damage the DDR machinery regulates many pathways of interest, including those controlling cell cycle regulation and programmed cell death (Jackson and Bartek, 2009). DNA damage and the DDR can also stimulate innate immune responses (Section 1.3.2). ATM has been shown to interact with NEMO to induce NF-κB signalling (Wu *et al*., 2006), and genotoxic damage has also been shown to activate IRF and IFN signalling (Brzostek-Racine *et al*., 2011; Kim *et al*., 1999). It is therefore a reasonable hypothesis that PAXX could also play a role in the responses to exogenous DNA stimuli.

Primary MEFs were used to explore potential roles for PAXX in innate immune responses to nucleic acids and HSV-1 because they are thought to be better models for innate immune responses than cell lines, and because they have previously been shown to increase transcription of IFN-I and cytokines in response to HSV-1 infection (Ferguson *et al*., 2012; Honda *et al*., 2005). Experiments were executed on passage one (P1) MEFs as it has been previously noted that MEFs lose intracellular DNA-stimulated NF-κB signalling at later passages (B. Ferguson unpublished observation; Chiu, Macmillan, & Chen, 2009). The MEFs were kindly generated by Dr Gabriel Balmus from WT and *Paxx*$^{-/-}$ embryos. The MEFs were either transfected with 2 μg/mL of concatenated DNA, transfected with 2 μg/mL of poly(I:C), infected with ΔICP0 HSV-1 at MOI 5, or left untreated (mock). The concentrations of nucleic acids and the MOI were chosen following successful stimulation with similar concentrations in previous experiments in our laboratory (Ferguson, unpublished data; Ferguson *et al*. 2012). Poly(I:C) was used as a positive control because it is a strong stimulator of innate immune responses and we expected that PAXX would not affect its ability to stimulate cells. Instead of using WT

HSV-1, ΔICP0 HSV-1 was used in experiments probing the innate immune response. This is because ICP0 significantly reduces the induction of IFN-I responses from infected cells, meaning that any differences in innate immune stimulation between MEF genotypes is masked by the inhibitory effects of ICP0 (Eidson *et al*., 2002b; Lin *et al*., 2004b; Mossman *et al*., 2001). Each condition was carried out in triplicate. Cells were harvested six hours after stimulation because we have previously observed strong responses at this time (Ferguson *et al*., 2012), the RNA was purified, and cDNA was created for gene expression analysis by qPCR (**Figure 11**). *Isg54* mRNA levels were measured to investigate stimulation of the IRF3-dependent signalling pathway because its transcription is IRF3-dependent (Navarro *et al*., 1998), *Nfkbia*, was measured because its activity is NF-κB-dependent (Rupec *et al*., 1999), and CXCL10 can be activated by both IRF3 and NF-κB (Spurrell *et al*., 2005). *Cjun* and *Cfos* expression was quantified to monitor MAPK signalling (Eriksson *et al*., 2007).

No differences were observed between cellular genotypes in the transcriptional response to ΔICP0 HSV-1 infection, suggesting that PAXX is not involved in innate immune sensing of HSV-1 in MEFs or that other DNA sensors such as cGAS create redundancy (**Figure 11**). Some differences were, however, noted following the transfection of DNA or RNA. Transfection of DNA lacking CpG motifs, which targets the STING-depending signalling pathways (Ishikawa and Barber, 2011), induced similar levels of *Cxcl10* and *Ifnb* in WT and *Paxx*$^{-/-}$ cells, but slightly lower *Isg54* and *Nfkbia* transcription was observed in *Paxx*$^{-/-}$ cells (**Figure 11A-D**). This may suggest that other DNA sensors such as cGAS create redundancy in some pathways but not in others. DNA stimulation did not induce a large change in expression of *Cjun* and *Cfos* in WT cells relative to mock treatment, but the difference was statistically significant (**Figure 11E** and **F**). In contrast, this response was completely abrogated in *Paxx*$^{-/-}$ cells, where *Cjun* and *Cfos* levels were not significantly different to those of mock-treated cells (**Figure 11 E** and **F**).

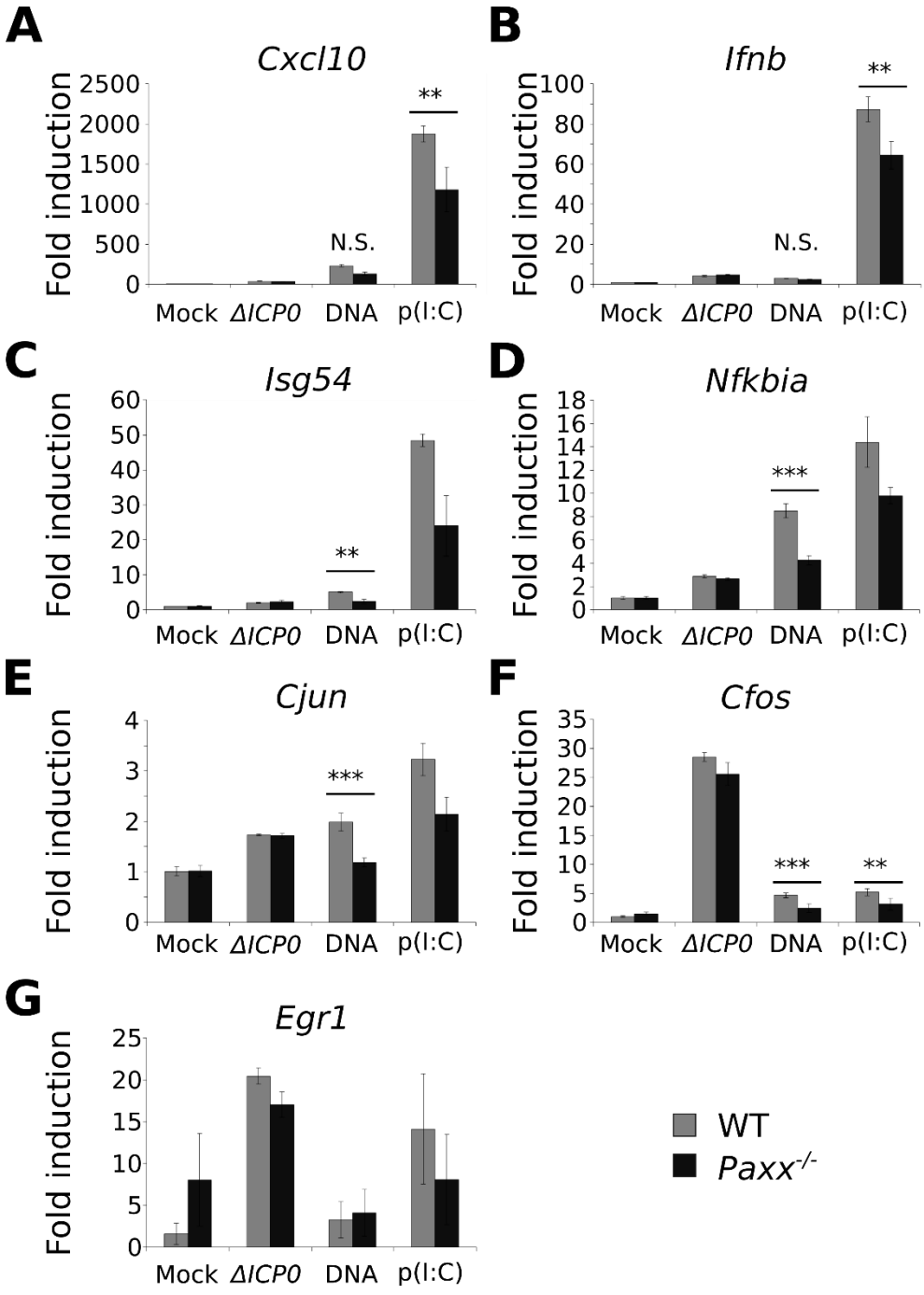

Figure 11: PAXX may affect innate immune signalling pathways in MEFs.

MEFs were infected with ΔICP0 HSV-1 at MOI 5, or stimulated with 2 μg/mL of concatenated DNA or poly(I:C). RNA was extracted six hours *post* infection. RNA was converted to cDNA, and relative expression levels of **A)** *Cxcl10*, **B)** *Ifnb*, **C)** Isg54, **D)** *Nfkbia*, **E)** *Cjun*, **F)** *Cfos*, and **G)** *Egr1* were analysed by qPCR and normalised to *Hprt*. All data points are the mean of a triplicate, and data is representative of three independent experiments. Error bars show intra-experimental mean +/- SEM, and statistical significance was calculated using the Student's t-test, and some instances of statistical significance was indicated using stars - * = <0.05, ** = p<0.02, *** = p<0.01.

Perhaps surprisingly, following the transfection of poly(I:C), an RNA mimetic that stimulates intracellular RNA PRRs, no differences were observed in *Nfkbia*, *Isg54* or *Cjun* transcription, but *Cxcl10* and *Cfos* levels were significantly higher in WT versus *Paxx*$^{-/-}$ cells (**Figure 11**).

Together these data suggest that PAXX may be required for innate responses to nucleic acids. These were most notable in response to DNA stimulation, but differences were also observed following poly(I:C) stimulation. However, no difference was observed in the response of different cellular genotypes to ΔICP0 HSV-1 infection.

3.8 RPE-1 cells do not initiate responses to DNA stimulation or ΔICP0 HSV-1 infection

We hypothesised that the defects in innate signalling observed in *Paxx*$^{-/-}$ MEFs could explain the increased production of infectious virus in these cells, and that innate immune signalling defects could also explain why *PAXX*$^{-/-}$ RPE-1 cells produce more infectious HSV-1 virions (**Figure 6**). Although immortalised with hTERT, RPE-1 cells retain epithelial characteristics and are not cancer-derived and so are less likely to have as many mutations in innate immune signalling pathways as other cell lines (Davis *et al*., 1995). We therefore decided to test whether these cells were suitable for studying the innate immune response. Several pilot experiments were carried out to characterise the innate immune response to intracellular nucleic acids and HSV-1 in WT RPE-1 cells. Cells were infected with ΔICP0 HSV-1 at an MOI of 4, or stimulated by transfecting 5 μg/mL of DNA or poly(I:C). Higher concentrations were used than in the experiments with MEFs because we knew that the transfection efficiency of RPE-1 cells is low, and because we expected responses to be weaker. RNA was harvested and mRNA expression was analysed by qPCR. DNA stimulation and ΔICP0 HSV-1 infection did not induce an increase in innate immune signalling pathways (**Figure 12**). Although poly(I:C) was able to induce *ISG54* and *CXCL10* transcription (**Figure 12A** and **E**), the fold-increase was considerably lower than would normally be expected. Although poor stimulation by DNA or poly(I:C) could be explained by poor transfection efficiency, this

does not explain the poor response following infection with ΔICP0 HSV-1. As such it is likely that RPE-1 cells are not strongly stimulated by nucleic acids.

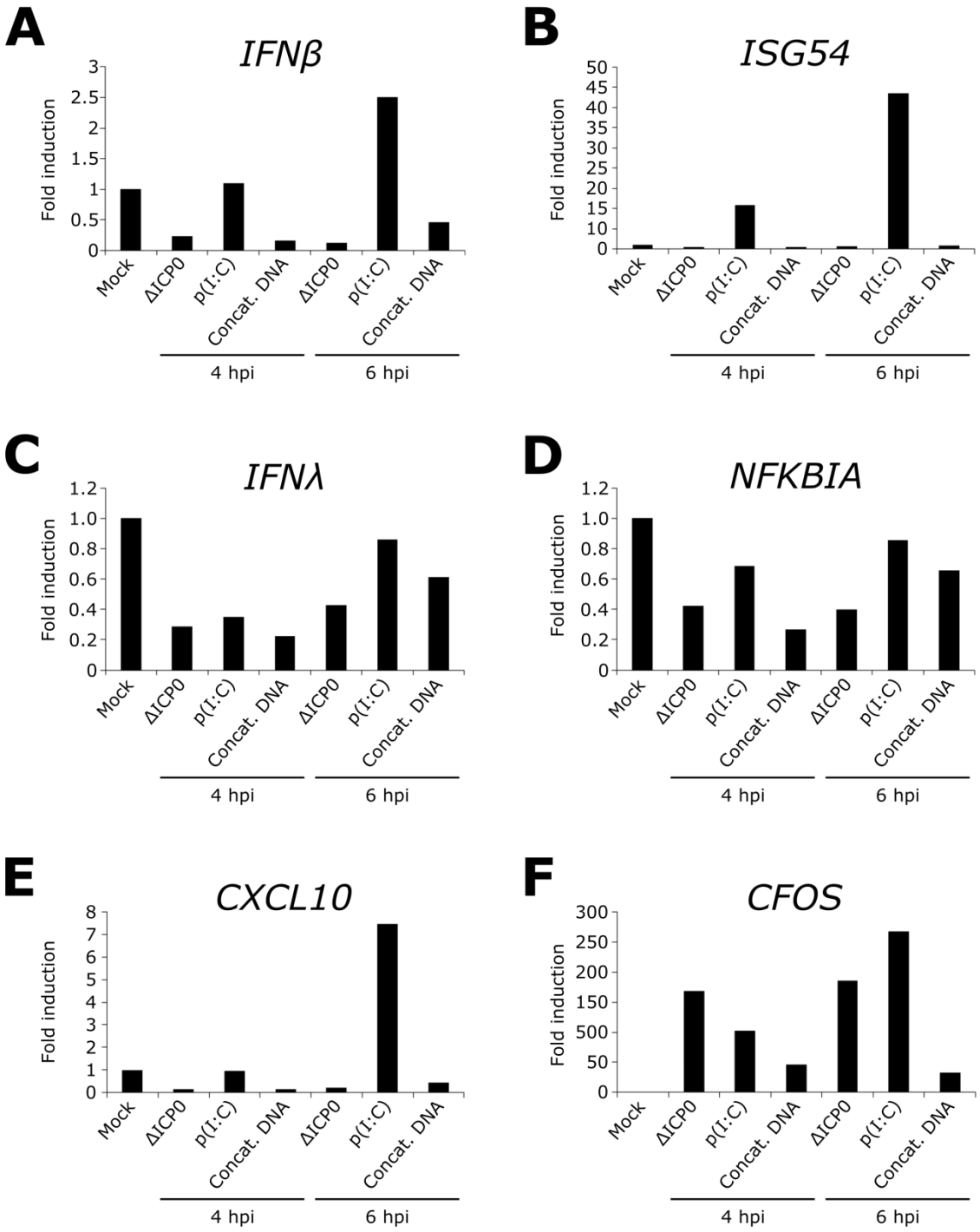

Figure 12: RPE-1 cells are not stimulated by infection or nucleic acid transfection.

WT RPE-1 cells were infected with ΔICP0 HSV-1 at MOI 4, transfected 5 μg/mL with linear DNA, transfected with 5 μg/mL of poly(I:C), or left untreated (mock). After 4 and 6 hours of infection or stimulation, the cells were harvested for RNA. qPCR was used to analyse gene expression of **A)** *IFNβ*, **B)** *ISG54*, **C)** *IFNλ*, **D)** *NFKBIA*, **E)** *CXCL10*, and **F)** *CFOS*, all relative to *GAPDH*. These data are representative of three independent experiments.

3.9 PAXX does not affect the expression of the HSV-1 genes tested

Although we were unable to consistently stimulate RPE-1 cells, we remained interested in potential roles of PAXX in the innate response to DNA and viral infection, and the effects that these may have on HSV-1. Reduced expression of EGR1, a MAPK transcription factor, reduces lethality of HSV-1 infection in mice (Chen *et al*., 2008), and EGR1 is able to bind to the promoter region of *ICP4* and *ICP22* and repress their expression (Bedadala *et al*., 2007). Following our observation that some MAPK signalling pathways are abrogated in *Paxx*$^{-/-}$ MEFs, we hypothesised that PAXX may indirectly affect *ICP4* and *ICP22* expression. As a control we also looked at expression of the immediate-early gene *ICP27*. WT and *PAXX*$^{-/-}$ cells were infected at MOI 5 for 4 or 8 hours, RNA was isolated, and qPCR was used to determine relative levels of viral gene transcripts during infection of RPE-1 cells. These times were selected so that early gene expression could be observed, and because we knew that replication started earlier than 8 hours *post* infection and so late gene expression should be observed. Only small differences were observed in *ICP27* or *ICP4* gene expression between WT and *PAXX*$^{-/-}$ cells at either time point, with *ICP27* expression slightly higher in KO cells, and *ICP4* expression higher in WT cells (**Figure 13A** and **B**).

Following our observation in Section 3.3 that *PAXX*$^{-/-}$ cells produce fewer viral genomes, we were also interested in late viral gene expression. Some HSV-1 genes, termed true (γ2) late, are only expressed after viral genome replication. We hypothesised that the expression of these genes may be lower in *PAXX*$^{-/-}$ cells. The expression of *gB* (γ1 late) and *US11* (γ2 true late) genes were unaffected by PAXX (**Figure 13C**). These data suggest that HSV-1 gene expression is unaffected by PAXX, and that the increased viral genome replication in WT cells does not manifest itself in late gene transcription.

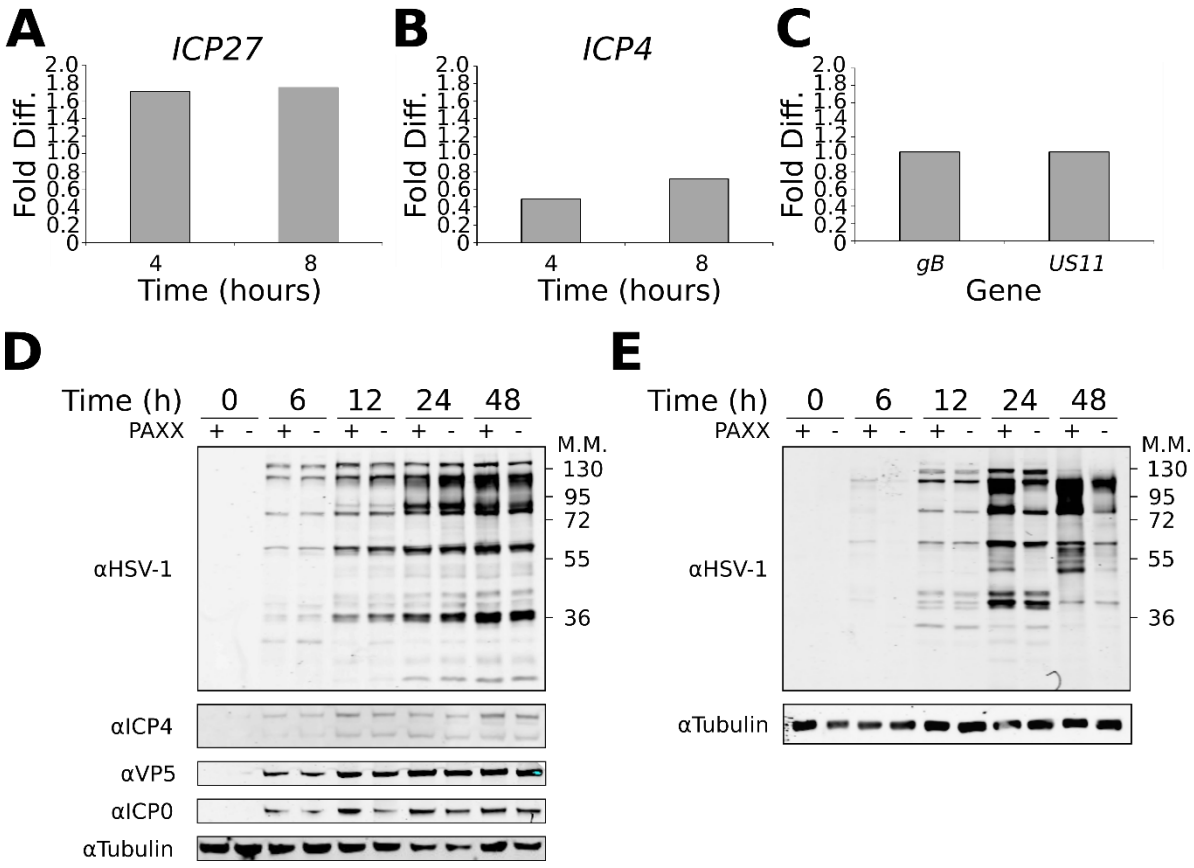

Figure 13: HSV-1 gene expression is unaffected by PAXX.

WT and *PAXX*$^{-/-}$ RPE-1 cells were infected with HSV-1 at an MOI of 5, and the RNA harvested after 4 or 8 hours. The gene expression of the immediate-early genes **A)** *ICP27* and **B)** *ICP4*, **C)** the γ1 late gene *gB*, and the γ2 true late gene *US11* were analysed by qPCR, and calculated relative to *GAPDH* expression. Samples were taken at four and eight hours after infection with the exception of *gB* and Us11 which were only sampled after eight hours. All data points show the fold increase in expression in *PAXX*$^{-/-}$ cells relative to WT cells, calculated from the mean of a triplicate, and data is representative of three experimental repeats. **D)** WT and *PAXX*$^{-/-}$ RPE-1 cells or **E)** WT or *Paxx*$^{-/-}$ MEFs were infected at an MOI of 1 and harvested at specified times *post* infection. Anti-HSV-1, anti-ICP0, or anti-ICP4 primary antibodies were used. Tubulin was used as a loading control in both cases. The data in **D)** was produced in collaboration with a colleague (I created the samples, and they did the western blotting). The data in **E)** was produced by a colleague. Both **D)** and **E)** are representative of three independent experiments.

3.10 PAXX may affect viral protein levels in MEFs, but not in RPE-1 cells.

By quantifying gene transcripts we have shown that there are no differences in viral gene expression in WT or *PAXX*$^{-/-}$ cells, but *post* transcriptional regulation means that this does not necessarily represent viral protein levels. To complement the analysis of viral gene expression a colleague investigated whether PAXX affects viral protein production (**Figure 13D** and **E**). For these experiments WT and *PAXX*$^{-/-}$ RPE-1 cells were infected with HSV-1 at MOI 1, and lysed at various time points *post* infection for immunoblotting. A polyclonal antibody raised against HSV-1 virions was used which is likely to recognise primarily capsid proteins, creating a bias towards late proteins. We also used antibodies recognising ICP4, VP5, and ICP0. There was no difference in expression of any of these genes during infection of RPE-1 cells (**Figure 13D**). However, we did observe less HSV-1 protein expression in *Paxx*$^{-/-}$ MEFs relative to their WT counterparts (**Figure 13E**). These data suggest that PAXX does not affect protein production in RPE-1 cells, but that PAXX may function to regulate HSV-1 protein production in MEFs.

3.11 PAXX localisation changes during HSV-1 infection

So far this chapter has focussed on defining PAXX as a restriction factor for HSV-1 and attempting to explain how this protein reduces the production of infectious HSV-1 virions. HSV-1 has, however, evolved to interfere with the function of many cellular restriction factors (Section 1.4.4), and so we hypothesised that HSV-1 may also regulate PAXX. This hypothesis is especially interesting given the observation that HSV-1-induced inhibition of the DDR may be a contributory factor towards the development of Alzheimer's Disease (De Chiara *et al*., 2016; Itzhaki, 2014). The NHEJ protein DNA-PKcs restricts HSV-1 and is degraded during during infection (Lees-Miller *et al*., 1996; Parkinson *et al*., 1999), so we therefore decided to investigate whether PAXX is also degraded during HSV-1 infection. To investigate whether HSV-1 degrades PAXX, U2OS cells were infected with WT HSV-1 at MOI 10, the cells were lysed at various time points *post* infection, and the nuclear and cytoplasmic fractions were separated prior to

immunoblotting (**Figure 14A**). U2OS cells were used because PAXX localisation during DSB repair has previously been investigated in these cells (Ochi *et al*., 2015). Antibodies against tubulin and PARP-1 were used as cytoplasmic and nuclear markers respectively to ensure that fractionation was effective, and an antibody against the HSV-1 protein VP22 was used to demonstrate productive HSV-1 infection. In uninfected cells PAXX was observed in both the nucleus and the cytoplasm, although the nature of the fractionation means that no conclusions can be drawn on relative amounts. Eight hours *post* infection a large reduction in the amount of nuclear PAXX was observed despite cytoplasmic levels remaining unaffected. A similar pattern was observed after 16 hours. Interestingly, overall levels of PAXX appeared to be unaffected (**Figure 14B**)

The cytoplasmic and nuclear fractionation kit used for the creation of the samples for immunoblotting primarily recovers soluble proteins, and the recovery of DNA-bound proteins is inefficient (ThermoFisher Scientific, 2017). It is therefore possible that if PAXX is directly or indirectly bound to the HSV-1 genome, less nuclear PAXX would be recovered. We therefore wanted to confirm our observations using confocal microscopy. U2OS cells were infected with a recombinant HSV-1 virus which encoded the capsid protein VP26 tagged with YFP, and lacked the protein gE. gE forms part of the HSV-1 IgG Fc receptor, and its absence prevents formation of the complex and reduces nonspecific binding of the primary and secondary antibodies (Bell *et al*., 1990). 16 hours *post* infection at MOI 1 over 80 % of cells exhibited a change in the localisation of PAXX from a nuclear (as observed by the DAPI stain and previously described by Ochi *et al*., 2015) to dispersed distribution, as compared with about 5 % of uninfected cells (**Figure 14D**). Of the 5 % of uninfected cells with dispersed PAXX staining, the majority had morphology or DAPI-staining which indicated that the cells were probably undergoing cell division, for example nuclear breakdown (**Figure 14C**), although this was not quantified. Throughout infection the proportion of cells in which PAXX distribution has changed increases (**Figure 14D**). These data support the observations made using immunoblotting, and suggest that HSV-1 infection induces the distribution changes of PAXX.

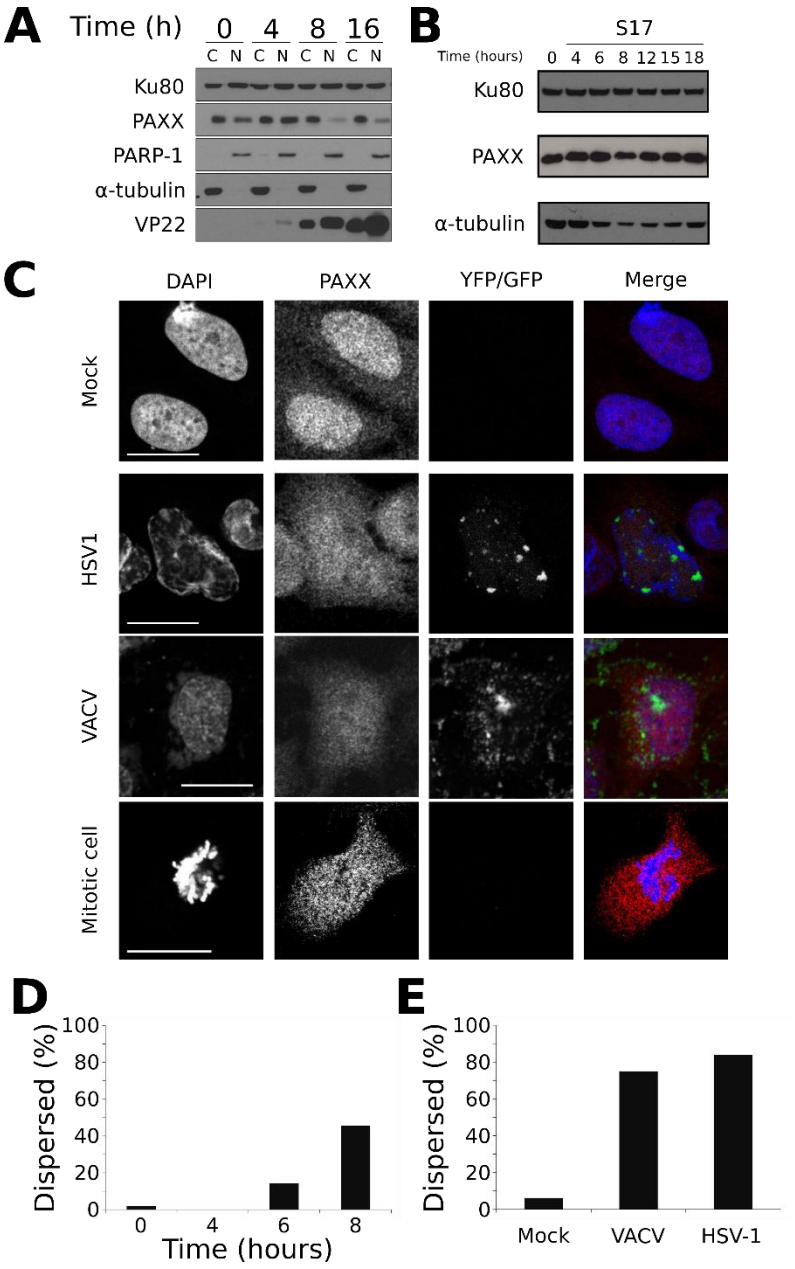

Figure 14: The distribution of PAXX changes during viral infection.

A) U2OS cells were infected at an MOI of 10. Cells were harvested at the indicated timepoints, and the cytoplasmic (C) and nuclear (N) fractions separated as described in section 2.9.2 Western blotting was used to observe PAXX. PARP-1 and tubulin controlled for fractionation, and VP22 demonstrated successful infection. Ku80 was used as a loading control. NI = not infected**. B)** U2OS cells were infected as in A), but protein samples were not fractionated so that overall levels of PAXX could be ascertained. **C)** U2OS cells were infected with ΔgE VP26-YFP HSV-1 or A5-GFP VACV at an MOI of 1 for 16 hours and analysed by immunofluorescence. Scale bars denote 20 μm. **D)** U2OS cells infected with ΔgE VP26-YFP HSV-1 at an MOI of 1 were fixed and stained for immunofluorescence. A minimum of 100 cells were counted, and the percentage of all cells that had dispersed, cytoplasmic PAXX staining was calculated. **E)** U2OS cells were infected with ΔgE VP26-YFP HSV-1 or VACV at an MOI of 1 for 16 hours, and processed and counted as in D). The data in this figure is representative of three independent experiments.

To investigate whether the nuclear localisation of the viral genome is important in the induction of PAXX distribution changes, we wanted to investigate whether a virus which replicates in the cytoplasm also induces these changes. Vaccinia virus (VACV) is a member of the *Poxviridae* family, and it replicates its dsDNA genome in the cytoplasm, making it a useful model for testing whether nuclear entry of the viral genome is required to trigger PAXX dispersal Interestingly, infection of U2OS cells with VACV at MOI 1 for 16 hours was also able to induce distribution changes of PAXX (**Figure 14E**). These data suggest that PAXX distribution changes are not specific to HSV-1, and that the trigger might be the genome of the viruses themselves.

3.12 Stimulation with DNA may be sufficient to induce changes in PAXX localisation

The loss of PAXX from the nucleus observed during HSV-1 and VACV infection could be actively induced by the virus, or could represent a cellular response to the infection. It has been reported that XLF, a NHEJ protein with homology to PAXX, translocates from the nucleus to the cytoplasm following DNA damage (Liu *et al*., 2015). We therefore hypothesised that changes in PAXX localisation could occur following the detection of the HSV-1 genome, and that the detection of any DNA with free ends may trigger this response. To test this hypothesis, we transfected U2OS cells with linear DNA, the pcDNA3.1 plasmid not encoding any protein, pcDNA3.1 encoding GFP, or poly(I:C). This experiment was designed to test whether DNA was sufficient to induce PAXX localisation changes, and whether any particular DNA structure was required. Poly(I:C) was intended as a control, although after observing differences in the innate immune responses of WT and *PAXX*$^{-/-}$ RPE-1 cells to poly(I:C) (**Figure 11**), we also recognised that poly(I:C) may also induce changes in PAXX. The transfection of all DNA species was sufficient to induce changes in PAXX localisation (preliminary data, **Figure 15**) but, poly(I:C) was unable to induce the response, suggesting that the induction of PAXX localisation changes is specific to DNA (**Figure 15**). This preliminary data suggests that the changes observed in the localisation of PAXX during HSV-1 infection may be induced by the detection of the viral genome. It is interesting that circular DNA that lacks free ends is sufficient to induce this response.

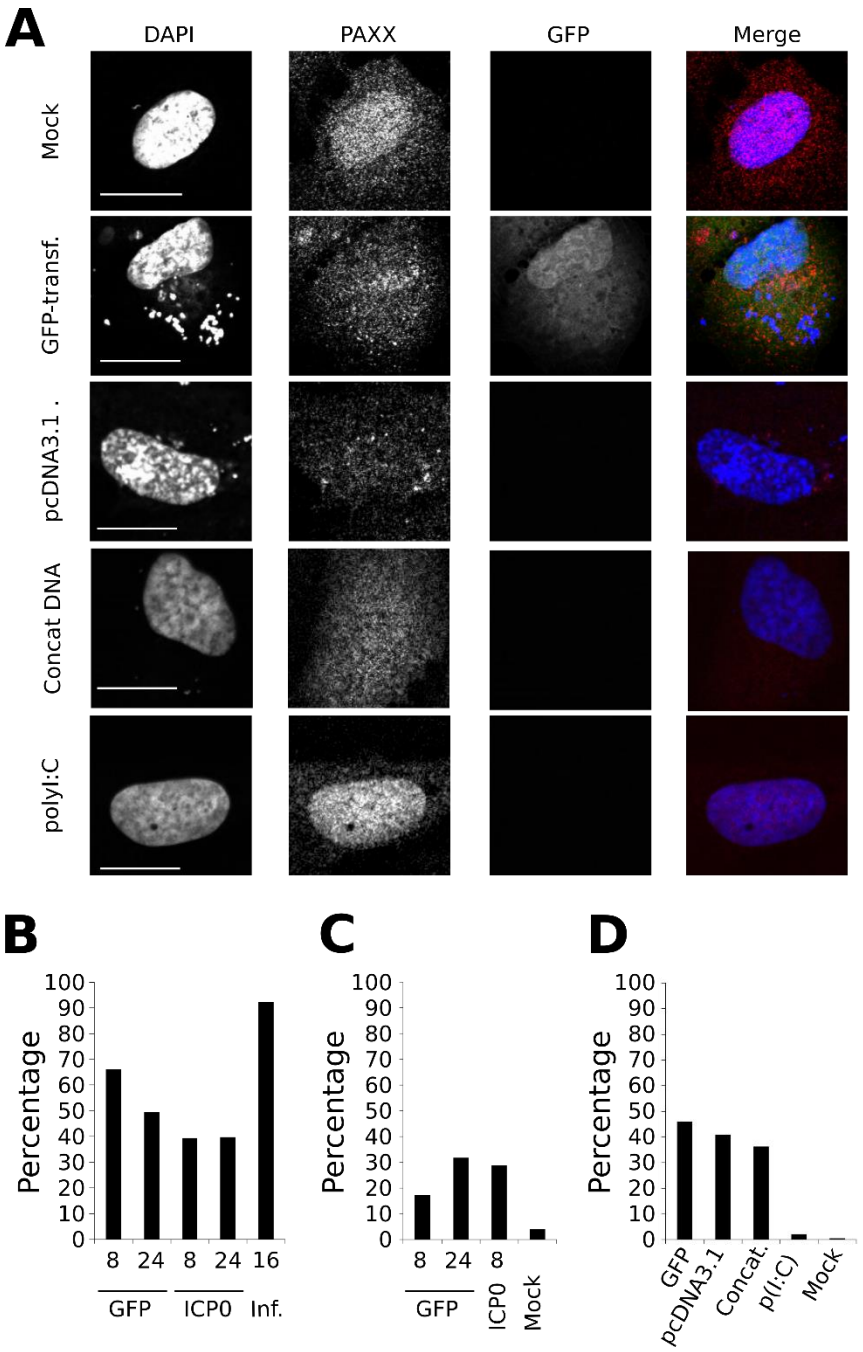

Figure 15: DNA is sufficient to induce distribution changes of PAXX.

A) U2OS cells were transfected with pcDNA3.1 expressing GFP, 'empty' pcDNA3.1, or polyI:C for 24 hours, and fixed and stained for immunofluorescence. **B)** GFP-tagged *ICP0* was transfected into U2OS cells, and immunofluorescence was used to quantify the percentage of GFP-positive cells in which PAXX distribution changed relative to cells that have either been infected or transfected with *GFP*. **C)** As in B), except cells displaying PAXX localisation changes are presented as a percentage of all cells. **D)** The percentage of all cells with dispersed PAXX was quantified 24 hours after the transfection of a plasmid expressing GFP-FLAG, an 'empty plasmid (pcDNA3.1), linear DNA, or poly(I:C). The data in this figure is representative of two independent experiments and is therefore only preliminary. The experiments need to be repeated.

3.13 Discussion

Many DNA repair proteins have been shown to influence HSV-1 infection (Section 1.2.6). The NHEJ proteins LIG4 and XRCC4 promote HSV-1 infection (Muylaert and Elias, 2007), while the Ku heterodimer and DNA-PKcs restrict viral infection (Parkinson *et al*., 1999; Smith *et al*., 2014; Taylor and Knipe, 2004). This chapter has explored the role of PAXX, a relatively recently discovered member of the NHEJ machinery, during HSV-1 infection. *PAXX*$^{-/-}$ human cells and *Paxx*$^{-/-}$ murine cells produce a larger titre of infectious virus than their WT counterparts, suggesting that PAXX restricts HSV-1 infection. We hypothesised that this restriction would be caused by PAXX directly binding the viral genome and inhibiting replication, or that PAXX may be involved in the activation of an innate immune response to DNA. We have tested both hypotheses and shown that surprisingly *PAXX*$^{-/-}$ cells produced fewer viral genomes during lytic infection than their WT counterparts, and that PAXX is not required for innate transcriptional responses to HSV-1 infection. Although we have not identified the mechanism which explains the restriction of HSV-1 by PAXX, we have uncovered a potential role of PAXX in MAPK signalling in MEFs. In addition we have observed that during HSV-1 infection PAXX is lost from the nucleus. Preliminary data suggests that the changes in subcellular localisation of PAXX can be induced by DNA species, but not by the RNA analogue poly(I:C). Although we have not determined a mechanism to explain how PAXX restricts HSV-1 we have made many interesting and novel observations, and we will now discuss the implications of these observations and the hypotheses that we can derive from them. However, it is important to note that characterisation of the *PAXX*$^{-/-}$ RPE-1 cells through genome sequencing and western blot analysis is required to strengthen these conclusions.

3.13.1 PAXX and the HSV-1 genome

The fact that *PAXX*$^{-/-}$ cells produce more infectious virus (**Figure 6**) but contain fewer viral genomes (**Figure 7**) is perhaps our most informative observation. These data indicate that viral genome replication is not disrupted by the presence of PAXX, and is, in fact, faster. It is not the first time that a DDR protein has been shown to both promote and restrict HSV-1 infection; ATR is recruited to viral replication centres and is essential

for efficient virus production, yet HSV-1 also inhibits its activity (Mohni *et al*., 2010, 2013).

Models explaining the mechanism of HSV-1 genome replication, more specifically whether rolling circle replication or recombination is responsible for creating concatemers, remain controversial (Smith and Weller, 2015; Weller and Coen, 2012). This is because factors from both the HR and NHEJ pathways have been shown to be beneficial to HSV-1 infection (Section 1.2.6). It is not clear whether HSV-1 balances competing NHEJ and HR functions, or whether these factors function in conjunction. It is interesting to hypothesise that HSV-1 recruits factors from different pathways to fulfil a custom function, thereby allowing for maximum control over the end result. It is conceivable that PAXX could be utilised to recruit LIG4 and XRCC4, two NHEJ factors which have already been shown to enhance HSV-1 genome replication and virion production (Muylaert and Elias, 2007). It would be interesting to consider whether the loss of beneficial HR factors (e.g. ATM, WRN), PAXX and LIG4/XRCC4 is epistatic in reducing HSV-1 genome replication.

It has been proposed that DNA-PKcs supports circularisation of the genome (Smith *et al*. 2014; Section 1.2.6), a process which could be important in genome replication but which has also been linked to increase latency of HSV-1 (Efstathiou *et al*., 1986; Jackson and DeLuca, 2003). It is also conceivable that circularised genomes would not be able to be packaged into capsids. It is natural to hypothesise that PAXX could contribute to genome circularisation, and this could explain the reduced production of infectious virions despite increased replication in the presence of PAXX. Analysis by southern blotting suggests that the amount of endless genomes is indeed reduced in *PAXX*$^{-/-}$ cells, supporting this argument (**Figure 8B**). In contrast the ratios between endless and monomeric forms of viral genomes remain similar between WT and *PAXX*$^{-/-}$ cells at all times observed (**Figure 8B**), suggesting that PAXX is not required for subsequent replication, and that the reduced total amount of viral genomes present is due to the initial defect in the formation of endless genomes.

The reduced viral genome replication observed by southern blotting was in keeping with the qPCR data showing fewer viral genomes in *PAXX*$^{-/-}$ cells. Further evidence that

PAXX does not restrict HSV-1 genome replication comes from our study of viral gene expression. True late (γ2) HSV-1 genes such as US11 should only be expressed following viral DNA replication (Kibler *et al*., 1991). Despite the increased replication of the viral genome observed in WT RPE-1 cells, there is no correlative increase in US11 expression (**Figure 13**). As far as we are aware the relationship between the number of viral genomes and gene expression has not been characterised, so it cannot be said that a correlation should necessarily be observed. On the other hand, this may indicate that a higher proportion of the genomes produced in the WT cells are not transcriptionally functional. The observation that PAXX does not affect viral gene expression is important in itself because many DDR proteins have been linked to the silencing of viral gene expression, for example IFI16, RNF8 and RNF168, and DNA-PKcs (Lilley *et al*., 2010; Orzalli *et al*., 2013; Smith and Weller, 2015).

We also considered the hypothesis that PAXX affects the packaging of the viral genome. Although we found no difference in the proportion of endless genomes, PAXX could create other structural changes that prevent efficient packaging. However, current dogma indicates that the fragments Q and S (**Figure 8**) should only be observed from encapsidated, mature viral DNA because cleavage occurs during packaging (Heming *et al*., 2014; Muylaert and Elias, 2007). Therefore the detection of the Q and S fragments in the southern blot suggest that packaging is occurring in WT and *PAXX*$^{-/-}$ cells with comparable efficiency. However, many of the inferences that underlie this dogma are based on comparisons to pseudorabies virus and bacteriophages (Selvarajan Sigamani *et al*., 2013), not based on experiments in HSV-1. The best evidence for concomitant packaging and cleavage of the HSV-1 genome is that the capsid protein UL6 is required for the formation of Q and S BamHI fragments, even though UL6 is not required for assembly of the terminase complex (Patel *et al*., 1996). One study proposed that cleavage is possible without packaging using a mutant in the terminase complex component UL15, but the authors of this study acknowledge that the mutant probably initiates packaging and packaging is subsequently aborted as opposed to the cleavage occurring in the absence of packaging (Yang *et al*., 2011). To avoid any doubt and avoid unnecessary assumptions, we decided to use a separate method to assess how HSV-1 packaging is affected by PAXX. Electron microscopy was used to count virions in the

nucleus because it has previously been reported that virions lacking DNA or with defective DNA that is significantly too short do not exit the nucleus (Ladin *et al*., 1980; Vlazny *et al*., 1982). Interestingly, contrary to the conclusions of the above studies, low numbers of type A and type B capsids were observed outside of the nucleus in both WT and *PAXX*$^{-/-}$ RPE-1 cells, and in some instances these even appeared to have undergone wrapping (data not shown). We did not, however, identify any change in the frequency of packaging defects between WT and *PAXX*$^{-/-}$ cells (**Figure 9**) using electron microscopy. This observation could be tested by extracting viral protein and viral DNA from purified virions, and comparing the protein:DNA ratio observed in *PAXX*$^{-/-}$ and WT cells.

3.13.2 PAXX and infectious virion production

We have showed that PAXX does not affect HSV-1 gene expression or protein production in RPE-1 cells (**Figure 13A-D**), but have observed differences in total HSV-1 protein production in MEFs (**Figure 13E**). In contrast to RPE-1 cells, in MEFs we observed differences in MAPK responses to DNA stimulation (**Figure 11**), and MAPK pathways have been linked to the transcriptional activity of some genes (e.g. *ICP4* and *ICP22* – **Section 3.9**), so it would be interesting to look at HSV-1 gene transcription in MEFs. However, the lack of PAXX-dependent restriction on viral gene expression or protein production in RPE-1 cells suggests that this mechanism is not responsible for the reduced production of infectious virions in *PAXX*$^{-/-}$ RPE-1 cells.

We have observed that *PAXX*$^{-/-}$ RPE-1 cells release a higher proportion of infectious virions into the growth medium. It is interesting to note that Ku70 has been proposed to be important for the internalisation, but not cell adhesion, of the bacterium *Rickettsia conorii* (Chan *et al*., 2009; Martinez *et al*., 2005), and it would be interesting to investigate whether PAXX is also involved in this process. This observation may impact on the low MOI growth curves because convection currents or diffusion may move these virions away from a developing plaque, resulting in the infection of more cells early. Each cell has a limited capacity for viral production, and so dispersing the infection in this way would be likely to allow viral production early in infection to be faster. It would be

interesting to eliminate this variable by conducting a growth curve with semi-solid medium to prevent viral spread through the medium.

Virions which contain DNA are not necessarily infectious; HSV-1 infection creates a high particle:PFU ratio, caused by the production of a large number of non-infectious, defective particles (Frenkel *et al*., 1975; Watson *et al*., 1963). The genomes of defective particles would be detected by southern blotting because the genome must contain the 'ac' fragment to be packaged (Vlazny *et al*., 1982), and this contains the sequence detected by our assay. This would potentially explain why WT cells create more copies of the HSV-1 genome than *PAXX*$^{-/-}$ cells during infection, but produce fewer infectious virions. It is therefore a possibility that PAXX alters the particle:PFU ratio of HSV-1, and it future work should investigate whether this is the case.

3.13.3 PAXX and the innate immune response

We have also investigated whether PAXX is involved in the regulation of innate immune responses. The data suggest that, in MEFs, PAXX might contribute to the initiation of innate signalling pathways following nucleic acid stimulation, but not during HSV-1 infection. The difference in responses of WT and *Paxx*$^{-/-}$ cells to ΔICP0 HSV-1 may be abrogated because of other inhibitors of the IRF3 pathway, or as a result of PAXX relocalisation (**Section 3.11**). The strongest phenotype was observed in MAPK signalling pathways; loss of PAXX in MEFs abrogated *Cfos* and *Cjun* transcription following stimulation with DNA (**Figure 11**). *Paxx*$^{-/-}$ MEFs also exhibited reduced transcription of IRF-3- and NF-κB-dependent genes. DNA death pathways constitute one area in which we have not investigated potential roles for PAXX. DNA-PKcs and Ku70 have been linked to the induction of apoptosis following DNA DSBs, although the PAXX homologue XLF is not involved (Abe *et al*., 2008). It would be interesting to further explore whether the delayed CPE observed in *Paxx*$^{-/-}$ MEFs (Section 3.2) is linked to abrogated signalling pathways.

We had originally hypothesised that PAXX may affect the innate immune response to DNA because it can bind indirectly to DNA and because other DDR proteins have been implicated as innate immune sensors of DNA (Section 1.3.1). It is therefore

interesting to note that the loss of PAXX also had effects on cytoplasmic poly(I:C)-driven transcription of *Cxcl10* and *Cjun* (**Figure 11**). This does raise concerns that PAXX might instead be involved in transcription rather than innate sensing. However, PAXX may indeed be involved in orchestrating an innate response to RNA, so it would therefore be interesting to investigate whether PAXX affects RNA virus infection using a similar experimental approach as we have taken here.

Together, these data provide justification for further exploration of a potential role of PAXX in the innate immune response. Unfortunately our resources were limited, and we were unable to continue experimentation on first passage MEFs. Accordingly we attempted to investigate the role of PAXX in RPE-1 cells. Unfortunately neither ΔICP0 HSV-1 infection nor cytoplasmic DNA stimulation were sufficient to induce elevated transcription of any of the genes investigated in WT RPE-1. We have observed low transfection efficiency in RPE-1 cells which may help explain the lack of response to DNA, but we know that these cells are infected by ΔICP0 HSV-1 (**Figure 24**) so it is likely that there is an intrinsic defect in pattern recognition receptor signalling in these cells. Interestingly innate immune transcription was stimulated in RPE-1 cells following poly(I:C) transfection, but this was not pursued further.

Following the observation that *Paxx*$^{-/-}$ MEFs have reduced MAPK responses, we wanted to find an alternative MAPK stimulator to study the requirement for PAXX. In contrast to DNA transfection, we found that PMA was able to induce transcriptional responses in WT RPE-1 cells. Unfortunately, the transcriptional responses of RPE-1 cells to PMA were too inconsistent for the production of reliable data. The poor transcriptional responses of innate immune genes to DNA stimulation and the inconsistency of MAPK gene transcription following PMA stimulation highlight the importance of using primary cells for innate immune studies. Taken together these data suggest that, although innate responses may contribute to the increase in infectious virus produced by *Paxx*$^{-/-}$ MEFs, it is unable to explain the same phenotype in RPE-1 cells.

3.13.4 Changes in subcellular PAXX distribution

We hypothesised that PAXX may be degraded by HSV-1, but found that instead PAXX localisation changes during HSV-1 infection, and we have observed these HSV-1-induced changes in in multiple systems (**Figure 14**). From six hours *post* infection, the proportion of cells with changes in PAXX localisation increases with time (**Figure 14D**). After 16 hours, PAXX was dispersed in over 80 % of cells. Our data show that a small proportion of uninfected cells also exhibited these changes in PAXX localisation, but the morphology and genome structure of these cells suggested that they were undergoing cell division (**Figure 14C**). PAXX distribution changes during cell division are perhaps unsurprising given the breakdown of the nuclear envelope during mitosis. During infection HSV-1 halts the cell cycle at one of either the G1/S or G2/M checkpoints (Li *et al*., 2008b), so it is interesting to note that no cells were observed with PAXX distribution changes after four hours of infection. It is possible that after four hours of infection HSV-1 had initiated a cell-cycle checkpoint, thereby preventing mitosis-dependent PAXX localisation changes, but had not yet induced changes in the distribution of PAXX itself.

More work is required to establish the mechanism and implications of the changes in PAXX localisation. Some DNA-repair proteins exit the nucleus following DNA damage, for example Ku80 and WRN (Dejmek *et al*., 2009). We therefore tested the ability of exogenous DNA to induce PAXX localisation changes, and preliminary data suggests that transfection of DNA, but not poly(I:C), is sufficient to induce the change in localisation (**Figure 15**). Interestingly circular DNA species can trigger the localisation changes of PAXX; it is possible that the plasmid is digested upon entry into the cells, but it is also conceivable that unlike NHEJ, stimulation of changes in PAXX do not require free DNA ends.

These preliminary data suggest that it may be viral genomes, not viral proteins, which induce changes in PAXX distribution, although further repetition of these experiments is required to confirm that DNA is sufficient to induce the chenage. Interestingly, the homologue of PAXX, XLF, is phosphorylated by Akt following DNA damage, resulting in relocalisation from the nucleus to the cytoplasm where it is

subsequently degraded (Liu *et al*., 2015). It is possible that exogenous DNA triggers Akt activity which in turn induces PAXX relocalisation. However, we do not observe a reduction in cytoplasmic PAXX protein levels which might be indicative of degradation, suggesting that this mechanism might not be responsible. Regardless, it would be interesting to investigate whether Akt is required for PAXX localisation changes. An alternative hypothesis is exemplified by another DDR protein, IFI16, which has been shown to form an inflammasome complex and relocalise from the nucleus to the cytoplasm following HSV-1 infection (Johnson *et al*., 2013). It is especially tempting to speculate that PAXX may have a similar function given the potential role of PAXX in innate immune sensing or signalling. However the dynamics of the change in IFI16 distribution is much faster than that of PAXX, with increases in cytoplasmic IFI16 observed as early as 2 hours *post* infection as compared with 6 hours with PAXX.

3.13.5 HSV-1, the DDR, and PAXX

Following DNA damage a number of different DNA repair pathways can be stimulated, and the decision regarding repair mechanism is determined by a number of factors including the form of DNA lesion and cell cycle stage. It is tempting to consider the role of the DDR proteins during HSV-1 infection in terms of their pathways, and to brand each pathway as either promoting or inhibiting HSV-1 infection. However, different proteins from the same pathway can have polarising effects on HSV-1 infection, and HSV-1 has evolved to activate and inhibit individual proteins accordingly. For example, cells deficient in the HR proteins ATM, MRN, or WRN are less efficient at HSV-1 production (Balasubramanian *et al*., 2010; Lilley *et al*., 2005; Taylor and Knipe, 2004), yet the HR pathway as a whole is suppressed during HSV-1 infection (Schumacher *et al*., 2012).

Indeed, a single protein can be both beneficial and detrimental to HSV-1. Activity of ATR is inhibited by HSV-1, yet ATR is recruited to viral replication centres and is essential for efficient virus production (Mohni *et al*., 2010, 2013). It has been suggested that this is because although the protein ATR promotes HSV-1 genome replication, the pathways it stimulates downstream are deleterious (Smith and Weller, 2015). A similar conclusion is plausible for PAXX; PAXX may enhance HSV-1 genome replication, but it

may also signal to downstream pathways which have detrimental effects. This would help reconcile the seemingly paradoxical data that PAXX aids viral genome replication (**Figure 7**) but restricts the production of infectious virions (**Figure 6**). Parallels can be drawn between this hypothesis and data for DNA-PKcs which suggests that DNA-PKcs may be involved in the circularisation of the HSV-1 genome (Jackson and DeLuca, 2003; Smith *et al*., 2014), despite its known detrimental effects on HSV-1 (Ferguson *et al*., 2012; Lees-Miller *et al*., 1996; Parkinson *et al*., 1999).

As a relatively new discovery, the roles of PAXX in NHEJ are still to be fully elucidated. As our understanding of PAXX in this context improves, we may also gain insight into how PAXX functions during infection. Already it is able to inform our future investigations. For instance, PAXX and XLF are redundant in the repair of simple DSBs, yet cooperate in repairing complex lesions (Kumar *et al*., 2016; Xing *et al*., 2015); indeed the function of PAXX in NHEJ has been described as masked by XLF (Tadi *et al*., 2016). Future work should therefore consider whether XLF and PAXX function cooperatively during HSV-1 infection, and this may help us to disentangle the conflicting roles PAXX appears to play.

3.13.6 Summary

The data presented in this chapter show that PAXX is able to restrict the production of infectious HSV-1 virions, as is demonstrated by the increased numbers of infectious virions produced by *PAXX*$^{-/-}$ cells. We tested the hypothesis that PAXX may be detrimental for HSV-1 genome replication, but showed that *PAXX*$^{-/-}$ cells supported lower levels of viral genome replication and we did not identify any defects in viral genome structure or packaging into virions. However we did observe that MEFs lacking PAXX showed a reduced innate response to DNA, although it is unclear whether RPE-1 cells are able to respond to these stimuli at all. Finally, PAXX distribution may change following stimulation with DNA or DNA virus infection, but the mechanisms and implications remain to be elucidated. Work is also required to characterise the *PAXX*$^{-/-}$ RPE-1 cells, preferably through sequencing of the genome and western blotting analysis.

In summary, we have identified that PAXX is able to restrict HSV-1 infection, and made some progress towards understanding the mechanisms by which this is achieved. However, further work is required to fully disentangle what are likely to be multiple roles for PAXX in HSV-1 infection. To address this, the next chapter will explore the potential roles of PAXX during HSV-1 infection *in vivo*.

4 The role of PAXX in vivo

4.1 Introduction

In Chapter 3 we have shown that PAXX restricts HSV-1 infection in both human and murine cells. In the murine system, fibroblasts (MEFs) lacking PAXX produce more infectious virus during infection. We also showed that these cells might have impaired MAPK responses following DNA stimulation. MAPKs have pleiotropic roles *in vivo*, regulating multiple aspects of innate and adaptive immunity including pattern recognition receptor signalling and the differentiation and activation of T lymphocytes (reviewed Rincón, Flavell, & Davis, 2001). Indeed, MAPKs affect HSV-1 infection outcome in mice (Chen *et al*., 2008). We therefore postulated that the absence of PAXX might impact HSV-1 *in vivo* so, to further assess the physiological relevance of our findings in Chapter 3, we infected mice lacking PAXX with HSV-1 and analysed the outcome of infection.

The observations in Chapter 3 were made in cell culture, and investigating the *in vivo* role of a protein is significantly more complicated because there are many more processes that may be affected by loss of function experiments in a whole organism. NHEJ factors are required for V(D)J recombination to different extents, and therefore the development of lymphocytes in NHEJ mutant mice varies (Section 1.3.3.1). *Prkdc*$^{-/-}$ mice exhibit a SCID phenotype (Blunt *et al*., 1995; Kirchgessner *et al*., 1995; Kurimasa *et al*., 1999b). The loss of XLF results in mild to severe immunodeficiency in humans (Cipe *et al*., 2014; Ijspeert *et al*., 2016), although in XLF-deficient mice V(D)J recombination is only slightly reduced (Balmus *et al*., 2016; Li *et al*., 2008a). In contrast XRCC4 mutations in humans do not cause a SCID phenotype (Murray *et al*., 2015). Since lymphocyte populations can affect the outcome of virus infection, we therefore wanted to investigate whether PAXX was required for V(D)J recombination and lymphocyte production.

Another implication of NHEJ defects *in vivo* is genomic instability. In cell culture genomic instability can create immunostimulatory micronuclei or lead to DNA leaking into the cytoplasm (Glück et al., 2017b; Harding et al., 2017; Mackenzie et al., 2017), triggering DNA sensing pathways and inducing autoinflammation. Autoinflammatory

disease can cause pathology in the skin or central nervous system (CNS) (Rodero and Crow, 2016; Woodbine *et al*., 2013), and these tissues are both very relevant to HSV-1 infection. NHEJ mutations have also been linked to growth defects and microcephaly in both humans and mice (Bunting and Nussenzweig, 2013). In humans, mutations in *XRCC4, ATR,* and *NHEJ1* (encoding XLF) can cause immunodeficiency, primordial dwarfism, and microcephaly (Buck *et al*., 2006; Cipe *et al*., 2014; Murray *et al*., 2015; O'Driscoll *et al*., 2003; Ogi *et al*., 2012; Qvist *et al*., 2011; Shaheen *et al*., 2014). In mice, deficiency in XRCC4 or LIG4 expression is embryonic-lethal due to defective neurogenesis and lymphogenesis (Gao *et al*., 1998, 2000), and Ku70-deficient mice are about half the size of wild type counterparts at all ages (Gu *et al*., 1997). These examples indicate why it is important that we considered the role of PAXX in this context before exploring its role in controlling HSV-1 infection.

The aims of the experiments in this chapter are to characterise the morphological, neurological, and adaptive immune development of *Paxx*$^{-/-}$ mice, and to subsequently investigate whether PAXX contributes to the control of HSV-1 in mice.

4.2 PAXX expression might not affect brain weight

Defects in DNA repair machinery are often associated with microcephaly (Woodbine *et al*., 2014). A partial explanation for this is that defects in DNA repair machinery are also linked to type I interferonopathies, manifestations of which generally either affect the skin or the CNS, and many have been shown to result in neurological defects (Rodero and Crow, 2016; Woodbine *et al*., 2013). We therefore investigated whether PAXX-deficiency caused defects in brain size. PCR genotyping was used to confirm that WT and *Paxx*$^{-/-}$ mice were of the correct genetic background (**Figure 16A**). The brains of *Paxx*$^{-/-}$ mice were weighed, a common measure of the extent of microcephaly and neuronal cell death (Huang *et al*., 2016; Li *et al*., 2008a; Pulvers *et al*., 2010), and compared to their WT counterparts. Preliminary data suggests that *Paxx*$^{-/-}$ mice do not show any defects in brain weight (**Figure 16B**). Certainly, *Paxx*$^{-/-}$ mice do not display overtly abnormal growth, and there were no obvious behavioural defects which may have been indicative of neurological complications.

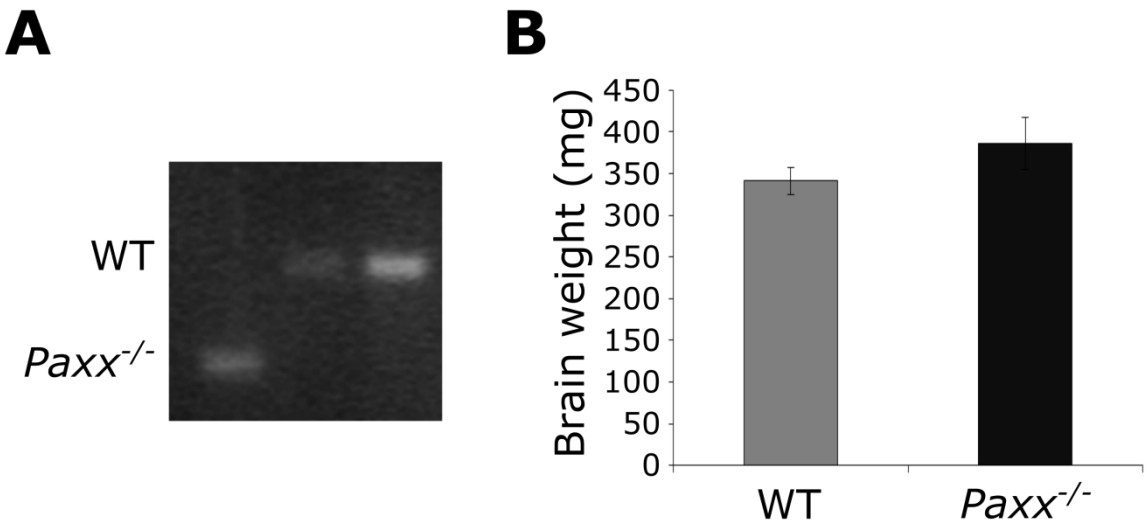

Figure 16: *Paxx*$^{-/-}$ mice have brains of normal weight.

A) The genotypes of WT and *Paxx*$^{-/-}$ mice were confirmed using PCR for each experiment conducted. **B)** The brains of six mice from each genotype were weighed in a single experiment. Preliminary data from a single experiment suggests that the brains of *Paxx*$^{-/-}$ mice do not have significantly different masses to those of WT mice. Error bars denote intra-experimental mean +/- standard error of the mean (SEM).

4.3 Paxx$^{-/-}$ *mice have normal lymphocyte populations*

NHEJ factors are important in V(D)J recombination and lymphogenesis (Section 1.3.3), and PAXX and XLF show redundancy in human and mouse V(D)J recombination (Kumar *et al*., 2016; Lescale *et al*., 2016). We therefore wanted to investigate whether lymphocyte development was normal in *Paxx*$^{-/-}$ mice. The spleen and lymph nodes were collected from WT and *Paxx*$^{-/-}$ mice, and cells were isolated. These organs were selected for analysis because they contain large numbers and high proportions of lymphocytes. The isolated cells were stained using antibodies (Section 2.10.8) raised against CD45 (a marker for lymphocytes), CD19 (a marker for B lymphocytes), CD3 (a marker for T lymphocytes), CD4 (a marker for T helper lymphocytes), and CD8 (a marker for cytotoxic T lymphocytes), and then analysed by flow cytometry. The flow cytometer was operated by a colleague for all experiments shown in this chapter, but I was responsible for all other stages of the experiments. **Figure 17A** shows the gating strategy used to

analyse the isolated cells. We were particularly interested in $CD45^+$ lymphocytes because they require V(D)J recombination for their development, and because T lymphocytes are particularly important in the control of HSV-1 in mice (Section 1.5.3).

The total numbers of cells recovered were similar between WT and *Paxx*$^{-/-}$ samples (data not shown), and so the proportion of each cell type was determined to avoid using absolute counts where variation in the isolation protocol could confound analysis. The proportion of all cells in the lymph node and spleen which had CD45, a marker of lymphocytes, was unchanged in *Paxx*$^{-/-}$ mice (**Figure 17B** and **2G**). The $CD45^+$ populations were further subdivided into $CD3^+$ T lymphocytes, and $CD19^+$ B lymphocytes. The proportion of $CD45^+$ cells which had CD3 (T lymphocytes) was unchanged in *PAXX*$^{-/-}$ cells (**Figure 17C** and **Figure 17H**), as were the proportions of T lymphocytes with CD4 (**Figure 17D** and **Figure 17I**) or CD8 markers (**Figure 17E** and **Figure 17J**). Similarly, the proportion of $CD45^+$ cells with CD19 was not affected by PAXX (**Figure 17F** and **Figure 17K**). We were therefore able to conclude that *Paxx*$^{-/-}$ mice were able to create normal lymphocyte populations, and that V(D)J recombination was not deficient. Whilst we can be confident in this conclusion, further experiments are required to determine whether there is a significant difference in lymphocyte populations between genotypes, because the experiment has only been conducted twice with two mice per group.

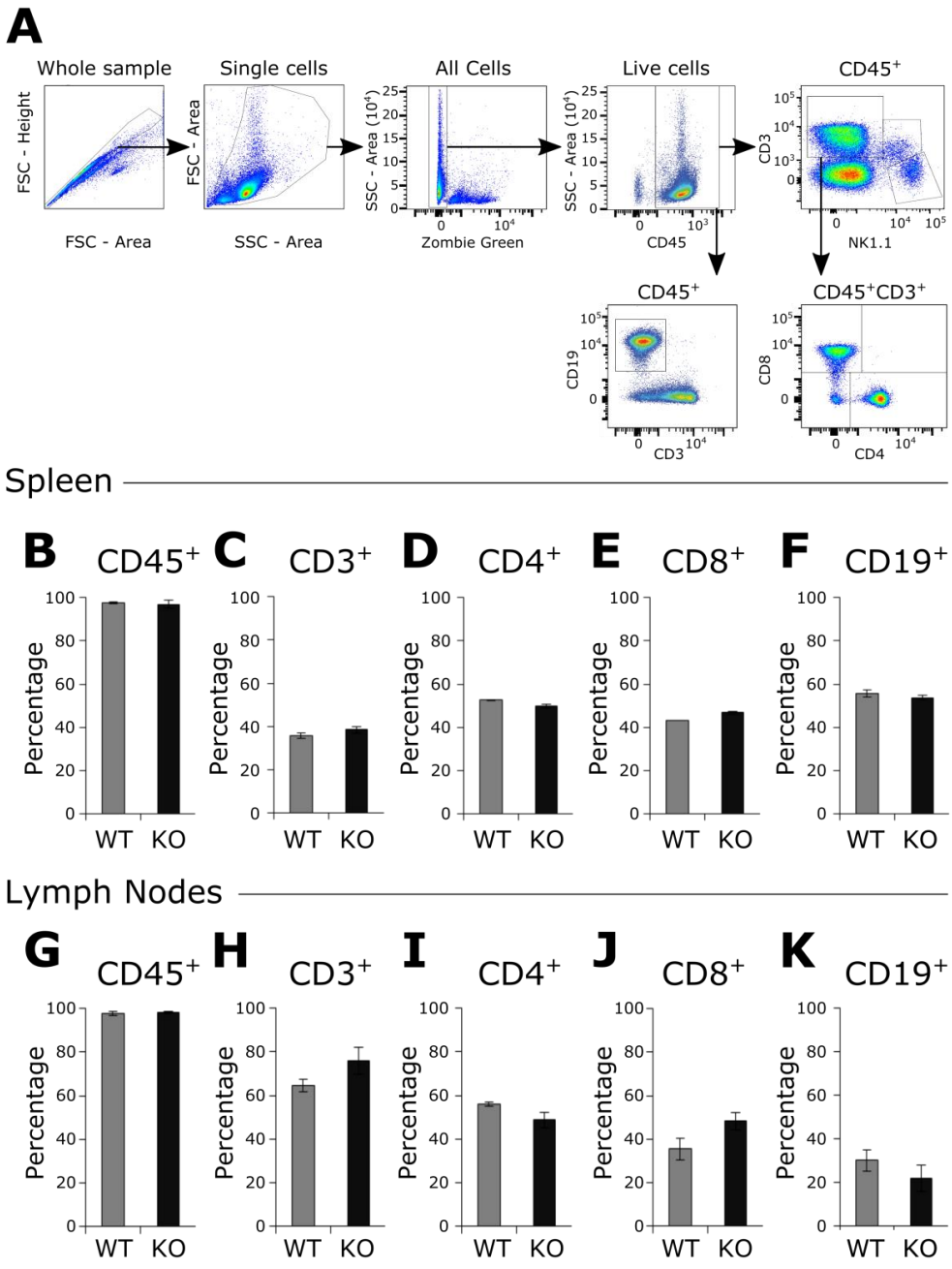

Figure 17: *Paxx*$^{-/-}$ mice have normal lymphocyte populations in the spleen and lymph nodes.

A) Cells extracted from the spleen were analysed by flow cytometry using the gating protocol illustrated. Doublets and dead cells were removed from analysis, and CD45$^+$ cells were isolated. CD19 and CD3 were used to identify B and T lymphocytes, respectively. NK1.1$^+$CD3$^+$ cells were removed to discount NKT cells, and CD8 and CD4 were used to identify CD3$^+$ subsets. Cells were isolated from the spleen and analysed to determine the proportions of **B**) CD45$^+$ cells, **C)** CD45$^+$ cells that are CD3$^+$, **D)** CD3$^+$ cells that are CD4$^+$, **E)** CD3$^+$ cells that are CD8$^+$, and **F)** CD45$^+$ cells that are CD19$^+$. Cells were isolated from the lymph nodes and analysed to determine the proportions of **G)** CD45$^+$ cells, **H)** CD45$^+$ cells that are CD3$^+$, **I)** CD3$^+$ cells that are CD4$^+$, **J)** CD3$^+$ cells that are CD8$^+$, and **K)** CD45$^+$ cells that are CD19$^+$. Two mice were used per group. Error bars denote intra-experimental mean +/- SEM. Data representative of two independent experiments.

4.4 PAXX is not required to restrict HSV-1 infection in vivo

Having shown that the *Paxx*$^{-/-}$ mice did not have a SCID phenotype, which could confound any observations made in response to infection of these mice with pathogens, we wanted to investigate the role of PAXX during HSV-1 infection in mice. We showed in Section 3.2 that *Paxx*$^{-/-}$ MEFs and *PAXX*$^{-/-}$ RPE-1 cells supported the production of more infectious HSV-1 virions in comparison with WT cells. We therefore hypothesised that *Paxx*$^{-/-}$ mice may have a reduced capacity to control HSV-1 infection. To test this 1×10^6 PFU of HSV-1 expressing a firefly luciferase gene under the control of a CMV promoter was injected intradermally into the whisker pads of four mice per genotype, and PBS of the same volume was injected into two control mice for each genotype. HSV-1 infection is generally asymptomatic in mice, but in cases where mice are severely compromised in their ability to control HSV-1 infection, pathology may be observed (Kollias *et al*., 2015). Pathology is generally in the form of neurological complications or weight loss, and so we monitored mice for both during infection. No neurological pathology was observed in any mice. The weight of the mice was measured daily, and there was no significant change in the weight of either WT or *Paxx*$^{-/-}$ mice during infection (**Figure 18A**). Sometimes lesions can form on the lips or, in the event of anterograde transport along the ocular nerves, the eyes (Kollias *et al*., 2015), but no lesions were observed in any mice.

Although no pathology was observed in WT or *Paxx*$^{-/-}$ mice, *Paxx*$^{-/-}$ mice may still have a reduced ability to control HSV-1 infection. In mice HSV-1 spreads from the whisker pads to the trigeminal ganglia where it usually establishes latency, but in mice that are compromised in their ability to control the virus, lytic infection is established and the virus spreads to other tissues (Kollias *et al*., 2015). HSV-1 expressing luciferase was used so that the locatio of HSV-1 infection can be determined using an *in vitro* imaging system (IVIS). Mice are injected with luciferin, and 20 minutes later they were anaesthetised and placed into the IVIS. The firefly luciferase produced by HSV-1 catalyses the oxidation of luciferin, and light is emitted as a by-product. The location and intensity of the light is detected by the IVIS, allowing for interpretation of the location

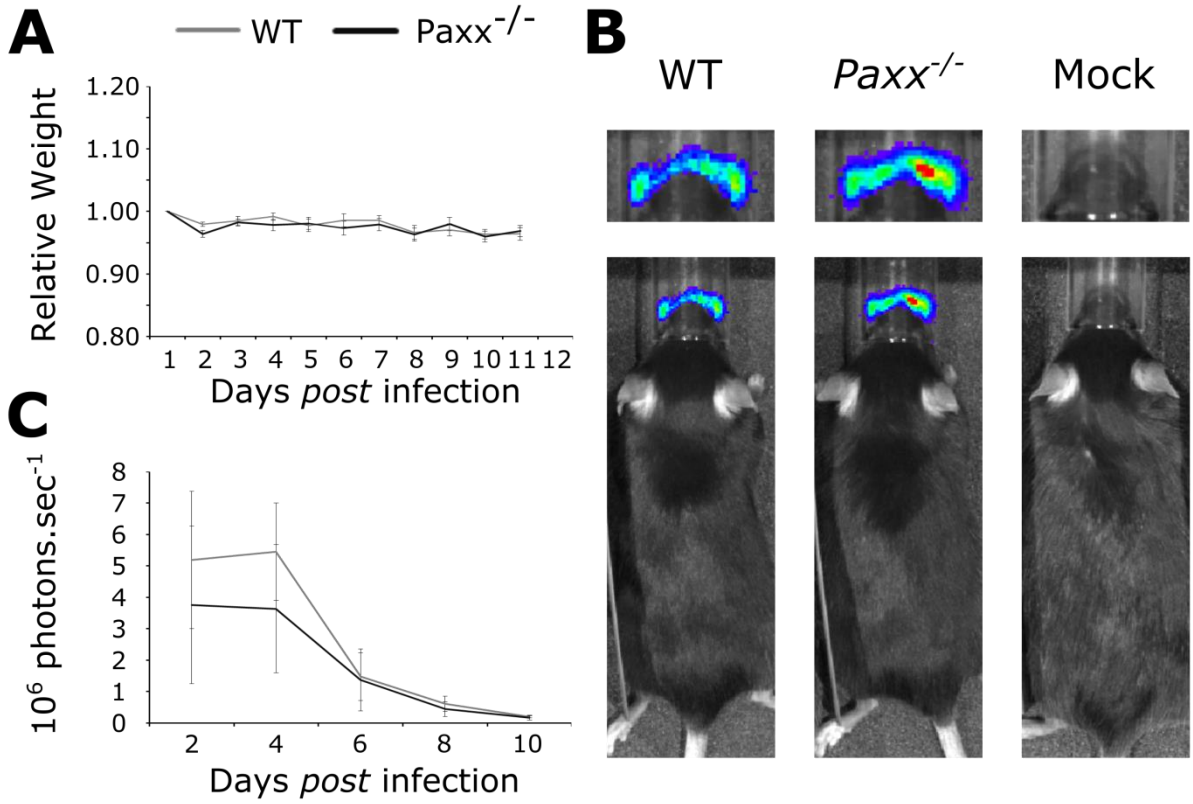

Figure 18: PAXX deficiency does not affect outcome of HSV-1 infection *in vivo*.

WT and *Paxx*$^{-/-}$ mice were infected intradermally in the whisker pads with 1 x 10^6 PFU of HSV-1 expressing luciferase, or with PBS (mock). **A)** The weight of each mouse was monitored throughout the experiment and is shown as the weight relative to its initial weight. The graph only shows infected mice and is representative of two experiments each with three mice per group. **B)** IVIS was used to observe the spread of the viral infection. Representative examples after 6 days of infection are shown. The top panel shows a magnified image of the nasal area, while the bottom panel shows an image of the whole body. **C)** IVIS was used to quantify the luciferase activity during the course of infection. Mock infected mice are not shown, and three mice were used per group. The graph shows a representative example of two independent experiments. Error bars denote intra-experimental mean +/- SEM.

and amount of virus during infection. This system was used to observe the spread of HSV-1 in infected mice every second day *post* infection.

Signal above background was not observed in WT or *Paxx*$^{-/-}$ mock-treated (uninfected) mice at any time (**Figure 18B**). Signal was observed in the nasal area of infected WT mice after 2 days, the first time luciferase activity was measured (**Figures 18B** and **C**). For the duration of the study, signal was limited to this region in all WT

mice. After 6 days of infection, the total signal observed in WT mice had started to drop, suggesting that lytic infection was being controlled (**Figure 18C**). After 10 days of infection total luciferase activity was at background levels.

In general, the infection of *Paxx*$^{-/-}$ mice followed was very similar to that observed in WT mice (**Figures 18B** and **C**). However, in one experiment a *Paxx*$^{-/-}$ individual had luciferase signal that aligned with the brain after 4 days of infection, but it had been cleared by day 6. Spread of HSV-1 infection to the brain is often observed in mice unable to effectively control HSV-1 infection following lip inoculation (Kastrukoff *et al*., 1982). Otherwise there was no indication from the localisation or intensity of luciferase production that the *Paxx*$^{-/-}$ mice were any less competent at controlling HSV-1 infection than their WT counterparts. We repeated this experiment and found similar results with the same conclusions. We therefore concluded that PAXX is not required for the restriction of HSV-1 infection in mice, although a further repetition of the experiment would enhance our confidence in this conclusion.

4.5 PAXX deficiency does not result in changes to lymphocyte populations during infection

Mutations in some NHEJ factors can cause a SCID phenotype in mice and humans because they are required for V(D)J recombination, an important part of lymphocyte maturation (Section 1.3.3.1). We have observed that *Paxx*$^{-/-}$ mice have normal lymphocyte populations in the absence of infection (Section 4.3), and that they are able to control HSV-1 to a similar extent as their WT counterparts (Section 4.4). However, we wanted to investigate whether there was an observable difference in the lymphocyte populations of *Paxx*$^{-/-}$ mice relative to their WT counterparts during infection.

To test for differences between lymphocyte populations, cells were isolated from the spleen or lymph node 11 days after infection, stained, and analysed by flow cytometry using the gating strategy shown in **Figure 17A**. After the removal of doublets and dead cells, CD45^{+} cells were subdivided into CD3^{-}CD19^{+} B cells and CD3^{+}NK1.1^{-} T cells, the latter of which were further subdivided into CD8^{+} and CD4^{+} cells. B cells and T cells were also stained for CD62L, a marker indicative of lymphocyte memory. Proportions of

different cell types were then calculated. 11 days after infection the proportion of the different lymphocyte population was similar to uninfected controls in both the spleen (**Figure 19**) and lymph nodes (**Figure 20**). These data show that at these times after infection the relative proportions of lymphocyte subsets are not different between infected and uninfected mice. *Paxx*$^{-/-}$ mice do not have significantly different proportions of lymphocyte subsets compared to WT mice.

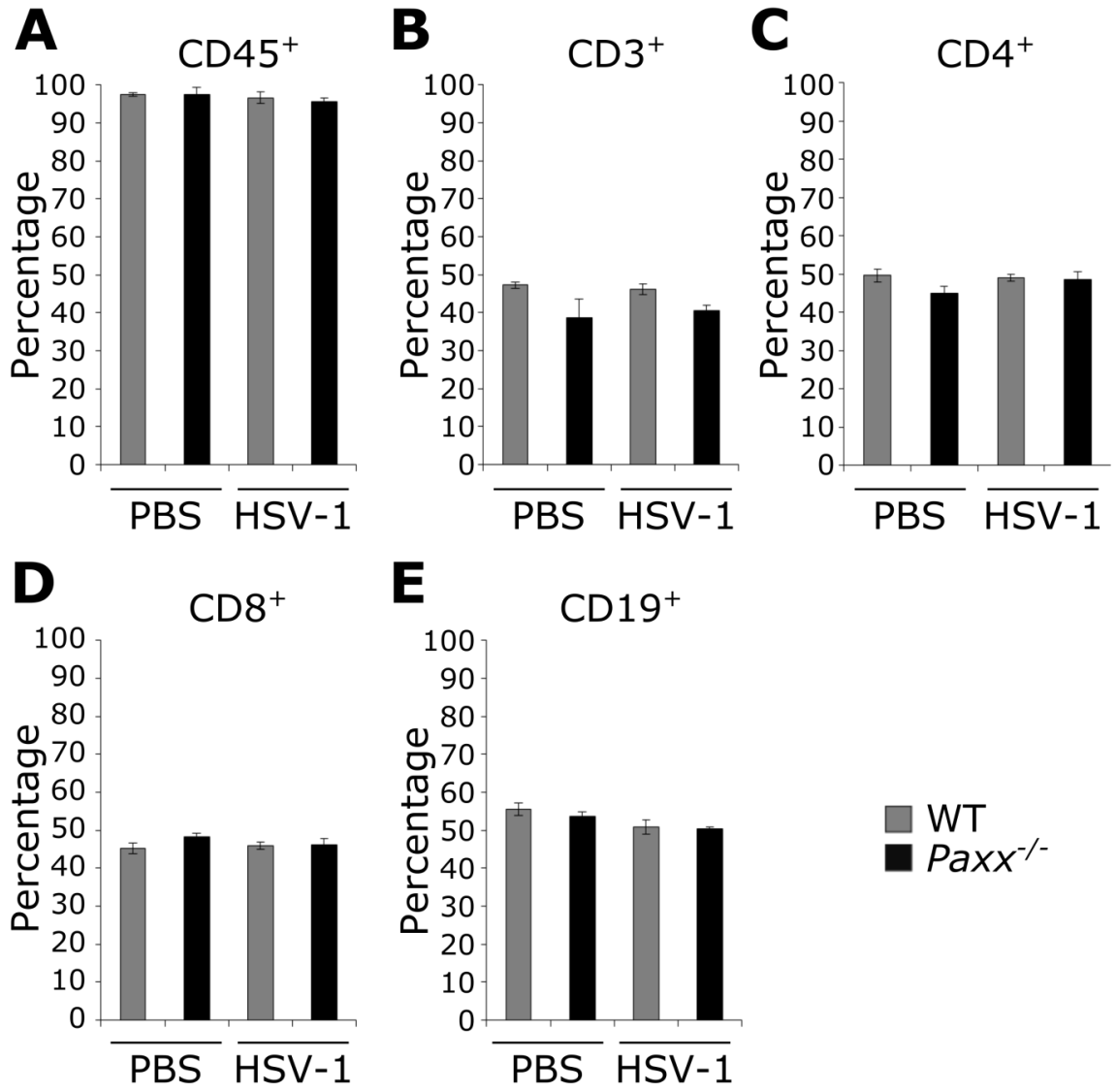

Figure 19: HSV-1 infection does not alter the relative proportions of lymphocytes from the spleen.

WT and *Paxx*$^{-/-}$ mice were infected intradermally in the whisker pads with 1 x 10^6 PFU of HSV-1 expressing luciferase, or with PBS. Cells were isolated from the spleen after 11 days and analysed by flow cytometry using the gating strategy shown in Figure 17 to determine the proportions of **A)** CD45$^+$ cells, **B)** CD45$^+$ cells that are CD3$^+$, **C)** CD3$^+$ cells that are CD4$^+$, **D)** CD3$^+$ cells that are CD8$^+$, and **E)** CD45$^+$ cells that are CD19$^+$. Infected groups consisted of three mice, mock groups had two mice. Error bars denote intra-experimental mean +/- SEM. Figures are representative of two independent experiments.

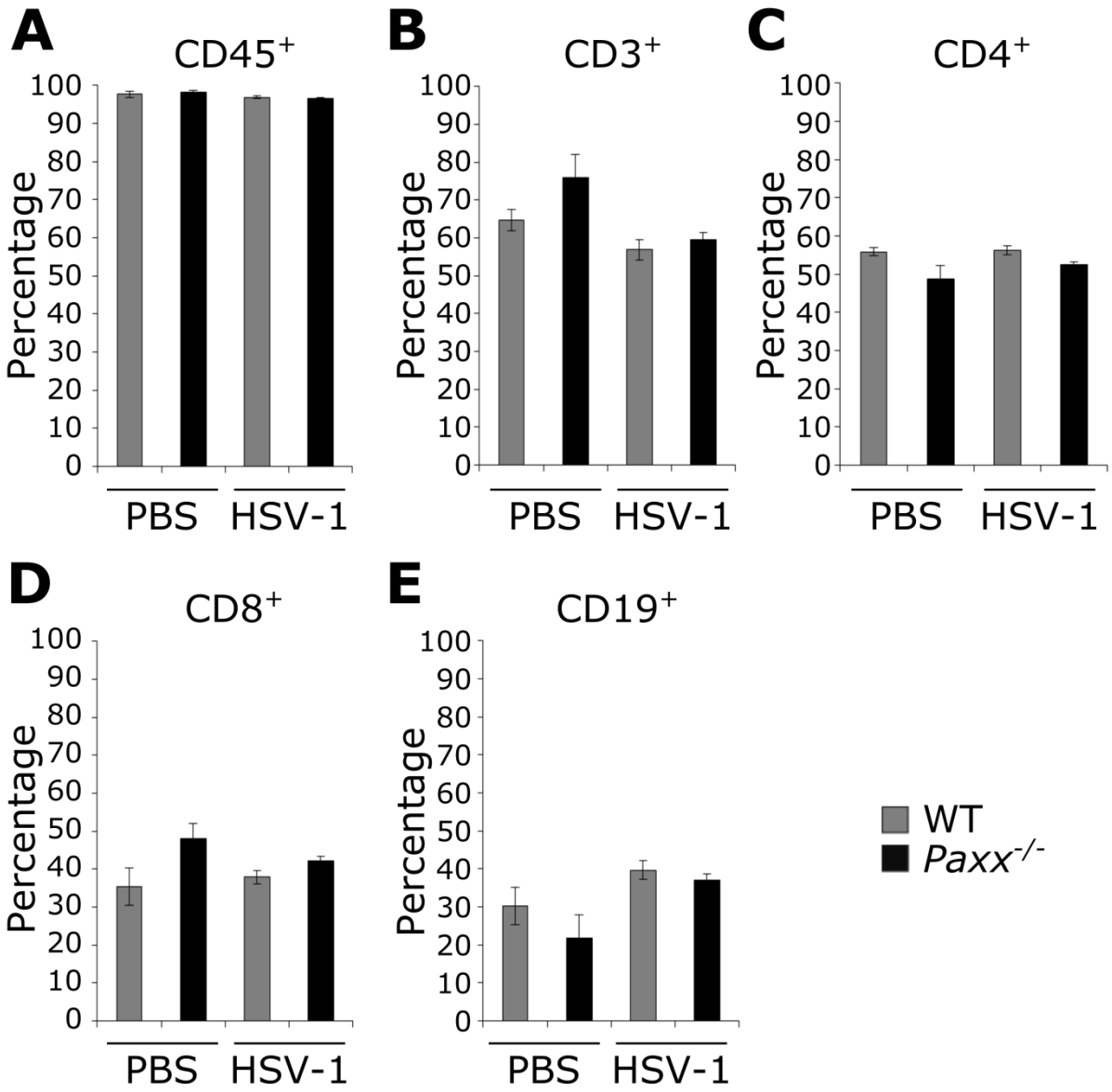

Figure 20: HSV-1 infection does not alter the relative proportions of lymphocytes from the lymph nodes. WT and *Paxx*$^{-/-}$ mice were infected intradermally in the whisker pads with 1 x 10^6 PFU of HSV-1 expressing luciferase, or with PBS. Cells were isolated from lymph nodes after 11 days and analysed by flow cytometry using the gating strategy shown in Figure 17 to determine the proportions of **A)** CD45$^+$ cells, **B)** CD45$^+$ cells that are CD3$^+$, **C)** CD3$^+$ cells that are CD4$^+$, **D)** CD3$^+$ cells that are CD8$^+$, and **E)** CD45$^+$ cells that are CD19$^+$. Infected groups consisted of three mice, mock groups had two mice. Error bars denote intra-experimental mean +/- SEM. Figures are representative of two independent experiments.

4.6 PAXX is not required for the stimulation of lymphocytes with PMA

After the observation that the proportions of lymphocyte subpopulations remain similar between WT and *Paxx*$^{-/-}$ cells, we wanted to investigate whether lymphocytes isolated from the two genotypes were equally primed for activation following infection. Phorbol myristate acetate (PMA) activates T lymphocytes, and can be used to investigate the proportion of T lymphocytes primed to respond (Touraine *et al*., 1977).

Lymphocytes were extracted from the spleen or lymph nodes of infected and uninfected mice, were stimulated with PMA or left unstimulated, and analysed by flow cytometry to investigate production of IFNγ and TNFα, and the expression of CD62L (**Figure 21A**). IFNγ was studied because it is a marker of lymphocyte activation and is important in restricting HSV-1 infection (Section 1.5.3). TNFα is produced by activated T lymphocytes (Cuturi *et al*., 1987; Sung *et al*., 1988). CD62L is used as a marker of naïve T cell lymphocytes (Picker *et al*., 1993). Unstimulated cells were used to determine appropriate thresholds for analysis (**Figure 21B**). The T lymphocytes were activated by the PMA (**Figure 21B** and **C**), but there were not any significant differences between WT and *Paxx*$^{-/-}$ lymphocytes in the expression of any of these proteins in CD4^{+} or CD8^{+} T lymphocytes (**Figure 22**). This suggests that PAXX is not required for the activation of lymphocytes by PMA.

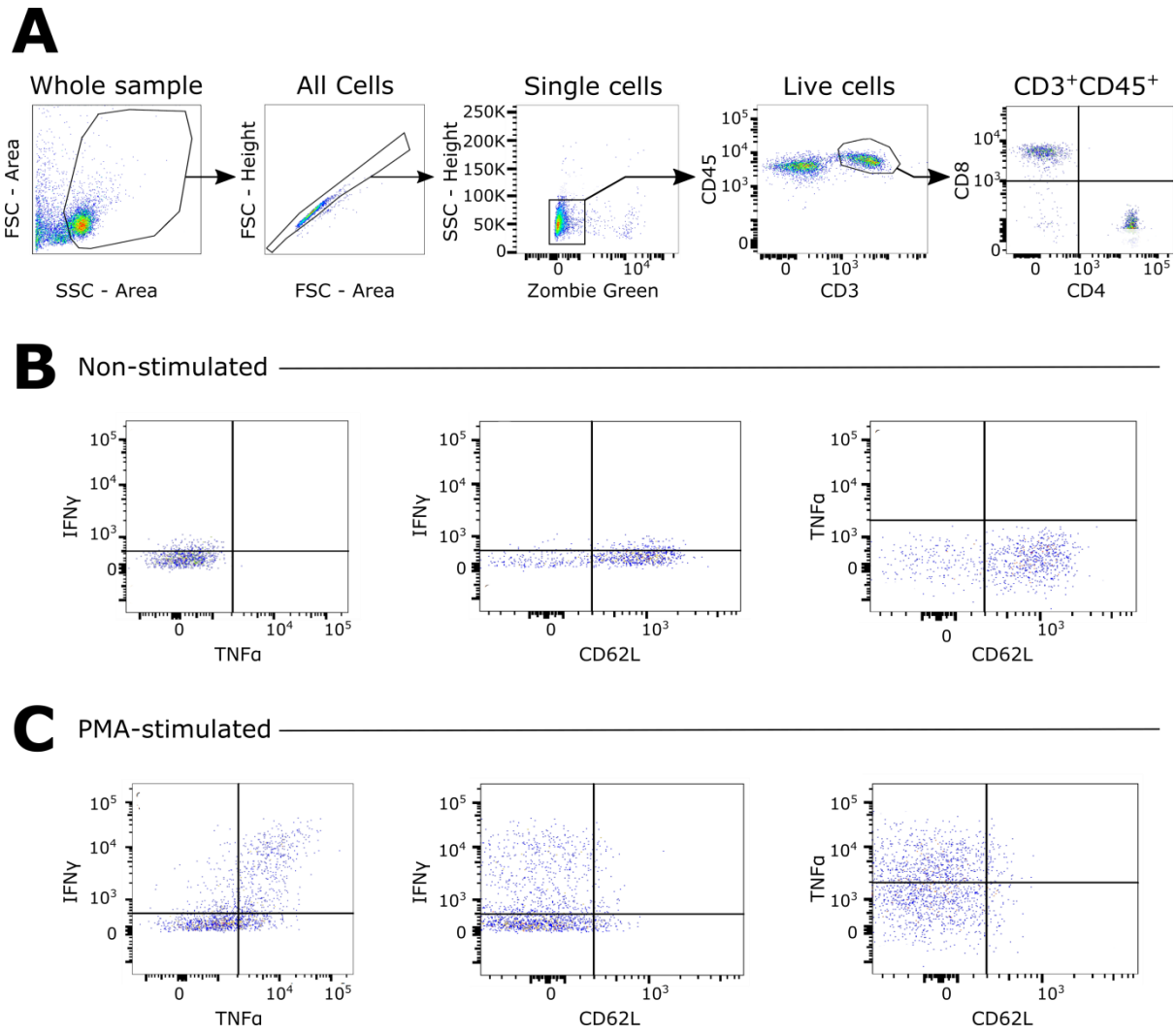

Figure 21: Gating strategy and examples of flow cytometry analysis.

Three WT mice were infected intradermally in the whisker pads with 1 x 10^6 PFU of HSV-1 expressing luciferase, and two were injected with PBS. Cells were isolated from the spleen after 11 days, stimulated with PMA or left unstimulated for four hours. **A)** Cellular debris was excluded from analysis using forward and side scatter. Single cells were isolated from doublets, and analysed using Zombie green so that only live cells were selected for analysis. $CD45^+CD3^+$ cells were isolated, and split into $CD4^+CD8^-$ and $CD4^-CD8^+$ subpopulations. $CD4^+CD8^+$ cells were not included in subsequent analysis. **B)** and **C)** The isolated subsets were then analysed for IFNγ, TNFα, and CD62L. **B)** An example of non-stimulated $CD4^+CD8^-$ cell staining. **C)** An example of PMA-stimulated $CD4^+CD8^-$ cell staining. FSC – forward scatter; SSC – side scatter. Figures are representative of two independent experiments.

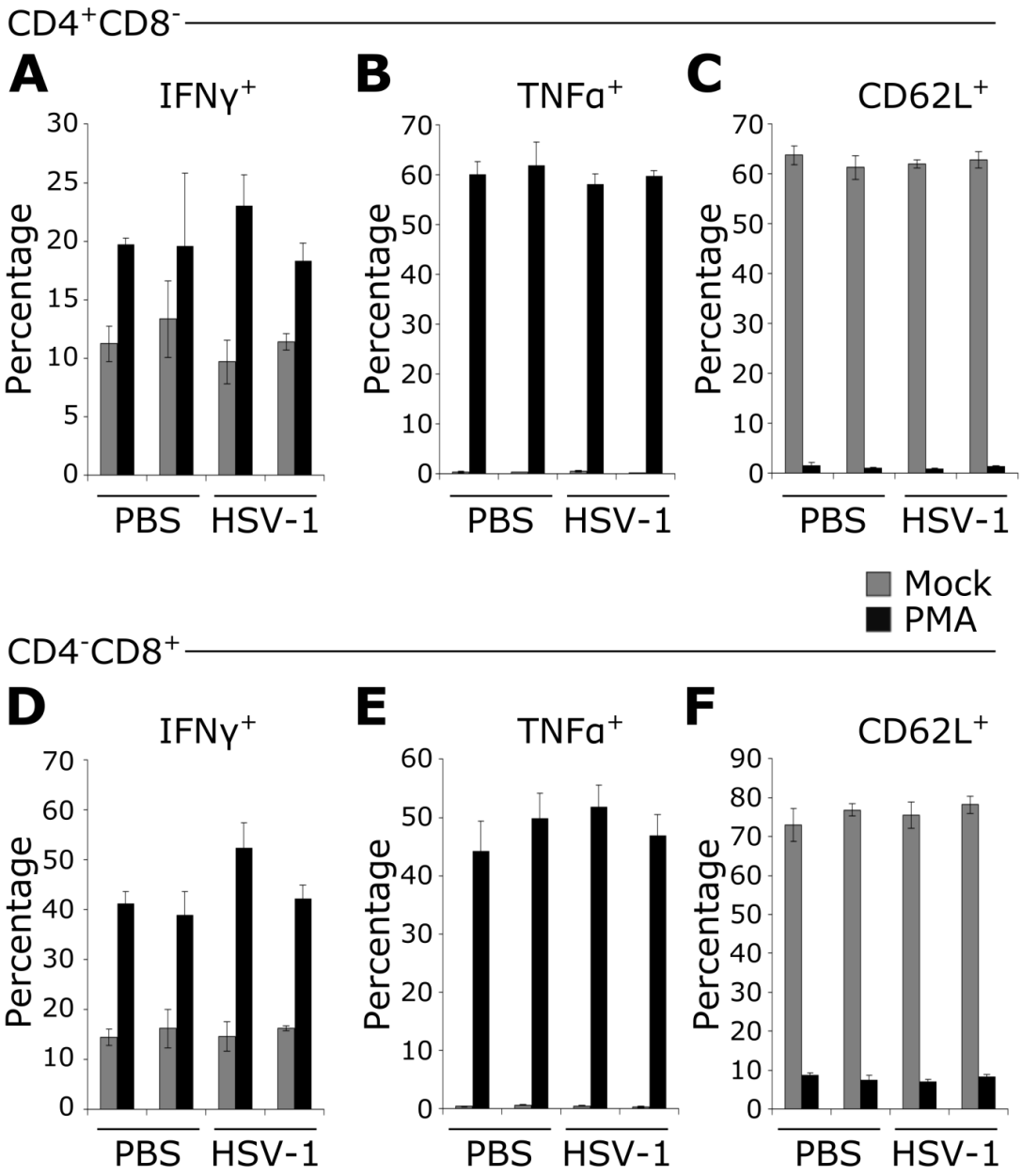

Figure 22: *Paxx*$^{-/-}$ lymphocytes respond to PMA stimulation.

WT and Paxx$^{-/-}$ mice were infected intradermally in the whisker pads with 1 x 10^6 PFU of HSV-1 expressing luciferase, or with PBS. Cells were isolated from the spleen after 11 days, stimulated with PMA (black bars) or left unstimulated (grey bars) for four hours, and analysed by flow cytometry using the gating strategy shown in Figure 21. This analysis was used to determine proportions of $CD3^+$ $CD4^+$ cells expressing **A)** IFNγ, **B)** TNFα, and **C)** CD62L, and $CD3^+$ $CD8^+$ lymphocytes expressing **D)** IFNγ, **E)** TNFα, and **F)** CD62L. Error bars denote intra-experimental mean +/- SEM. N.S. = no significant difference. Figures are representative of two independent experiments, except for figures C) and F) which depict a single experiment. Infected groups consisted of three mice, mock groups had two mice.

4.7 $gB_{498-505}$ stimulates expression of IFNγ but not TNFα, and does not reduce CD62L presentation.

PMA is a generic stimulator of T lymphocytes, so we wanted to stimulate lymphocytes with the peptide $gB_{498-505}$ (amino acids 498-505 from gB; SSIEFARL) to test HSV-1-specific responses. $gB_{498-505}$ is from the major HSV-1 antigen, gB, which was selected because it is considered an immunodominant antigen during HSV-1 infection (Khanna *et al*., 2003; Wallace *et al*., 1999). Cells were stimulated with 10^{-7} to 10^{-6} M of $gB_{498-505}$ for four hours, and analysed by flow cytometry using the same gating strategy described in **Figure 22A**. $CD4^+$ and $CD8^+$ cells both produced IFNγ in response to all concentrations of $gB_{498-505}$ tested, and the levels were similar to those following PMA stimulation (**Figure 23A** and **D**). In contrast to PMA stimulation, $gB_{498-505}$-stimulated T cells did not produce TNFα (**Figure 23B** and **E**) or lose CD62L (**Figure 23C** and **F**). Since the activation observed was incomplete, we did not explore stimulation with $gB_{498-505}$ further.

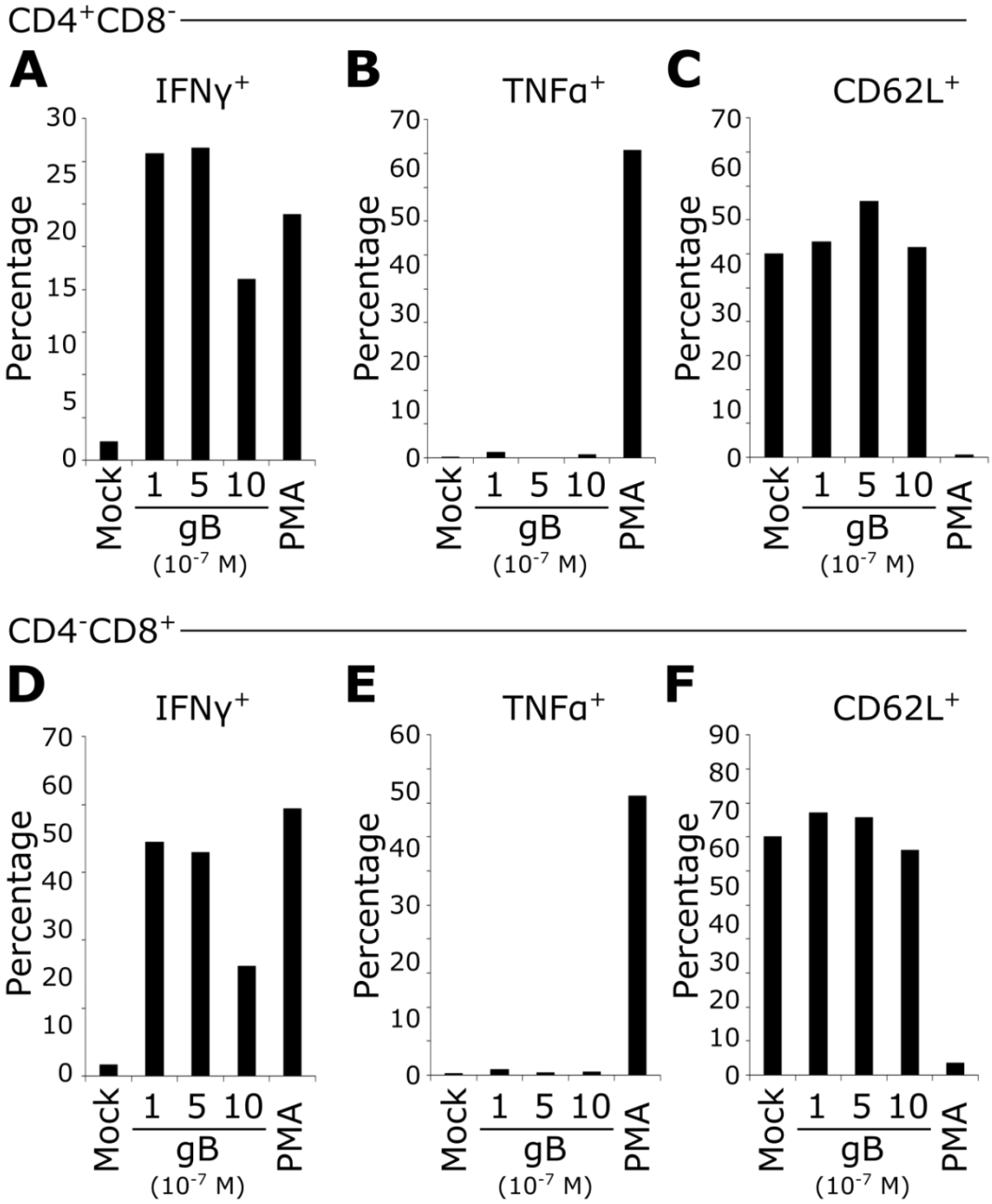

Figure 23: The gB peptide, SSIEFARL, is able to induce IFNγ in CD3+ cells from WT mice, but does not induce TNFα production or loss of CD62L presentation.

WT mice were infected intradermally in the whisker pads with 1 x 10^6 PFU of HSV-1 expressing luciferase. Cells were isolated from the spleen after 11 days, stimulated with PMA, stimulated with varying concentrations of the gB peptide, or left unstimulated for four hours. Cells were analysed by flow cytometry using the gating strategy shown in Figure 21. Analysis determined the proportion of CD4+CD8- cells expressing **A)** IFNγ, **B)** TNFα, and **C)** CD62L, and the proportion of CD4-CD8+ cells expressing **D)** IFNγ, **E)** TNFα, and **F)** CD62L. Error bars denote intra-experimental mean +/- SEM. Data representative of one experiment. Infected groups consisted of three mice, mock groups had two mice.

4.8 Discussion

In Chapter 3 we showed that PAXX restricts HSV-1 infection in cell culture. We were therefore interested in whether PAXX restricts HSV-1 infection *in vivo*. Before testing this hypothesis we wanted to investigate whether *Paxx*$^{-/-}$ mice have normal development, in part to ensure that there are no confounding pathologies exhibited by these mice. *Xrcc6*$^{-/-}$ mice are roughly 50 % of the size of WT mice (Gu *et al*., 1997), and defects in XRCC4 have been shown to cause primordial dwarfism in humans (Murray *et al*., 2015). However, *Paxx*$^{-/-}$ mice did not share this phenotype. DNA damage has been shown to stimulate the innate immune response (Brzostek-Racine *et al*., 2011; Kim *et al*., 1999; Wu *et al*., 2006), and DNA repair-deficiencies can lead to genomic instability which can create immunostimulatory micronuclei or lead to DNA leaking into the cytoplasm (Mackenzie *et al*., 2017). As a result, DNA sensing pathways can be triggered, and autoinflammation may occur *in vivo*. Autoinflammatory disease often manifests itself in at least one of the skin or CNS, often both (Rodero and Crow, 2016), and these tissues are both very relevant to HSV-1 infection. Mutations in human *PRKDC* have been shown to result in neurological complications as well as SCID (Woodbine *et al*., 2013). We did not observe pathology in the skin of *Paxx*$^{-/-}$ mice (data not shown). The behaviour of *Paxx*$^{-/-}$ mice was not indicative of neurological problems, and the weights of their brains were not different to those of WT mice (**Figure** 16**B**). Although this suggested that the loss of *Paxx* expression did not have major adverse effects on the skin and CNS of the mice, it would be interesting to look directly at IFN-I levels in *Paxx*$^{-/-}$ mice using ELISA (enzyme-linked immunosorbent assay).

The DNA repair machinery has also been shown to be important in the development of lymphocytes. DNA-PKcs is required for V(D)J recombination, and therefore *Prkdc*$^{-/-}$ mice lack B and T cell lymphocytes and exhibit a SCID phenotype (Blunt *et al*., 1995; Kirchgessner *et al*., 1995; Kurimasa *et al*., 1999b; Woodbine *et al*., 2013). Ku70 and Ku80 have also been shown to be required for efficient V(D)J recombination, although *Xrcc6*$^{-/-}$ (Ku70$^{-/-}$) mice are still able to achieve inefficient V(D)J recombination which is sufficient for the production of some abnormal T cells (Gu *et al*., 1997; Taccioli *et al*., 1994). Although humans with XRCC4 mutations do not have a SCID phenotype (Murray *et al*.,

2015), we therefore hypothesised that PAXX may also be important for V(D)J recombination. We used flow cytometry to show that the spleens and lymph nodes of *Paxx*$^{-/-}$ mice contained both B and T lymphocyte populations, and that the proportions of the different lymphocytes were similar to those of WT mice (**Figure 17**). This suggests that PAXX is not required for V(D)J recombination in mice, and others have made the same conclusion (Balmus *et al*., 2016). As discussed in Chapter 3, it would be interesting to account for potential redundancy between PAXX and XLF by comparing *Paxx*$^{-/-}$*Nhej1*$^{-/-}$ to single knockouts, but an inducible or tissue-specific system would be required *in vivo* due to the embryonic lethality of the double knockout (Balmus *et al*., 2016).

Having confirmed that *Paxx*$^{-/-}$ mice do not have overt developmental defects and that they have normal lymphocyte populations we wanted to investigate whether PAXX restricts HSV-1 infection *in vivo*. Mice unable to control HSV-1 infection usually lose weight and allow spread of the virus to the brain (Kollias *et al*., 2015). Neither WT nor *Paxx*$^{-/-}$ mice lost weight during infection with HSV-1 (**Figure 18A**). We also monitored the spread of HSV-1 expressing luciferase using IVIS. Following intradermal injection into the whisker pads, HSV-1 established infection in the noses of both WT and *Paxx*$^{-/-}$ mice (**Figure 18B**). There was one instance in a *Paxx*$^{-/-}$ mouse where signal was observed in the brain at day four, but this had been cleared by day six and otherwise signal was limited to the nasal area. By day six mice of both genotypes had started to clear the infection, and the luciferase activity detected dropped (**Figure 18C**). There were no significant differences in the luciferase activity detected between WT and *Paxx*$^{-/-}$ mice at any time during infection, and both genotypes had almost cleared the lytic infection by day ten. We also showed that after 11 days of infection the relative proportions of lymphocyte subsets had not changed. However, this analysis was only conducted at one time *post* infection, and so analysis would need to be conducted at other times *post* infection to ensure that our conclusions are robust.

These data suggest that PAXX is not required to restrict and clear HSV-1 infection *in vivo*, but there are a number of ways in which this conclusion could be tested further. In Chapter 3 we showed that PAXX restricts the production of infectious virus, and so it would be interesting to infect WT and *Paxx*$^{-/-}$ mice and to titrate the infectious virus

produced. Similarly, applying other techniques developed in Chapter 3 to determine viral genome copy numbers and genome structures would be informative, especially when considering a potential role for PAXX in the establishment of HSV-1 latency. Finally, the protocol could be adapted to better assess the immune response to HSV-1 infection in both genotypes. For example, ELISA could be used to investigate the innate immune response to infection, and antibody titres could be analysed using a plaque neutralisation assay. However, we decided that we could not ethically justify pursuing our original hypotheses further.

Although we had concluded that PAXX is not required to restrict and clear lytic HSV-1 infection *in vivo*, we investigated whether WT and *Paxx*$^{-/-}$ T cells were equally primed for activation following HSV-1 infection. To establish whether PAXX is required for the activation and IFNγ production of T cells in mice, lymphocytes isolated from the spleen and lymph nodes were activated with PMA and stained for IFNγ, TNFα, and CD62L. Lymphocytes from both WT and *Paxx*$^{-/-}$ mice were activated by PMA, regardless of whether they were isolated from individuals infected with HSV-1 or not, as is evidenced by an increased proportion of lymphocytes expressing IFNγ and TNFα, and the reduced proportion of lymphocytes expressing CD62L (**Figure 22**). There were no observable differences between the activation of WT and *Paxx*$^{-/-}$ lymphocytes, and this was true for both CD4^{+} and CD8^{+} lymphocytes (**Figure 22**). It is also interesting to consider that in Chapter 3 we observed that PAXX might be involved in MAPK signalling, and MAPK signalling has been shown to be important for activation and IFNγ production in CD4^{+} (Dong *et al*., 1998, 2000; Sabapathy *et al*., 1999) and CD8^{+} T cells (Merritt *et al*., 2000). This is exemplified by the activation of T cells by the generic MAPK stimulator, PMA. Furthermore, c-Jun is important in effector CD8^{+} T lymphocyte differentiation (Kuroda *et al*., 2011). However, these data suggest that PAXX is not required for PMA-induced activation of T lymphocytes, and that if MAPK signalling is defective in *Paxx*$^{-/-}$ cells, it does not affect T lymphocyte activation.

In addition to the general activation state of T lymphocytes, we also wanted to look at a HSV-1-specific activator of T lymphocytes, and so we explored the potential of using the gB$_{498\text{-}505}$ peptide from the HSV-1 glycoprotein gB. gB$_{498\text{-}505}$ is thought to be targeted by

70-90 % of HSV-1-specific $CD8^+$ T cells (Wallace *et al*., 1999). Although $gB_{498-505}$ activated IFNγ production in $CD4^+$ and $CD8^+$ cells, it did not stimulate T lymphocytes to produce TNFα or to remove CD62L (**Figure 23**). We therefore did not pursue $gB_{498-505}$ stimulation of T lymphocytes further.

Together, the data from this chapter show that *Paxx*$^{-/-}$ mice develop normally and do not have an overt pathological phenotype. We have also shown that PAXX is not required for the creation of lymphocytes, and that *Paxx*$^{-/-}$ lymphocytes are able to respond normally to PMA stimulation. Having presented our data on the role of PAXX during HSV-1 infection both in cell culture and *in vivo*, Chapter 5 will investigate the role of DNA-PKcs, another NHEJ protein, during HSV-1 infection.

5 The role of DNA-PKcs during HSV-1 infection

5.1 Introduction

In Chapters 3 and 4 we have discussed the role of PAXX during HSV-1 infection. In this chapter we will explore the role of another NHEJ protein, DNA-PKcs, in the same context. This is a subject of interest because the DNA-PK complex restricts HSV-1 infection, and, in response, HSV-1 has evolved to induce DNA-PKcs protein degradation (Lees-Miller *et al*., 1996; Parkinson *et al*., 1999). Human *PRKDC*$^{-/-}$ malignant glioma cells produce more infectious HSV-1 virus than their WT counterparts after two days of infection (Parkinson *et al*., 1999). The mechanisms by which DNA-PKcs inhibits HSV-1 infection are not currently known, and we hope to address this issue in this chapter.

There are multiple potential mechanisms through which DNA-PKcs could restrict HSV-1, and not all of these have been studied in the context of HSV-1 infection. Firstly, DNA-PKcs functions as an innate immune sensor of DNA, and the cytokine responses to HSV-1 infection are reduced in *Prkdc*$^{-/-}$ mice relative to their WT counterparts (Ferguson *et al*., 2012; Morchikh *et al*., 2017). It has also been proposed that the DNA-PK complex may contribute to HSV-1 genome circularisation, and therefore induce latency (Smith *et al*., 2014). This hypothesis is consistent with the observation that ICP0 promotes lytic HSV-1 infection (Jackson and DeLuca, 2003). Finally, DNA-PK can initiate some programmed cell death pathways, most notably apoptosis (Section 1.1.2.3), but this has not been investigated during HSV-1 infection.

The aim of the experiments in this chapter was to begin exploring the different roles of DNA-PKcs during HSV-1 infection, and to ultimately provide a more complete picture about how DNA-PKcs regulates HSV-1 infection.

5.2 HSV-1-induced degradation of DNA-PK complex components is cell-type specific

It has previously been reported that DNA-PKcs is degraded during HSV-1 infection, and that ICP0 is responsible for inducing this (Lees-Miller *et al*., 1996; Parkinson *et al*., 1999). However DNA-PKcs levels are stable during HSV-1 infection of rat cortical

neurons, whereas Ku80 is degraded (De Chiara *et al*., 2016). DNA-PKcs degradation has also been reported as absent in Vero cells, derived from the kidney of African green monkeys, however the authors only checked seven hours *post* infection, which may be too early to be conclusive (Wilkinson and Weller, 2004). We hoped that studying the cell type-dependency of DNA-PKcs and Ku80 degradation might help us to better understand the function of these proteins during HSV-1 infection. To further investigate this, RPE-1, U2OS, and HFFF cells were infected at MOI 10 with HSV-1, and protein was harvested at various times *post* infection for analysis by immunoblotting. We also infected cells with ΔICP0 HSV-1 to test whether DNA-PKcs degradation is dependent on ICP0 as described. RPE-1 cells were used because they are of epithelial origin, a natural target for HSV-1 infection, and for continuity with the experiments in Chapter 4. U2OS cells were chosen because they are permissive to **Δ**ICP0 infection, and so we hypothesised that the ICP0-induced degradation of DNA-PKcs might not be required for HSV-1 infection in these cells. HFFF cells were used at an early passage because they are fibroblasts that have the attributes of primary cells. As was expected, a drop in DNA-PKcs protein levels was observed in RPE-1 and HFFF cells (**Figure** 24**A** and **B**), but unexpectedly DNA-PKcs protein levels were stable in U2OS cells (**Figure** 24**C**). The reduction in DNA-PKcs protein was not observed in RPE-1 and HFFF cells infected with ΔICP0 HSV-1, suggesting that ICP0 is responsible for inducing DNA-PKcs degradation in these cells. HSV-1 infection of rat cortical cells induced a reduction in Ku80 protein (De Chiara *et al*., 2016). In all of the cells tested here, however, both Ku70 and Ku80 protein levels were stable. VP22 expression confirms that ΔICP0 HSV-1 successfully infected the cells. PARP-1 is cleaved by a range of host proteases and is indicative of the activation of cell death pathways (Chaitanya *et al*., 2010). HFFFs have no cleaved PARP-1, which may indicate that alternative or no cell death pathways are activated. In contrast RPE-1 cells exhibit a lot of PARP-1 cleavage. This suggests that PARP-1 cleavage and DNA-PKcs degradation are disconnected. VP22 expression and PARP-1 degradation is delayed relative to the kinetics observed with WT HSV-1, suggesting that the kinetics of ΔICP0 HSV-1 infection are slower. Finally, multiple bands are observed in RPE-1 cells when using an antibody recognising the N-terminus of DNA-PKcs for immunoblotting, and following HSV-1 infection all of these bands disappear, suggesting

that these bands may represent isoforms, degradation products, or differential *post*-transcriptional modification of DNA-PKcs.

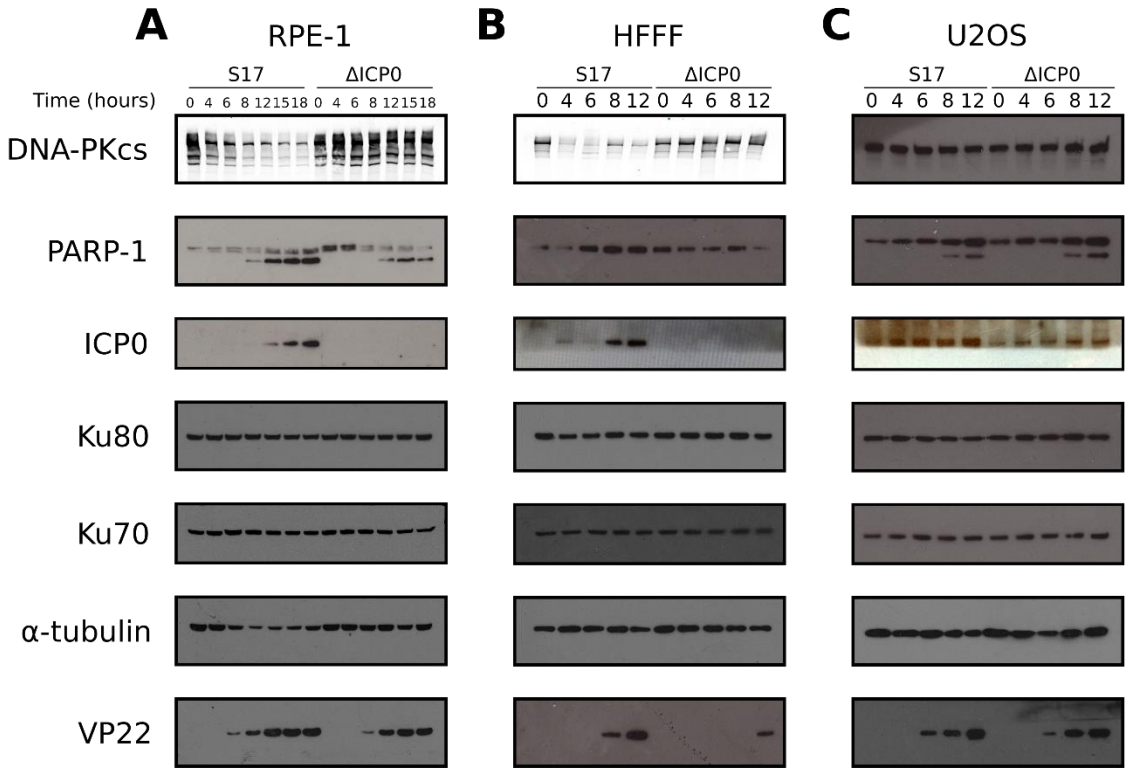

Figure 24: DNA-PKcs degradation is cell-type specific.

A) RPE-1, **B)** HFFF, and **C)** U2OS cells were infected with WT or ΔICP0 HSV-1 at MOI 10. At the indicated times *post* infection whole cell lysates were created. Immunoblotting was used to analyse the levels of DNA-PKcs, Ku70, and Ku80. PARP-1 levels were observed because cleavage of PARP-1 is indicative of caspase activation and cell death pathways. Tubulin was used as a loading control, and VP22 was used to demonstrate successful infection. Blotting for ICP0 showed that the ΔICP0 HSV-1 does not express ICP0. Data are representative of three independent experiments.

5.3 *PRKDC*$^{-/-}$ RPE-1 cells are not permissive to ΔICP0 HSV-1 infection

Infection of most cell types with **Δ**ICP0 HSV-1 at a low MOI does not produce infectious virions, but U2OS cells are permissive to **Δ**ICP0 HSV-1 infection (Deschamps and Kalamvoki, 2017). It has recently been proposed that this is due to dysfunctional STING signalling (Deschamps and Kalamvoki, 2017), in keeping with observations that ICP0 inhibits the IRF3 pathway (Lin *et al*., 2004a). STING signalling is impaired in response to DNA stimulation in the absence of DNA-PKcs (Ferguson *et al*., 2012; Morchikh *et al*., 2017). It has also been proposed ICP0-induced degradation of DNA-PKcs helps prevent progression to latency because DNA-PKcs may induce circularisation of the viral genome (Smith *et al*., 2014). Therefore abrogating DNA-PKcs expression may be sufficient to prevent both innate immune activation and viral latency resulting from the absence of ICP0. We therefore hypothesised that *PRKDC*$^{-/-}$ cells would be permissive to **Δ**ICP0 infection.

To test this hypothesis, CRISPR/Cas9 genome editing was used to create *PRKDC*$^{-/-}$ RPE-1 cells. RPE-1 cells were used in this study because we had already observed that ΔICP0 HSV-1 can infect these cells, and because ICP0 was required for the degradation of DNA-PKcs in these cells (**Figure 24A**). To maximise confidence that any phenotypes observed in *PRKDC*$^{-/-}$ cells would be due to the targeted genetic lesion rather than off-target effects of CRISPR, we created single guide RNAs (sgRNAs) that targeted two different sites in the *PRKDC* gene. The first sgRNA was designed to create an insertion or deletion mutation (InDel) at the N-terminus to create a frame-shift and disrupt the rest of the gene (**Figure 255A**). The second sgRNA created an InDel at the C-terminal end of the kinase domain. This mutant is of additional interest because previous studies have shown that the 83 C-terminal amino acids are required for DNA-PKcs NHEJ activity (Blunt *et al*., 1996), but not for the innate sensing of cytoplasmic DNA (Ferguson *et al*., 2012). Therefore if a lesion here does not create a functional KO, this could be used to help us to disentangle the two roles of DNA-PKcs during HSV-1 infection. RPE-1 cells were treated with CRISPR/Cas9 (Section 2.7.1), clones were created, and DNA-PKcs expression of the clones was tested using immunoblotting with an antibody recognising

the N-terminus of DNA-PKcs showed that a clone created with an sgRNA targeting the kinase domain did not express DNA-PKcs, but that two clones created with the sgRNA targeting the N-terminus did (**Figure 255B**). Given that the sgRNA targeted the kinase domain towards the C-terminus, this suggests that the truncated version may be degraded, and immunofluorescence was used to confirm that this clone (referred to as *PRKDC*$^{-/-}$ RPE-1 cells hereafter) did not express DNA-PKcs (**Figure 255C**). We therefore decided to use this clone in our analysis. We attempted to sequence the site at which we expected the mutation to be made, but had technical difficulty. Although the immunoblot and immunofluorescence have increased our confidence that this clone is a KO, a sequence should be attained in the future to further increase confidence in the clone. DNA-PKcs is a 469 kDa protein, and the *PRKDC* gene (excluding introns) is 13509 bp in length. As a result, rescue of the gene with current technology was not feasible.

To test our hypothesis that *PRKDC*$^{-/-}$ cells are permissive for **Δ**ICP0 infection, monolayers of WT RPE-1 cells, *PRKDC*$^{-/-}$ RPE-1 cells, and U2OS cells were infected with 30 PFU of WT or **Δ**ICP0 HSV-1 so that plaque formation could be observed. WT virus was able to form plaques in all cell types, while **Δ**ICP0 HSV-1 only formed plaques in U2OS cells (**Table 10**). ΔICP0 HSV-1 is often able to overcome restriction at higher MOIs (Everett *et al*., 2004), and both WT and *PRKDC*$^{-/-}$ RPE-1 cells showed CPE plaque formation, an indicator of productive infection, after infection with ΔICP0 HSV-1 at MOI 4.

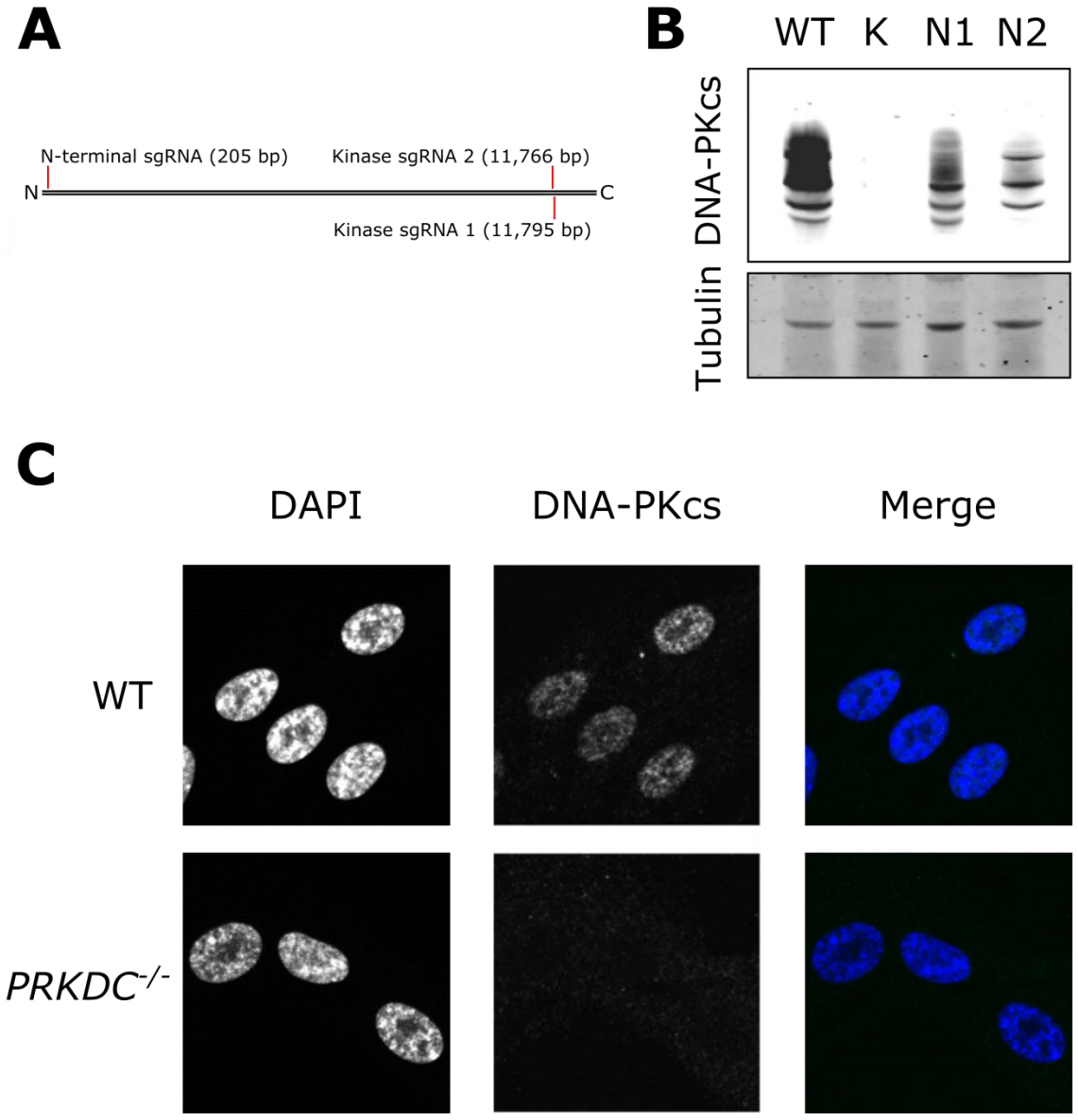

Figure 25: CRISPR/Cas9 was employed to create *PRKDC*$^{-/-}$ RPE-1 cells.

A) Map of sgRNA binding sites in *PRKDC*. **B)** Immunoblotting using an antibody recognising the N-terminus of DNA-PKcs was used to confirm the loss of DNA-PKcs expression in the clone where DNA-PKcs was targeted at the kinase domain (K), and two clones that were targeted at the N-terminus (N1 and N2). **C)** Immunofluorescence using an antibody recognising the N-terminus of DNA-PKcs was used to ensure that the *PRKDC*$^{-/-}$ clone was not a mixed population of WT and *PRKDC*$^{-/-}$ cells. Data is representative of three independent experiments.

	S17	ΔICP0	
	30 PFU	30 PFU	MOI 4
WT RPE-1	+	-	+
PRKDC$^{-/-}$ RPE-1	+	-	+
U2OS	+	+	+

Table 10: DNA-PKcs does not affect whether RPE-1 cells are permissive to ΔICP0 HSV-1 infection.
WT RPE-1 cells, *PRKDC*$^{-/-}$ RPE-1 cells, and WT U2OS cells were infected with 30 PFU of WT (S17) HSV-1 or ΔICP0 HSV-1, or at MOI 4 with ΔICP0 HSV-1. After 5 days of infection the cells were stained with crystal violet solution. The formation or absence of plaques in each condition is denoted by a '+' or '-', respectively. Data are representative of three independent experiments.

5.4 DNA-PKcs may alter the kinetics of infectious HSV-1 virion production

Although *PRKDC*$^{-/-}$ RPE-1 cells were not permissive to **Δ**ICP0 infection, this result does not preclude DNA-PKcs from having a role in regulating HSV-1. Indeed, it has previously been reported that after two days of infection *PRKDC*$^{-/-}$ human malignant glioma cells produce a higher titre of HSV-1 or **Δ**ICP0 than WT cells (Parkinson *et al*., 1999). However, the WT human malignant glioma cells were permissive to ΔICP0 HSV-1 infection and the loss of DNA-PKcs expression affected WT and ΔICP0 HSV-1 titres to a similar extent, indicating that these cells do not behave like most other cells during HSV-1 infection. We therefore wanted to investigate whether DNA-PKcs-deficient cells also produce more infectious virions when derived from a non-cancerous cell line. We also wanted to investigate how DNA-PKcs affects the kinetics of infectious HSV-1 virion production because LIG4- and XRCC4-deficient cells are delayed in their production of infectious HSV-1 virions (Muylaert and Elias, 2007). WT and *PAXX*$^{-/-}$ RPE-1 cells were infected at an MOI of 0.01 or 4, and the output of infectious virus was quantified by titration on Vero cells. MOI 0.01 was used to investigate multi-step infection dynamics, while MOI 4 was used to investigate single-step infection (as described in more detail in Section 3.2), and both experiments were repeated twice. In one experiment at MOI 0.01, WT RPE-1 cells produced significantly more infectious virions than *PRKDC*$^{-/-}$ RPE-1 cells 24 hours *post* infection, but 48 hours *post* infection the infectious virion production in *PRKDC*$^{-/-}$ RPE-1 cells had surpassed that of WT cells (**Figure 26A**). In the second repeat the titres of infectious virus were similar 24 hours *post* infection, but *PRKDC*$^{-/-}$ RPE-1 cells produced significantly more infectious virus 48 hours *post* infection (**Figure 26B**). The preliminary nature of these results is highlighted by their inconsistencies, and further repeats are required for any conclusions to be drawn. The experimental repeats at MOI 4 were more consistent in the shape of the curve, although there was a 10-fold difference between repeats (**Figure 26C and D**). 12 hours *post* infection at MOI 4 WT cells produced significantly more infectious virions than WT RPE-1 cells, but this phenotype was reversed 48 hours *post* infection where *PRKDC*$^{-/-}$ RPE-1 cells produced more infectious

virions than WT cells. Although these results are more consistent, further repeats are required before strong conclusions can be made.

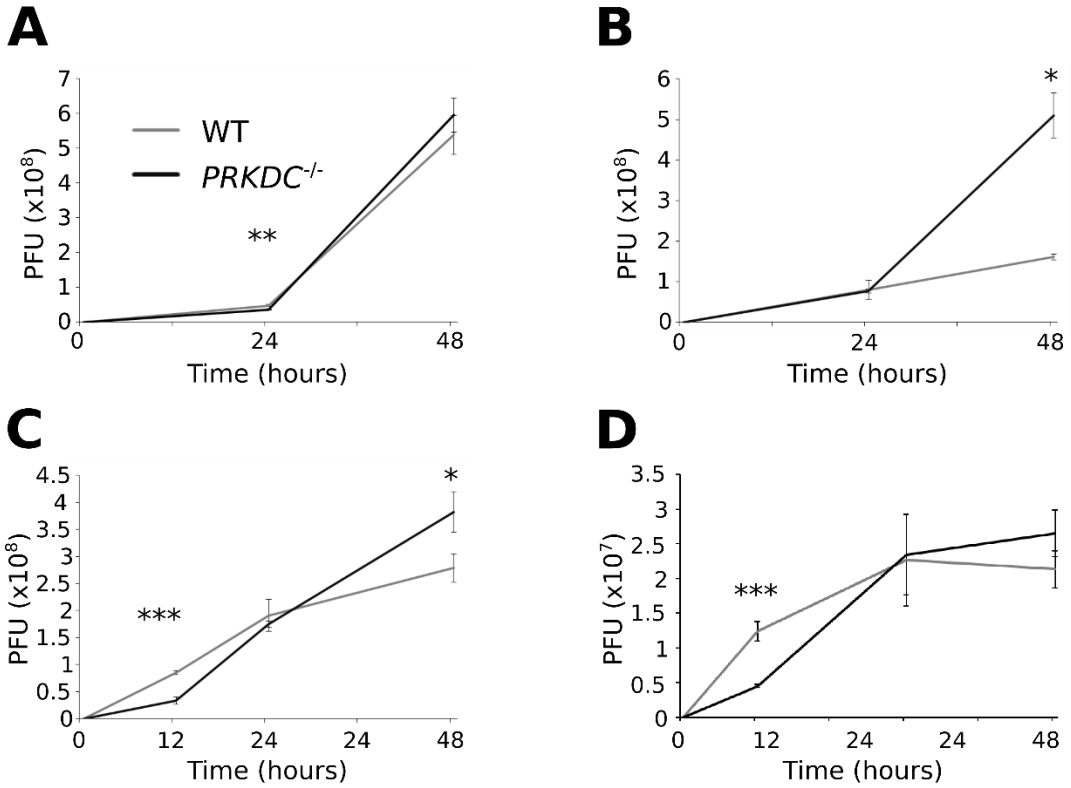

Figure 26: HSV-1 infection of *PRKDC*$^{-/-}$ cells produces fewer infectious virions than WT cells early in infection, but more later in infection.

A) and **B)** show two experiments where WT and *PRKDC*$^{-/-}$ RPE-1 cells were infected at MOI 0.01, and at the indicated times *post* infection the number of infectious virions was quantified by titration onto Vero cells. **C)** and **D)** show two experiments with the same setup as in A) and B), but at MOI 4. All data points are the mean of a biological triplicate, and error bars show intra-experimental mean +/- standard error of the mean (SEM). Statistical significance, calculated using the Student's t-test, is indicated using stars - * = $p<0.05$, ** = $p<0.02$, *** = $p<0.01$.

5.5 Endless HSV-1 genomes can be observed in cells lacking DNA-PKcs.

It has been proposed that DNA-PKcs may be required for the circularisation of the HSV-1 genome (Smith *et al*., 2014). We therefore hypothesised that *PRKDC*$^{-/-}$ RPE-1 cells produce less infectious virus than WT cells 12 hours *post* infection at MOI 4 (**Figure 26B**) because DNA-PKcs is required for genome circularisation, and therefore for efficient rolling circle replication of the HSV-1 genome. HSV-1 genome circularisation is correlated with HSV-1 latency (Jackson and DeLuca, 2003; Rock and Fraser, 1985; Smith *et al*., 2014), so this may also explain why WT cells produce fewer infectious virions than *PRKDC*$^{-/-}$ 48 hours *post* infection. We therefore wanted to investigate whether HSV-1 genome circularisation occurs efficiently in absence of DNA-PKcs. To test this, WT and *PRKDC*$^{-/-}$ cells were infected with HSV-1 at MOI 4, and the viral genomes were analysed by southern blotting to detect endless forms of the genome (Section 2.6.8). Preliminary results suggest that WT and *PRKDC*$^{-/-}$ cells support similar levels of HSV-1 circularisation at 5 hours post infection (**Figure 27**). There also appears to be less viral

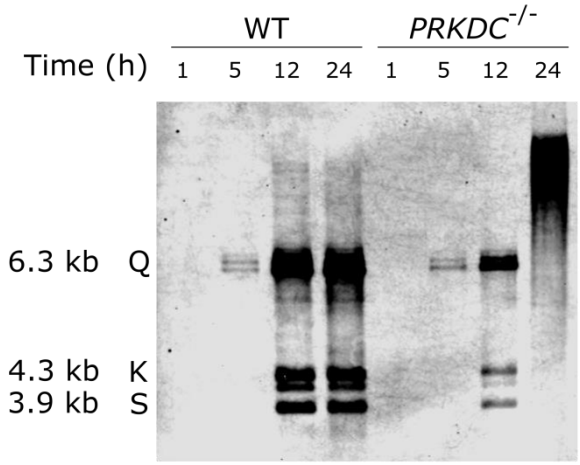

Figure 27: Endless HSV-1 genome form efficiently in *PRKDC*$^{-/-}$ cells, but genome replication is restricted. WT and *PRKDC*$^{-/-}$ cells were infected at MOI 4, and total cellular and viral DNA was isolated at indicated times *post* infection. The DNA extracts were digested with BamHI, and the HSV-1 S, K, and Q fragments were visualised by southern blot. The same total mass of DNA was added to each well. The sizes of the K, Q, and S fragments are indicated. This preliminary experiment has only been performed once.

DNA in *PRKDC*$^{-/-}$ cells after 12 hours of infection in a manner reminiscent of that observed in *PAXX*$^{-/-}$ cells (Section 3.4, **Figure 8**). The smear observed in the *PRKDC*$^{-/-}$ sample after 24 hours is likely to be due to problems with the BamHI digestion of the viral DNA and so requires repeating prior to full analysis of the results. Although these data suggest that DNA-PKcs is not required for HSV-1 genome circularisation, and that genome replication is less efficient in the absence of PAXX, several repeats of this experiment are required before robust conclusions can be made.

5.6 Prkdc$^{-/-}$ *primary murine skin fibroblasts respond normally to DNA stimulation and infection*

DNA-PKcs is an innate sensor of cytoplasmic DNA (Section 1.3.1.2), but the exact mechanisms of its function are not well characterised. We wanted to further investigate the role of DNA-PKcs in innate immunity, but wanted to use an alternative model to RPE-1 cells due to the poor stimulation of innate pathways in these cells and because non-primary cells such as RPE-1 cells generally produce low levels of IFNβ (Section 3.8). A method was optimised to culture primary murine skin fibroblasts (MSFs) from WT C129 and *Prkdc*$^{-/-}$ C129 mice (**Section 2.10.9**). To test the responsiveness of these cells to innate immune stimuli, WT MSFs were infected with ΔICP0 HSV-1 at MOI 5, or transfected with 5 μg/mL of concatenated DNA. ΔICP0 HSV-1 was used because ICP0 induces the degradation of DNA-PKcs (Lees-Miller *et al*., 1996; Parkinson *et al*., 1999), and also inhibits innate immune responses to infection (Eidson *et al*., 2002b; Lin *et al*., 2004b; Mossman *et al*., 2001). Cells were harvested six hours after stimulation because we have previously observed significantly increased transcription of IFNβ and other genes at this time (Ferguson *et al*., 2012), the RNA was purified, and cDNA was created for gene expression analysis by qPCR. The culture of MSFs *ex vivo* produced a low yield of cells for a given area of skin, and the MSFs progressed to senescence after two passages, so culturing large numbers of cells was difficult. Therefore, we did not create biological repeats for this experiment. However, we were able to show that after six hours both infection with ΔICP0 HSV-1 and stimulation with concatenated DNA were sufficient to induce *Ifnb*, *Cxcl10*, *Isg15*, and *Ifna* transcription in WT MSFs (**Figure 28A-D**).

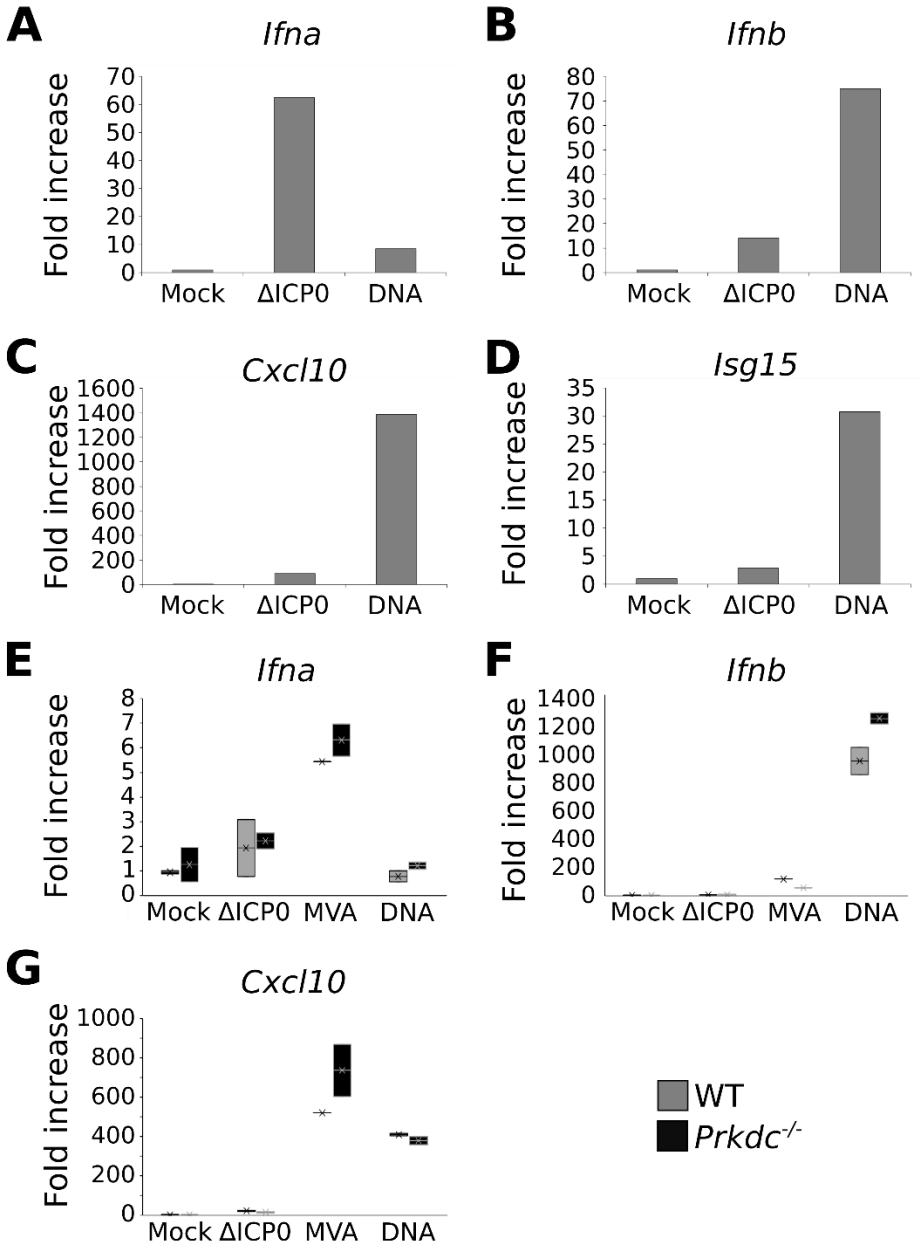

Figure 28: *Prkdc*$^{-/-}$ murine skin fibroblasts respond normally to infection and DNA transfection.

Murine skin fibroblasts (MSFs) were cultured *ex vivo* from mice, and used within the first two passages. WT MSFs from C57BL/6 mice were infected with ΔICP0 HSV-1 at MOI 5, stimulated by transfecting 5 μg/mL of concatenated DNA, or left untreated (mock), and the transcription levels of **A)** *Ifna*, **B)** *Ifnb*, **C)** *Cxcl10*, and **D)** *Isg15* after six hours were determined relative to *Hprt* by qPCR. These graphs were created from data without biological repeats. In a separate experiment, WT and *Prkdc*$^{-/-}$ MSFs from C129 mice were infected with ΔICP0 HSV-1 at MOI 5, infected with MVA at MOI 5, transfected with 5 μg/mL of concatenated DNA, or left untreated (mock). Transcription levels of **E)** *Ifna*, **F)** *Ifnb*, and **G)** *Cxcl10* were quantified after five hours using qPCR, and calculated relative to *Hprt*. The boxes represent two biological repeats, and the lines and crosses represent the mean. Data are representative of two independent experiments.

Having demonstrated that WT MSFs were responsive to infection and stimulation with DNA, we compared the responses of WT and *Prkdc*$^{-/-}$ MSFs. We aimed to establish whether DNA-PKcs-dependent DNA sensing was compartment-dependent, and so we compared the cytoplasmic-replicating VACV with the nuclear-replicating HSV-1 in this context. WT and *Prkdc*$^{-/-}$ MSFs were infected with MVA at MOI 5. MVA is an attenuated form of VACV which lacks many innate immune modulators, resulting in greater stimulation of innate immune signalling pathways than WT VACV. We had hoped to conduct this experiment under the same conditions as in **Figure 28**, but infected *Prkdc*$^{-/-}$ cells had very advanced cytopathic effect (CPE) six hours *post* infection with ΔICP0 HSV-1, and we were concerned that cell death pathways may interfere with innate immune signalling pathways. We therefore tested transcription levels five hours *post* stimulation instead. This difference in timing can explain some differences between levels of stimulation, for example lower levels of *Ifnb* transcription five hours *post* ΔICP0 HSV-1 infection as compared with six hours *post* infection (**Figure 28B** and **F**). Nevertheless good stimulation was observed for most treatments and genes. Although mean transcription levels were generally higher in WT MSFs than *Prkdc*$^{-/-}$ MSFs, there were no instances where this was statistically significant. It is interesting to note that in both WT and *Prkdc*$^{-/-}$ MSFs at both five and six hours *post* infection, the *Ifna* genes are the only ones which have higher levels of transcription following ΔICP0 HSV-1 infection than following concatenated DNA transfection (**Figure 28A** and **E**).

5.7 PRKDC$^{-/-}$ RPE-1 cells exhibit advanced CPE during HSV-1 infection

While conducting the above experiments we observed that *PRKDC*$^{-/-}$ RPE-1 cells and *Prkdc*$^{-/-}$ MSFs showed more advanced CPE during infection than WT cells. Indeed, the advanced CPE of *Prkdc*$^{-/-}$ MSFs after six hours was significant enough that we decided to change our experimental design while testing the innate immune responses of MSFs (**Section 5.6**). The processes behind HSV-1-induced CPE are poorly understood; despite work showing the potential for qualitative analysis of cellular volume using stereological analysis (Motamedifar and Noorafshan, 2008), this method does not capture the extent of morphology changes, and analysis in the literature remains largely

qualitative and subjective. To represent our observation we infected WT and *PRKDC*$^{-/-}$ RPE-1 cells with HSV-1 at MOI 0.01, and photographed the cell monolayer at various times post infection (**Figure 29**). RPE-1 cells were used because we have previously observed this phenotype in these cells, and because *Prkdc*$^{-/-}$ MSFs were not easily cultured *ex vivo* at a large enough scale for this experiment. CPE was first observed after 24 hours in cells of both genotypes, but *PRKDC*$^{-/-}$ cells appeared more rounded, and the plaque appeared larger. 48 hours *post* infection with HSV-1 at MOI 0.01, almost all *PRKDC*$^{-/-}$ RPE-1 cells exhibited advanced CPE, whereas WT cells were still forming individual plaques. 72 hours *post* infection all *PRKDC*$^{-/-}$ cells had dissociated from the plate, while many WT cells still did not show signs of CPE.

To further probe the advanced CPE in *PRKDC*$^{-/-}$ cells, we also examined CPE following infection at MOI 4 (**Figure 30**). Most *PRKDC*$^{-/-}$ cells had CPE after only 12 hours of infection, as compared with very few WT cells. After 24 hours most *PRKDC*$^{-/-}$ had advanced CPE, whilst WT cells were forming plaques. 48 hours *post* infection all *PRKDC*$^{-/-}$ cells were fully detached from the plate, and almost all WT cells displayed signs of at least early CPE. This phenotype is disconnected from our preliminary observations that early in infection WT RPE-1 cells may produce more infectious HSV-1 virions (**Figure 26**).

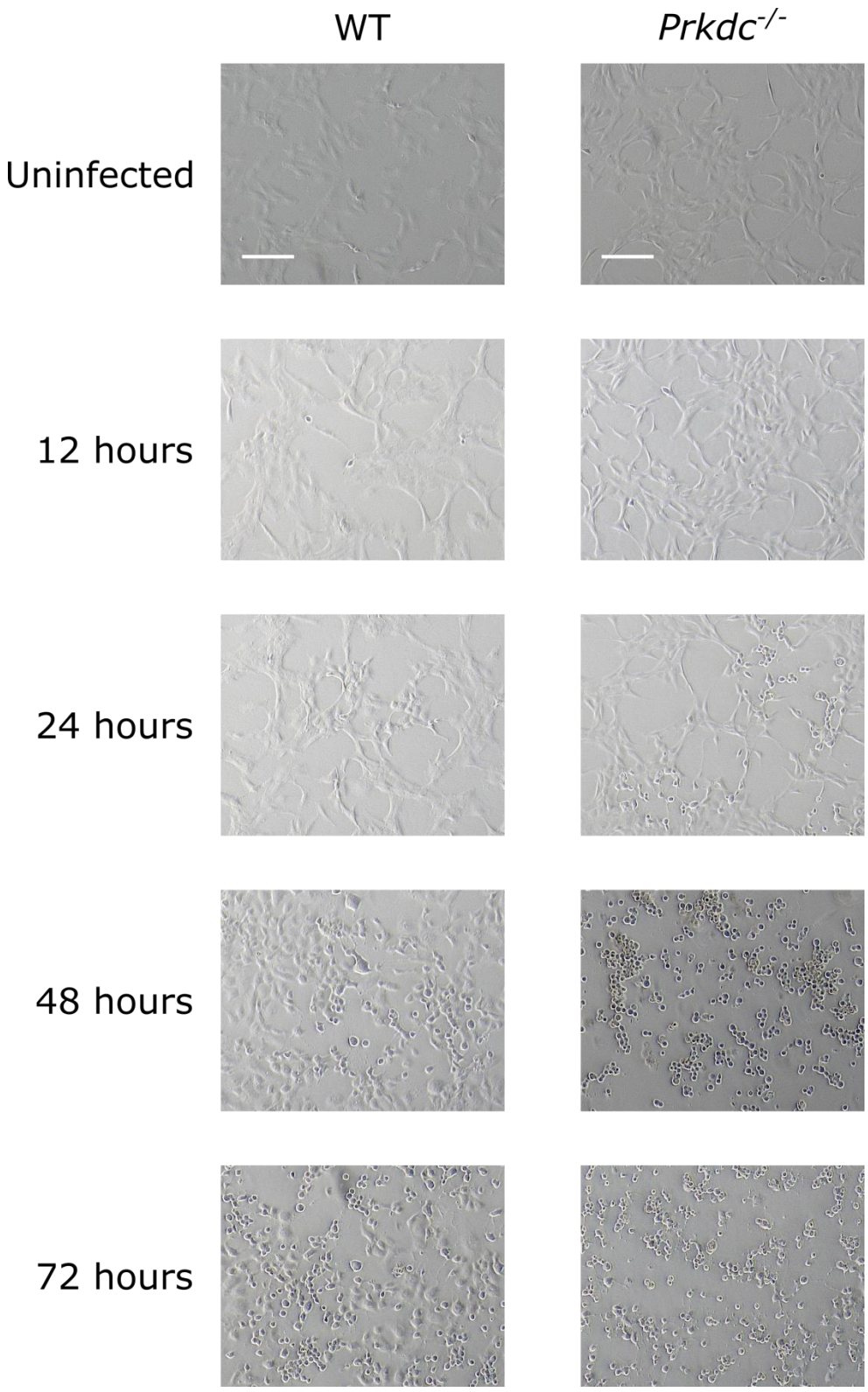

Figure 29: *PRKDC*$^{-/-}$ RPE-1 cells exhibit advanced CPE during HSV-1 infection at low MOI.

WT and *PRKDC*$^{-/-}$ RPE-1 cells were infected with HSV-1 at MOI 0.01 and photographed at the indicated times *post* infection using a Zeiss Vert.A1 microscope with an AxioCam Mrc camera. The scale bars represent 100 μm**.** Data are representative of three independent experiments.

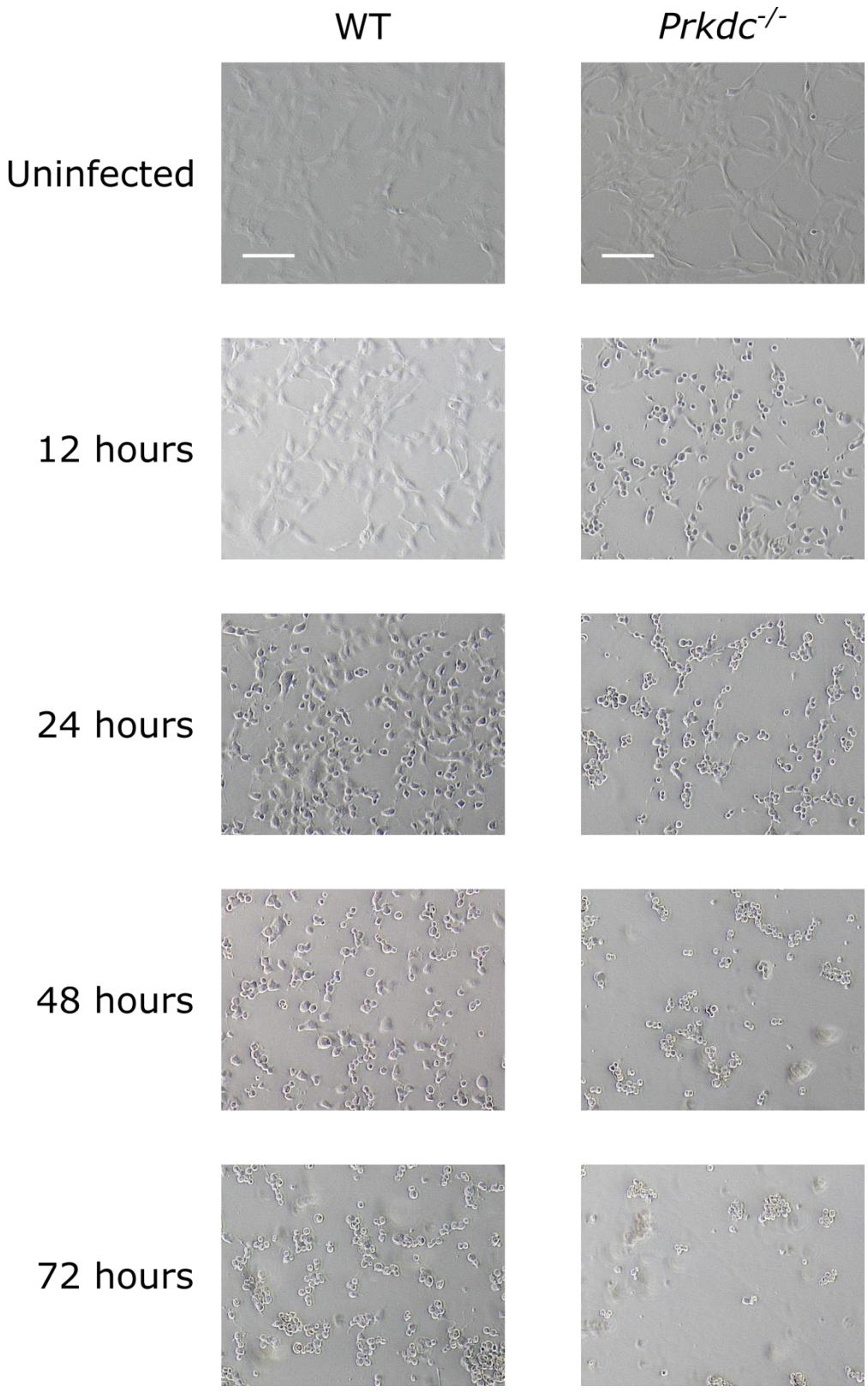

Figure 30: *PRKDC*$^{-/-}$ RPE-1 cells exhibit advanced CPE during HSV-1 infection at high MOI.

WT and *PRKDC*$^{-/-}$ RPE-1 cells were infected with HSV-1 at MOI 4 and photographed at the indicated times *post* infection a Zeiss Vert.A1 microscope with an AxioCam Mrc camera. The scale bars represent 100 μm. Data are representative of three independent experiments.

5.8 Discussion

There is a growing literature on the functions of DNA repair proteins during DNA virus infection (Section 1.2), and their impact on HSV-1 infection is an area of ongoing investigation (Section 1.2.6). DNA-PKcs was amongst the first DNA repair proteins to be identified as a factor regulating HSV-1 infection following the discovery that it was degraded by ICP0, and that human malignant glioma cells deficient in DNA-PKcs expression produce more infectious HSV-1 virions two days *post* infection (Lees-Miller *et al*., 1996; Parkinson *et al*., 1999). Further work showed that DNA-PKcs is involved in the induction of cytokine transcriptional responses during HSV-1 infection *in vivo*, and to DNA in cultured cells (Ferguson *et al*., 2012; Morchikh *et al*., 2017). The innate immune roles of DNA-PKcs might be sufficient to explain the detrimental impact of DNA-PKcs on HSV-1 infection, but this link has not been formalised, and there are alternative explanations. For instance, there have been roles proposed for DNA-PKcs during HSV-1 genome replication, including the inhibitory effects of DNA-PKcs-induced circularisation of the HSV-1 genome (Smith *et al*., 2014), but these have not been tested experimentally. Similarly, although DNA-PKcs has previously been linked to cell death pathways (Section 1.1.2.3), this has not been characterised in the context of HSV-1 infection.

This chapter aimed to investigate these roles of DNA-PKcs during HSV-1 infection, and as part of this we created *PRKDC*$^{-/-}$ RPE-1 cells using CRISPR/Cas9 and used immunoblotting and immunofluorescence to demonstrate that DNA-PKcs is not expressed at detectable levels in these cells (**Figure 255**). We attempted to address some of the limitations of CRISPR/Cas9 by creating multiple clones, but unfortunately this was not successful. Future work should try some alternative sgRNAs, preferably targeting the N-terminus of *PRKDC*, and sequence the clones to demonstrate that the CRISPR/Cas9 worked as intended.

Although these limitations are important to address, the phenotypes we have observed make sense in the context of what is already known about DNA-PKcs, and we remain confident that they are due to the reduction in DNA-PKcs expression. We will

now discuss these phenotypes and some of the interesting implications arising from our work.

5.8.1 DNA-PKcs degradation during HSV-1 infection

The first reports of an interaction between DNA-PKcs and HSV-1 arose following the observation that the HSV-1 protein ICP0 induces the degradation of DNA-PKcs (Lees-Miller *et al*., 1996; Parkinson *et al*., 1999). It has previously been reported that this degradation is not observed in Vero cells (African green monkey kidney fibroblasts) (Wilkinson and Weller, 2004), although this observation was made only 7 hours *post* infection which may be too early to be conclusive. Insignificant changes in DNA-PKcs protein levels have also been observed in rat cortical cells, although this was at MOI 0.01 and using HSV-1 strain F (De Chiara *et al*., 2016). Other proteins important in restricting HSV-1 are known to be degraded by ICP0, including IFI16 (Johnson et al., 2013; Orzalli et al., 2016). WhetherICP0 has a direct effect on cGAS is unknown, but ICP0 targets other components of the pathway for degradation, such as STING (Kalamvoki and Roizman, 2014), and inhibits IRF3 and IRF7 activation (Lin et al., 2004b).

We tested the effect of HSV-1 infection on DNA-PKcs protein levels in RPE-1, U2OS, and HFFF cells. A drop in DNA-PKcs protein levels was observed in RPE-1 and HFFF cells, although degradation appeared to be faster in the latter (**Figure 24A** and **B**). This reduction in DNA-PKcs protein was dependent on ICP0, and so it is likely that ICP0 is inducing degradation of DNA-PKcs as previously described (Lees-Miller *et al*., 1996; Parkinson *et al*., 1999). We observed that DNA-PKcs protein levels are stable during HSV-1 infection of U2OS cells (**Figure 24C**), which has not been reported previously. During HSV-infection ICP0 initially localises to promyelocytic leukaemia (PML) nuclear bodies and induces their degradation (Cuchet-Lourenço *et al*., 2012). U2OS cells have defects in expression of the PML nuclear body components ATRX and Daxx, and it has been proposed that this is why U2OS cells are permissive to ΔICP0 HSV-1 infection (Lukashchuk and Everett, 2010). Normally ICP0 induces the degradation of a number of factors whilst interacting with the PML nuclear bodies, so this may be why DNA-PKcs degradation is not observed in U2OS cells. It would be interesting to look at other

degradation targets of ICP0 and determine whether these are degraded during infection of U2OS cells.

Ku80 protein levels drop during HSV-1 infection of rat cortical cells (De Chiara *et al*., 2016), but levels were stable in all cell types that we tested. In fact, we found that Ku70 and Ku80 protein levels were more stable than α-tubulin, levels of which frequently varied independently of other proteins. ICP0 dismantles microtubule networks during infection, and is also able to bind to α-tubulin, although there is no direct evidence of ICP0-induced degradation of α-tubulin (Liu *et al*., 2010).

5.8.2 DNA-PKcs, genome replication, and infectious virus production

Although functions for DNA-PKcs in the regulation of HSV-1 genome replication have been proposed, to our knowledge these have not yet been investigated. Our preliminary southern blotting data suggest that DNA-PKcs is not required for the formation of endless genomes, and that five hours *post* infection the signal of the K fragment is similar between WT and *PRKDC*$^{-/-}$ RPE-1 cells (**Figure 27**). However, later in infection the HSV-1 genome replicates less efficiently in *PRKDC*$^{-/-}$ cells, suggesting that DNA-PKcs may actually promote HSV-1 infection. Alternatively, it is possible that the reduced genome replication observed in *PRKDC*$^{-/-}$ cells is linked to the advanced CPE observed in these cells (**Figure 29** and **Figure 30**; Section 5.8.4).

It is interesting that less HSV-1 genome replication is observed by 12 and 24 hours post infection in both *PRKDC*$^{-/-}$ and *PAXX*$^{-/-}$ RPE-1 cells (**Figure 8**; **Figure 27**), however different mechanisms may be at play; *PRKDC*$^{-/-}$ cells do not have a defect in the formation of endless genomes after five hours, whereas *PAXX*$^{-/-}$ RPE-1 cells do have fewer endless genomes than WT cells. This suggests that PAXX and DNA-PKcs may be functioning differently in HSV-1 genome replication, but it is important to remember that the experiment with *PRKDC*$^{-/-}$ cells needs to be repeated before strong conclusions can be made. It would also be interesting to complement these experiments with qPCR to quantify viral genome copy number, as we have done with PAXX (**Figure 7**).

Preliminary growth curve experiment suggest that at early times *post* infection with HSV-1, *PRKDC*$^{-/-}$ RPE-1 cells produce significantly fewer infectious virions than WT RPE-1 cells (**Figure 26A** and **B**). This was observed 12 hours *post* infection at MOI 0.01, and 24 hours *post* infection at MOI 4 WT RPE-1 cells. At both MOIs, later in infection *PRKDC*$^{-/-}$ RPE-1 cells end up producing more infectious virus. This is an unusual dynamic, and suggests that either cells lacking DNA-PKcs are delayed in producing HSV-1 virions, or that there are different phases during which DNA-PKcs has different effects upon infectious virion production. Given the multiple roles of DNA-PKcs, it is easy to suggest examples for the second hypothesis, for example early in infection DNA-PKcs could promote genome replication (as observed by southern blot and qPCR) while later in infection DNA-PKcs could create an antiviral state by triggering an innate immune response (Section 5.8.3). These hypotheses are limited by the preliminary nature of the experiments, and repetition of the experiments are required before any conclusions can be made. However, the observation that *PRKDC*$^{-/-}$ RPE-1 cells produce more infectious virus at later stages of HSV-1 infection is in agreement with the observation that *PRKDC*$^{-/-}$ human malignant glioma cells produce more infectious virions after two days of infection than their WT counterparts (Parkinson *et al*., 1999).

It is notable that in RPE-1 cells the DNA-PKcs protein is mostly degraded by eight hours *post* infection, yet we continue to notice its effects on genome replication and infectious virion production long after this time. Naturally, this raises questions regarding the CRISPR/Cas9 clone that we have used, and this major limitation of our experiments needs to be addressed in future work. However, some of our observations, for example the advanced CPE phenotype in DNA-PKcs-deficient cells (Section 5.8.4), have been confirmed in MSFs, which raises our confidence in these data. There are also other explanations for the long-lasting effects of DNA-PKcs; most notably, that we continue to observe DNA-PKcs protein at a low level in RPE-1 cells throughout the first 18 hours of HSV-1 infection (**Figure 24**). It is also possible that DNA-PKcs will have initiated multiple DDR pathways which will have long-lasting effects on the cell. Finally, any innate immune roles of DNA-PKcs are also likely to have long-lasting effects on HSV-1 genome replication and infectious virion production.

If our results are reproducible, it would be interesting to consider the role of other NHEJ factors in HSV-1 genome replication and infectious virion production. LIG4 and XRCC4 are so far the only NHEJ factors published to affect these processes, and are required for the formation of endless HSV-1 genomes, and for efficient production of infectious virions (Muylaert and Elias, 2007). This phenotype is different from PAXX and DNA-PKcs, and so it would be interesting to consider whether other factors, such as Ku and XLF, share one of the phenotypes, or have novel functions during HSV-1 infection.

In light of the data which show that DNA-PKcs may in fact promote the production of infectious HSV-1 virions early in infection, it is perhaps unsurprising that we did not find that *PRKDC*$^{-/-}$ RPE-1 cells were permissive to ΔICP0 HSV-1 infection (Section 5.3). In fact, given the potentially beneficial role of DNA-PKcs early in infection, the loss of DNA-PKcs might make these cells even more hostile to ΔICP0 HSV-1 infection. It would therefore be interesting to test whether cells normally permissive to ΔICP0 HSV-1, for example U2OS cells, produce fewer infectious virions if DNA-PKcs expression or activity is abrogated.

5.8.3 DNA-PKcs and the innate immune response to DNA

DNA-PKcs is a cytoplasmic sensor of DNA (Ferguson *et al*., 2012; Morchikh *et al*., 2017), and we hoped to further investigate this function of DNA. Our experiments testing the innate immune responses of RPE-1 cells in Chapter 3 showed that RPE-1 cells are not easily stimulated by DNA or ΔICP0 HSV-1 infection (**Figure 12**). We therefore optimised a system to isolate and culture MSFs from WT and *Prkdc*$^{-/-}$ mice *ex vivo*. Although transcription of *Cxcl10* and interferons was generally slightly higher in WT MSFs than *Prkdc*$^{-/-}$ MSFs, these differences were not significantly different (**Figure 28**).

DNA-sensing is likely to be critical for IFN-I production, and viruses have evolved multiple mechanisms to inhibit the DNA-sensing pathway. There are numerous putative innate immune sensors of cytoplasmic DNA, and it has not been determined why so many should exist. However, there are a number of theories as to why this might be (Unterholzner, 2013), including that innate immune sensing pathways are cell-type specific, and that some receptors may have a degree of redundancy. ICP0 targets DNA-

PKcs for degradation and it may also target IFI16, but it has not been shown to inhibit cGAS (Cuchet-Lourenco et al., 2013; Lees-Miller et al., 1996; Orzalli et al., 2012). As such, prevention of ICP0 expression might not be sufficient to prevent inhibition of DNA-sensing pathways, and thereby observe their effects on IFN and cytokine production. Furthermore, HSV-1 infection in the absence of ICP0 expression can destabilise STING, which would dampen innate immune responses in all cell types (Kalamvoki and Roizman, 2014). Any of these hypotheses could be used to explain why DNA-PKcs does not appear to be important in stimulating an innate immune transcriptional response in these MSFs.

5.8.4 DNA-PKcs, CPE, and cell death

The advanced CPE observed in DNA-PKcs-deficient cells during HSV-1 infection (**Figure 29** and **Figure 30**) is interesting, and we have observed the phenotype enough times to be confident that it is reproducible. However, it is important that the implications of this are not overstated, and, ultimately, more experiments are required to understand the cause and mechanism of this phenotype. However, for the purpose of this thesis, it remains interesting to consider potential explanations of our observations.

DNA-PKcs has functions in cell death, and these generally appear to be pro-apoptotic (Hill and Lee, 2010; Wang *et al*., 2000, 2016). DNA-PKcs phosphorylates γH_2AX and induces apoptosis following DNA damage and TNF-related apoptosis-inducing ligand (TRAIL) treatment (Hill and Lee, 2010; Solier and Pommier, 2009; Solier *et al*., 2009). DNA-PKcs also induces apoptosis in lymphocytes *via* p53 activation (Callén *et al*., 2009), including during integration of the HIV-1 genome into the host genome (Cooper *et al*., 2013).

It is therefore interesting that DNA-PKcs-deficient cells show CPE more quickly than WT cells, because it might be expected that DNA-PKcs would promote cell death. At this point it is important to clarify that we are indeed observing CPE and not cell death, two very different things. However, it is tempting to hypothesise that although DNA-PKcs is required for driving apoptosis, in its absence other forms of cell death or stress occur. These alternative pathways may even create an environment more conducive for HSV-1

genome replication late in infection, a potential explanation for the higher titres of virus observed late in infection in *PRKDC*$^{-/-}$ RPE-1 cells than in WT cells (**Figure 26**). Although HSV-1 activates necroptosis in mouse cells, it inhibits the necroptotic pathway in human cells, making this pathway unlikely to be the cause of the CPE (Guo et al., 2015; Wang et al., 2014; Yu and He, 2016), The role of pyroptosis during HSV-1 infection has not been studied in depth, and so this could be a potential candidate.

It would be of great interest to the field to test these hypotheses. It would be interesting to investigate whether PARP-1 cleavage observed during HSV-1 infection of RPE-1 cells (**Figure 24A**) is still observed in *PRKDC*$^{-/-}$ cells. There are also multiple assays available to test which cell death pathways are activated in infected cells (Kepp *et al*., 2011). Following the identification of relevant cell death pathways, specific cell death inhibitors could be used during HSV-1 infection to test whether the CPE phenotype could be rescued, and to investigate the impact of these inhibitors on infectious HSV-1 production.

An alternative explanation to cell death is that the increased production of HSV-1 in DNA-PKcs-deficient cells is sufficient to cause CPE through the stresses placed on cellular metabolism. However, the difference in CPE is disproportionate to the increase of infectious virus production in *PRKDC*$^{-/-}$ cells, and five hours *post* infection is very early to be observing stress-induced CPE in *Prkdc*$^{-/-}$ MSFs. Therefore, although further experiments would be required to confirm this, we think it is unlikely that metabolic stress is the cause of HSV-1-induced CPE in the absence of DNA-PKcs.

5.8.5 Summary

The data presented in this chapter has given some insight into the functions of DNA-PKcs during HSV-1 infection, but there is much yet to be understood about its role. Our data suggest that DNA-PKcs is beneficial to the early production of infectious virions, but restricts infectious virion production late in infection. Preliminary data suggest that HSV-1 genome replication is supported by DNA-PKcs. In the absence of DNA-PKcs, both RPE-1 cells and MSFs displayed advanced levels of CPE, which might be indicative of interesting roles of DNA-PKcs in regulating cell death pathways.

Together, these data support the argument that DNA-PKcs has multiple functions during HSV-1 infection, and that further study of these will give insight into a number of pathways important in viral infection.

Concluding remarks

In this study we have investigated how HSV-1 infection is affected by PAXX and DNA-PKcs, two NHEJ factors about which little is known in this context. We observed that cells deficient in either of PAXX or DNA-PKcs support reduced viral genome replication but increased production of infectious virus late during infection relative to WT cells, indicating that they restrict HSV-1 infection.

PAXX has not previously been studied in the context of viral infection. We demonstrated that viral gene expression and protein production was unaffected by PAXX deficiency, and that EM shows normal packaging and wrapping of virions in *PAXX*$^{-/-}$ cells. We also showed that PAXX is not required to control HSV-1 infection in mice, or for the production or activation of lymphocytes. Interestingly, however, PAXX may have functions in the innate immune response to DNA. Future work should seek to address whether PAXX influences the particle:PFU ratio of HSV-1, as this one possible explanation of our data.

DNA-PKcs has previously been studied during viral infection, although this is limited within the context of HSV-1 infection. We confirmed previous reports that DNA-PKcs is degraded in infection, but observed that this is not the case in U2OS cells. We hypothesised that this may be linked to U2OS cells being permissive to ΔICP0 HSV-1, but the *PRKDC*$^{-/-}$ RPE-1 cells we generated with CRISPR/Cas9 do not support ΔICP0 HSV-1 infection. We also showed that *Prkdc*$^{-/-}$ MSFs were able to initiate innate immune gene expression following HSV-1 infection or nucleic acid stimulation, suggesting that DNA-PKcs is not important for detecting cytoplasmic DNA in these cells. Finally, *Prkdc*$^{-/-}$ MSFs and *PRKDC*$^{-/-}$ RPE-1 cells exhibit CPE faster than their WT counterparts, an observation which may have implications for our understanding of the drivers of cell death, and which demonstrates that HSV-1 is a useful model for studying cellular fate during infection.

This study has shown that both PAXX and DNA-PKcs restrict HSV-1 infection, and provides the basis for further exploration of the mechanisms involved. In conjunction with those previously described, multiple NHEJ factors have now been shown to be

beneficial or detrimental to HSV-1 infection, and future work should consider how these different NHEJ factors interact during HSV-1 infection. Rather than a linear pathway, it is likely that complexes form and direct multiple pathways, much like in the DDR response to DSBs. Indeed, this is not limited to NHEJ - HSV-1 directs different DDR factors from multiple repair pathways to promote infection, and instead of considering DDR pathways in isolation, progress is likely to come from studying the combined effects of such factors.

As such, our study not only contributes to the understanding of the effects of NHEJ on HSV-1, but rather should be seen in the context the entire DDR response. Understanding the interactions between viruses and the DDR will enable new approaches to control viral infection, but is also increasingly recognised as important in a myriad of other areas including cancer, neurological diseases, and autoimmune diseases.

Bibliography

Abe, T., and Barber, G.N. (2014). Cytosolic-DNA-mediated, STING-dependent proinflammatory gene induction necessitates canonical NF-κB activation through TBK1. J. Virol. *88*, 5328–5341.

Abe, T., Ishiai, M., Hosono, Y., Yoshimura, A., Tada, S., Adachi, N., Koyama, H., Takata, M., Takeda, S., Enomoto, T., et al. (2008). KU70/80, DNA-PKcs, and Artemis are essential for the rapid induction of apoptosis after massive DSB formation. Cell. Signal. *20*, 1978–1985.

Ablasser, A., Goldeck, M., Cavlar, T., Deimling, T., Witte, G., Röhl, I., Hopfner, K.-P., Ludwig, J., and Hornung, V. (2013). cGAS produces a 2′-5′-linked cyclic dinucleotide second messenger that activates STING. Nature *498*.

Ablasser, A., Hemmerling, I., Schmid-Burgk, J.L., Behrendt, R., Roers, A., and Hornung, V. (2014). TREX1 Deficiency Triggers Cell-Autonomous Immunity in a cGAS-Dependent Manner. J. Immunol. *192*.

Abraham, R.T. (2004). PI 3-kinase related kinases: "big" players in stress-induced signaling pathways. DNA Repair (Amst). *3*, 883–887.

Adamo, A., Collis, S.J., Adelman, C.A., Silva, N., Horejsi, Z., Ward, J.D., Martinez-Perez, E., Boulton, S.J., and La Volpe, A. (2010). Preventing Nonhomologous End Joining Suppresses DNA Repair Defects of Fanconi Anemia. Mol. Cell *39*, 25–35.

Ahel, I., Rass, U., El-Khamisy, S.F., Katyal, S., Clements, P.M., McKinnon, P.J., Caldecott, K.W., and West, S.C. (2006). The neurodegenerative disease protein aprataxin resolves abortive DNA ligation intermediates. Nature *443*, 713–716.

Alekseev, O., Donovan, K., and Azizkhan-Clifford, J. (2014). Inhibition of Ataxia Telangiectasia Mutated (ATM) Kinase Suppresses Herpes Simplex Virus Type 1 (HSV-1) Keratitis. Invest. Ophthalmol. Vis. Sci. *55*, 706–715.

Almine, J.F., O'Hare, C.A.J., Dunphy, G., Haga, I.R., Naik, R.J., Atrih, A., Connolly, D.J., Taylor, J., Kelsall, I.R., Bowie, A.G., et al. (2017). IFI16 and cGAS cooperate in the activation of STING during DNA sensing in human keratinocytes. Nat. Commun. *8*, 14392.

Amatya, P.N., Kim, H.-B., Park, S.-J., Youn, C.-K., Hyun, J.-W., Chang, I.-Y., Lee, J.-H., and You, H.J. (2012). A role of DNA-dependent protein kinase for the activation of AMP-activated protein kinase in response to glucose deprivation. Biochim. Biophys. Acta - Mol. Cell Res. *1823*, 2099–2108.

Anacker, D.C., Gautam, D., Gillespie, K.A., Chappell, W.H., and Moody, C.A. (2014). Productive replication of human papillomavirus 31 requires DNA repair factor Nbs1. J. Virol. *88*, 8528–8544.

Arya, R., and Bassing, C.H. (2017). V(D)J Recombination Exploits DNA Damage Responses to Promote Immunity. Trends Genet. *33*, 479–489.

Bailey, S.M., Meyne, J., Chen, D.J., Kurimasa, A., Li, G.C., Lehnert, B.E., and Goodwin, E.H. (1999). DNA double-strand break repair proteins are required to cap the ends of mammalian chromosomes. Proc. Natl. Acad. Sci. U. S. A. *96*, 14899–14904.

Baker, A., Rohleder, K.J., Hanakahi, L.A., and Ketner, G. (2007). Adenovirus E4 34k and E1b 55k oncoproteins target host DNA ligase IV for proteasomal degradation. J. Virol. *81*, 7034–7040.

Balasubramanian, N., Bai, P., Buchek, G., Korza, G., and Weller, S.K. (2010). Physical interaction between the herpes simplex virus type 1 exonuclease, UL12, and the DNA double-strand break-sensing MRN complex. J. Virol. *84*, 12504–12514.

Balmus, G., Barros, A.C., Wijnhoven, P.W.G., Lescale, C., Hasse, H.L., Boroviak, K., le Sage, C., Doe, B., Speak, A.O., Galli, A., et al. (2016). Synthetic lethality between PAXX and XLF in mammalian development. Genes Dev. *30*, 2152–2157.

Baram-Pinto, D., Shukla, S., Gedanken, A., and Sarid, R. (2010). Inhibition of HSV-1 Attachment, Entry, and Cell-to-Cell Spread by Functionalized Multivalent Gold Nanoparticles. Small *6*, 1044–1050.

Baritaud, M., Cabon, L., Delavallée, L., Galán-Malo, P., Gilles, M.-E., Brunelle-Navas, M.-N., and Susin, S.A. (2012). AIF-mediated caspase-independent necroptosis requires ATM and DNA-PK-induced histone H2AX Ser139 phosphorylation. Cell Death Dis. *3*, e390.

Bedadala, G.R., Pinnoji, R.C., and Hsia, S.-C. V (2007). Early Growth Response gene 1 (Egr-1) regulates HSV-1 ICP4 and ICP22 gene expression. Cell Res. *17*, 546–555.

Bell, S., Cranage, M., Borysiewicz, L., and Minson, T. (1990). Induction of immunoglobulin G Fc receptors by recombinant vaccinia viruses expressing glycoproteins E and I of herpes simplex virus type 1. J. Virol. *64*, 2181–2186.

Ben-Hur, T., Hadar, J., Shtram, Y., Gilden, D.H., and Becker, Y. (1983). Neurovirulence of herpes simplex virus type 1 depends on age in mice and thymidine kinase expression. Arch. Virol. *78*, 303–308.

Bernstein, C., Bernstein, H., Payne, C.M., and Garewal, H. (2002). DNA repair/pro-apoptotic dual-role proteins in five major DNA repair pathways: fail-safe protection against carcinogenesis. Mutat. Res. Mutat. Res. *511*, 145–178.

Bernstein, N.K., Williams, R.S., Rakovszky, M.L., Cui, D., Green, R., Karimi-Busheri, F., Mani, R.S., Galicia, S., Koch, C.A., Cass, C.E., et al. (2005). The Molecular Architecture of the Mammalian DNA Repair Enzyme, Polynucleotide Kinase. Mol. Cell *17*, 657–670.

Beskow, C., Skikuniene, J., Holgersson, A., Nilsson, B., Lewensohn, R., Kanter, L., and Viktorsson, K. (2009). Radioresistant cervical cancer shows upregulation of the

NHEJ proteins DNA-PKcs, Ku70 and Ku86. Br. J. Cancer *101*, 816–821.

Bhargava, R., Onyango, D.O., and Stark, J.M. (2016). Regulation of Single-Strand Annealing and its Role in Genome Maintenance. Trends Genet. *32*, 566–575.

Bhatia, T., Wood, J., Iyengar, S., Narayanan, S.S., Beniwal, R.P., Prasad, K.M., Chen, K., Yolken, R.H., Dickerson, F., Gur, R.C., et al. (2017). Emotion discrimination in humans: Its association with HSV-1 infection and its improvement with antiviral treatment. Schizophr. Res.

Blackford, A.N., Patel, R.N., Forrester, N.A., Theil, K., Groitl, P., Stewart, G.S., Taylor, A.M.R., Morgan, I.M., Dobner, T., Grand, R.J.A., et al. (2010). Adenovirus 12 E4orf6 inhibits ATR activation by promoting TOPBP1 degradation. Proc. Natl. Acad. Sci. U. S. A. *107*, 12251–12256.

Blinov, V.M., Zverev, V. V., Krasnov, G.S., Filatov, F.P., and Shargunov, A. V. (2017). Viral component of the human genome. Mol. Biol. *51*, 205–215.

Blondeau, C., Pelchen-Matthews, A., Mlcochova, P., Marsh, M., Milne, R.S.B., and Towers, G.J. (2013). Tetherin Restricts Herpes Simplex Virus 1 and Is Antagonized by Glycoprotein M. J. Virol. *87*, 13124–13133.

Blunt, T., Finnie, N.J., Taccioli, G.E., Smith, G.C.., Demengeot, J., Gottlieb, T.M., Mizuta, R., Varghese, A.., Alt, F.W., Jeggo, P.A., et al. (1995). Defective DNA-dependent protein kinase activity is linked to V(D)J recombination and DNA repair defects associated with the murine scid mutation. Cell *80*, 813–823.

Blunt, T., Gell, D., Fox, M., Taccioli, G.E., Lehmann, A.R., Jackson, S.P., and Jeggo, P.A. (1996). Identification of a nonsense mutation in the carboxyl-terminal region of DNA-dependent protein kinase catalytic subunit in the scid mouse. Proc. Natl. Acad. Sci. U. S. A. *93*, 10285–10290.

Bol, V. (2015). Abstract 2915: Identification of the mechanisms of radiosensitization by human papillomavirus (HPV) in head and neck cancer cell lines. Cancer Res. *75*.

Bouquet, F., Ousset, M., Biard, D., Fallone, F., Dauvillier, S., Frit, P., Salles, B., and Muller, C. (2011). A DNA-dependent stress response involving DNA-PK occurs in hypoxic cells and contributes to cellular adaptation to hypoxia. J. Cell Sci. *124*.

Brzostek-Racine, S., Gordon, C., Van Scoy, S., and Reich, N.C. (2011). The DNA damage response induces IFN. J. Immunol. *187*, 5336–5345.

Buck, D., Moshous, D., de Chasseval, R., Ma, Y., le Deist, F., Cavazzana-Calvo, M., Fischer, A., Casanova, J.-L., Lieber, M.R., and de Villartay, J.-P. (2006). Severe combined immunodeficiency and microcephaly in siblings with hypomorphic mutations in DNA ligase IV. Eur. J. Immunol. *36*, 224–235.

Bunting, S.F., and Nussenzweig, A. (2013). End-joining, translocations and cancer. Nat. Rev. Cancer *13*, 443–454.

Cai, W., and Schaffer, P.A. (1992). Herpes simplex virus type 1 ICP0 regulates expression of immediate-early, early, and late genes in productively infected cells. J. Virol. *66*, 2904–2915.

Cai, W.H., Gu, B., and Person, S. (1988). Role of glycoprotein B of herpes simplex virus type 1 in viral entry and cell fusion. J. Virol. *62*, 2596–2604.

Callén, E., Jankovic, M., Wong, N., Zha, S., Chen, H.-T., Difilippantonio, S., Di Virgilio, M., Heidkamp, G., Alt, F.W., Nussenzweig, A., et al. (2009). Essential Role for DNA-PKcs in DNA Double-Strand Break Repair and Apoptosis in ATM-Deficient Lymphocytes. Mol. Cell *34*, 285–297.

Campadelli-Fiume, G., and Menotti, L. (2007). Entry of alphaherpesviruses into the cell (Cambridge University Press).

Cantin, E., Tanamachi, B., Openshaw, H., Mann, J., and Clarke, K. (1999). Gamma interferon (IFN-gamma) receptor null-mutant mice are more susceptible to herpes simplex virus type 1 infection than IFN-gamma ligand null-mutant mice. J. Virol. *73*, 5196–5200.

Cantin, E.M., Hinton, D.R., Chen, J., and Openshaw, H. (1995). Gamma interferon expression during acute and latent nervous system infection by herpes simplex virus type 1. J. Virol. *69*, 4898–4905.

Caricchio, R., McPhie, L., and Cohen, P.L. (2003). Ultraviolet B Radiation-Induced Cell Death: Critical Role of Ultraviolet Dose in Inflammation and Lupus Autoantigen Redistribution. J. Immunol. *171*.

Carson, C.T., Schwartz, R.A., Stracker, T.H., Lilley, C.E., Lee, D. V, and Weitzman, M.D. (2003). The Mre11 complex is required for ATM activation and the G2/M checkpoint. EMBO J. *22*, 6610–6620.

Carson, C.T., Orazio, N.I., Lee, D. V, Suh, J., Bekker-Jensen, S., Araujo, F.D., Lakdawala, S.S., Lilley, C.E., Bartek, J., Lukas, J., et al. (2009). Mislocalization of the MRN complex prevents ATR signaling during adenovirus infection. EMBO J. *28*, 652–662.

Ceccaldi, R., Sarangi, P., and D'Andrea, A.D. (2016). The Fanconi anaemia pathway: new players and new functions. Nat. Rev. Mol. Cell Biol. *17*, 337–349.

Cerboni, C., Fionda, C., Soriani, A., Zingoni, A., Doria, M., Cippitelli, M., and Santoni, A. (2014). The DNA Damage Response: A Common Pathway in the Regulation of NKG2D and DNAM-1 Ligand Expression in Normal, Infected, and Cancer Cells. Front. Immunol. *4*, 508.

Chaitanya, G.V., Steven, A.J., and Babu, P.P. (2010). PARP-1 cleavage fragments: signatures of cell-death proteases in neurodegeneration. Cell Commun. Signal. *8*, 31.

Chan, D.W., Ye, R., Veillette, C.J., and Lees-Miller, S.P. (1999). DNA-Dependent Protein Kinase Phosphorylation Sites in Ku 70/80 Heterodimer †. Biochemistry *38*, 1819–

1828.

Chan, Y.G.Y., Cardwell, M.M., Hermanas, T.M., Uchiyama, T., and Martinez, J.J. (2009). Rickettsial outer-membrane protein B (rOmpB) mediates bacterial invasion through Ku70 in an actin, c-Cbl, clathrin and caveolin 2-dependent manner. Cell. Microbiol. *11*, 629–644.

Chang, H.H.Y., Watanabe, G., Gerodimos, C.A., Ochi, T., Blundell, T.L., Jackson, S.P., and Lieber, M.R. (2016). Different DNA End Configurations Dictate Which NHEJ Components Are Most Important for Joining Efficiency. J. Biol. Chem. *291*, 24377–24389.

Chelbi-Alix, M., Wietzerbin, J., Everett, R.D., and Chelbi-Alix, M.K. (2007). PML and PML nuclear bodies: Implications in antiviral defence. Biochimie *89*, 819–830.

Chen, S.-H., Yao, H.-W., Chen, I.-T., Shieh, B., Li, C., and Chen, S.-H. (2008). Suppression of transcription factor early growth response 1 reduces herpes simplex virus lethality in mice. J. Clin. Invest. *118*, 3470–3477.

De Chiara, G., Marcocci, M.E., Sgarbanti, R., Civitelli, L., Ripoli, C., Piacentini, R., Garaci, E., Grassi, C., and Palamara, A.T. (2012). Infectious agents and neurodegeneration. Mol. Neurobiol. *46*, 614–638.

De Chiara, G., Racaniello, M., Mollinari, C., Marcocci, M.E., Aversa, G., Cardinale, A., Giovanetti, A., Garaci, E., Palamara, A.T., and Merlo, D. (2016). Herpes Simplex Virus-Type1 (HSV-1) Impairs DNA Repair in Cortical Neurons. Front. Aging Neurosci. *8*, 242.

Chiu, Y.-H., Macmillan, J.B., and Chen, Z.J. (2009). RNA polymerase III detects cytosolic DNA and induces type I interferons through the RIG-I pathway. Cell *138*, 576–591.

Choi, Y.J., Li, H., Son, M.Y., Wang, X., Fornsaglio, J.L., Sobol, R.W., Lee, M., Vijg, J., Imholz, S., Dollé, M.E.T., et al. (2014). Deletion of Individual Ku Subunits in Mice Causes an NHEJ-Independent Phenotype Potentially by Altering Apurinic/Apyrimidinic Site Repair. PLoS One *9*, e86358.

Chumduri, C., Gurumurthy, R.K., Zietlow, R., and Meyer, T.F. (2016). Subversion of host genome integrity by bacterial pathogens. Nat. Rev. Mol. Cell Biol. *17*, 659–673.

Cipe, F.E., Aydogmus, C., Babayigit Hocaoglu, A., Kilic, M., Kaya, G.D., Yilmaz Gulec, E., and Yilmaz Gulec, E. (2014). Cernunnos/XLF Deficiency: A Syndromic Primary Immunodeficiency. Case Rep. Pediatr. *2014*, 614238.

Cliffe, A.R., and Knipe, D.M. (2008). Herpes simplex virus ICP0 promotes both histone removal and acetylation on viral DNA during lytic infection. J. Virol. *82*, 12030–12038.

Cooper, A., García, M., Petrovas, C., Yamamoto, T., Koup, R.A., and Nabel, G.J. (2013). HIV-1 causes CD4 cell death through DNA-dependent protein kinase during

viral integration. Nature *498*, 376–379.

Costantini, S., Woodbine, L., Andreoli, L., Jeggo, P.A., and Vindigni, A. (2007). Interaction of the Ku heterodimer with the DNA ligase IV/Xrcc4 complex and its regulation by DNA-PK. DNA Repair (Amst). *6*, 712–722.

Crameri, M., Bauer, M., Caduff, N., Walker, R., Steiner, F., Franzoso, F.D., Gujer, C., Boucke, K., Kucera, T., Zbinden, A., et al. (2018). MxB is an interferon-induced restriction factor of human herpesviruses. Nat. Commun. *9*, 1980.

Craxton, A., Somers, J., Munnur, D., Jukes-Jones, R., Cain, K., and Malewicz, M. (2015). XLS (c9orf142) is a new component of mammalian DNA double-stranded break repair. Cell Death Differ. *22*, 890–897.

Cridland, J.A., Curley, E.Z., Wykes, M.N., Schroder, K., Sweet, M.J., Roberts, T.L., Ragan, M.A., Kassahn, K.S., and Stacey, K.J. (2012). The mammalian PYHIN gene family: phylogeny, evolution and expression. BMC Evol. Biol. *12*, 140.

Crow, Y.J., Hayward, B.E., Parmar, R., Robins, P., Leitch, A., Ali, M., Black, D.N., van Bokhoven, H., Brunner, H.G., Hamel, B.C., et al. (2006). Mutations in the gene encoding the 3′-5′ DNA exonuclease TREX1 cause Aicardi-Goutières syndrome at the AGS1 locus. Nat. Genet. *38*, 917–920.

Cuchet-Lourenco, D., Anderson, G., Sloan, E., Orr, A., and Everett, R.D. (2013). The viral ubiquitin ligase ICP0 is neither sufficient nor necessary for degradation of the cellular DNA sensor IFI16 during HSV-1 infection. J. Virol. JVI.02474–13 – .

Cuchet-Lourenço, D., Vanni, E., Glass, M., Orr, A., and Everett, R.D. (2012). Herpes simplex virus 1 ubiquitin ligase ICP0 interacts with PML isoform I and induces its SUMO-independent degradation. J. Virol. *86*, 11209–11222.

Cui, X., Yu, Y., Gupta, S., Cho, Y.-M., Lees-Miller, S.P., and Meek, K. (2005). Autophosphorylation of DNA-dependent protein kinase regulates DNA end processing and may also alter double-strand break repair pathway choice. Mol. Cell. Biol. *25*, 10842–10852.

Cunha, C.W., Taylor, K.E., Pritchard, S.M., Delboy, M.G., Komala Sari, T., Aguilar, H.C., Mossman, K.L., and Nicola, A. V (2015). Widely Used Herpes Simplex Virus 1 ICP0 Deletion Mutant Strain dl1403 and Its Derivative Viruses Do Not Express Glycoprotein C Due to a Secondary Mutation in the gC Gene. PLoS One *10*, e0131129.

Curtin, N.J. (2012). DNA repair dysregulation from cancer driver to therapeutic target. Nat. Rev. Cancer *12*, 801–817.

Cuturi, M.C., Murphy, M., Costa-Giomi, M.P., Weinmann, R., Perussia, B., and Trinchieri, G. (1987). Independent regulation of tumor necrosis factor and lymphotoxin production by human peripheral blood lymphocytes. J. Exp. Med. *165*, 1581–1594.

d'Adda di Fagagna, F., Hande, M.P., Tong, W.-M., Roth, D., Lansdorp, P.M., Wang,

Z.-Q., and Jackson, S.P. (2001). Effects of DNA nonhomologous end-joining factors on telomere length and chromosomal stability in mammalian cells.

Dahl, J., You, J., and Benjamin, T.L. (2005). Induction and utilization of an ATM signaling pathway by polyomavirus. J. Virol. *79*, 13007–13017.

Daniel, R., Katz, R.A., and Skalka, A.M. (1999). A Role for DNA-PK in Retroviral DNA Integration. Science (80-.). *284*.

Darbinyan, A., Siddiqui, K.M., Slonina, D., Darbinian, N., Amini, S., White, M.K., and Khalili, K. (2004). Role of JC virus agnoprotein in DNA repair. J. Virol. *78*, 8593–8600.

Davis, A.J., and Chen, D.J. (2013). DNA double strand break repair via non-homologous end-joining. Transl. Cancer Res. *2*, 130–143.

Davis, A.A., Bernstein, P.S., Bok, D., Turner, J., Nachtigal, M., and Hunt, R.C. (1995). A human retinal pigment epithelial cell line that retains epithelial characteristics after prolonged culture. Invest. Ophthalmol. Vis. Sci. *36*, 955–964.

Davis, A.J., Lee, K.-J., and Chen, D.J. (2013). The N-terminal region of the DNA-dependent protein kinase catalytic subunit is required for its DNA double-stranded break-mediated activation. J. Biol. Chem. *288*, 7037–7046.

DeCaprio, J.A., and Garcea, R.L. (2013). A cornucopia of human polyomaviruses. Nat. Rev. Microbiol. *11*, 264–276.

Dejmek, J., Iglehart, J.D., and Lazaro, J.-B. (2009). DNA-Dependent Protein Kinase (DNA-PK)–Dependent Cisplatin-Induced Loss of Nucleolar Facilitator of Chromatin Transcription (FACT) and Regulation of Cisplatin Sensitivity by DNA-PK and FACT. Mol. Cancer Res. *7*.

Della-Maria, J., Zhou, Y., Tsai, M.-S., Kuhnlein, J., Carney, J.P., Paull, T.T., and Tomkinson, A.E. (2011). Human Mre11/human Rad50/Nbs1 and DNA ligase IIIalpha/XRCC1 protein complexes act together in an alternative nonhomologous end joining pathway. J. Biol. Chem. *286*, 33845–33853.

Desai, P., Watkins, S.C., and Person, S. (1994). The size and symmetry of B capsids of herpes simplex virus type 1 are determined by the gene products of the UL26 open reading frame. J. Virol. *68*, 5365–5374.

Deschamps, T., and Kalamvoki, M. (2017). Impaired STING Pathway in Human Osteosarcoma U2OS Cells Contributes to the Growth of ICP0-Null Mutant Herpes Simplex Virus. J. Virol. *91*, e00006–e00017.

Dey, D., Dahl, J., Cho, S., and Benjamin, T.L. (2002). Induction and bypass of p53 during productive infection by polyomavirus. J. Virol. *76*, 9526–9532.

Dobbs, T.A., Tainer, J.A., and Lees-Miller, S.P. (2010). A structural model for

regulation of NHEJ by DNA-PKcs autophosphorylation. DNA Repair (Amst). *9*, 1307–1314.

Dong, C., Yang, D.D., Wysk, M., Whitmarsh, A.J., Davis, R.J., and Flavell, R.A. (1998). Defective T Cell Differentiation in the Absence of Jnk1. Science (80-.). *282*.

Dong, C., Yang, D.D., Tournier, C., Whitmarsh, A.J., Xu, J., Davis, R.J., and Flavell, R.A. (2000). JNK is required for effector T-cell function but not for T-cell activation. Nature *405*, 91–94.

Douglas, P., Gupta, S., Morrice, N., Meek, K., and Lees-Miller, S.P. (2005). DNA-PK-dependent phosphorylation of Ku70/80 is not required for non-homologous end joining. DNA Repair (Amst). *4*, 1006–1018.

Dutta, D., Dutta, S., Veettil, M.V., Roy, A., Ansari, M.A., Iqbal, J., Chikoti, L., Kumar, B., Johnson, K.E., Chandran, B., et al. (2015). BRCA1 Regulates IFI16 Mediated Nuclear Innate Sensing of Herpes Viral DNA and Subsequent Induction of the Innate Inflammasome and Interferon-?? Responses. PLoS Pathog. *11*, e1005030.

Efstathiou, S., Minson, A.C., Field, H.J., Anderson, J.R., and Wildy, P. (1986). Detection of herpes simplex virus-specific DNA sequences in latently infected mice and in humans. J. Virol. *57*, 446–455.

Eidson, K.M., Hobbs, W.E., Manning, B.J., Carlson, P., and DeLuca, N.A. (2002a). Expression of Herpes Simplex Virus ICP0 Inhibits the Induction of Interferon-Stimulated Genes by Viral Infection. J. Virol. *76*, 2180–2191.

Eidson, K.M., Hobbs, W.E., Manning, B.J., Carlson, P., and DeLuca, N.A. (2002b). Expression of Herpes Simplex Virus ICP0 Inhibits the Induction of Interferon-Stimulated Genes by Viral Infection. J. Virol. *76*, 2180–2191.

Eriksson, M., Taskinen, M., and Leppä, S. (2007). Mitogen activated protein kinase-dependent activation of c-Jun and c-Fos is required for neuronal differentiation but not for growth and stress response in PC12 cells. J. Cell. Physiol. *210*, 538–548.

Espejel, S., Franco, S., Sgura, A., Gae, D., Bailey, S.M., Taccioli, G.E., and Blasco, M.A. (2002a). Functional interaction between DNA-PKcs and telomerase in telomere length maintenance. EMBO J. *21*, 6275–6287.

Espejel, S., Franco, S., Rodríguez-Perales, S., Bouffler, S.D., Cigudosa, J.C., and Blasco, M.A. (2002b). Mammalian Ku86 mediates chromosomal fusions and apoptosis caused by critically short telomeres. EMBO J. *21*, 2207–2219.

Evans, C.J., and Aguilera, R.J. (2003). DNase II: genes, enzymes and function. Gene *322*, 1–15.

Everett, R.D. (1984). Trans activation of transcription by herpes virus products: requirement for two HSV-1 immediate-early polypeptides for maximum activity. EMBO J. *3*, 3135–3141.

Everett, R.D., Boutell, C., and Orr, A. (2004). Phenotype of a herpes simplex virus type 1 mutant that fails to express immediate-early regulatory protein ICP0. J. Virol. *78*, 1763–1774.

Ferguson, B.J., Mansur, D.S., Peters, N.E., Ren, H., and Smith, G.L. (2012). DNA-PK is a DNA sensor for IRF-3-dependent innate immunity. Elife *1*, e00047.

Fields, B.N., Knipe, D.M. (David M., and Howley, P.M. (2007). Fields virology (Wolters Kluwer Health/Lippincott Williams & Wilkins).

Figueiredo, N., Chora, A., Raquel, H., Pejanovic, N., Pereira, P., Hartleben, B., Neves-Costa, A., Moita, C., Pedroso, D., Pinto, A., et al. (2013). Anthracyclines induce DNA damage response-mediated protection against severe sepsis. Immunity *39*, 874–884.

Forrester, N.A., Sedgwick, G.G., Thomas, A., Blackford, A.N., Speiseder, T., Dobner, T., Byrd, P.J., Stewart, G.S., Turnell, A.S., and Grand, R.J.A. (2011). Serotype-specific inactivation of the cellular DNA damage response during adenovirus infection. J. Virol. *85*, 2201–2211.

Frenkel, N., Jacob, R.J., Honess, R.W., Hayward, G.S., Locker, H., and Roizman, B. (1975). Anatomy of herpes simplex virus DNA. III. Characterization of defective DNA molecules and biological properties of virus populations containing them. J. Virol. *16*, 153–167.

Friedman, E. (2002). Immune Modulation by Ionizing Radiation and its Implications for Cancer Immunotherapy. Curr. Pharm. Des. *8*, 1765–1780.

Gao, Y., Sun, Y., Frank, K.M., Dikkes, P., Fujiwara, Y., Seidl, K.J., Sekiguchi, J.M., Rathbun, G.A., Swat, W., Wang, J., et al. (1998). A Critical Role for DNA End-Joining Proteins in Both Lymphogenesis and Neurogenesis. Cell *95*, 891–902.

Gao, Y., Ferguson, D.O., Xie, W., Manis, J.P., Sekiguchi, J., Frank, K.M., Chaudhuri, J., Horner, J., DePinho, R.A., and Alt, F.W. (2000). Interplay of p53 and DNA-repair protein XRCC4 in tumorigenesis, genomic stability and development. Nature *404*, 897–900.

Gasser, S., Orsulic, S., Brown, E.J., and Raulet, D.H. (2005). The DNA damage pathway regulates innate immune system ligands of the NKG2D receptor. Nature *436*, 1186–1190.

Gentili, M., Kowal, J., Tkach, M., Satoh, T., Lahaye, X., Conrad, C., Boyron, M., Lombard, B., Durand, S., Kroemer, G., et al. (2015). Transmission of innate immune signaling by packaging of cGAMP in viral particles. Science (80-.). *349*.

Gilden, D., and Nagel, M.A. (2016). Neurological complications of human herpesvirus infections. In International Neurology, (Chichester, UK: John Wiley & Sons, Ltd), pp. 316–322.

Gilley, D., Tanaka, H., Hande, M.P., Kurimasa, A., Li, G.C., Oshimura, M., and Chen, D.J. (2001). DNA-PKcs is critical for telomere capping. Proc. Natl. Acad. Sci. U. S. A. *98*,

15084–15088.

Glück, S., Guey, B., Gulen, M.F., Wolter, K., Kang, T.-W., Schmacke, N.A., Bridgeman, A., Rehwinkel, J., Zender, L., and Ablasser, A. (2017a). Innate immune sensing of cytosolic chromatin fragments through cGAS promotes senescence. Nat. Cell Biol. *19*, 1061–1070.

Glück, S., Guey, B., Gulen, M.F., Wolter, K., Kang, T.-W., Schmacke, N.A., Bridgeman, A., Rehwinkel, J., Zender, L., and Ablasser, A. (2017b). Innate immune sensing of cytosolic chromatin fragments through cGAS promotes senescence. Nat. Cell Biol. *19*, 1061–1070.

Gonzalez-Dosal, R., Horan, K.A., Rahbek, S.H., Ichijo, H., Chen, Z.J., Mieyal, J.J., Hartmann, R., and Paludan, S.R. (2011). HSV Infection Induces Production of ROS, which Potentiate Signaling from Pattern Recognition Receptors: Role for S-glutathionylation of TRAF3 and 6. PLoS Pathog. *7*, e1002250.

Goodwin, J.F., and Knudsen, K.E. (2014). Beyond DNA repair: DNA-PK function in cancer. Cancer Discov. *4*, 1126–1139.

Gottlieb, T.M., and Jackson, S.P. (1993). The DNA-dependent protein kinase: Requirement for DNA ends and association with Ku antigen. Cell *72*, 131–142.

Goytisolo, F.A., Samper, E., Edmonson, S., Taccioli, G.E., and Blasco, M.A. (2001). The absence of the dna-dependent protein kinase catalytic subunit in mice results in anaphase bridges and in increased telomeric fusions with normal telomere length and G-strand overhang. Mol. Cell. Biol. *21*, 3642–3651.

Grabowska, A., Chumbley, G., Carter, N., and Loke, Y.W. (1990). Interferon-gamma enhances mRNA and surface expression of class I antigen on human extravillous trophoblast. Placenta *11*, 301–308.

Gregory, D.A., and Bachenheimer, S.L. (2008). Characterization of mre11 loss following HSV-1 infection. Virology *373*, 124–136.

Gu, H., Zheng, Y., and Roizman, B. (2013). Interaction of herpes simplex virus ICP0 with ND10 bodies: a sequential process of adhesion, fusion, and retention. J. Virol. *87*, 10244–10254.

Gu, Y., Seidl, K.J., Rathbun, G.A., Zhu, C., Manis, J.P., van der Stoep, N., Davidson, L., Cheng, H.-L., Sekiguchi, J.M., Frank, K., et al. (1997). Growth Retardation and Leaky SCID Phenotype of Ku70-Deficient Mice. Immunity *7*, 653–665.

Guo, H., Omoto, S., Harris, P.A., Finger, J.N., Bertin, J., Gough, P.J., Kaiser, W.J., and Mocarski, E.S. (2015). Herpes simplex virus suppresses necroptosis in human cells. Cell Host Microbe *17*, 243–251.

Gupta, S., and Meek, K. (2005). The leucine rich region of DNA-PKcs contributes to its innate DNA affinity. Nucleic Acids Res. *33*, 6972–6981.

Halford, W.P., Halford, K.J., and Pierce, A.T. (2005a). Mathematical analysis demonstrates that interferons- and - interact in a multiplicative manner to disrupt herpes simplex virus replication. J. Theor. Biol. *234*, 439–454.

Halford, W.P., Maender, J.L., and Gebhardt, B.M. (2005b). Re-evaluating the role of natural killer cells in innate resistance to herpes simplex virus type 1. Virol. J. *2*, 56.

Harding, S.M., Benci, J.L., Irianto, J., Discher, D.E., Minn, A.J., and Greenberg, R.A. (2017). Mitotic progression following DNA damage enables pattern recognition within micronuclei. Nature *548*, 466–470.

Hart, L.S., Yannone, S.M., Naczki, C., Orlandoţ, J.S., Waters, S.B., Akman, S.A., Chen, D.J., Ornellesţ, D., and Koumenis, C. (2004). The Adenovirus E4orf6 Protein Inhibits DNA Double Strand Break Repair and Radiosensitizes Human Tumor Cells in an E1B-55K-independent Manner*.

Hart, L.S., Ornelles, D., and Koumenis, C. (2007). The adenoviral E4orf6 protein induces atypical apoptosis in response to DNA damage. J. Biol. Chem. *282*, 6061–6067.

Hartley, K.O., Gell, D., Smith, G.C.., Zhang, H., Divecha, N., Connelly, M.A., Admon, A., Lees-Miller, S.P., Anderson, C.W., and Jackson, S.P. (1995). DNA-dependent protein kinase catalytic subunit: A relative of phosphatidylinositol 3-kinase and the ataxia telangiectasia gene product. Cell *82*, 849–856.

zur Hausen, H. (2002). Papillomaviruses and cancer: from basic studies to clinical application. Nat. Rev. Cancer *2*, 342–350.

Hayward, A. (2017). Origin of the retroviruses: when, where, and how? Curr. Opin. Virol. *25*, 23–27.

Heilingloh, C.S., Muhl-Zurbes, P., Steinkasserer, A., and Kummer, M. (2014). Herpes simplex virus type 1 ICP0 induces CD83 degradation in mature dendritic cells independent of its E3 ubiquitin ligase function. J. Gen. Virol. *95*, 1366–1375.

Hellberg, T., Paßvogel, L., Schulz, K.S., Klupp, B.G., and Mettenleiter, T.C. (2016). Nuclear Egress of Herpesviruses. In Advances in Virus Research, pp. 81–140.

Heming, J.D., Huffman, J.B., Jones, L.M., and Homa, F.L. (2014). Isolation and characterization of the herpes simplex virus 1 terminase complex. J. Virol. *88*, 225–236.

Hemmi, H., Takeuchi, O., Kawai, T., Kaisho, T., Sato, S., Sanjo, H., Matsumoto, M., Hoshino, K., Wagner, H., Takeda, K., et al. (2000). A Toll-like receptor recognizes bacterial DNA. Nature *408*, 740–745.

Heyer, W.-D., Ehmsen, K.T., and Liu, J. (2010). Regulation of Homologous Recombination in Eukaryotes. Annu. Rev. Genet. *44*, 113–139.

Hill, R., and Lee, P.W. (2010). The DNA-dependent protein kinase (DNA-PK): More than just a case of making ends meet? Cell Cycle *9*, 3460–3469.

Hochrein, H., Schlatter, B., O'Keeffe, M., Wagner, C., Schmitz, F., Schiemann, M., Bauer, S., Suter, M., and Wagner, H. (2004). Herpes simplex virus type-1 induces IFN-alpha production via Toll-like receptor 9-dependent and -independent pathways. Proc. Natl. Acad. Sci. U. S. A. *101*, 11416–11421.

Hoeben, R.C., and Uil, T.G. (2013). Adenovirus DNA replication. Cold Spring Harb. Perspect. Biol. *5*, a013003.

Hollinshead, M., Johns, H.L., Sayers, C.L., Gonzalez-Lopez, C., Smith, G.L., and Elliott, G. (2012). Endocytic tubules regulated by Rab GTPases 5 and 11 are used for envelopment of herpes simplex virus. EMBO J. *31*, 4204–4220.

Homa, F.L., and Brown, J.C. (1997). Capsid assembly and DNA packaging in herpes simplex virus. Rev. Med. Virol. *7*, 107–122.

Honda, K., Yanai, H., Negishi, H., Asagiri, M., Sato, M., Mizutani, T., Shimada, N., Ohba, Y., Takaoka, A., Yoshida, N., et al. (2005). IRF-7 is the master regulator of type-I interferon-dependent immune responses. Nature *434*, 772–777.

Hong, C.-S., Chiang, C.-Y., and Tsao, P.-, J.-H. (1999). Rapid induction of cytokine gene expression in the lung after single and fractionated doses of radiation. Int. J. Radiat. Biol. *75*, 1421–1427.

Hor, J.L., Heath, W.R., and Mueller, S.N. (2017). Neutrophils are dispensable in the modulation of T cell immunity against cutaneous HSV-1 infection. Sci. Rep. *7*, 41091.

Hornung, V., Ablasser, A., Charrel-Dennis, M., Bauernfeind, F., Horvath, G., Caffrey, D.R., Latz, E., and Fitzgerald, K.A. (2009). AIM2 recognizes cytosolic dsDNA and forms a caspase-1-activating inflammasome with ASC. Nature *458*, 514–518.

Hosoi, Y., Watanabe, T., Nakagawa, K., Matsumoto, Y., Enomoto, A., Morita, A., Nagawa, H., and Suzuki, N. (2004). Up-regulation of DNA-dependent protein kinase activity and Sp1 in colorectal cancer. Int. J. Oncol. *25*, 461–468.

Huang, W.-C., Abraham, R., Shim, B.-S., Choe, H., and Page, D.T. (2016). Zika virus infection during the period of maximal brain growth causes microcephaly and corticospinal neuron apoptosis in wild type mice. Sci. Rep. *6*, 34793.

Huffman, J.B., Daniel, G.R., Falck-Pedersen, E., Huet, A., Smith, G.A., Conway, J.F., and Homa, F.L. (2017). The C Terminus of the Herpes Simplex Virus UL25 Protein Is Required for Release of Viral Genomes from Capsids Bound to Nuclear Pores. J. Virol. *91*, JVI.00641–17.

Ijspeert, H., Rozmus, J., Schwarz, K., Warren, R.L., van Zessen, D., Holt, R.A., Pico-Knijnenburg, I., Simons, E., Jerchel, I., Wawer, A., et al. (2016). XLF deficiency results in reduced N-nucleotide addition during V(D)J recombination. Blood *128*, 650–659.

Iliakis, G., Wang, Y., Guan, J., and Wang, H. (2003). DNA damage checkpoint control in cells exposed to ionizing radiation. Oncogene *22*, 5834–5847.

Ishii, K.J., Kawagoe, T., Koyama, S., Matsui, K., Kumar, H., Kawai, T., Uematsu, S., Takeuchi, O., Takeshita, F., Coban, C., et al. (2008). TANK-binding kinase-1 delineates innate and adaptive immune responses to DNA vaccines. Nature *451*, 725–729.

Ishikawa, H., and Barber, G.N. (2011). The STING pathway and regulation of innate immune signaling in response to DNA pathogens. Cell. Mol. Life Sci. *68*, 1157–1165.

Ishikawa, H., Ma, Z., and Barber, G.N. (2009). STING regulates intracellular DNA-mediated, type I interferon-dependent innate immunity. Nature *461*, 788–792.

Itzhaki, R.F. (2014). Herpes simplex virus type 1 and Alzheimer's disease: increasing evidence for a major role of the virus. Front. Aging Neurosci. *6*, 202.

Itzhaki, R.F. (2017). Herpes simplex virus type 1 and Alzheimer's disease: possible mechanisms and signposts. FASEB J. *31*, 3216–3226.

Jackson, S.A., and DeLuca, N.A. (2003). Relationship of herpes simplex virus genome configuration to productive and persistent infections. Proc. Natl. Acad. Sci. U. S. A. *100*, 7871–7876.

Jackson, S.P., and Bartek, J. (2009). The DNA-damage response in human biology and disease. Nature *461*, 1071–1078.

Jackson, S.P., MacDonald, J.J., Lees-Miller, S., and Tjian, R. (1990). GC box binding induces phosphorylation of Sp1 by a DNA-dependent protein kinase. Cell *63*, 155–165.

Jeanson, L., Subra, F., Vaganay, S., Hervy, M., Marangoni, E., Bourhis, J., and Mouscadet, J.-F. (2002). Effect of Ku80 Depletion on the Preintegrative Steps of HIV-1 Replication in Human Cells. Virology *300*, 100–108.

Jin, S., Kharbanda, S., Mayer, B., Kufe, D., and Weaver, D.T. (1997). Binding of Ku and c-Abl at the kinase homology region of DNA-dependent protein kinase catalytic subunit. J. Biol. Chem. *272*, 24763–24766.

Jin, T., Xu, X., and Hereld, D. (2008). Chemotaxis, chemokine receptors and human disease. Cytokine *44*, 1–8.

Johnson, A.J., Chu, C.-F., and Milligan, G.N. (2008). Effector CD4+ T-cell involvement in clearance of infectious herpes simplex virus type 1 from sensory ganglia and spinal cords. J. Virol. *82*, 9678–9688.

Johnson, D.C., Frame, M.C., Ligas, M.W., Cross, A.M., and Stow, N.D. (1988). Herpes simplex virus immunoglobulin G Fc receptor activity depends on a complex of two viral glycoproteins, gE and gI. J. Virol. *62*, 1347–1354.

Johnson, K.E., Chikoti, L., and Chandran, B. (2013). Herpes simplex virus 1 infection induces activation and subsequent inhibition of the IFI16 and NLRP3 inflammasomes. J. Virol. *87*, 5005–5018.

Jolicoeur, P., and Baltimore, D. (1976). Effect of Fv-1 gene product on proviral DNA formation and integration in cells infected with murine leukemia viruses. Proc. Natl. Acad. Sci. U. S. A. *73*, 2236–2240.

Kalamvoki, M., and Roizman, B. (2014). HSV-1 degrades, stabilizes, requires, or is stung by STING depending on ICP0, the US3 protein kinase, and cell derivation. Proc. Natl. Acad. Sci. U. S. A. 1323414111 – .

Kang, M.J., Jung, S.M., Kim, M.J., Bae, J.H., Kim, H.B., Kim, J.Y., Park, S.J., Song, H.S., Kim, D.W., Kang, C.D., et al. (2008). DNA-dependent protein kinase is involved in heat shock protein-mediated accumulation of hypoxia-inducible factor-1α in hypoxic preconditioned HepG2 cells. FEBS J. *275*, 5969–5981.

Karo, J.M., Schatz, D.G., and Sun, J.C. (2014). The RAG recombinase dictates functional heterogeneity and cellular fitness in natural killer cells. Cell *159*, 94–107.

Karpova, A.Y., Trost, M., Murray, J.M., Cantley, L.C., and Howley, P.M. (2002). Interferon regulatory factor-3 is an in vivo target of DNA-PK. Proc. Natl. Acad. Sci. U. S. A. *99*, 2818–2823.

Karttunen, H., Savas, J.N.N., McKinney, C., Chen, Y.-H., Yates, J.R.R., Hukkanen, V., Huang, T.T.T., and Mohr, I. (2014). Co-opting the Fanconi Anemia Genomic Stability Pathway Enables Herpesvirus DNA Synthesis and Productive Growth. Mol. Cell *55*, 111–122.

Kastrukoff, L., Hamada, T., Schumacher, U., Long, C., Doherty, P.C., and Koprowski, H. (1982). Central nervous system infection and immune response in mice inoculated into the lip with herpes simplex virus type 1. J. Neuroimmunol. *2*, 295–305.

Kastrukoff, L.F., Lau, A.S., and Thomas, E.E. (2012). The effect of mouse strain on herpes simplex virus type 1 (HSV-1) infection of the central nervous system (CNS). Herpesviridae *3*, 4.

Kepp, O., Galluzzi, L., Lipinski, M., Yuan, J., and Kroemer, G. (2011). Cell death assays for drug discovery. Nat. Rev. Drug Discov. *10*, 221–237.

Khanna, K.K., and Jackson, S.P. (2001). DNA double-strand breaks: signaling, repair and the cancer connection. Nat. Genet. *27*, 247–254.

Khanna, K.M., Bonneau, R.H., Kinchington, P.R., and Hendricks, R.L. (2003). Herpes simplex virus-specific memory CD8+ T cells are selectively activated and retained in latently infected sensory ganglia. Immunity *18*, 593–603.

Kibler, P.K., Duncan, J., Keith, B.D., Hupel, T., and Smiley, J.R. (1991). Regulation of herpes simplex virus true late gene expression: sequences downstream from the US11 TATA box inhibit expression from an unreplicated template. J. Virol. *65*, 6749–6760.

Kim, E.T., White, T.E., Brandariz-Núñez, A., Diaz-Griffero, F., and Weitzman, M.D. (2013). SAMHD1 restricts herpes simplex virus 1 in macrophages by limiting DNA

replication. J. Virol. *87*, 12949–12956.

Kim, T.K., Kim, T., Kim, T.Y., Lee, W.G., and Yim, J. (2000). Chemotherapeutic DNA-damaging Drugs Activate Interferon Regulatory Factor-7 by the Mitogen-activated Protein Kinase Kinase-4-c-Jun NH2-Terminal Kinase Pathway. Cancer Res. *60*.

Kim, T.Y.K., Kim, T.Y.K., Song, Y.H., Min, I.M., Yim, J., and Kim, T.Y.K. (1999). Activation of interferon regulatory factor 3 in response to DNA-damaging agents. J. Biol. Chem. *274*, 30686–30689.

Kirchgessner, C., Patil, C., Evans, J., Cuomo, C., Fried, L., Carter, T., Oettinger, M., and Brown, J. (1995). DNA-dependent kinase (p350) as a candidate gene for the murine SCID defect. Science (80-.). *267*.

Knickelbein, J.E., Khanna, K.M., Yee, M.B., Baty, C.J., Kinchington, P.R., and Hendricks, R.L. (2008). Noncytotoxic lytic granule-mediated CD8+ T cell inhibition of HSV-1 reactivation from neuronal latency. Science *322*, 268–271.

Kobiyama, K., Jounai, N., Aoshi, T., Tozuka, M., Takeshita, F., Coban, C., and Ishii, K. (2013). Innate Immune Signaling by, Genetic Adjuvants for, DNA Vaccination. Vaccines *1*, 278–292.

Kollias, C.M., Huneke, R.B., Wigdahl, B., and Jennings, S.R. (2015). Animal models of herpes simplex virus immunity and pathogenesis. J. Neurovirol. *21*, 8–23.

Kondo, S., Kono, T., Sauder, D., and McKenzie, R. (1993). IL-8 Gene Expression and Production in Human Keratinocytes and Their Modulation by UVB. J. Invest. Dermatol. *101*, 690–694.

Kondo, T., Kobayashi, J., Saitoh, T., Maruyama, K., Ishii, K.J., Barber, G.N., Komatsu, K., Akira, S., and Kawai, T. (2013). DNA damage sensor MRE11 recognizes cytosolic double-stranded DNA and induces type I interferon by regulating STING trafficking. Proc. Natl. Acad. Sci. U. S. A. *110*, 2969–2974.

Koonin, E. V., and Starokadomskyy, P. (2016). Are viruses alive? The replicator paradigm sheds decisive light on an old but misguided question. Stud. Hist. Philos. Sci. Part C Stud. Hist. Philos. Biol. Biomed. Sci. *59*, 125–134.

Koyuncu, E., Budayeva, H.G., Miteva, Y. V, Ricci, D.P., Silhavy, T.J., Shenk, T., and Cristea, I.M. (2014). Sirtuins are evolutionarily conserved viral restriction factors. MBio *5*, e02249–14.

Krieser, R.J., MacLea, K.S., Longnecker, D.S., Fields, J.L., Fiering, S., and Eastman, A. (2002). Deoxyribonuclease IIalpha is required during the phagocytic phase of apoptosis and its loss causes perinatal lethality. Cell Death Differ. *9*, 956–962.

Ku, C.H., and Ferguson, B.J. (2014). Stimulation of Cytoplasmic DNA Sensing Pathways In Vitro and In Vivo. J. Vis. Exp. e51593–e51593.

Kumar, V., Alt, F.W., and Frock, R.L. (2016). PAXX and XLF DNA repair factors are functionally redundant in joining DNA breaks in a G1-arrested progenitor B-cell line. Proc. Natl. Acad. Sci. *113*, 10619–10624.

Kummer, M., Turza, N.M., Muhl-Zurbes, P., Lechmann, M., Boutell, C., Coffin, R.S., Everett, R.D., Steinkasserer, A., and Prechtel, A.T. (2007). Herpes simplex virus type 1 induces CD83 degradation in mature dendritic cells with immediate-early kinetics via the cellular proteasome. J. Virol. *81*, 6326–6338.

Kurimasa, A., Kumano, S., Boubnov, N. V, Story, M.D., Tung, C.S., Peterson, S.R., and Chen, D.J. (1999a). Requirement for the kinase activity of human DNA-dependent protein kinase catalytic subunit in DNA strand break rejoining. Mol. Cell. Biol. *19*, 3877–3884.

Kurimasa, A., Ouyang, H., Dong, L.J., Wang, S., Li, X., Cordon-Cardo, C., Chen, D.J., and Li, G.C. (1999b). Catalytic subunit of DNA-dependent protein kinase: impact on lymphocyte development and tumorigenesis. Proc. Natl. Acad. Sci. U. S. A. *96*, 1403–1408.

Kuroda, S., Yamazaki, M., Abe, M., Sakimura, K., Takayanagi, H., and Iwai, Y. (2011). Basic leucine zipper transcription factor, ATF-like (BATF) regulates epigenetically and energetically effector CD8 T-cell differentiation via Sirt1 expression. Proc. Natl. Acad. Sci. U. S. A. *108*, 14885–14889.

Kurosawa, A., Saito, S., So, S., Hashimoto, M., Iwabuchi, K., Watabe, H., and Adachi, N. (2013). DNA Ligase IV and Artemis Act Cooperatively to Suppress Homologous Recombination in Human Cells: Implications for DNA Double-Strand Break Repair. PLoS One *8*, e72253.

Kutler, D.I., Wreesmann, V.B., Goberdhan, A., Ben-Porat, L., Satagopan, J., Ngai, I., Huvos, A.G., Giampietro, P., Levran, O., Pujara, K., et al. (2003). Human Papillomavirus DNA and p53 Polymorphisms in Squamous Cell Carcinomas From Fanconi Anemia Patients. CancerSpectrum Knowl. Environ. *95*, 1718–1721.

Ladin, B.F., Blankenship, M.L., and Ben-Porat, T. (1980). Replication of herpesvirus DNA. V. Maturation of concatemeric DNA of pseudorabies virus to genome length is related to capsid formation. J. Virol. *33*, 1151–1164.

Lai, M., Zimmerman, E.S., Planelles, V., and Chen, J. (2005). Activation of the ATR pathway by human immunodeficiency virus type 1 Vpr involves its direct binding to chromatin in vivo. J. Virol. *79*, 15443–15451.

Lau, A., Swinbank, K.M., Ahmed, P.S., Taylor, D.L., Jackson, S.P., Smith, G.C.M., and O'Connor, M.J. (2005). Suppression of HIV-1 infection by a small molecule inhibitor of the ATM kinase. Nat. Cell Biol. *7*, 493–500.

Lee, H.K., Zamora, M., Linehan, M.M., Iijima, N., Gonzalez, D., Haberman, A., and Iwasaki, A. (2009). Differential roles of migratory and resident DCs in T cell priming

after mucosal or skin HSV-1 infection. J. Exp. Med. *206*.

Lee, K.-J., Jovanovic, M., Udayakumar, D., Bladen, C.L., and Dynan, W.S. (2004). Identification of DNA-PKcs phosphorylation sites in XRCC4 and effects of mutations at these sites on DNA end joining in a cell-free system. DNA Repair (Amst). *3*, 267–276.

Lees-Miller, S.P., Sakaguchi, K., Ullrich, S.J., Appella, E., and Anderson, C.W. (1992). Human DNA-activated protein kinase phosphorylates serines 15 and 37 in the amino-terminal transactivation domain of human p53. Mol. Cell. Biol. *12*, 5041–5049.

Lees-Miller, S.P., Long, M.C., Kilvert, M.A., Lam, V., Rice, S.A., and Spencer, C.A. (1996). Attenuation of DNA-dependent protein kinase activity and its catalytic subunit by the herpes simplex virus type 1 transactivator ICP0. J. Virol. *70*, 7471–7477.

Lempiäinen, H., and Halazonetis, T.D. (2009). Emerging common themes in regulation of PIKKs and PI3Ks. EMBO J. *28*, 3067–3073.

Lescale, C., Lenden Hasse, H., Blackford, A.N.N., Balmus, G., Bianchi, J.J., Yu, W., Bacoccina, L., Jarade, A., Clouin, C., Sivapalan, R., et al. (2016). Specific Roles of XRCC4 Paralogs PAXX and XLF during V(D)J Recombination. Cell Rep. *16*, 2967–2979.

Li, N., and Karin, M. (1998). Ionizing radiation and short wavelength UV activate NF-kappaB through two distinct mechanisms. Proc. Natl. Acad. Sci. U. S. A. *95*, 13012–13017.

Li, G., Alt, F.W., Cheng, H.-L., Brush, J.W., Goff, P.H., Murphy, M.M., Franco, S., Zhang, Y., and Zha, S. (2008a). Lymphocyte-specific compensation for XLF/cernunnos end-joining functions in V(D)J recombination. Mol. Cell *31*, 631–640.

Li, H., Baskaran, R., Krisky, D.M., Bein, K., Grandi, P., Cohen, J.B., and Glorioso, J.C. (2008b). Chk2 is required for HSV-1 ICP0-mediated G2/M arrest and enhancement of virus growth. Virology *375*, 13–23.

Li, L., Olvera, J.M., Yoder, K.E., Mitchell, R.S., Butler, S.L., Lieber, M., Martin, S.L., and Bushman, F.D. (2001). Role of the non-homologous DNA end joining pathway in the early steps of retroviral infection. EMBO J. *20*, 3272–3281.

Li, S., Kanno, S., Watanabe, R., Ogiwara, H., Kohno, T., Watanabe, G., Yasui, A., and Lieber, M.R. (2011). Polynucleotide kinase and aprataxin-like forkhead-associated protein (PALF) acts as both a single-stranded DNA endonuclease and a single-stranded DNA 3′ exonuclease and can participate in DNA end joining in a biochemical system. J. Biol. Chem. *286*, 36368–36377.

Li, X.-D., Wu, J., Gao, D., Wang, H., Sun, L., and Chen, Z.J. (2013). Pivotal roles of cGAS-cGAMP signaling in antiviral defense and immune adjuvant effects. Science *341*, 1390–1394.

Li, Y., Wu, Y., Zheng, X., Cong, J., Liu, Y., Li, J., Sun, R., Tian, Z.G., and Wei, H.M. (2016). Cytoplasm-Translocated Ku70/80 Complex Sensing of HBV DNA Induces

Hepatitis-Associated Chemokine Secretion. Front. Immunol. *7*, 569.

Lieber, M.R. (2010). The mechanism of double-strand DNA break repair by the nonhomologous DNA end-joining pathway. Annu. Rev. Biochem. *79*, 181–211.

Lilley, C.E., Carson, C.T., Muotri, A.R., Gage, F.H., and Weitzman, M.D. (2005). DNA repair proteins affect the lifecycle of herpes simplex virus 1. Proc. Natl. Acad. Sci. U. S. A. *102*, 5844–5849.

Lilley, C.E., Chaurushiya, M.S., Boutell, C., Landry, S., Suh, J., Panier, S., Everett, R.D., Stewart, G.S., Durocher, D., and Weitzman, M.D. (2010). A viral E3 ligase targets RNF8 and RNF168 to control histone ubiquitination and DNA damage responses. EMBO J. *29*, 943–955.

Lilly, F. (1970). Fv-2: identification and location of a second gene governing the spleen focus response to Friend leukemia virus in mice. J. Natl. Cancer Inst. *45*, 163–169.

Lin, R., Noyce, R.S., Collins, S.E., Everett, R.D., and Mossman, K.L. (2004a). The Herpes Simplex Virus ICP0 RING Finger Domain Inhibits IRF3- and IRF7-Mediated Activation of Interferon-Stimulated Genes. J. Virol. *78*, 1675–1684.

Lin, R., Noyce, R.S., Collins, S.E., Everett, R.D., and Mossman, K.L. (2004b). The Herpes Simplex Virus ICP0 RING Finger Domain Inhibits IRF3- and IRF7-Mediated Activation of Interferon-Stimulated Genes. J. Virol. *78*, 1675–1684.

Lindahl, T. (1993). Instability and decay of the primary structure of DNA. Nature *362*, 709–715.

van Lint, A.L., Murawski, M.R., Goodbody, R.E., Severa, M., Fitzgerald, K.A., Finberg, R.W., Knipe, D.M., and Kurt-Jones, E.A. (2010). Herpes simplex virus immediate-early ICP0 protein inhibits Toll-like receptor 2-dependent inflammatory responses and NF-kappaB signaling. J. Virol. *84*, 10802–10811.

Liu, C., Srihari, S., Cao, K.-A.L., Chenevix-Trench, G., Simpson, P.T., Ragan, M.A., and Khanna, K.K. (2014). A fine-scale dissection of the DNA double-strand break repair machinery and its implications for breast cancer therapy. Nucleic Acids Res. *42*, 6106–6127.

Liu, M., Schmidt, E.E., Halford, W.P., Roizman, B., and Weller, S. (2010). ICP0 Dismantles Microtubule Networks in Herpes Simplex Virus-Infected Cells. PLoS One *5*, e10975.

Liu, P., Gan, W., Guo, C., Xie, A., Gao, D., Guo, J., Zhang, J., Willis, N., Su, A., Asara, J.M., et al. (2015). Akt-mediated phosphorylation of XLF impairs non-homologous end-joining DNA repair. Mol. Cell.

Liu, T., Khanna, K.M., Chen, X., Fink, D.J., and Hendricks, R.L. (2000). CD8(+) T cells can block herpes simplex virus type 1 (HSV-1) reactivation from latency in sensory neurons. J. Exp. Med. *191*, 1459–1466.

Liu, X., Shao, Z., Jiang, W., Lee, B.J., and Zha, S. (2017). PAXX promotes KU accumulation at DNA breaks and is essential for end-joining in XLF-deficient mice. *8*, 13816.

Looker, K.J., Magaret, A.S., May, M.T., Turner, K.M.E., Vickerman, P., Gottlieb, S.L., and Newman, L.M. (2015). Global and Regional Estimates of Prevalent and Incident Herpes Simplex Virus Type 1 Infections in 2012. PLoS One *10*, e0140765.

Lukashchuk, V., and Everett, R.D. (2010). Regulation of ICP0-null mutant herpes simplex virus type 1 infection by ND10 components ATRX and hDaxx. J. Virol. *84*, 4026–4040.

Ma, Y., Pannicke, U., Schwarz, K., and Lieber, M.R. (2002). Hairpin opening and overhang processing by an Artemis/DNA-dependent protein kinase complex in nonhomologous end joining and V(D)J recombination. Cell *108*, 781–794.

Ma, Y., Pannicke, U., Lu, H., Niewolik, D., Schwarz, K., and Lieber, M.R. (2005). The DNA-dependent Protein Kinase Catalytic Subunit Phosphorylation Sites in Human Artemis. J. Biol. Chem. *280*, 33839–33846.

Mackenzie, K.J., Carroll, P., Martin, C.-A., Murina, O., Fluteau, A., Simpson, D.J., Olova, N., Sutcliffe, H., Rainger, J.K., Leitch, A., et al. (2017). cGAS surveillance of micronuclei links genome instability to innate immunity. Nature *548*, 461.

Mansur, D.S., Smith, G.L., and Ferguson, B.J. (2014). Intracellular sensing of viral DNA by the innate immune system. Microbes Infect. *16*, 1002–1012.

Maréchal, A., and Zou, L. (2013). DNA damage sensing by the ATM and ATR kinases. Cold Spring Harb. Perspect. Biol. *5*.

Mari, P.-O., Florea, B.I., Persengiev, S.P., Verkaik, N.S., Brüggenwirth, H.T., Modesti, M., Giglia-Mari, G., Bezstarosti, K., Demmers, J.A.A., Luider, T.M., et al. (2006). Dynamic assembly of end-joining complexes requires interaction between Ku70/80 and XRCC4. Proc. Natl. Acad. Sci. U. S. A. *103*, 18597–18602.

Martin, G.M., Smith, A.C., Ketterer, D.J., Ogburn, C.E., and Disteche, C.M. (1985). Increased chromosomal aberrations in first metaphases of cells isolated from the kidneys of aged mice. Isr. J. Med. Sci. *21*, 296–301.

Martinez, J.J., Seveau, S., Veiga, E., Matsuyama, S., and Cossart, P. (2005). Ku70, a Component of DNA-Dependent Protein Kinase, Is a Mammalian Receptor for Rickettsia conorii. Cell *123*, 1013–1023.

Mboko, W.P., Mounce, B.C., Wood, B.M., Kulinski, J.M., Corbett, J.A., and Tarakanova, V.L. (2012). Coordinate regulation of DNA damage and type I interferon responses imposes an antiviral state that attenuates mouse gammaherpesvirus type 68 replication in primary macrophages. J. Virol. *86*, 6899–6912.

McConnell, K.R., Dynan, W.S., and Hardin, J.A. (1997). The DNA-dependent protein

kinase catalytic subunit (p460) is cleaved during Fas-mediated apoptosis in Jurkat cells. J. Immunol. *158*.

McGeoch, D.J., Dalrymple, M.A., Davison, A.J., Dolan, A., Frame, M.C., McNab, D., Perry, L.J., Scott, J.E., and Taylor, P. (1988). The Complete DNA Sequence of the Long Unique Region in the Genome of Herpes Simplex Virus Type 1. J. Gen. Virol. *69*, 1531–1574.

McGettrick, A.F., and O'Neill, L.A.J. (2004). The expanding family of MyD88-like adaptors in Toll-like receptor signal transduction. Mol. Immunol. *41*, 577–582.

McKinney, C.C., Hussmann, K.L., and McBride, A.A. (2015). The Role of the DNA Damage Response throughout the Papillomavirus Life Cycle. Viruses *7*, 2450–2469.

Merritt, C., Enslen, H., Diehl, N., Conze, D., Davis, R.J., and Rincón, M. (2000). Activation of p38 mitogen-activated protein kinase in vivo selectively induces apoptosis of CD8(+) but not CD4(+) T cells. Mol. Cell. Biol. *20*, 936–946.

Mettenleiter, T.C. (2002). Herpesvirus assembly and egress. J. Virol. *76*, 1537–1547.

Mistrik, M., and Bartek, J. (2015). What a "Ku"incidence!: parallel discoveries of a new DNA repair factor. Cell Death Differ. *22*, 888–889.

Mocarski, E.S., and Roizman, B. (1982). Structure and role of the herpes simplex virus DNA termini in inversion, circularization and generation of virion DNA. Cell *31*, 89–97.

Mohni, K.N., Livingston, C.M., Cortez, D., and Weller, S.K. (2010). ATR and ATRIP are recruited to herpes simplex virus type 1 replication compartments even though ATR signaling is disabled. J. Virol. *84*, 12152–12164.

Mohni, K.N., Mastrocola, A.S., Bai, P., Weller, S.K., and Heinen, C.D. (2011). DNA mismatch repair proteins are required for efficient herpes simplex virus 1 replication. J. Virol. *85*, 12241–12253.

Mohni, K.N., Dee, A.R., Smith, S., Schumacher, A.J., and Weller, S.K. (2013). Efficient herpes simplex virus 1 replication requires cellular ATR pathway proteins. J. Virol. *87*, 531–542.

Moody, C.A., and Laimins, L.A. (2009). Human papillomaviruses activate the ATM DNA damage pathway for viral genome amplification upon differentiation. PLoS Pathog. *5*, e1000605.

Moody, C.A., and Laimins, L.A. (2010). Human papillomavirus oncoproteins: pathways to transformation. Nat. Rev. Cancer *10*, 550–560.

Morchikh, M., Cribier, A., Raffel, R., Amraoui, S., Cau, J., Severac, D., Dubois, E., Schwartz, O., Bennasser, Y., and Benkirane, M. (2017). HEXIM1 and NEAT1 Long Non-coding RNA Form a Multi-subunit Complex that Regulates DNA-Mediated Innate Immune Response. Mol. Cell *67*, 387–399.e5.

Moshous, D., Li, L., Chasseval, R. de, Philippe, N., Jabado, N., Cowan, M.J., Fischer, A., and Villartay, J.-P. de (2000). A new gene involved in DNA double-strand break repair and V(D)J recombination is located on human chromosome 10p. Hum. Mol. Genet. *9*, 583–588.

Moshous, D., Callebaut, I., de Chasseval, R., Corneo, B., Cavazzana-Calvo, M., Le Deist, F., Tezcan, I., Sanal, O., Bertrand, Y., Philippe, N., et al. (2001). Artemis, a Novel DNA Double-Strand Break Repair/V(D)J Recombination Protein, Is Mutated in Human Severe Combined Immune Deficiency. Cell *105*, 177–186.

Mossman, K.L., Saffran, H.A., and Smiley, J.R. (2000). Herpes Simplex Virus ICP0 Mutants Are Hypersensitive to Interferon. J. Virol. *74*, 2052–2056.

Mossman, K.L., Macgregor, P.F., Rozmus, J.J., Goryachev, A.B., Edwards, A.M., and Smiley, J.R. (2001). Herpes simplex virus triggers and then disarms a host antiviral response. J. Virol. *75*, 750–758.

Motamedifar, M., and Noorafshan, A. (2008). Cytopathic effect of the herpes simplex virus type 1 appears stereologically as early as 4h after infection of Vero cells. Micron *39*, 1331–1334.

Mukherjee, B., Kessinger, C., Kobayashi, J., Chen, B.P.C., Chen, D.J., Chatterjee, A., and Burma, S. (2006). DNA-PK phosphorylates histone H2AX during apoptotic DNA fragmentation in mammalian cells. DNA Repair (Amst). *5*, 575–590.

Murray, J.E., van der Burg, M., IJspeert, H., Carroll, P., Wu, Q., Ochi, T., Leitch, A., Miller, E.S., Kysela, B., Jawad, A., et al. (2015). Mutations in the NHEJ component XRCC4 cause primordial dwarfism. Am. J. Hum. Genet. *96*, 412–424.

Muylaert, I., and Elias, P. (2007). Knockdown of DNA Ligase IV/XRCC4 by RNA Interference Inhibits Herpes Simplex Virus Type I DNA Replication. J. Biol. Chem. *282*, 10865–10872.

Nagashunmugam, T., Lubinski, J., Wang, L., Goldstein, L.T., Weeks, B.S., Sundaresan, P., Kang, E.H., Dubin, G., and Friedman, H.M. (1998). In vivo immune evasion mediated by the herpes simplex virus type 1 immunoglobulin G Fc receptor. J. Virol. *72*, 5351–5359.

Navarro, L., Mowen, K., Rodems, S., Weaver, B., Reich, N., Spector, D., and David, M. (1998). Cytomegalovirus activates interferon immediate-early response gene expression and an interferon regulatory factor 3-containing interferon-stimulated response element-binding complex. Mol. Cell. Biol. *18*, 3796–3802.

Nick McElhinny, S.A., Snowden, C.M., McCarville, J., and Ramsden, D.A. (2000). Ku recruits the XRCC4-ligase IV complex to DNA ends. Mol. Cell. Biol. *20*, 2996–3003.

Novak, N., and Peng, W. (2005). Dancing with the enemy: the interplay of herpes simplex virus with dendritic cells. Clin. Exp. Immunol. *0*, 050911055050015.

O'Driscoll, M., Ruiz-Perez, V.L., Woods, C.G., Jeggo, P.A., and Goodship, J.A. (2003). A splicing mutation affecting expression of ataxia–telangiectasia and Rad3–related protein (ATR) results in Seckel syndrome. Nat. Genet. *33*, 497–501.

Ochi, T., Blackford, A.N., Coates, J., Jhujh, S., Mehmood, S., Tamura, N., Travers, J., Wu, Q., Draviam, V.M., Robinson, C. V., et al. (2015). PAXX, a paralog of XRCC4 and XLF, interacts with Ku to promote DNA double-strand break repair. Science (80-.). *347*, 185–188.

Ogi, T., Walker, S., Stiff, T., Hobson, E., Limsirichaikul, S., Carpenter, G., Prescott, K., Suri, M., Byrd, P.J., Matsuse, M., et al. (2012). Identification of the first ATRIP-deficient patient and novel mutations in ATR define a clinical spectrum for ATR-ATRIP Seckel Syndrome. PLoS Genet. *8*, e1002945.

Okabe, Y., Kawane, K., Akira, S., Taniguchi, T., and Nagata, S. (2005). Toll-like receptor-independent gene induction program activated by mammalian DNA escaped from apoptotic DNA degradation. J. Exp. Med. *202*, 1333–1339.

Orzalli, M.H., DeLuca, N.A., and Knipe, D.M. (2012). Nuclear IFI16 induction of IRF-3 signaling during herpesviral infection and degradation of IFI16 by the viral ICP0 protein. Proc. Natl. Acad. Sci. U. S. A. *109*, E3008–E3017.

Orzalli, M.H., Conwell, S.E., Berrios, C., DeCaprio, J.A., and Knipe, D.M. (2013). Nuclear interferon-inducible protein 16 promotes silencing of herpesviral and transfected DNA. Proc. Natl. Acad. Sci. U. S. A. *110*, E4492–E4501.

Orzalli, M.H., Broekema, N.M., Diner, B.A., Hancks, D.C., Elde, N.C., Cristea, I.M., and Knipe, D.M. (2015). cGAS-mediated stabilization of IFI16 promotes innate signaling during herpes simplex virus infection. Proc. Natl. Acad. Sci. U. S. A. *112*, E1773–E1781.

Orzalli, M.H., Broekema, N.M., and Knipe, D.M. (2016). Varying Roles of Herpes Simplex Virus 1 ICP0 and Vhs in Loss of Cellular IFI16 in Different Cell Types. J. Virol. JVI.00939–16.

Ouellet Lavallée, G., and Pearson, A. (2015). Upstream binding factor inhibits herpes simplex virus replication. Virology *483*, 108–116.

Pancholi, N.J., Price, A.M., and Weitzman, M.D. (2017). Take your PIKK: tumour viruses and DNA damage response pathways. Philos. Trans. R. Soc. London B Biol. Sci. *372*.

Panek, R.B., and Benveniste, E.N. (1995). Class II MHC gene expression in microglia. Regulation by the cytokines IFN-gamma, TNF-alpha, and TGF-beta. J. Immunol. *154*, 2846–2854.

Parkinson, J., Lees-Miller, S.P., and Everett, R.D. (1999). Herpes Simplex Virus Type 1 Immediate-Early Protein Vmw110 Induces the Proteasome-Dependent Degradation of the Catalytic Subunit of DNA-Dependent Protein Kinase. J. Virol. *73*, 650–657.

Patel, A.H., Rixon, F.J., Cunningham, C., and Davison, A.J. (1996). Isolation and Characterization of Herpes Simplex Virus Type 1 Mutants Defective in the UL6 Gene. Virology *217*, 111–123.

Perez-Caballero, D., Zang, T., Ebrahimi, A., McNatt, M.W., Gregory, D.A., Johnson, M.C., and Bieniasz, P.D. (2009). Tetherin inhibits HIV-1 release by directly tethering virions to cells. Cell *139*, 499–511.

Perry, J., and Kleckner, N. (2003). The ATRs, ATMs, and TORs Are Giant HEAT Repeat Proteins. Cell *112*, 151–155.

Perry, J.J.P., Yannone, S.M., Holden, L.G., Hitomi, C., Asaithamby, A., Han, S., Cooper, P.K., Chen, D.J., and Tainer, J.A. (2006). WRN exonuclease structure and molecular mechanism imply an editing role in DNA end processing. Nat. Struct. Mol. Biol. *13*, 414–422.

Perry, J.J.P., Asaithamby, A., Barnebey, A., Kiamanesch, F., Chen, D.J., Han, S., Tainer, J.A., and Yannone, S.M. (2010). Identification of a coiled coil in werner syndrome protein that facilitates multimerization and promotes exonuclease processivity. J. Biol. Chem. *285*, 25699–25707.

Picker, L.J., Treer, J.R., Ferguson-Darnell, B., Collins, P.A., Buck, D., and Terstappen, L.W. (1993). Control of lymphocyte recirculation in man. I. Differential regulation of the peripheral lymph node homing receptor L-selectin on T cells during the virgin to memory cell transition. J. Immunol. *150*.

Pierce, A.T., DeSalvo, J., Foster, T.P., Kosinski, A., Weller, S.K., and Halford, W.P. (2005). Beta interferon and gamma interferon synergize to block viral DNA and virion synthesis in herpes simplex virus-infected cells. J. Gen. Virol. *86*, 2421–2432.

Povirk, L.F., Zhou, T., Zhou, R., Cowan, M.J., and Yannone, S.M. (2007). Processing of 3'-phosphoglycolate-terminated DNA double strand breaks by Artemis nuclease. J. Biol. Chem. *282*, 3547–3558.

Prasad, K.M., Watson, A.M.M., Dickerson, F.B., Yolken, R.H., and Nimgaonkar, V.L. (2012). Exposure to herpes simplex virus type 1 and cognitive impairments in individuals with schizophrenia. Schizophr. Bull. *38*, 1137–1148.

Price, B.D., and D'Andrea, A.D. (2013). Chromatin remodeling at DNA double-strand breaks. Cell *152*, 1344–1354.

Pulvers, J.N., Bryk, J., Fish, J.L., Wilsch-Bräuninger, M., Arai, Y., Schreier, D., Naumann, R., Helppi, J., Habermann, B., Vogt, J., et al. (2010). Mutations in mouse Aspm (abnormal spindle-like microcephaly associated) cause not only microcephaly but also major defects in the germline. Proc. Natl. Acad. Sci. U. S. A. *107*, 16595–16600.

Qvist, P., Huertas, P., Jimeno, S., Nyegaard, M., Hassan, M.J., Jackson, S.P., and Børglum, A.D. (2011). CtIP Mutations Cause Seckel and Jawad Syndromes. PLoS Genet. *7*, e1002310.

Ran, F.A., Hsu, P.D., Wright, J., Agarwala, V., Scott, D.A., and Zhang, F. (2013). Genome engineering using the CRISPR-Cas9 system. Nat. Protoc. *8*, 2281–2308.

Raulet, D.H. (2003). Roles of the NKG2D immunoreceptor and its ligands. Nat. Rev. Immunol. *3*, 781–790.

Rincón, M., Flavell, R.A., and Davis, R.J. (2001). Signal transduction by MAP kinases in T lymphocytes. Oncogene *20*, 2490–2497.

Rivera-Calzada, A., Maman, J.D.P., Spagnolo, L., Pearl, L.H., Llorca, O., Llorca, O., Maman, J.D.P., Spagnolo, L., Pearl, L.H., and Llorca, O. (2005). Three-dimensional structure and regulation of the DNA-dependent protein kinase catalytic subunit (DNA-PKcs). Structure *13*, 243–255.

Roberts, S.A., Strande, N., Burkhalter, M.D., Strom, C., Havener, J.M., Hasty, P., and Ramsden, D.A. (2010). Ku is a 5′-dRP/AP lyase that excises nucleotide damage near broken ends. Nature *464*, 1214–1217.

Rock, D.L., and Fraser, N.W. (1985). Latent herpes simplex virus type 1 DNA contains two copies of the virion DNA joint region. J. Virol. *55*, 849–852.

Rodero, M.P., and Crow, Y.J. (2016). Type I interferon–mediated monogenic autoinflammation: The type I interferonopathies, a conceptual overview. J. Exp. Med. *213*.

Rogakou, E.P., Pilch, D.R., Orr, A.H., Ivanova, V.S., and Bonner, W.M. (1998). DNA double-stranded breaks induce histone H2AX phosphorylation on serine 139. J. Biol. Chem. *273*, 5858–5868.

Roizman, B. (1985). The Herpesviruses : Volume 3 (Springer US).

Roshal, M., Kim, B., Zhu, Y., Nghiem, P., and Planelles, V. (2003). Activation of the ATR-mediated DNA damage response by the HIV-1 viral protein R. J. Biol. Chem. *278*, 25879–25886.

Roth, S., Rottach, A., Lotz-Havla, A.S., Laux, V., Muschaweckh, A., Gersting, S.W., Muntau, A.C., Hopfner, K.-P., Jin, L., Vanness, K., et al. (2014). Rad50-CARD9 interactions link cytosolic DNA sensing to IL-1β production. Nat. Immunol. *15*, 538–545.

Royer, D.J., Cohen, A., and Carr, D. (2015). The Current State of Vaccine Development for Ocular HSV-1 Infection. Expert Rev. Ophthalmol. *10*, 113–126.

Royer, D.J., Gurung, H.R., Jinkins, J.K., Geltz, J.J., Wu, J.L., Halford, W.P., and Carr, D.J.J. (2016). A Highly Efficacious Herpes Simplex Virus 1 Vaccine Blocks Viral Pathogenesis and Prevents Corneal Immunopathology via Humoral Immunity. J. Virol. *90*, 5514–5529.

Rupec, R.A., Poujol, D., Grosgeorge, J., Carle, G.F., Livolsi, A., Peyron, J.F., Schmid, R.M., Baeuerle, P.A., and Messer, G. (1999). Structural analysis, expression, and

chromosomal localization of the mouse ikba gene. Immunogenetics *49*, 395–403.

Sabapathy, K., Hu, Y., Kallunki, T., Schreiber, M., David, J.-P., Jochum, W., Wagner, E.F., and Karin, M. (1999). JNK2 is required for efficient T-cell activation and apoptosis but not for normal lymphocyte development. Curr. Biol. *9*, 116–125.

Saitoh, T., Fujita, N., Yoshimori, T., and Akira, S. (2010). Regulation of dsDNA-induced innate immune responses by membrane trafficking. Autophagy *6*, 430–432.

Sand-Dejmek, J., Adelmant, G., Sobhian, B., Calkins, A.S., Marto, J., Iglehart, D.J., and Lazaro, J.-B. (2011). Concordant and opposite roles of DNA-PK and the "facilitator of chromatin transcription" (FACT) in DNA repair, apoptosis and necrosis after cisplatin. Mol. Cancer *10*, 74.

Sattentau, Q. (2008). Avoiding the void: cell-to-cell spread of human viruses. Nat. Rev. Microbiol. *6*, 815–826.

Schatz, D.G., and Ji, Y. (2011). Recombination centres and the orchestration of V(D)J recombination. Nat. Rev. Immunol. *11*, 251–263.

Schirm, J., and Mulkens, P.S. (1997). Bell's palsy and herpes simplex virus. APMIS *105*, 815–823.

Schoggins, J.W., and Rice, C.M. (2011). Interferon-stimulated genes and their antiviral effector functions. Curr. Opin. Virol. *1*, 519–525.

Schulz, O., Pichlmair, A., Rehwinkel, J., Rogers, N.C., Scheuner, D., Kato, H., Takeuchi, O., Akira, S., Kaufman, R.J., and Reis e Sousa, C. (2010). Protein kinase R contributes to immunity against specific viruses by regulating interferon mRNA integrity. Cell Host Microbe *7*, 354–361.

Schumacher, A.J., Mohni, K.N., Kan, Y., Hendrickson, E.A., Stark, J.M., and Weller, S.K. (2012). The HSV-1 Exonuclease, UL12, Stimulates Recombination by a Single Strand Annealing Mechanism. PLoS Pathog. *8*, e1002862.

Selvarajan Sigamani, S., Zhao, H., Kamau, Y.N., Baines, J.D., and Tang, L. (2013). The structure of the herpes simplex virus DNA-packaging terminase pUL15 nuclease domain suggests an evolutionary lineage among eukaryotic and prokaryotic viruses. J. Virol. *87*, 7140–7148.

Servant, M.J., ten Oever, B., LePage, C., Conti, L., Gessani, S., Julkunen, I., Lin, R., and Hiscott, J. (2001). Identification of distinct signaling pathways leading to the phosphorylation of interferon regulatory factor 3. J. Biol. Chem. *276*, 355–363.

Severini, A., Scraba, D.G., and Tyrrell, D.L. (1996). Branched structures in the intracellular DNA of herpes simplex virus type 1. J. Virol. *70*, 3169–3175.

Sfeir, A., and Symington, L.S. (2015). Microhomology-Mediated End Joining: A Back-up Survival Mechanism or Dedicated Pathway? Trends Biochem. Sci. *40*, 701–714.

Shah, G.A., and O'Shea, C.C. (2015). Viral and Cellular Genomes Activate Distinct DNA Damage Responses. Cell *162*, 987–1002.

Shaheen, R., Faqeih, E., Ansari, S., Abdel-Salam, G., Al-Hassnan, Z.N., Al-Shidi, T., Alomar, R., Sogaty, S., and Alkuraya, F.S. (2014). Genomic analysis of primordial dwarfism reveals novel disease genes. Genome Res. *24*, 291–299.

Sheehy, A.M., Gaddis, N.C., Choi, J.D., and Malim, M.H. (2002). Isolation of a human gene that inhibits HIV-1 infection and is suppressed by the viral Vif protein. Nature *418*, 646–650.

Shintani, S., Mihara, M., Li, C., Nakahara, Y., Hino, S., Nakashiro, K.-I., and Hamakawa, H. (2003). Up-regulation of DNA-dependent protein kinase correlates with radiation resistance in oral squamous cell carcinoma. Cancer Sci. *94*, 894–900.

Shirata, N., Kudoh, A., Daikoku, T., Tatsumi, Y., Fujita, M., Kiyono, T., Sugaya, Y., Isomura, H., Ishizaki, K., and Tsurumi, T. (2005). Activation of ataxia telangiectasia-mutated DNA damage checkpoint signal transduction elicited by herpes simplex virus infection. J. Biol. Chem. *280*, 30336–30341.

Sibanda, B.L., Chirgadze, D.Y., and Blundell, T.L. (2010). Crystal structure of DNA-PKcs reveals a large open-ring cradle comprised of HEAT repeats. Nature *463*, 118–121.

Simmons, A., and Nash, A.A. (1987). Effect of B cell suppression on primary infection and reinfection of mice with herpes simplex virus. J. Infect. Dis. *155*, 649–654.

Sinclair, A., Yarranton, S., and Schelcher, C. (2006). DNA-damage response pathways triggered by viral replication. Expert Rev. Mol. Med. *8*, 1–11.

Smith, G. (2012). Herpesvirus transport to the nervous system and back again. Annu. Rev. Microbiol. *66*, 153–176.

Smith, S., and Weller, S.K. (2015). HSV-I and the cellular DNA damage response. Future Virol. *10*, 383–397.

Smith, C.M., Belz, G.T., Wilson, N.S., Villadangos, J.A., Shortman, K., Carbone, F.R., and Heath, W.R. (2003). Cutting Edge: Conventional CD8α+ Dendritic Cells Are Preferentially Involved in CTL Priming After Footpad Infection with Herpes Simplex Virus-1. J. Immunol. *170*.

Smith, M.C., Boutell, C., and Davido, D.J. (2011). HSV-1 ICP0: paving the way for viral replication. Future Virol. *6*, 421–429.

Smith, S., Reuven, N., Mohni, K.N., Schumacher, A.J., and Weller, S.K. (2014). Structure of the HSV-1 genome: manipulation of nicks and gaps can abrogate infectivity and alter the cellular DNA damage response. J. Virol. *88*, 10146–10156.

Sodeik, B. (1997). Microtubule-mediated Transport of Incoming Herpes Simplex Virus 1Capsids to the Nucleus. J. Cell Biol. *136*, 1007–1021.

Solier, S., and Pommier, Y. (2009). The apoptotic ring: A novel entity with phosphorylated histones H2AX and H2B, and activated DNA damage response kinases. Cell Cycle *8*, 1853–1859.

Solier, S., Sordet, O., Kohn, K.W., and Pommier, Y. (2009). Death receptor-induced activation of the Chk2- and histone H2AX-associated DNA damage response pathways. Mol. Cell. Biol. *29*, 68–82.

Song, Q., Lees-Miller, S.P., Kumar, S., Zhang, Z., Chan, D.W., Smith, G.C., Jackson, S.P., Alnemri, E.S., Litwack, G., Khanna, K.K., et al. (1996). DNA-dependent protein kinase catalytic subunit: a target for an ICE-like protease in apoptosis. EMBO J. *15*, 3238–3246.

Sowd, G.A., Mody, D., Eggold, J., Cortez, D., Friedman, K.L., Fanning, E., Sowd 1¤, G.A., Mody, D., Eggold, J., Cortez, D., et al. (2014). SV40 utilizes ATM kinase activity to prevent non-homologous end joining of broken viral DNA replication products. PLoS Pathog. *10*, e1004536.

Sparrer, K.M.J., Gableske, S., Zurenski, M.A., Parker, Z.M., Full, F., Baumgart, G.J., Kato, J., Pacheco-Rodriguez, G., Liang, C., Pornillos, O., et al. (2017). TRIM23 mediates virus-induced autophagy via activation of TBK1. Nat. Microbiol. *2*, 1543–1557.

Spurrell, J.C.L., Wiehler, S., Zaheer, R.S., Sanders, S.P., and Proud, D. (2005). Human airway epithelial cells produce IP-10 (CXCL10) in vitro and in vivo upon rhinovirus infection. Am. J. Physiol. - Lung Cell. Mol. Physiol. *289*.

Stetson, D.B., and Medzhitov, R. (2006). Recognition of Cytosolic DNA Activates an IRF3-Dependent Innate Immune Response. Immunity *24*, 93–103.

Stetson, D.B., Ko, J.S., Heidmann, T., and Medzhitov, R. (2008). Trex1 Prevents Cell-Intrinsic Initiation of Autoimmunity. Cell *134*, 587–598.

Stiff, T., O'Driscoll, M., Rief, N., Iwabuchi, K., Löbrich, M., and Jeggo, P.A. (2004). ATM and DNA-PK Function Redundantly to Phosphorylate H2AX after Exposure to Ionizing Radiation. Cancer Res. *64*.

Stow, N.D., and Stow, E.C. (1986). Isolation and Characterization of a Herpes Simplex Virus Type 1 Mutant Containing a Deletion within the Gene Encoding the Immediate Early Polypeptide Vmw110. J. Gen. Virol. *67*, 2571–2585.

Stracker, T.H., Carson, C.T., and Weitzman, M.D. (2002). Adenovirus oncoproteins inactivate the Mre11–Rad50–NBS1 DNA repair complex. Nature *418*, 348–352.

Stracker, T.H., Lee, D. V, Carson, C.T., Araujo, F.D., Ornelles, D.A., and Weitzman, M.D. (2005). Serotype-specific reorganization of the Mre11 complex by adenoviral E4orf3 proteins. J. Virol. *79*, 6664–6673.

Stronach, E.A., Chen, M., Maginn, E.N., Agarwal, R., Mills, G.B., Wasan, H., and Gabra, H. (2011). DNA-PK mediates AKT activation and apoptosis inhibition in

clinically acquired platinum resistance. Neoplasia *13*, 1069–1080.

Sui, H., Zhou, M., Imamichi, H., Jiao, X., Sherman, B.T., Lane, H.C., and Imamichi, T. (2017). STING is an essential mediator of the Ku70-mediated production of IFN-λ1 in response to exogenous DNA. Sci. Signal. *10*.

Sun, L., Wu, J., Du, F., Chen, X., and Chen, Z.J. (2013). Cyclic GMP-AMP synthase is a cytosolic DNA sensor that activates the type I interferon pathway. Science *339*, 786–791.

Sun, Z., Xiao, B., Jha, H.C., Lu, J., Banerjee, S., and Robertson, E.S. (2014). Kaposi's Sarcoma-Associated Herpesvirus-Encoded LANA Can Induce Chromosomal Instability through Targeted Degradation of the Mitotic Checkpoint Kinase Bub1. J. Virol. *88*, 7367–7378.

Sung, S.S., Bjorndahl, J.M., Wang, C.Y., Kao, H.T., and Fu, S.M. (1988). Production of tumor necrosis factor/cachectin by human T cell lines and peripheral blood T lymphocytes stimulated by phorbol myristate acetate and anti-CD3 antibody. J. Exp. Med. *167*.

Surova, O., and Zhivotovsky, B. (2013). Various modes of cell death induced by DNA damage. Oncogene *32*, 3789–3797.

Surpris, G., and Poltorak, A. (2016). The expanding regulatory network of STING-mediated signaling. Curr. Opin. Microbiol. *32*, 144–150.

Suspène, R., Aynaud, M.-M., Koch, S., Pasdeloup, D., Labetoulle, M., Gaertner, B., Vartanian, J.-P., Meyerhans, A., and Wain-Hobson, S. (2011). Genetic editing of herpes simplex virus 1 and Epstein-Barr herpesvirus genomes by human APOBEC3 cytidine deaminases in culture and in vivo. J. Virol. *85*, 7594–7602.

Sveda, M.M., and Soeiro, R. (1976). Host restriction of Friend leukemia virus: synthesis and integration of the provirus. Proc. Natl. Acad. Sci. U. S. A. *73*, 2356–2360.

Svennerholm, B., Jeansson, S., Vahlne, A., and Lycke, E. (1991). Involvement of glycoprotein C (gC) in adsorption of herpes simplex virus type 1 (HSV-1) to the cell. Arch. Virol. *120*, 273–279.

Taccioli, G., Gottlieb, T., Blunt, T., Priestley, A., Demengeot, J., Mizuta, R., Lehmann, A., Alt, F., Jackson, S., and Jeggo, P. (1994). Ku80: product of the XRCC5 gene and its role in DNA repair and V(D)J recombination. Science (80-.). *265*.

Tadi, S.K., Tellier-Lebègue, C., Nemoz, C., Drevet, P., Audebert, S., Roy, S., Meek, K., Charbonnier, J.-B., and Modesti, M. (2016). PAXX Is an Accessory c-NHEJ Factor that Associates with Ku70 and Has Overlapping Functions with XLF. Cell Rep. *17*, 541–555.

Tanaka, Y., and Chen, Z.J. (2012). STING specifies IRF3 phosphorylation by TBK1 in the cytosolic DNA signaling pathway. Sci. Signal. *5*, ra20.

Tang, M.L.F., Khan, M.K.N., Croxford, J.L., Tan, K.W., Angeli, V., and Gasser, S. (2014). The DNA damage response induces antigen presenting cell-like functions in fibroblasts. Eur. J. Immunol. *44*, 1108–1118.

Taylor, T.J., and Knipe, D.M. (2004). Proteomics of herpes simplex virus replication compartments: association of cellular DNA replication, repair, recombination, and chromatin remodeling proteins with ICP8. J. Virol. *78*, 5856–5866.

ThermoFisher Scientific (2017). NE-PER™ Nuclear and Cytoplasmic Extraction Reagents.

Tong, L., and Stow, N.D. (2010). Analysis of herpes simplex virus type 1 DNA packaging signal mutations in the context of the viral genome. J. Virol. *84*, 321–329.

Tonotsuka, N., Hosoi, Y., Miyazaki, S., Miyata, G., Sugawara, K., Mori, T., Ouchi, N., Satomi, S., Matsumoto, Y., Nakagawa, K., et al. (2006). Heterogeneous expression of DNA-dependent protein kinase in esophageal cancer and normal epithelium. Int. J. Mol. Med. *18*, 441–447.

Törmänen Persson, H., Aksaas, A.K., Kvissel, A.K., Punga, T., Engström, Å., Skålhegg, B.S., and Akusjärvi, G. (2012). Two Cellular Protein Kinases, DNA-PK and PKA, Phosphorylate the Adenoviral L4-33K Protein and Have Opposite Effects on L1 Alternative RNA Splicing. PLoS One *7*, e31871.

Touraine, J.L., Hadden, J.W., Touraine, F., Hadden, E.M., Estensen, R., and Good, R.A. (1977). Phorbol myristate acetate: a mitogen selective for a T-lymphocyte subpopulation. J. Exp. Med. *145*, 460–465.

Trigg, B.J., and Ferguson, B.J. (2015). Functions of DNA damage machinery in the innate immune response to DNA virus infection. Curr. Opin. Virol. *15*, 56–62.

Tubbs, A., and Nussenzweig, A. (2017). Endogenous DNA Damage as a Source of Genomic Instability in Cancer. Cell *168*, 644–656.

Turnell, A.S., and Grand, R.J. (2012). DNA viruses and the cellular DNA-damage response. J. Gen. Virol. *93*, 2076–2097.

Turner, A., Bruun, B., Minson, T., and Browne, H. (1998). Glycoproteins gB, gD, and gHgL of herpes simplex virus type 1 are necessary and sufficient to mediate membrane fusion in a Cos cell transfection system. J. Virol. *72*, 873–875.

Uematsu, N., Weterings, E., Yano, K., Morotomi-Yano, K., Jakob, B., Taucher-Scholz, G., Mari, P.-O., van Gent, D.C., Chen, B.P.C., and Chen, D.J. (2007). Autophosphorylation of DNA-PKCS regulates its dynamics at DNA double-strand breaks. J. Cell Biol. *177*, 219–229.

Unterholzner, L. (2013). The interferon response to intracellular DNA: why so many receptors? Immunobiology *218*, 1312–1321.

Unterholzner, L., Keating, S.E., Baran, M., Horan, K.A., Jensen, S.B., Sharma, S., Sirois, C.M., Jin, T., Latz, E., Xiao, T.S., et al. (2010). IFI16 is an innate immune sensor for intracellular DNA. Nat. Immunol. *11*, 997–1004.

Vanhove, W., Peeters, P.M., Staelens, D., Schraenen, A., Van der Goten, J., Cleynen, I., De Schepper, S., Van Lommel, L., Reynaert, N.L., Schuit, F., et al. (2015). Strong Upregulation of AIM2 and IFI16 Inflammasomes in the Mucosa of Patients with Active Inflammatory Bowel Disease. Inflamm. Bowel Dis. *21*, 2673–2682.

Vlazny, D.A., Kwong, A., and Frenkel, N. (1982). Site-specific cleavage/packaging of herpes simplex virus DNA and the selective maturation of nucleocapsids containing full-length viral DNA. Proc. Natl. Acad. Sci. U. S. A. *79*, 1423–1427.

Volcy, K., and Fraser, N.W. (2013). DNA damage promotes herpes simplex virus-1 protein expression in a neuroblastoma cell line. J. Neurovirol. *19*, 57–64.

Wallace, M.E., Keating, R., Heath, W.R., and Carbone, F.R. (1999). The cytotoxic T-cell response to herpes simplex virus type 1 infection of C57BL/6 mice is almost entirely directed against a single immunodominant determinant. J. Virol. *73*, 7619–7626.

Wang, H., and Xu, X. (2017). Microhomology-mediated end joining: new players join the team. Cell Biosci. *7*, 6.

Wang, R., Zheng, X., Zhang, L., Zhou, B., Hu, H., Li, Z., Zhang, L., Lin, Y., and Wang, X. (2017). Histone H4 expression is cooperatively maintained by IKKβ and Akt1 which attenuates cisplatin-induced apoptosis through the DNA-PK/RIP1/IAPs signaling cascade. Sci. Rep. *7*, 41715.

Wang, S., Guo, M., Ouyang, H., Li, X., Cordon-Cardo, C., Kurimasa, A., Chen, D.J., Fuks, Z., Ling, C.C., and Li, G.C. (2000). The catalytic subunit of DNA-dependent protein kinase selectively regulates p53-dependent apoptosis but not cell-cycle arrest. Proc. Natl. Acad. Sci. U. S. A. *97*, 1584–1588.

Wang, S., Long, J., and Zheng, C. (2012). The potential link between PML NBs and ICP0 in regulating lytic and latent infection of HSV-1. Protein Cell *3*, 372–382.

Wang, X., Li, Y., Liu, S., Yu, X., Li, L., Shi, C., He, W., Li, J., Xu, L., Hu, Z., et al. (2014). Direct activation of RIP3/MLKL-dependent necrosis by herpes simplex virus 1 (HSV-1) protein ICP6 triggers host antiviral defense. Proc. Natl. Acad. Sci. U. S. A. *111*, 15438–15443.

Wang, Y., Sun, H., Wang, J., Wang, H., Meng, L., Xu, C., Jin, M., Wang, B., Zhang, Y., Zhang, Y., et al. (2016). DNA-PK-mediated phosphorylation of EZH2 regulates the DNA damage-induced apoptosis to maintain T-cell genomic integrity. Cell Death Dis. *7*, e2316.

Wang, Y.-G., Nnakwe, C., Lane, W.S., Modesti, M., and Frank, K.M. (2004). Phosphorylation and Regulation of DNA Ligase IV Stability by DNA-dependent Protein Kinase. J. Biol. Chem. *279*, 37282–37290.

Ward, S.A., and Weller, S.K. (Sandra K. (2011). Alphaherpesviruses : molecular virology (Caister Academic Press).

Watson, D.H., Russell, W.C., and Wildy, P. (1963). Electron microscopic particle counts on herpes virus using the phosphotungstate negative staining technique. Virology *19*, 250–260.

Weaver, A.N., Cooper, T.S., Rodriguez, M., Trummell, H.Q., Bonner, J.A., Rosenthal, E.L., and Yang, E.S. (2015). DNA double strand break repair defect and sensitivity to poly ADP-ribose polymerase (PARP) inhibition in human papillomavirus 16-positive head and neck squamous cell carcinoma. Oncotarget *6*, 26995–27007.

Weir, J.P. (2001). Regulation of herpes simplex virus gene expression. Gene *271*, 117–130.

Weller, S.K., and Coen, D.M. (2012). Herpes simplex viruses: mechanisms of DNA replication. Cold Spring Harb. Perspect. Biol. *4*, a013011.

Wilkinson, D.E., and Weller, S.K. (2004). Recruitment of Cellular Recombination and Repair Proteins to Sites of Herpes Simplex Virus Type 1 DNA Replication Is Dependent on the Composition of Viral Proteins within Prereplicative Sites and Correlates with the Induction of the DNA Damage Response. J. Virol. *78*, 4783–4796.

Wilkinson, D.E., and Weller, S.K. (2006). Herpes simplex virus type I disrupts the ATR-dependent DNA-damage response during lytic infection. J. Cell Sci. *119*, 2695–2703.

Williams, D.R., Lee, K.-J., Shi, J., Chen, D.J., and Stewart, P.L. (2008). Cryo-EM structure of the DNA-dependent protein kinase catalytic subunit at subnanometer resolution reveals alpha helices and insight into DNA binding. Structure *16*, 468–477.

Wong, R.H.F., Chang, I., Hudak, C.S.S., Hyun, S., Kwan, H.-Y., and Sul, H.S. (2009). A role of DNA-PK for the metabolic gene regulation in response to insulin. Cell *136*, 1056–1072.

Woo, S.-R., Corrales, L., and Gajewski, T.F. (2015). Innate Immune Recognition of Cancer. Annu. Rev. Immunol. *33*, 445–474.

Woodbine, L., Neal, J.A., Sasi, N.-K., Shimada, M., Deem, K., Coleman, H., Dobyns, W.B., Ogi, T., Meek, K., Davies, E.G., et al. (2013). PRKDC mutations in a SCID patient with profound neurological abnormalities. J. Clin. Invest. *123*, 2969–2980.

Woodbine, L., Gennery, A.R., and Jeggo, P.A. (2014). The clinical impact of deficiency in DNA non-homologous end-joining. DNA Repair (Amst). *16*, 84–96.

Wu, J., Sun, L., Chen, X., Du, F., Shi, H., Chen, C., and Chen, Z.J. (2013). Cyclic GMP-AMP is an endogenous second messenger in innate immune signaling by cytosolic DNA. Science *339*.

Wu, Z.-H., Shi, Y., Tibbetts, R.S., and Miyamoto, S. (2006). Molecular linkage

between the kinase ATM and NF-kappaB signaling in response to genotoxic stimuli. Science *311*, 1141–1146.

Xing, J., Wu, X., Vaporciyan, A.A., Spitz, M.R., and Gu, J. (2008). Prognostic significance of ataxia-telangiectasia mutated, DNA-dependent protein kinase catalytic subunit, and Ku heterodimeric regulatory complex 86-kD subunit expression in patients with nonsmall cell lung cancer. Cancer *112*, 2756–2764.

Xing, M., Yang, M., Huo, W., Feng, F., Wei, L., Jiang, W., Ning, S., Yan, Z., Li, W., Wang, Q., et al. (2015). Interactome analysis identifies a new paralogue of XRCC4 in non-homologous end joining DNA repair pathway. *6*, 6233.

Xu, Y. (2006). DNA damage: a trigger of innate immunity but a requirement for adaptive immune homeostasis. Nat. Rev. Immunol. *6*, 261–270.

Yaneva, M., Kowalewski, T., and Lieber, M.R. (1997). Interaction of DNA-dependent protein kinase with DNA and with Ku: biochemical and atomic-force microscopy studies. *16*.

Yang, K., Wills, E.G., and Baines, J.D. (2011). A mutation in UL15 of herpes simplex virus 1 that reduces packaging of cleaved genomes. J. Virol. *85*, 11972–11980.

Yannone, S.M., Roy, S., Chan, D.W., Murphy, M.B., Huang, S., Campisi, J., and Chen, D.J. (2001). Werner syndrome protein is regulated and phosphorylated by DNA-dependent protein kinase. J. Biol. Chem. *276*, 38242–38248.

Yano, K., and Chen, D.J. (2008). Live cell imaging of XLF and XRCC4 reveals a novel view of protein assembly in the non-homologous end-joining pathway. Cell Cycle *7*, 1321–1325.

Yano, K., Morotomi-Yano, K., Wang, S.-Y., Uematsu, N., Lee, K.-J., Asaithamby, A., Weterings, E., and Chen, D.J. (2008). Ku recruits XLF to DNA double-strand breaks. EMBO Rep. *9*, 91–96.

Yoo, S., and Dynan, W.S. (1999). Geometry of a complex formed by double strand break repair proteins at a single DNA end: recruitment of DNA-PKcs induces inward translocation of Ku protein. Nucleic Acids Res. *27*, 4679–4686.

Yoshida, H., Okabe, Y., Kawane, K., Fukuyama, H., and Nagata, S. (2005). Lethal anemia caused by interferon-β produced in mouse embryos carrying undigested DNA. Nat. Immunol. *6*, 49–56.

Yu, X., and He, S. (2016). The interplay between human herpes simplex virus infection and the apoptosis and necroptosis cell death pathways. Virol. J. *13*, 77.

Yu, Y., Wang, W., Ding, Q., Ye, R., Chen, D., Merkle, D., Schriemer, D., Meek, K., and Lees-Miller, S.P. (2003). DNA-PK phosphorylation sites in XRCC4 are not required for survival after radiation or for V(D)J recombination. DNA Repair (Amst). *2*, 1239–1252.

Yu, Y., Mahaney, B.L., Yano, K.-I., Ye, R., Fang, S., Douglas, P., Chen, D.J., and Lees-Miller, S.P. (2008). DNA-PK and ATM phosphorylation sites in XLF/Cernunnos are not required for repair of DNA double strand breaks. DNA Repair (Amst). *7*, 1680–1692.

Zhao, X., Madden-Fuentes, R.J., Lou, B.X., Pipas, J.M., Gerhardt, J., Rigell, C.J., and Fanning, E. (2008). Ataxia telangiectasia-mutated damage-signaling kinase- and proteasome-dependent destruction of Mre11-Rad50-Nbs1 subunits in Simian virus 40-infected primate cells. J. Virol. *82*, 5316–5328.

Zimmerman, E.S., Chen, J., Andersen, J.L., Ardon, O., Dehart, J.L., Blackett, J., Choudhary, S.K., Camerini, D., Nghiem, P., and Planelles, V. (2004). Human immunodeficiency virus type 1 Vpr-mediated G2 arrest requires Rad17 and Hus1 and induces nuclear BRCA1 and gamma-H2AX focus formation. Mol. Cell. Biol. *24*, 9286–9294.